arXiv:hep-lat/0703020v1 20 Mar 2007

UNIVERSITÀ DEGLI STUDI DI MILANO
Facoltà di Scienze Matematiche Fisiche e Naturali
CORSO DI DOTTORATO DI RICERCA IN
Fisica, Astrofisica e Fisica Applicata, Ciclo XIX

TESI DI DOTTORATO

Infra-Red divergences in large-N expansion

SETTORE SCIENTIFICO-DISCIPLINARE FIS/02

Relatore: Prof. Sergio CARACCIOLO
Relatore esterno: Prof. Andrea PELISSETTO
Coordinatore: Prof. Gianpaolo BELLINI

CANDIDATO
Bortolo Matteo MOGNETTI
Matr. R05424
Codice P.A.C.S.: 11.15.Pg, 11.10.Wx,
11.30.Rd, 12.40.Ee, 75.10.Hk.

Anno Accademico 2005-2006

Contents

1 Large-N expansions **11**
- 1.1 The model . . . 12
- 1.2 The large-N limit . . . 13
  - 1.2.1 Saddle-point solutions with $\mathcal{N}$ even . . . 15
- 1.3 Equation of state and scaling fields . . . 16
  - 1.3.1 $\mathcal{N} = 1$ . . . 16
  - 1.3.2 The general $\mathcal{N}$ odd case . . . 18
- 1.4 The $1/N$ calculation: propagator and effective vertices . . . 20
- 1.5 The failure of $1/N$ expansion . . . 22

2 Crossover in critical phenomena **27**
- 2.1 Critical crossover limit . . . 28
  - 2.1.1 Explicit two-loop perturbative calculation . . . 30
  - 2.1.2 Higher powers of the fields . . . 34
  - 2.1.3 The general argument . . . 35
  - 2.1.4 A unique definition for the renormalization functions $h_c(u)$ and $r_c(u)$ 36
  - 2.1.5 Higher than two dimension . . . 37
- 2.2 Multicritical crossover limit . . . 40
  - 2.2.1 One-loop computation . . . 41
  - 2.2.2 Two loop computation . . . 44
  - 2.2.3 Correction to u_{1c} and u_{2c} at two loop . . . 51
  - 2.2.4 Higher powers of the fields . . . 52

3 Large-N expansion of $O(N)$ models: the critical zero mode **55**
- 3.1 Effective Hamiltonian for the zero mode . . . 56
  - 3.1.1 Identities among effective vertices . . . 59
- 3.2 Critical crossover limit in the large-N case . . . 61
- 3.3 Crossover between mean-field and Ising behavior . . . 63
- 3.4 Critical behavior of $\langle \boldsymbol{\sigma}_x \cdot \boldsymbol{\sigma}_{x+\mu} \rangle$ . . . 66
- 3.5 Numerical results for selected Hamiltonians . . . 68
- 3.6 Conclusions . . . 70

4 Large-N expansion of $O(N)$ models: the multicritical zero mode **73**
- 4.1 Effective Hamiltonian for the zero mode . . . 74
  - 4.1.1 Basic definitions . . . 74
  - 4.1.2 Identities among the vertices of the effective Hamiltonian . . . 75

4.1.3 Translated zero-mode Hamiltonian 79
4.1.4 Structure of the translated vertices: another derivation 81
4.1.5 $k(m_0^2)$ near the MCP 84
4.2 Scaling Fields and the large N limit 86
4.2.1 $\mathcal{N} = 3$ case in two dimension 86
4.3 Conclusions 91

5 Fermionic Models with chiral symmetry 93
5.1 The model 94
5.2 Behavior for $N_f = \infty$ 96
5.3 Vertex, Propagator and the failure of $1/N$ expansion 100
5.4 The effective theory of the zero mode 103
5.5 The critical crossover limit 106
5.5.1 The general theory 107
5.5.2 Scaling behavior 108
5.5.3 Correlation functions 110
5.6 Conclusions 112

6 Crossover in tricritical models 115
6.1 The model 115
6.2 Gap-Equation. The $H_3 = 0$ case 116
6.3 $1/N$ Expansion and Crossover to Ising Behavior 118
6.4 On the stability of the Weakly-Coupled theory 119

A Properties of $x\mathcal{G}$ eq. (5.11) 121

B Relations among the Yukawa model, medium-range models, and field theory 123

Introduction

The investigation of non perturbative aspects of quantum field theories or statistical mechanic models is a fundamental topic in recent theoretical developments. These studies would give a more complete view of the structure of such theories (e.g. phase diagram), and are essential in order to elucidate non perturbative aspects like quark confinement in QCD or chiral symmetry restoration at finite temperature. Non perturbative techniques are both analytical and numerical. The most used numerical methods are Monte Carlo simulations that are very popular due to their universal setting.[1] On the other side concerning with non perturbative analytic approaches, the $1/N$ expansions [4] have a central role, that seems to increase in the last years. The general scheme of this expansion (see chapter 1) is to consider Hamiltonians with a large number N of fields (that goes to infinity) in such a way that the equations of motion are simplified and can be solved analytically. Proceeding in such a way one recovers solutions similar to those found using other schemes like Mean Field, variational methods or self-consistent approximations which reduce the interacting system to a interaction free one, with a self consistently determined parameter. For instance by considering a vectorial ϕ^4 theory, one can write

$$(\vec{\phi}^2)^2 \implies \vec{\phi}^2 \langle \vec{\phi}^2 \rangle$$

and can recover a free interaction with a mass term that must be fixed in a self consistent way, by computing $\langle \phi^2 \rangle$. However the $1/N$ expansion with respect to the previous methods has the advantage that can be improved in a systematic way by including $1/N$ fluctuations. What does one expect from such an expansion? Of course one would extract informations about the physical case (at finite N), so that one would detect for instance the presence of a phase transition studying the $N = \infty$ solution. This is not always possible. Indeed, due to the fact that the large N limit puts infinite degrees of freedom in a finite volume, one could observe several non analyticities in the partition function that are due to the taken limit instead of the thermodynamic limit $V \to \infty$. This is the problem of the pathologies of the large N limit and has been investigated in detail in [11] by comparing the large N expansion with the available exact solution in $d = 1$. In the case in which the large N expansion is not fictitious one would also try to get $1/N$ numerical corrections to the $N = \infty$ solution to compare with available data at finite N (for instance MC simulations). Another usually addressed advantage of the $1/N$ approaches is that the theory can be solved (in certain case) in a generic dimension,[2] while for instance conventional renormalization group equations usually can be solved only when the fixed point is very near the Gaussian point (like for instance in the ϵ expansion, $\epsilon \equiv 4 - d$).

---

[1] Maybe the claim is too optimistic. There are severe penalties related to MC simulations; the most popular are critical slowing down [1] or the sign problem in fermions system (e.g. [2]).

In this work we want to investigate several aspects of the $1/N$ expansion for models with a global $O(N)$ symmetry.[3] As stressed in [49] approaching a $1/N$ expansion one has to take care of two points (that are also two constraints of the theory):

i) The theory must be both Infra Red Finite and Renormalizable.

ii) The large N expansion is just a technique, with its own limitation. The extrapolation of results (also qualitative) to finite N must be discussed carefully.

Point *ii*) deals with the question (introduced above) of the (possible) pathologies introduced by the large N limit [11]. On the other hand, Renormalizability of large N actions [point *i*)] is quite delicate as the action for the auxiliary fields is usually not local.[4] A scheme to circumvent this difficulty is presented in [24] and [49]. In this work we mainly focus ourself on problems related to Infra Red singularities [point *i*)]. The fact that $1/N$ expansion is not Infra Red finite is usually addressed as a failure of the large N technique. There are several examples in which this happens. In this work we have studied the following cases: (a) Heisenberg models with generic ferromagnetic near neighbour interaction (chap. 1, 3, 4); (b) fermionic models (Yukawa and Gross-Neveu) at finite temperature (chap. 5); (c) a tricritical model with a six-th order interaction (chap. 6). First, we will show (recover) that all the models introduced above exhibit a Mean Field phase diagram for $N = \infty$. The failure of $1/N$ expansion calls for point *ii*): do the $N < \infty$ models show a critical point or the $N = \infty$ critical point is an artefact [11]? Scaling arguments for model (b) [50], a Monte Carlo Simulation for model (a) [82], and exact estimates for model (a) [79], suggest that the phase transition is present also at finite N with a critical behavior that is Ising like. These results suggest that the phase transition near an Infra Red singular point is present also in the physical sector $N < \infty$ so that (at least in the present cases) the large N limit does not produce artefacts. However a question remains open on the nature of the Critical Point (if present). In this work we will confirm the results of [50], [82] and [79] that for every N finite one observes an Ising phase transition. However in the large N limit the critical zone in which Ising behavior is observed scales with a proper power of $1/N$ reducing to zero in the spherical limit ($N = \infty$). This explains why only Mean Field is observed for $N = \infty$. This claim will be supported by the study of the effective interaction of the critical mode[5] that, for the models presented above, looks like a weakly coupled $u\varphi^4$ interaction (with $u \sim 1/N$) which exhibits an interesting crossover limit (called Critical crossover Limit) that matches

---

[2] However in the approaches we present, as soon as one include $1/N$ fluctuations, there are severals distinguo in the scheme proposed. Of course this is not unexpected (we refer to section 2.1.5 fore more details).

[3] For a review of $1/N$ expansion for this kind of models we recommend [49].

[4] This is due to the $\mathrm{tr}\log(\cdots)$ terms that appear in the action for the auxiliary fields (see for instance chapter 5 eq. 5.7), and it is due to the integration of the physical fields.

[5] Infra Red divergences are related to the appearance of a null eigenvalue in the inverse of the propagator P^{-1}, which eigenvector is usually named zero mode.

Ising and Mean Field criticality. The mechanism is the same of what observe in medium range models [36] [34], where now N plays the same role of R (R being the range of spin interaction).

The conclusion of this work are that for models (a), (b) and (c) the problem of Infra Red divergences can be solved using a generalized $1/N$ expansion which explains the universal[6] crossover between Mean Field and Ising (or Multicritical Points in chapter 4). We believe that the scheme proposed is quite general and can be applied to other models characterized by the presence of a zero mode.[7] However in principle it could happen that the weakly coupled interaction could be unstable (this is related to a negative mass term in the zero mode interaction); until now it is not clear to us if this is the sign that the $N = \infty$ critical point considered is unstable (we have developed the theory around the wrong point!) or the sign that now really the $N = \infty$ critical point is an artefact of the large N limit [point *ii*)]. Maybe, it seems that the answer to the previous question is not general but model dependent. Interesting also the fact that the method proposed gives a general scheme to compute $1/N$ corrections of the critical parameters, like for instance the critical temperature T_c. For example, in the critical models this can be done by studying the mass counterterm (and the magnetic one if the theory is not symmetric) that for $d < 4$ can be obtained by a computation in which only a finite number of diagrams enter[8] (see chap. 2). This is a very important point in order to check large N expansions with MC simulations. In sec. 3.5 we present some numerical predictions of a model that has been investigated in [82] by a MC simulation for $N = 3$. The fluctuations seem to match the $N = \infty$ with the $N = 3$ results but there are not enough precision for any claims. As future plan we would compute corrections to the critical temperature for the model simulated in [50]. In this case there is the advantage (instead of [82]) that there are simulations for several N ($N = 4, 12, 24$) so that (we believe) the check will give more precise answers.

Plan of the work

The aim of the first four chapters is to introduce the generalized large N formalism in the most general case (i.e. without any symmetry in the effective action). In order to do that we introduce Heisenberg models with general nearest neighbour ferromagnetic interaction

$$\mathcal{H} \;=\; -N\beta \sum_{\langle ij\rangle} W(1 + \boldsymbol{\sigma}_i \cdot \boldsymbol{\sigma}_j).$$

In **chapter 1** we show as for a large class of interaction W a continuous phase transition is present at finite temperature with Mean Field criticality. By an accurate choice of the interaction W, one is able to detect also multicritical points. However as soon as one tries to include $1/N$ fluctuations infra red divergences appear near the (multi)critical point and the $1/N$ expansion fails. This problem has been solved in **chapter 3** and **chapter 4** (respectively for the critical and for the multicritical case) by a careful study of the effective action of the critical mode[9] that looks like a weakly coupled φ^4 (φ^{2n}) theory. This exhibits an interesting universal crossover between classical to non classical criticality that has been just studied in the past for instance for medium range models [27] [34]. The studies of weakly coupled interactions have been presented in **chapter 2**. The discussion presented there, instead of the medium range models or field theoretical results, consider also the case in which $\mathbb{Z}_2$ symmetry is not present in the starting interaction but must be fixed by other renormalization conditions. The presentation presented in the first part of this work follows [56] and [57].[10]

---

[6] Indeed we will show that the crossover functions of all the models considered are the same apart two obvious normalization condition. Details on how to compare numerically models a) b) c) with field theory are given in app. B.

[7] This claim is supported by the general considerations presented in sec. 6.4.

[8] This is due to the fact that in a bare φ^4 theory, if $d < 4$ only a finite number of diagram must be regularized.

The problem of IR divergences is a well known problem in $1/N$ expansion [49] [14] [15]. This has suggested us to search to apply the same scheme used to study finite temperature (multi)critical points in Heisenberg models to investigate other physical interesting models that share the problem of $1/N$ infrared divergences. In particular in **chapter 5** we have focused our attention on system with N_f fermions coupled to a bosonic field through a Yukawa interaction,

$$\mathcal{H} \;=\; \frac{1}{2}(\partial\phi)^2 + p(\phi) + \sum_{f=1}^{N_f} \overline{\psi}_f \Big(\partial\!\!\!/ + g\phi\Big)\psi_f$$

in the large N_f limit.[11] The main result of this chapter will be to prove the claim that the crossover function obtained in the study of the Heisenberg model for $\mathcal{N} = 1$ can be used also for the fermionic model (they are universal).[12] We have just pointed out that an important check for the scheme proposed would be the computation of the $1/N$ correction to the critical temperature, to compare with the available results obtained in [50] for several N. In **chapter 6** we will consider a vectorial model $\vec{\phi} = \{\phi_1, \cdots \phi_N\}$ with a ϕ^6 interaction

$$\mathcal{H} \;=\; \vec{H}\phi + \frac{1}{2}(\partial\vec{\phi})^2 + \frac{r}{2}\vec{\phi}^2 + \frac{u}{4!}(\vec{\phi}^2)^2 + \frac{v}{6!}(\vec{\phi}^2)^3.$$

The phase diagram is rather well understood since a long time (e.g. [96]). For $\vec{H} \neq 0$ there are two line of second order phase transition (that usually are called wing lines) that meet together in a tricritical point for $\vec{H} = 0$. For the $N = \infty$ theory a Mean Field Behavior is observed along the wing lines while, due to symmetry arguments, one expect Ising behaviour for every N [96]. The apparent paradox can be solved including $1/N$ corrections in the same way of what we have done in the Heisenberg model.

---

[9] The appearance of a critical mode at the critical point is strictly related to infra red singularities.

[10] In [56] the critical points in $d = 2$ have been explicitly computed. The results have been then generalized in a straightforward way to the $d > 2$ case. However in the case in which the interaction is not symmetric in higher than two dimension the discussion is more involved (see sec. 2.1.5) although the conclusions remain unchanged.

[11] Similar consideration holds for the Gross Neveu model (see [24] sec. 31.9), that is a model with a four fermions interaction.

[12] However in this case, instead of the Heisenberg models, it was pointed out (using scaling arguments) time ago [50] the mechanism of the critical zone reduction for which the region size in which Ising fluctuations become relevant go to zero for $N_f \to \infty$, explaining the reason for which only Mean Field is observed for $N_f = \infty$.

As future application we plan to apply our multicritical scheme to the study of Yukawa models with nonzero chemical potential and finite temperature which is believed to have a phase diagram with a tricritical point. This is an interesting topic in order to investigate the phase diagram of QCD.

All the systems we have described are characterized by a global $O(N)$ symmetry. In models with local symmetry the Mean Field behavior of the large N limit is questionable and currently under investigation [43] (see also [58]). It could be interesting to use our approach in order to recover (or not) previous results [43].

Chapter 1

Large-N expansions

In this chapter we introduce the general technique commonly used in the study of models with $O(N)$ global symmetry in the limit in which N goes to infinity. The basic idea deals with the fact that the $O(N)$ quantities self-average for $N \to \infty$; in fact this can be seen as a consequence of central limit theorem [3]. Let we consider for instance the standard ϕ^4_x theory, where ϕ is a N component vectorial field and $\phi^4_x \equiv (\vec{\phi}^2_x)^2$ is the interacting term. In order to compute $O(N)$ symmetric observables one can guess that in the large N limit $\vec{\phi}^2_x$ self averages on a given expectation value $\alpha(x)$ with fluctuations that scale as $1/\sqrt{N}$. Concerning the expectation values, one can then write the equation reported into the introduction

$$\langle \phi(\mathbf{y})^2 \phi(\mathbf{x})^2 \rangle = \langle \phi(\mathbf{y})^2 \rangle \langle \phi(\mathbf{x})^2 \rangle + O\left(\frac{1}{\sqrt{N}}\right),$$

where now also fluctuations are included. In this work we implement the large N limit by introducing several auxiliary fields that are related to $O(N)$ invariant quantities of the model [49] [24]. This allows us to write an effective action in terms of the fields introduced. In literature there are also other methods that give the same results like for instance Hartree-Fock approximations [5]. Also in the point of view of stochastic quantization or in the Critical Dynamic [8] the Langevin equation becomes linear and self-consistent for large N replacing ϕ^2 with $\langle \phi^2 \rangle$. On the other hand a famous related model is the spherical model [6], that was shown to share the same critical behavior with $N = \infty$ spin systems [7]. However Hartree-Fock or self-consistent conditions give only the $N = \infty$ limit while the method of auxiliary fields gives the possibility to develop a systematic $1/N$ expansion. This is a fundamental necessity for our work which focuses on $1/N$ corrections.

As a prototype for IR divergences appearing in the large N limit, in sec. 1.1 we will introduce a general class of spin models (1.2) on a lattice, which exhibits a phase transition at finite temperature and spin-spin correlation length. In sec. 1.1 we also describe the recent interest in studying Hamiltonians (1.2). In sec. 1.2, after having introduced the auxiliary fields we study the saddle point equations (1.7-1.8-1.9) and the gap-equation (1.10) that give the physics for $N = \infty$. We study both models with critical and multicritical phase transitions. Multicritical points can be observed choosing very peculiar Hamiltonians (1.2) so that the set of equations (1.15) can be satisfied at the critical temperature $\beta_c < \infty$. We believe that the study of multicritical points is interesting because several physical systems undergo such a transitions. For example in the study of chiral symmetry in QCD several simplified models have been considered. In chapter 5 we investigate a Yukawa model[1] at finite temperature T that shows the same IR singularities of (1.2) near a critical point $T_c > 0$. We plan to study the model also with a finite chemical potential[2] $\mu > 0$ which is believed to exhibits a tricritical point so that our present investigation of multicritical interactions (1.2) could be useful. In sec. 1.3 we parametrize the gap-equation near the (multi)critical point obtaining the scaling fields and the equation of state (that are Mean Field like). In sec. 1.4 in order to include $1/N$ fluctuations we develop the theory around the saddle point solution giving the expression for the propagator and the vertices of the Hamiltonian for the auxiliary fields. We show as near the critical point the propagator is singular at zero external momentum. In sec. 1.5 we show that, because this singularity, the standard $1/N$ expansion breaks down.

1.1 The model

Motivated by condensed matter or field theory, a lot of work has been focused on the investigation of the following Hamiltonian

$$H = -N\beta \sum_{\langle ij \rangle} \boldsymbol{\sigma}_i \cdot \boldsymbol{\sigma}_j, \tag{1.1}$$

where $\boldsymbol{\sigma}_i$ is an N-dimensional unit spin and the sum is extended over all lattice nearest neighbours. Indeed (1.1) is usually used as the prototype of short-range interacting models with global $O(N)$ symmetry. In two dimension the model is disordered for all finite β [62] and it is described for $\beta \to \infty$ by the perturbative renormalization group [63], [64], [65]. The square-lattice model has been extensively studied numerically [66], [67], [68], [69], [70], [71], checking the perturbative predictions [72], [73], [74], [75] and the non-perturbative constants [76], [77], [78]. Recently more general models than (1.1) have received attentions

$$H = -N\beta \sum_{<ij>} W(1 + \boldsymbol{\sigma}_i \cdot \boldsymbol{\sigma}_j). \tag{1.2}$$

Indeed using exact estimates it has been pointed out in [79] that if one consider a generic $O(N)$ interaction (1.2) then for a large class of interactions W, a first-order phase transitions appear for $\beta > 0$ in two dimension.[3,4] In [82] a particular class of interactions depending on a parameter p is considered and studied by Monte Carlo simulations

$$W(x) \sim x^p. \tag{1.3}$$

---

[1] This model in the large N limit [24] behaves exactly as the Gross-Neveu model [9] [10].

[2] This is relevant for recent experimental progress in the physic of ultrarelativistic heavy-ion collisions.

[3] It [80] similar considerations are given for a gauge theory in $2 + 1$ dimensions.

[4] It is interesting to observe that this phase transition is not present for (1.1) although that the two continuum limit of (1.1) and (1.2) formally coincide. This is related to the fact that, according with [62], at the critical point the spin-spin correlation length is finite.

The results show, according with [79], the existence of a first order phase transition for high enough p at finite temperature.[5] Otherwise also a continuous phase transition for $p \approx 5$ is observed and numerical evidences suggest that it belongs to the Ising universality class. It is important to stress that according with [62] at the critical point (CP) the spin-spin correlation length remains finite while the critical parameter seems to be the energy $E = \boldsymbol{\sigma}_i \cdot \boldsymbol{\sigma}_j$, where i and j are neighbour. The same qualitative results of [82] was obtained in [55] taking the spherical limit ($N \to \infty$), but instead of the Ising criticality a Mean Field behavior was observed.

The apparent paradox has been solved in [56] where it has been shown that in the large N limit the width of the critical Ising zone (that is the region near p_c and β_c where fluctuations become important and Mean Field behavior is suppressed) reduces as a power of $1/N$ for $N \to \infty$. This explains why only Mean Field is detected for N strictly infinite. In this work we present the results obtained in [56] considering also interaction W depending on $\mathcal{N}$ tunable parameter p_i. We show the existence of multicritical points (MCP) for every model (with $\mathcal{N}$ odd) that can simultaneously satisfy $\mathcal{N}+1$ conditions (1.14) at the critical point $p_{1c} \cdots p_{\mathcal{N}c}, \beta_c$. Then following [56] we show how $1/N$ fluctuations don't destroy the $N = \infty$ critical points so that CP or MCP are present at finite N and cannot be considered an artefact of the large N limit [11]. Otherwise the Mean Field behaviour is destroyed as soon as one takes N finite. We explain this in term of a generalized $1/N$ expansion using a weakly coupled $\varphi^{\mathcal{N}+3}$ theory that will be introduced in chapter 2 and applied to (1.2) in chapters 3 and 4.

1.2 The large-N limit

The large-N limit for the model (1.2) has been discussed in detail in Ref. [55]. Proceeding in a standard way [49] we introduce three auxiliary fields $\lambda_{x\mu}$, $\rho_{x\mu}$, and μ_x in order to linearize the dependence of the Hamiltonian on the spins $\boldsymbol{\sigma}$ and to eliminate the constraint[6] $\boldsymbol{\sigma}_x^2 = 1$. The partition function becomes

$$Z = \int \prod_{x\mu} [d\rho_{x\mu} d\lambda_{x\mu}] \prod_x [d\mu_x d\boldsymbol{\sigma}_x] \, e^{-N\mathcal{H}}, \tag{1.4}$$

where

$$\mathcal{H} = -\frac{\beta}{2} \sum_{x\mu} \left[\lambda_{x\mu} + \lambda_{x\mu} \boldsymbol{\sigma}_x \cdot \boldsymbol{\sigma}_{x+\mu} - \lambda_{x\mu}\rho_{x\mu} + 2W(\rho_{x\mu})\right] + \frac{\beta}{2} \sum_x \left(\mu_x \boldsymbol{\sigma}_x^2 - \mu_x\right). \tag{1.5}$$

We develop the auxiliary fields near their saddle-point values

$$\lambda_{x\mu} = \alpha + \frac{1}{\sqrt{N}} \widehat{\lambda}_{x\mu}, \quad \rho_{x\mu} = \tau + \tfrac{1}{\sqrt{N}} \widehat{\rho}_{x\mu}, \quad \mu_x = \gamma + \frac{1}{\sqrt{N}} \widehat{\mu}_x. \tag{1.6}$$

---

[5] There are other numerical works with similar results for different Hamiltonians than (1.3), see e.g. [83]. However Hamiltonian (1.3) is peculiar with respect other models –like for instance RP^{N-1} models– because it does not have any symmetry.

[6] This constraint is usually irrelevant in the large N limit (see [24] sec. 30.6).

In Ref. [55] α, τ and γ were explicitly given. They can be written as

$$\begin{aligned}\gamma &= \alpha(4+m_0^2)/2, & (1.7)\\ \alpha &= 2W'(\tau), & (1.8)\\ \tau &= \overline{\tau}\left(m_0^2\right) \equiv 2+\frac{m_0^2}{4}-\frac{1}{4B_1(m_0^2)}, & (1.9)\\ \beta &= \frac{B_1(m_0^2)}{W'(\overline{\tau},p)}, & (1.10)\end{aligned}$$

where the parameter m_0 is related to the spin-spin correlation length $\xi_\sigma = 1/m_0$ and

$$B_n(m_0^2) \equiv \int_{\mathbf{q}} \frac{1}{(\hat{q}^2+m_0^2)^n}, \tag{1.11}$$

with the integral extended over the first Brillouin zone. The corresponding free energy can be written as

$$F = -\beta d W(\tau) + \frac{1}{2}\log I(m_0^2) + \frac{1}{2}L(m_0^2), \tag{1.12}$$

where

$$L(m_0^2) = \int_{\mathbf{p}} \log(\hat{p}^2+m_0^2). \tag{1.13}$$

In Ref. [55] it was shown that generic models may show first-order transitions. This happens when, for given β, there are several values of m_0^2 that solve the gap equation (1.10). Here, we will be interested at the endpoint of the first-order transition line for which the following two relations holds [55]

$$\frac{\partial\beta}{\partial m_0^2} = 0, \qquad \frac{\partial^2\beta}{\partial(m_0^2)^2} = 0 \qquad \frac{\partial^3\beta}{\partial(m_0^2)^3} < 0. \tag{1.14}$$

In order to recover the two previous conditions (1.14) one can use a family of one parameter of interactions $W(x) \equiv W(p;x)$ in (1.2) and tune both p and β to the critical point where (1.14) are satisfied. For instance in [82] and [79] the Hamiltonian 1.3 was considered as prototype of interactions W that show phase transitions. In [81] similar consideration to what obtained in [55] was given for the mixed O(N)-RP^{N-1} model $W(x) \sim x + px^2$. In this work we will consider the most generic one-parameter families of interactions that satisfy (1.14) for a critical point p_c, m_{0c}^2. More interesting we will consider also families of interaction that depend on $\mathcal{N}$ odd tunable parameters $W(x) \equiv W(p_1, \cdots p_{\mathcal{N}}; x)$ in oder to avoid the following multicritical conditions

$$\frac{\partial^i\beta}{\partial(m_0^2)^i} = 0, \qquad \frac{\partial^{\mathcal{N}+2}\beta}{\partial(m_0^2)^{\mathcal{N}+2}} < 0 \tag{1.15}$$

for $i = 1, \cdots \mathcal{N}+1$. This permit us to claim that for the Hamiltonian (1.2) not only Ising behavior can be observed but also multicritical points (described by scalar $\phi^{2\mathcal{N}+2}$ theory in chap. 2). This in principle gives us the possibility to study large-N physical system with multicritical point. In the next sub-section we show that solutions of (1.15) with $\mathcal{N}$ even are unstable; i.e. if (1.15) is realised for $m_0 = m_{0c}$ with $\mathcal{N}$ even, then another solution $\overline{m}$ always

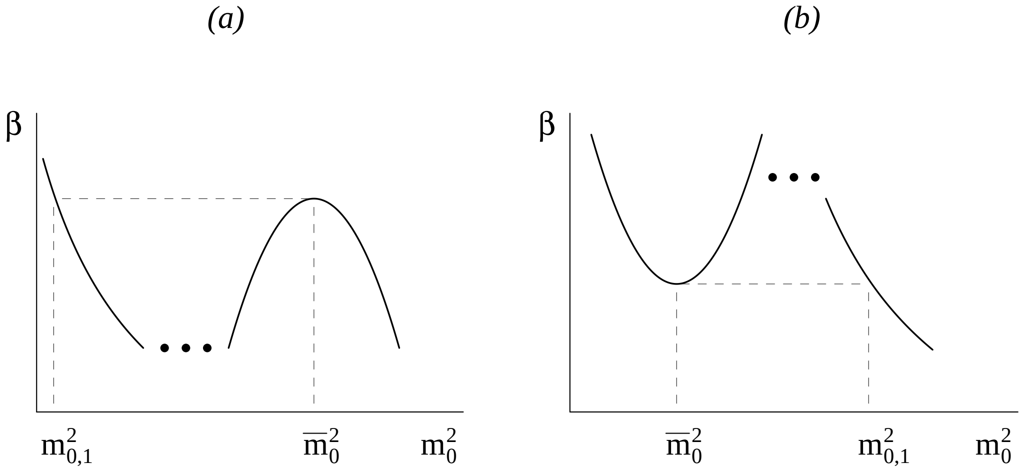

Figure 1.1: The two possibilities for $\beta(m_0^2)$ in the presence of a saddle-point with $\mathcal{N}$ even.

exists with $F(\overline{m}) < F(m_{0c})$. The previous conclusion remains unchanged for the point $\overline{m}$ that satisfy (1.14) or (1.15) with opposite sign in the dis-equalities. Then in sec. 5.3 we will recover the $N = \infty$ phase diagram for the model (1.2) obtaining the scaling fields as functions of p_i and β and explaining the mean field behavior.

1.2.1 Saddle-point solutions with $\mathcal{N}$ even

In this section we show that solutions of eq. (1.14) with $\mathcal{N}$ even are of no interest. Indeed, given $\overline{m}_0^2$ satisfying eq. (1.14) with $\mathcal{N}$ even there exists $m_{0,1}^2$ such that

$$\beta(m_{0,1}^2) = \beta(\overline{m}_0^2) \qquad\qquad F(m_{0,1}^2) < F(\overline{m}_0^2), \tag{1.16}$$

where $F(m_0^2)$ is the free energy (1.12). Thus, $\overline{m}_0^2$ is not the relevant solution and simply represents a metastable state.

We start by observing that, if $\mathcal{N}$ is even, $\overline{m}_0^2$ is a local maximum or minimum of the function $\beta(m_0^2)$. Since $\beta(m_0^2)$ vanishes for $m_0^2 \to \infty$, diverges for $m_0^2 \to 0$, and is always positive under the assumption that $W'(x)$ is positive for $1 \leq x \leq 2$, the function $\beta(m_0^2)$ must behave as in Fig. 1.1. If it is a local maximum, there exists $m_{0,1}^2$ such that $m_{0,1}^2 < \overline{m}_0^2$, $\beta(m_{0,1}^2) = \beta(\overline{m}_0^2)$ and $\beta(m_0^2) < \beta(m_{0,1}^2)$ for $m_{0,1}^2 < m_0^2 < \overline{m}_0^2$. Similar considerations can be made if $\overline{m}_0^2$ is a local minimum (see Fig. 1.1). Then, consider the free energy (1.12), a straightforward calculation gives

$$\frac{dF}{dm_0^2} = -2W(\tau)\frac{d\beta}{dm_0^2}. \tag{1.17}$$

Consider first case (a) of Fig. 1.1. Using eq. (1.17) we can write

$$F(\overline{m}_0^2) - F(m_{0,1}^2) = -2\beta(\overline{m}_0^2)\,[W(\tau(\overline{m}_0^2)) - W(\tau(m_{0,1}^2))]$$

$$+2\int_{m_{0,1}^2}^{\overline{m}_0^2} dm_0^2\, W'(\tau(m_0^2))\beta(m_0^2)\frac{d\tau}{dm_0^2}. \tag{1.18}$$

Now $W'(\tau) > 0$, $d\tau/dm_0^2 < 0$, $\beta(m_0^2) < \beta(\overline{m}_0^2)$ in the interval, so that

$$\begin{aligned}\int_{m_{0,1}^2}^{\overline{m}_0^2} dm_0^2\, W'(\tau(m_0^2))\beta(m_0^2)\frac{d\tau}{dm_0^2} &> \beta(\overline{m}_0^2)\int_{m_{0,1}^2}^{\overline{m}_0^2} dm_0^2\, W'(\tau(m_0^2))\frac{d\tau}{dm_0^2} \\ &= \beta(\overline{m}_0^2)[W(\tau(\overline{m}_0^2)) - W(\tau(m_{0,1}^2))]. \end{aligned} \tag{1.19}$$

If follows

$$F(\overline{m}_0^2) - F(m_{0,1}^2) > 0, \tag{1.20}$$

as required. In the case $\overline{m}_0^2$ is a local minimum the analysis is identical. If the disequalities (1.14) (1.15) have opposite sign one can repeat the discussion reported it is straightforward to recover the previous conclusion strictly following the case (a) of Fig. 1.1.

1.3 Equation of state and scaling fields

In this section we want to describe the phase diagram of the model outlining the mean field behavior. This is done in sec. 1.3.1 developing the gap-equation $\beta(m_0^2)$ near the critical point (1.14). In sec. 1.3.2 we generalize the discussion for a multi-critical point (1.15).

1.3.1 $\mathcal{N} = 1$

We wish now to parametrize the singular behavior for $\beta \to \beta_c$ and $p \to p_c$. Expanding the gap equation (1.10) near the critical point we obtain

$$\beta - \beta_c = \sum_{nm} a_{nm}(p - p_c)^n (m_0^2 - m_{0c}^2)^m. \tag{1.21}$$

Because of the definition of β_c we have $a_{00} = 0$. Moreover, eq. (1.14) implies that $a_{01} = a_{02} = 0$, $a_{03} < 0$. For $p = p_c$ we see that m_0^2 has the leading behavior

$$m_0^2 - m_{0c}^2 \approx \left(\frac{\beta - \beta_c}{a_{03}}\right)^{1/3}, \tag{1.22}$$

while for $\beta = \beta_c$, we have

$$m_0^2 - m_{0c}^2 \approx \left(-\frac{a_{10}(p - p_c)}{a_{03}}\right)^{1/3}. \tag{1.23}$$

The nonanalytic behavior with exponent 1/3 is observed along any straight line approaching the critical point, except that satisfying $\beta - \beta_c - a_{10}(p - p_c) = 0$. Therefore, the correct linear scaling field is

$$u_h \equiv \beta - \beta_c - a_{10}(p - p_c), \tag{1.24}$$

and we have $m_0^2 - m_{0c}^2 \sim u_h^{1/3}$ whenever $u_h \neq 0$. To include the case $u_h = 0$, we write the general scaling equation

$$m_0^2 - m_{0c}^2 = u_h^{1/3} f(x), \tag{1.25}$$

where $f(x)$ is a scaling function and x is a scaling variable to be determined. Then, we use again the gap equation (1.21). Keeping only the leading terms we obtain

$$u_h = a_{20}(p - p_c)^2 + a_{11}(p - p_c)u_h^{1/3} f(x) + a_{03} u_h f(x)^3, \tag{1.26}$$

so that

$$a_{03} f(x)^3 + a_{11}(p - p_c)u_h^{-2/3} f(x) - a_{20}(p - p_c)^2 u_h^{-1} - 1 = 0 \tag{1.27}$$

Since $(p - p_c)^2 u_h^{-1} = [(p - p_c)u_h^{-2/3}]^2 u_h^{1/3}$, the third term can be neglected. Thus, we may take (the prefactor has been introduced for later convenience)

$$x \equiv a_{11}(p - p_c)|u_h|^{-2/3}. \tag{1.28}$$

The function $f(x)$ satisfies

$$a_{03} f(x)^3 + x f(x) - 1 = 0. \tag{1.29}$$

Such an equation is exactly the mean-field equation for the magnetization. Indeed, if we consider the mean-field Hamiltonian

$$\mathcal{H} = -hM + \frac{t}{2}M^2 + \frac{u}{24}M^4, \tag{1.30}$$

the stationarity condition gives

$$-h + tM + \frac{u}{6}M^3 = 0, \tag{1.31}$$

which is solved by $M = h^{1/3}\hat{f}(t|h|^{-2/3})$, where $\hat{f}(x)$ satisfies eq. (1.29) with[7] $a_{03} = u/6$. It is thus clear that the scaling field (1.24) corresponds to h, while p corresponds to the temperature. Note that this identification is not unique, since only the line $H = 0$ is uniquely defined by the singular behavior. For instance, in the usual Ising case, we could define $t' = t + ah$ without changing the scaling equation of state, since $t|h|^{-2/3} = t'|h|^{-2/3} + ah^{1/3}$. Since the scaling limit is taken with $h \to 0$, $t \to 0$ at fixed $t|h|^{-2/3}$, we see that $t|h|^{-2/3} \approx t'|h|^{-2/3}$. In the Ising case, however, there is exact $\mathbb{Z}_2$ symmetry and thus the natural t variable is defined so that it is invariant under the symmetry. In our case we could define $u_t = p - p_c + A(\beta - \beta_c)$ and fix A by requiring the leading correction on any line (except $u_h = 0$) to be of order $u_h^{2/3}$ instead of order $u_h^{1/3}$, recovering in this way an approximate $\mathbb{Z}_2$ symmetry. For our purposes this is irrelevant and thus we will use $p - p_c$ as thermal scaling field.

Eq. (1.25) gives the leading behavior. It is also possible to compute the subleading corrections. We obtain for the leading one

$$m_0^2 - m_{0c}^2 = u_h^{1/3} f(x) + u_h^{2/3} g(x) + O(u_h), \tag{1.32}$$

---

[7] Notice that the sign of a_{03} implies that the low temperature phase is obtained –as expected– for $p > p_c$. However the sign of a_{03} is fundamental in order to guarantees the stability of the effective theory for the zero mode in chapter 3.

with

$$g(x) = -\frac{a_{20}x^2 + a_{12}a_{11}xf(x)^2 + a_{04}a_{11}^2 f(x)^4}{a_{11}^2(x + 3a_{03}f(x)^2)}. \tag{1.33}$$

Finally, let us discuss the singular behavior of the energy. We have

$$E = 2W(\overline{\tau}, p). \tag{1.34}$$

Such a function is regular in m_0^2 and p. Since $p - p_c \sim x|u_h|^{2/3}$ and $m_0^2 - m_{0c}^2 \sim u_h^{1/3}$, the leading term is obtained by expanding the previous equation in powers of $m_0^2 - m_{0c}^2$. Thus

$$E = 2W_c + 2W_c' \left.\frac{B_1^2 - B_2}{4B_1^2}\right|_{m_0 = m_{0c}} u_h^{1/3} f(x) + O(u_h^{2/3}). \tag{1.35}$$

where $W' = \partial W(x,p)/\partial x$ with $x = \overline{\tau}$ and the suffix c indicates that all quantities must be computed at the critical point.

1.3.2 The general $\mathcal{N}$ odd case

Following the same step of the previous section 1.3.1 we want now the expand the gap equation (1.10) near a multicritical point (1.15). First we present the $\mathcal{N} = 3$ case because it requires to consider non-linear terms in the definitions of the scaling fields, the generalization is then straightforward. We have

$$\beta - \beta_c = \sum_{\ell, i_1 i_2 i_3} a^{(\ell)}_{i_1 i_2 i_3} (p_1 - p_{1c})^{i_1} (p_2 - p_{2c})^{i_2} (p_3 - p_{3c})^{i_3} (m_0^2 - m_{0c}^2)^{\ell}. \tag{1.36}$$

with $a^{(\ell)}_{000} = 0$ for $0 \le \ell \le 4$ because of eq. (1.14). To simplify the notations we introduce a multi-index $A \equiv (i_1, i_2, i_3)$, rewrite the previous equation as

$$\beta - \beta_c = \sum_{\ell, A} a^{(\ell)}_A (p - p_c)^A (m_0^2 - m_{0c}^2)^{\ell}. \tag{1.37}$$

and define the linear scaling fields as

$$u_h = \beta - \beta_c - \sum_{A:[A]=1} a^{(0)}_A (p - p_c)^A, \tag{1.38}$$

$$u_1 = \sum_{A:[A]=1} a^{(1)}_A (p - p_c)^A, \tag{1.39}$$

$$u_2 = \sum_{A:[A]=1} a^{(2)}_A (p - p_c)^A, \tag{1.40}$$

$$u_3 = \sum_{A:[A]=1} a^{(3)}_A (p - p_c)^A, \tag{1.41}$$

where $[A] = a$ indicates indices i_1, i_2, i_3 such that $i_1 + i_2 + i_3 = a$. The gap equation becomes

$$\begin{aligned} u_h &= \sum_{\ell \ge 5} a^{(\ell)}_{000} (m_0^2 - m_{0c}^2)^{\ell} + (m_0^2 - m_{0c}^2) u_1 + (m_0^2 - m_{0c}^2)^2 u_2 + (m_0^2 - m_{0c}^2)^3 u_3 \\ &\quad + \sum_{\ell \ge 4} \sum_{A:[A]=1} a^{(\ell)}_A (p - p_c)^A (m_0^2 - m_{0c}^2)^{\ell} + \sum_{\ell = 0} \sum_{A:[A]\ge 2} a^{(\ell)}_A (p - p_c)^A (m_0^2 - m_{0c}^2)^{\ell}. \end{aligned} \tag{1.42}$$

From this equation one can read the correct scalings. We have $m_0^2 - m_{0c}^2 \sim u_h^{1/5}$ and, as a consequence, $u_j \sim u_h (m_0^2 - m_{0c}^2)^{-j} \sim u_h^{1-j/5}$. Moreover, expressing $p_i - p_{ic}$ in terms of u_i, we obtain $p_i - p_{ic} \sim u_3 \sim u_h^{2/5}$. Thus, close to the multicritical point we expect

$$m_0^2 - m_{0c}^2 = u_h^{1/5} f(x_1, x_2, x_3), \tag{1.43}$$

where the scaling variables x_j are defined by $x_j \equiv u_j u_h^{j/5-1}$. If we now substitute this Ansatz in eq. (1.42) we find however a difficulty. All terms in the equation should vanish close to the MCP as u_h or faster. On the other hand, the terms with $[A] = 2$ and $\ell = 0$ vanish only as $u_h^{4/5}$. Thus, they are the dominant ones and make the Ansatz (1.43) inconsistent. There is a very simple way out of this problem. It is enough to include these terms in the definition of u_h and consider the nonlinear scaling field

$$u_h = \beta - \beta_c - \sum_{A:[A]=1,2} a_A^{(0)} (p - p_c)^A. \tag{1.44}$$

With this definition the dangerous terms are no longer present in eq. (1.42) and in the scaling limit, $u_h \to 0$, $u_i \to 0$, at fixed x_i, we obtain

$$a_{000}^{(5)} f^5 + x_3 f^3 + x_2 f^2 + x_1 f - 1 = 0, \tag{1.45}$$

which is exactly the mean-field scaling equation of state for a generic ϕ^6 theory with Hamiltonian

$$\mathcal{H} = -\phi + \frac{x_1}{2}\phi^2 + \frac{x_2}{3}\phi^3 + \frac{x_3}{4}\phi^4 + \frac{a_{000}^{(5)}}{6}\phi^6. \tag{1.46}$$

Note the absence of the ϕ^5 term, which, if present, can always be eliminated by performing an appropriate shift of the fields.

The generalization to generic values of $\mathcal{N}$ is straightforward. We define

$$\begin{aligned} u_h &\equiv \beta - \beta_c - \sum_{A:[A]\le m_0} a_A^{(0)} (p - p_c)^A && (1.47)\\ u_i &\equiv \sum_{A:[A]\le m_i} a_A^{(i)} (p - p_c)^A && (1.48)\\ x_i &\equiv u_i u_h^{i/(\mathcal{N}+2)-1}, && (1.49) \end{aligned}$$

$i = 1, \ldots, \mathcal{N}$, which imply $(p_i - p_{ic}) \sim u_h^{2/(\mathcal{N}+2)}$ and $(m_0^2 - m_{0c}^2) \sim u_h^{1/(\mathcal{N}+2)}$. The integers m_i must be determined by requiring that

$$\sum_{A:[A]>m_\ell} a_A^{(\ell)} (p - p_c)^A (m_0^2 - m_{0c}^2)^\ell \tag{1.50}$$

is of order u_h^α with $\alpha > 1$ for $0 \le \ell \le \mathcal{N}$. It follows

$$\frac{2m_\ell + 2 + \ell}{\mathcal{N} + 2} > 1, \tag{1.51}$$

so that

$$m_\ell = \left\lfloor \frac{\mathcal{N}-\ell}{2} \right\rfloor + 1, \tag{1.52}$$

where $\lfloor x \rfloor$ indicates the largest integer that is smaller than or equal to x. In terms of these variables we have therefore in the scaling limit

$$m_0^2 - m_{0c}^2 = u_h^{1/(\mathcal{N}+2)} f(x_1, \ldots, x_{\mathcal{N}}), \tag{1.53}$$

where the scaling function satisfies the mean-field equation of state of a $\phi^{3+\mathcal{N}}$ theory:

$$a_{0,\ldots,0}^{(2+\mathcal{N})} f^{2+\mathcal{N}} + \sum_{j=1}^{\mathcal{N}} x_j f^j - 1 = 0. \tag{1.54}$$

This discussion also clarifies why only the case $\mathcal{N}$ odd is relevant. If $\mathcal{N}$ is even we obtain a ϕ^n theory with n odd, which is unstable, providing another indication for the instability of the corresponding solution.

1.4 The $1/N$ calculation: propagator and effective vertices

In order to develop the standard $1/N$ expansion we insert the fields expansion (1.6) into the action for the auxiliary fields (1.5). Taking a short-hand notation we define a five-component field Ψ_A

$$\Psi = (\hat{\mu}, \hat{\lambda}_1, \hat{\lambda}_2, \hat{\rho}_1, \hat{\rho}_2), \tag{1.55}$$

then $\mathcal{H}$ can be written as

$$\begin{aligned} \mathcal{H} &= \frac{1}{2}\int_{\mathbf{p}} \sum_{A_1 A_2} \Psi_{A_1}(-\mathbf{p}) P^{-1}_{A_1 A_2}(\mathbf{p}) \Psi_{A_2}(\mathbf{p}) \qquad (1.56) \\ &+ \sum_{n=3} \frac{1}{n!}\frac{1}{N^{n/2-1}} \int_{\mathbf{p}_1} \cdots \int_{\mathbf{p}_n} \delta\left(\sum_i \mathbf{p}_i\right) \sum_{A_1,\ldots,A_n} V^{(n)}_{A_1,\ldots,A_n}(\mathbf{p}_1,\ldots,\mathbf{p}_n) \Psi_{A_1}(\mathbf{p}_1)\cdots\Psi_{A_n}(\mathbf{p}_n), \end{aligned}$$

where the indices A_i run from 1 to 5 and we have neglected the constant part $F(m_0^2)$ (1.12). Notice that in (1.56) the linear term disappears due to the gap equations (1.7-1.8-1.9). The propagator can be explicitly written as[8]

$$\mathbf{P^{-1}}(\mathbf{p}) = -\frac{1}{W'^2} \begin{pmatrix} \frac{1}{2}A_{0,0} & -\frac{1}{2}A_{1,0} & -\frac{1}{2}A_{0,1} & 0 & 0 \\ -\frac{1}{2}A_{1,0} & \frac{1}{2}A_{2,0} & \frac{1}{2}A_{1,1} & -\frac{1}{2}\beta W'^2 & 0 \\ -\frac{1}{2}A_{0,1} & \frac{1}{2}A_{1,1} & \frac{1}{2}A_{0,2} & 0 & -\frac{1}{2}\beta W'^2 \\ 0 & -\frac{1}{2}\beta W'^2 & 0 & \beta W'' W'^2 & 0 \\ 0 & 0 & -\frac{1}{2}\beta W'^2 & 0 & \beta W'' W'^2 \end{pmatrix}, \tag{1.57}$$

---

[8] It is useful to write the Fourier transform of $\hat{\lambda}_x$ as $\hat{\lambda}(\mathbf{p}) = e^{-ip_\mu/2}\sum_x e^{-ip\cdot x}\hat{\lambda}_x$. This makes all vertices and propagators real.

where W should always be intended as a function of $\bar{\tau}(m_0^2)$,

$$A_{i,j}(\mathbf{p}, m_0^2) \equiv \int_{\mathbf{q}} \frac{\cos^i q_x \cos^j q_y}{[m_0^2 + \widehat{(q+\frac{p}{2})}^2][m_0^2 + \widehat{(q-\frac{p}{2})}^2]}, \tag{1.58}$$

and $\hat{p}^2 \equiv 4(\sin^2 p_x/2 + \sin^2 p_y/2)$.

For $p \to 0$, by using the algebraic algorithm described in App. A of Ref. [74], it is easy to express the integrals $A_{i,j}(0, m_0^2)$ in terms of the integrals $B_n(m_0^2)$ defined in eq. (1.11) with $n = 1, 2$. Explicitly we have

$$\begin{aligned}
A_{00}(\mathbf{0}, m_0^2) &= B_2, \\
A_{10}(\mathbf{0}, m_0^2) &= A_{01}(\mathbf{0}, m_0^2) = \left(1 + \frac{m_0^2}{4}\right) B_2 - \frac{1}{4} B_1, \\
A_{11}(\mathbf{0}, m_0^2) &= -\frac{1}{8}(4 + m_0^2) B_1 + \frac{1}{8}(8 + 8m_0^2 + m_0^4) B_2, \\
A_{20}(\mathbf{0}, m_0^2) &= A_{02}(\mathbf{0}, m_0^2) = \frac{1}{8} + B_2 - \frac{1}{8}(4 + m_0^2) B_1.
\end{aligned} \tag{1.59}$$

Vertices are analogously computed. It is easy to check that the only nonvanishing contributions for which some A_i is equal to 4 or 5 are

$$V^{(n)}_{4\ldots4}(\mathbf{p}_1, \ldots, \mathbf{p}_n) = V^{(n)}_{5\ldots5}(\mathbf{p}_1, \ldots, \mathbf{p}_n) = -\beta W^{(n)}(\bar{\tau}). \tag{1.60}$$

If all indices satisfy $A_i \leq 3$, then

$$\begin{aligned}
&V^{(n)}_{A_1,\ldots,A_n}(\mathbf{p}_1, \ldots, \mathbf{p}_n) \delta(\sum_i \mathbf{p}_i) = \qquad (1.61) \\
&= \frac{(-1)^{n+1}}{[W'(\bar{\tau})]^n} \left\{ \prod_{i=1}^{n} \left[\int_{\mathbf{q}_i} \delta(\mathbf{q}_{i+1} - \mathbf{q}_i - \mathbf{p}_i) \frac{1}{\hat{q}_i^2 + m_0^2} R_{A_i}(\mathbf{p}_i, \mathbf{q}_i) \right] + \text{permutations} \right\},
\end{aligned}$$

where

$$R_1(\mathbf{p}, \mathbf{q}) = 1, \qquad R_2(\mathbf{p}, \mathbf{q}) = -\cos(q_x + p_x/2), \qquad R_3(\mathbf{p}, \mathbf{q}) = -\cos(q_y + p_y/2). \tag{1.62}$$

The permutations should made the quantity in braces symmetric under any exchange of $(\mathbf{p}_i, A_i)$ [the total number of needed terms is $(n-1)!/2$]. As already discussed in Ref. [55], at the critical point the inverse propagator at zero momentum has a vanishing eigenvalue. Indeed, a straightforward computation gives

$$\det \mathbf{P}^{-1}(\mathbf{0}) \;\; = \;\; K_{0,\text{det}} s_1, \tag{1.63}$$

where $K_{0,\text{det}}$ is given by

$$K_{0,\text{det}} \equiv -\frac{B_1^3}{128 W'^6} \left[4 B_1 W' - (1 - m_0^2 (8 + m_0^2) B_2) W'' \right], \tag{1.64}$$

and

$$s_1 \equiv -\frac{\partial \beta}{\partial m_0^2} = \frac{1}{4 B_1 W'^2} (4 B_1 B_2 W' + B_1^2 W'' - B_2 W''). \tag{1.65}$$

Eq. (1.63) shows that the determinant vanishes at the critical point—hence there is at least one vanishing eigenvalue—since there $\partial\beta/\partial m_0^2 = 0$. The corresponding eigenvector can be written as

$$\mathbf{z} = \left(2\frac{A_{01}(\mathbf{0}, m_0^2)}{A_{00}(\mathbf{0}, m_0^2)}, 1, 1, \frac{1}{2W''}, \frac{1}{2W''}\right) \tag{1.66}$$

computed at the critical point. Indeed,

$$\sum_{B=1}^{5} (P^{-1})_{AB}(\mathbf{0}) z_B = \frac{B_1}{4B_2 W''} s_1(0,1,1,0,0)_A. \tag{1.67}$$

Note that there is always only one zero mode. Indeed, at the critical point, we have from eq. (1.65)

$$W'' = -\frac{4B_1B_2}{B_1^2 - B_2} W', \tag{1.68}$$

so that we can write at criticality

$$K_{0,\mathrm{det}} = -\frac{B_1^4[B_1^2 - (8+m_0^2)m_0^2B_2^2]}{32(B_1^2 - B_2)} \frac{1}{W'^5}. \tag{1.69}$$

We have verified numerically that the prefactor of $1/W'^5$ (that is independent of W so that is the same for all the interactions that one consider) is always finite and negative, so that $K_{0,\mathrm{det}}$ is always nonvanishing. Thus, if we consider (multi)critical interaction, for $p_i = p_{ci}$ the determinant $\det \mathbf{P}^{-1}(\mathbf{0})$ vanishes as $(m_0^2 - m_0^2)^{\mathcal{N}+1}$ that is the scaling of eigenvalue associated with the zero mode, cf. Eq. (1.67). Thus, there can only be a single eigenvector with zero eigenvalue. This means that the effective action for the zero mode will be (see chapter 3) a scalar interaction. However choosing different $\mathcal{N}$ will change drastically the nature of this.

1.5 The failure of $1/N$ expansion

Now we want to show as the appearance of a zero mode (see sec. 1.4) invalidate the standard large-N expansion. Because of the zero mode, it is natural to express the fields in terms of a new basis. For each m_0^2 and p, given the inverse propagator $P^{-1}_{AB}(\mathbf{p})$, there exists an orthogonal matrix $U(\mathbf{p}; m_0^2, p)$ such that $U^T P^{-1} U$ is diagonal. If $v_A(\mathbf{p}; m_0^2, p) \equiv U_{A1}(\mathbf{p}; m_0^2, p)$ is the eigenvector that correspond to the zero eigenvalue for $\mathbf{p} = 0$ at the critical point and $Q_{Aa}(\mathbf{p}; m_0^2, p) \equiv U_{A,a+1}(\mathbf{p}; m_0^2, p)$, $a = 1, \dots 4$ are the other eigenvectors, we define new fields $\Phi_A(\mathbf{p})$ by writing

$$\Psi_A(\mathbf{p}) \equiv \sum_B U_{AB}(\mathbf{p})\Phi_B(\mathbf{p}) = v_A(\mathbf{p})\phi(\mathbf{p}) + \sum_a Q_{Aa}(\mathbf{p})\varphi_a(\mathbf{p}), \tag{1.70}$$

where $\Phi = (\phi, \varphi_a)$. Eq. (1.70) defines the fields Φ_A up to a sign. For definiteness we shall assume $v_A(\mathbf{p})$ to be such that, at the critical point,

$$v_A(\mathbf{0}) = z_A / (\sum_B z_B^2)^{1/2}. \tag{1.71}$$

We do not specify the sign of φ_a since it will not play any role in the following.

The new field ϕ corresponds to the zero mode, while the four fields φ_a are the noncritical (massive) modes. The effective Hamiltonian for the fields Φ has an expansion analogous to that presented in eq. (1.56) for Ψ. The propagator $\hat{P}_{AB}(\mathbf{p})$ of Φ is

$$\hat{P}_{AB}(\mathbf{p}) = \sum_{CD} P_{CD}(\mathbf{p}) U_{CA}(\mathbf{p}) U_{DB}(\mathbf{p}), \tag{1.72}$$

while the effective vertices are related to the previous ones by

$$\hat{V}^{(n)}_{A_i,\ldots,A_n}(\mathbf{p}_1,\ldots,\mathbf{p}_n) = \sum_{B_1,\ldots,B_n} V^{(n)}_{B_1,\ldots,B_n}(\mathbf{p}_1,\ldots,\mathbf{p}_n) U_{B_1A_1}(\mathbf{p}_1;m_0,p)\cdots U_{B_nA_n}(\mathbf{p}_n;m_0,p). \tag{1.73}$$

Note that $\hat{P}_{AB}(\mathbf{p})$ is diagonal by definition, i.e., $\hat{P}_{AB}(\mathbf{p}) = \delta_{AB}\hat{P}_{AA}(\mathbf{p})$. Relation (1.63) implies

$$\hat{P}_{11}(\mathbf{0}) \sim s_1 \sim (p_i - p_{ic}), (m_0^2 - m_{0c}^2)^{\mathcal{N}+2} \tag{1.74}$$

close to the critical point. Now we want to show that due to the singular behavior of $\hat{P}$ (1.74) the standard $1/N$ expansion fails near the critical point. Suppose we want to compute the expectation value of the n-th point function of the critical mode χ_n

$$\chi_n \equiv \int \mathrm{d}\mathbf{x}_2\cdots\mathrm{d}\mathbf{x}_n < \varphi(\mathbf{0})\varphi(\mathbf{x}_2)\cdots\varphi(\mathbf{x}_n) >_{\text{connected}} \tag{1.75}$$

In order to do that one can use the effective action for the zero mode $\mathcal{H}_{\text{eff}}$, in which the massive mode φ_a (1.70) have been integrated out. The study of $\mathcal{H}_{\text{eff}}$ is the main subject of the chapter 3. There we will show that at the critical point $p_i = p_{ci}$ the effective vertices $V^{(n)}$ behave as (in the infra-red limit, for $j = 1\cdots\mathcal{N}+3$)

$$V^{(n)}(\mathbf{p}_i, m_0^2; p_i = p_{ci}) \approx l_n(m_0^2 - m_{0c}^2)^{k-n} + \sum_i \alpha_i^{(n)}\mathbf{p}_i^2 + \cdots \tag{1.76}$$

where $k = \mathcal{N}+3$ if one considers the zero mode defined in (1.70) or $k = \mathcal{N}+4$ if one translate the zero mode (1.70) by a constant factor so that $l_{\mathcal{N}+2} = 0$.[9] If we consider then a general ℓ-loops graph $D_{n,\ell}$ entering into the computation of χ_n [eq. (1.75)] with N_j $j-$legs vertices ($j = 3,\cdots,\mathcal{N}+1$) and N_{int} internal line, neglecting ultraviolet divergences, by using eq. (1.74) and eq. (1.76) the following scaling relation holds[10]

$$\begin{aligned} D_{n,\ell} &\sim (m_0^2 - m_{0c}^2)^{-2n-2N_{\text{int}}+d\ell+\sum_{j=1}^{\mathcal{N}+1}(k-N_j)} \\ &= (m_0^2 - m_{0c}^2)^{-2n+k\mathcal{N}-1-3N_{\text{int}}+(d+1)\ell}, \end{aligned} \tag{1.77}$$

d being the dimension of the Euclidean space. In (1.77) we have used the topological relation

$$N_{\text{int}} = \ell + \sum_j N_j - 1 \tag{1.78}$$

---

[9] However in the considerations reported in this section we can take k undefined.

[10] In eq. (1.77)we neglect contributions coming from $\mathcal{N}+2$-legs vertex, however the general claim remains unchanged.

and we have neglected possible logarithmic corrections. The $1/N$ expansion is a loop expansion around the saddle point solution. Consider for instance the $d = 2$ case, from (1.77-1.78)

$$D_{n,\ell} \sim (m_0^2 - m_{0c}^2)^{-2n+k\mathcal{N}-1-3(\sum_j N_j-1)}. \tag{1.79}$$

Looking at eq. (1.79) it is clear how if one considers higher order in the $1/N$ expansion new more severe algebraic infrared divergences appear while in principle one expect only logarithmic contributions. This is the clear sign of the breakdown of the standard $1/N$ expansion. In order to solve the problem one has to consider a non-perturbative approach based on the study of weakly coupled scalar theories which are studied in chapter 2 and will be applied to the effective zero mode interaction $\mathcal{H}_{\text{eff}}$ in chapter 3. One can guess that divergences appearing in (1.79) cancel when explicitly Feynman diagrams are evaluated. One can convince that this is not the case considering for instance χ_2 at one loop. There are three different diagrams entering into the computation, one with a four-legs vertex ($\sim m^{-4}\log m^2$) and two built with a couple of three-legs vertices ($\sim m^{-6}$, $\sim m^{-4}$) so that there is no chance for any cancellation (we have defined $m \equiv m_0^2 - m_{0c}^2$). On the other hand this $1/N$ contributions cannot match with $1/N$ corrections of the $N = \infty$ result $\chi_2 \sim 1/(m_0^2 - m_{0c}^2)^2$

$$\begin{aligned}\chi_2 &\sim \frac{1}{\left(m_0^2 - m_{0c}^2 + \frac{a}{N}\right)^{2+b/N}} \\ &= \frac{1}{(m_0^2 - m_{0c}^2)^2}\left(1 - \frac{b}{2N}\log(m_0^2 - m_{0c}^2)^2 - \frac{2a}{N}\frac{1}{(m_0^2 - m_{0c}^2)}\right).\end{aligned} \tag{1.80}$$

In the previous equation (1.80) we generate (with respect to the leading order) only Δm^{-1} and $\log \Delta m$ divergences, while in principle, using the scaling arguments reported above, one would match m^{-4} and m^{-2} divergences.

The problem of Infra Red Divergences is well known in large N expansion [49] and it is usually addressed as a failure of $1/N$ expansion. They are not peculiar of the Heisenberg models introduced above (1.2) but are also present in other models like Gross-Neveu and Yukawa theory at finite temperature [12] [49] [96]. It is important to stress that for the previous models at zero temperature $1/N$ expansion works well [49] [24] [13]. In this case, concerning universal coefficients for instance, one finds the $N = \infty$ value and then standard perturbation theory is able to get $1/N$ corrections (e.g. [13]). This works exactly in the same way of $1/N$ expansion of the vector $\lambda\Phi^4$ model: one finds for instance[11] for $N = \infty$ $\nu = 1/(d-2)$ (e.g. [17] [18]) and fluctuations around the saddle point solution can be resummed giving a $1/N$ correction [19] [20] ($\epsilon \equiv 4 - d$)

$$\begin{aligned}\nu &= \frac{1}{d-2} - \frac{2(3-\epsilon)}{N(2-\epsilon)(4-\epsilon)}X_1 + O\left(\frac{1}{N^2}\right) \\ X_1 &= \frac{4\sin(\pi\epsilon/2)\Gamma(2-\epsilon)}{\pi\Gamma(1-\epsilon/2)\Gamma(2-\epsilon/2)}\end{aligned}$$

However when the temperature is finite the Infra Red Divergences become more severe so that the perturbative series cannot be useful [14] [15]. This can be understood also looking at the standard perturbation theory in which nonanalytic terms appear if the temperature is not zero [14]. For a discussion of the finite temperature see also sec. 10 of [16]. For the case we have investigated we suggest that one cannot correct the $N = \infty$ critical behavior because critical exponents are discontinuous for $N = \infty$. However one observes a crossover between the two different critical region that will be illustrated in the next chapter.

---

[11] With ν commonly one refers to the critical exponent related to the critical behaviour of the order parameter M near the critical point $M \sim (-t)^\nu$, t being the reduced temperature $t = (T - T_c)/T_c$.

Chapter 2

Crossover in critical phenomena

In the past decades a huge amount of work (experimental, theoretical and numerical) has been devoted to the study of the nature of critical points in physical system characterised by a large number of elementary components (since now "spins"). In particular –from the theoretical point of view– the possibility to apply field theoretic methods (e.g. [24], [25]) to implement basic physical assumptions like *scaling invariance* of the *universal* quantities at the critical point (e.g. [23]), has allowed to obtain accurate predictions for these observables in the scaling region $\tau \ll 1$ [$\tau \equiv (T-T_c)/T_c$, T being the temperature].[1] Outside the scaling region[2] (physically dominated by correlations between the degrees of freedom of the system) one expects to recover the physical picture given by mean-field approximations which is supposed to be dominated by the short range interaction of the spins. Several works [27] [28] [29] [30] [31] [32] [33] [34] [35] [36] [37] have investigated the nature of the crossover between the mean field region and the non trivial critical region (for instance Ising in simple fluid). Using the language of Wilson renormalization group theory, the main effort of the theoretical works is to resum the infinity set of irrelevant operators that becomes important as soon as one leaves the scaling region (for instance ϕ^6, ϕ^8, ... in the Ising theory), tuning a minimal set of adjustable non universal parameters [27] [28]. This description is valid because the introduction of the irrelevant operators leads simply to a multiplicative renormalization of this set of free parameters. Accordance with experiments is under investigations [38] [39] [40] [41] [42]. For simple liquid it seems to work, however for complex fluid the field theoretic methods is questionable.[3]

In this chapter we will investigate the *universal* crossover behavior that is observed for a family of scalar models in the weakly coupled limit. We do that because similar interactions will be obtained considering the effective interactions for the zero mode in large-N expansions affected by infrared singularities that are the main topic of this work. In order to understand the nature of the problem, let us consider for instance the following interaction

---

[1] For a review on the argument with a complete list of theoretical and experimental references see [26].

[2] Instead of "scaling region" we could use also "critical region".

[3] In condensed matter system (contrarily to field theory) the cut-off Λ^{-1} has a physical origin related to some size of the basic constituents. In simple fluid we have $\Lambda \approx 1$ and one can reach the condition $\xi/\Lambda^{-1} \gg 1$ that is necessary in order to apply RG. In complex fluid Λ^{-1} is not simply related to inter-molecular distance (think for instance to a polymer solution) and the previous condition could not be satisfied [42]. Maybe the understanding of these problems (for which techniques presented in this work could be useful) deserves future investigations.

$$\mathcal{H} \;=\; \frac{1}{2}(\partial\phi)^2 + \frac{r}{2}\phi^2 + \frac{u}{4!}\phi^4. \tag{2.1}$$

Tuning both $u \to 0$ or $t \equiv r - r_c \to 0$ in (2.1), the two universal behaviour (Ising for $r = r_c$, Mean Field for $u = 0$) enter into competition; keeping a proper scaling variable $x \equiv tu^{-\alpha}$ fixed one expect to compute the observables (in particular critical exponents) as functions of x

$$\langle \mathcal{O} \rangle_{\mathcal{H}} \sim f_{\mathcal{O}}(tu^{-\alpha})$$

and to recover Ising (Mean Field) behavior by taking $x \to 0$ ($x \to \infty$). The previous statements have been demonstrated in a series of theoretical works [29] [30]. More interesting it has been shown that the crossover functions $f_{\mathcal{O}}$ are independent of the regularization used (i.e. they are universal). This means that in principle one can compute this functions using e.g. field theory [29], spin system with medium range interaction [32] [35] [36] [37], or polymer systems [35].

In this chapter we consider more general interactions than (2.1) or that considered in [29] [30]. The reason is that in our large-N computation we will obtain an effective action for the zero mode without $\mathbb{Z}_2$ symmetry [$\phi \to -\phi$ in eq. (2.1)], so that we need to include also odd-legs vertices and higher than four-legs vertices. Our goals will be to show that including proper counterterms, in the limit in which our crossover is defined, the crossover functions remain unchanged with respect to the symmetric case. In some sense we recover algebraically the $\mathbb{Z}_2$ symmetry that is then dynamically broken.[4] This will permit us to investigate the nature of the Ising Mean-Field crossover in $O(N)$ models with a critical zero mode (chapter 3). The presentation given follows [56]. In section 2.2 we will also consider the case in which the four- and five-legs vertices are tuned to zero at the critical point so that one needs to generalize (2.1) including also a ϕ^6 operator. This will permit us to describe (see chapter 4) the crossover in $O(N)$ models with multicritical zero mode which effective theory will be described by an interaction similar to that presented in sec. 2.2. We stress that the basic point that permits us to apply the results presented in this chapter to our large-N models, is that the appearance of a zero mode [i.e. $r \to 0$ in eq. (2.2)] is accompanied by the relations $V^{(3)}(\mathbf{0},\mathbf{0},\mathbf{0}) = 0$ (and similar relations, involving higher order vertices, in the case of multicritical zero mode).

2.1 Critical crossover limit

We wish now to discuss the critical behavior of the following generic Hamiltonian

$$\begin{aligned}\mathcal{H}_{\text{eff}} \;=\;& H\varphi(\mathbf{0}) + \frac{1}{2}\int_{\mathbf{p}}[K(\mathbf{p}) + r]\varphi(\mathbf{p})\varphi(-\mathbf{p}) \\ &+ \frac{\sqrt{u}}{3!}\int_{\mathbf{p}}\int_{\mathbf{q}} V^{(3)}(\mathbf{p},\mathbf{q},-\mathbf{p}-\mathbf{q})\varphi(\mathbf{p})\varphi(\mathbf{q})\varphi(-\mathbf{p}-\mathbf{q}) \\ &+ \frac{u}{4!}\int_{\mathbf{p}}\int_{\mathbf{q}}\int_{\mathbf{s}} V^{(4)}(\mathbf{p},\mathbf{q},\mathbf{s},-\mathbf{p}-\mathbf{q}-\mathbf{s})\varphi(\mathbf{p})\varphi(\mathbf{q})\varphi(\mathbf{s})\varphi(-\mathbf{p}-\mathbf{q}-\mathbf{s})\end{aligned} \tag{2.2}$$

---

[4] This is similar to what happen when one wants to investigate chiral symmetry using Wilson fermion.

in some particular range of parameters that we will specify in the following. We use a square lattice to regularize (2.2), however most of the considerations reported in the following easily apply also to sharp-cut off regularization (used in chiral models) simply replacing the integration over the first Brillouin zone with an integration over $\mathbf{p} < \Lambda$. On the other hand the magnetic and thermal regularization $h_c(u)$ $r_c(u)$ depend of the regularization chosen. One is free to impose both $V^{(3)}(\mathbf{0},\mathbf{0},\mathbf{0}) = 0$ and $K(\mathbf{p}) \approx \mathbf{p}^2$ normalizing and translating φ by a constant factor $\varphi(\mathbf{p}) \to \alpha\varphi(\mathbf{p}) + k\delta(\mathbf{p})$ while $V^{(4)}(\mathbf{0},\mathbf{0},\mathbf{0},\mathbf{0}) = 1$ can be obtained normalizing u. In the models to which we have applied our formalism, H and r are functions of the two tunable parameter (for instance p and T in Heisenberg models introduced in chapter 1, or M and T in Yukawa models chap. 5), while the coupling parameter u goes to zero like $1/N$ in the spherical limit. Simple considerations show that for $u \to 0$ Hamiltonian (2.2) exhibits a nontrivial limit only if both H and r go to zero.

Let us first review the case $V^{(3)}(\mathbf{0},\mathbf{0},\mathbf{0}) = 0$. There is an interesting critical limit, the so-called Critical Crossover Limit (CCL) [27] [28] [29]. Indeed, one can show that, by properly defining a function $r_c(u)$, in the limit $u \to 0$, $t \equiv r - r_c(u) \to 0$, and $H \to 0$ at fixed H/u and t/u, the n-point susceptibility χ_n, i.e. the zero-momentum n-point connected correlation function

$$\chi_n = \langle \varphi^n(\mathbf{0}) \rangle_{\text{connected}}$$

has the following scaling form

$$\chi_n \approx u t^{-n} f_n^{\text{symm}}(t/u, H/u). \tag{2.3}$$

The scaling function $f_n^{\text{symm}}(x,y)$ is universal, i.e. it does not depend on the explicit form of $K(\mathbf{p})$ and of $V^{(4)}(\mathbf{p},\mathbf{q},\mathbf{r},\mathbf{s})$ as long as the normalization conditions fixed above are satisfied. The definition of $r_c(u)$ has been discussed in Ref. [29] for the continuum model and in Ref. [32] for the more complex case of medium-range models. Developing the standard expansion in u one can compute $r_c(u)$ which is obtained requiring that χ_2 scales according to eq. (2.3) in the critical crossover limit. If $r_c(u) = r_1 u + O(u^2)$, then at one loop we have

$$\chi_2 = \frac{1}{t} - \frac{u}{t^2}\left[r_1 + \frac{1}{2}\int_{\mathbf{p}} \frac{V^{(4)}(\mathbf{0},\mathbf{0},\mathbf{p},-\mathbf{p})}{K(\mathbf{p}) + t}\right] + O(u^2). \tag{2.4}$$

For $t \to 0$

$$\int_{\mathbf{p}} \frac{V^{(4)}(\mathbf{0},\mathbf{0},\mathbf{p},-\mathbf{p})}{K(\mathbf{p}) + t} \approx \int_{\mathbf{p}} \frac{1}{\hat{p}^2 + t} + \text{constant} = -\frac{1}{4\pi}\ln t + \text{constant}, \tag{2.5}$$

where $\hat{p}^2 = 4\sin^2(p_1/2) + 4\sin^2(p_2/2)$. Thus, we obtain

$$\chi_2 = \frac{1}{t} - \frac{u}{t^2}\left[r_1 - \frac{1}{8\pi}\ln u - \frac{1}{8\pi}\ln\frac{t}{u} + \text{constant}\right] + O(u^2). \tag{2.6}$$

Therefore, if we define

$$r_c(u) = \frac{u}{8\pi}\ln u, \tag{2.7}$$

the susceptibility χ_2 scales according to eq. (2.3). Actually one can show that (2.7) is sufficient to regularize the theory to all order in the perturbation theory. Indeed in the continuum two-dimensional theory there is only one primitively divergent graph, the one-loop tadpole, and therefore only a one-loop mass counterterm is needed to make the theory finite. However the exact knowledge (to all order) of $r_c(u)$ is a non-perturbative problem and leaves some ambiguity in the definition. This will be discussed in sec. 2.1.4.

In this work we will consider the more general case in which also the three-leg vertex is present in (2.2). We will show that, if one properly defines functions $r_c(u)$ and $h_c(u)$, then in the limit $u \to 0$, $t \equiv r - r_c(u) \to 0$, and $h \equiv H - h_c(u) \to 0$ at fixed h/u and t/u, the n-point susceptibility χ_n has the scaling form (2.3) with h replacing H and with the same scaling functions $f_n^{\rm symm}$ of the symmetric case. The previous statement easily follows from the condition $V^{(3)}(\mathbf{0},\mathbf{0},\mathbf{0}) = 0$. Indeed considering the continuum limit of the action (2.2)

$$\mathcal{H}_{\rm eff} = \int \mathrm{d}^2x \frac{1}{2}\varphi(x)(\Box + r)\varphi(x) + \frac{v_3\sqrt{u}}{3!}\varphi(x)^2\Box\varphi(x) + \frac{u}{4!}\varphi(x)^4 \tag{2.8}$$

and making the change of variable $x = yu^{-1/2}$, defining $\phi(x) = \varphi(x/\sqrt{u})$, we obtain

$$\mathcal{H}_{\rm eff} \approx \int \mathrm{d}^2y \frac{1}{2}\phi(y)(\Box + r/u)\phi(y) + \frac{v_3\sqrt{u}}{3!}\phi(y)^2\Box\phi(y) + \frac{1}{4!}\phi(y)^4 \,. \tag{2.9}$$

In the previous equation (2.9) it is clear how in the critical crossover limit ($u \to 0$) the three legs vertex can be neglected, so that the critical crossover coincide with that of the symmetric theory (2.3) . However in the previous naive discussion we do not have taken into account divergences that come from this contribution. This divergences must be carefully taken into account by proper counter-terms that define $h_c(u)$ introduced above.

We will first prove this result at two loops and then we will give a general argument that applies to all perturbative orders. Notice that it is enough to consider the case $h = 0$. Indeed, if eq. (2.3) is valid for $h = 0$ and any n, then

$$\begin{aligned}\chi_n(h) &= \sum_{m=0} \frac{1}{m!}\chi_{n+m}(h=0)h^m \approx \sum_{m=0}\frac{1}{m!}ut^{-n-m}f^{\rm symm}_{n+m}(t/u,0)h^m = \\ &= ut^{-n}\sum_{m=0}\frac{1}{m!}f^{\rm symm}_{n+m}(t/u,0)(t/u)^{-m}(h/u)^m. \end{aligned} \tag{2.10}$$

which proves eq. (2.3) for all values of h.

2.1.1 Explicit two-loop perturbative calculation

At tree level, all contributions to χ_n that contain three-leg vertices vanish because $V^{(3)}(\mathbf{0},\mathbf{0},\mathbf{0}) = 0$. Therefore, χ_n is identical to χ_n in the $\mathbb{Z}_2$-symmetric φ^4 theory; in particular $\chi_{2n+1} = 0$. At one-loop order, graphs contributing to χ_n are formed by a single loop made of a three-leg vertices and of b four-leg vertices, with $a + 2b = n$. Each of them contributes a term of the form

$$\frac{u^{n/2}}{t^n}\int_{\mathbf{p}} \frac{V_3^a(\mathbf{p})V_4^b(\mathbf{p})}{[K(\mathbf{p}) + t]^{a+b}}, \tag{2.11}$$

where $V_3(\mathbf{p}) \equiv V^{(3)}(\mathbf{0},\mathbf{p},-\mathbf{p})$ and $V_4(\mathbf{p}) \equiv V^{(4)}(\mathbf{0},\mathbf{0},\mathbf{p},-\mathbf{p})$. The leading contribution for $t \to 0$ is obtained by replacing each quantity with its small-$\mathbf{p}$ behavior, i.e. $V_4(\mathbf{p}) \approx 1$,

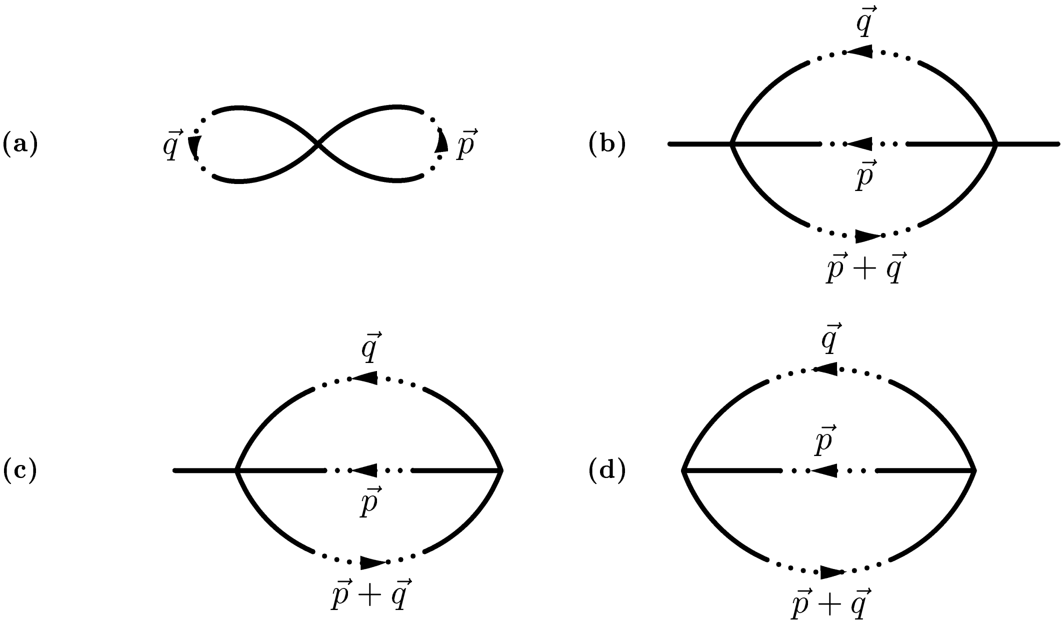

Figure 2.1: The four topologies appearing at two loops. Dots indicate parts of the graphs with additional external legs.

$V_3(\mathbf{p}) \sim \hat{p}^2$, and $K(\mathbf{p}) \approx \hat{p}^2$, with $\hat{p}^2 = 4\sin^2(p_1/2) + 4\sin^2(p_2/2)$. Then, we obtain a contribution proportional to

$$\frac{u^{n/2}}{t^n} \int_{\mathbf{p}} \frac{(\hat{p}^2)^a}{(\hat{p}^2+t)^{a+b}}. \tag{2.12}$$

Now, for $t \longrightarrow 0$ we have

$$\int_{\mathbf{p}} \frac{(\hat{p}^2)^a}{(\hat{p}^2+t)^{a+b}} \sim \begin{cases} 1 & \text{for } b=0 \\ \ln t & \text{for } b=1 \\ t^{1-b} & \text{for } b \geq 2. \end{cases} \tag{2.13}$$

Therefore, for $t \longrightarrow 0$, $u \longrightarrow 0$ at fixed t/u, we have

$$t^n \chi_n / u \sim \begin{cases} u^{n/2-1} & \text{for } b=0 \\ u^{n/2-1}\ln t & \text{for } b=1 \\ u^{n/2-b} = u^{a/2} & \text{for } b \geq 2. \end{cases} \tag{2.14}$$

Thus, all contributions vanish except those with: (i) $n=1$, $a=1$, $b=0$; (ii) $n=2$, $a=2$, $b=0$; (iii) n even, $b=n/2$, $a=0$. Contributions (iii) are those that appear in the standard theory without φ^3 interaction. Let us now show that contributions (i) and (ii) can be eliminated by redefining $r_c(u)$ and $h_c(u)$. Consider first χ_1. At one loop we have

$$\frac{t}{u}\chi_1 = -\frac{h_c(u)}{u} - \frac{1}{2\sqrt{u}} \int_{\mathbf{p}} \frac{V_3(\mathbf{p})}{K(\mathbf{p})+t} + O(\sqrt{u}). \tag{2.15}$$

For $t \to 0$ we have

$$\int_{\mathbf{p}} \frac{V_3(\mathbf{p})}{K(\mathbf{p})+t} = \int_{\mathbf{p}} \frac{V_3(\mathbf{p})}{K(\mathbf{p})} + O(t \ln t). \tag{2.16}$$

Thus, if we define

$$h_c(u) = -\frac{1}{2}\sqrt{u} \int_{\mathbf{p}} \frac{V_3(\mathbf{p})}{K(\mathbf{p})}, \tag{2.17}$$

then $t\chi_1/u \sim O(t \ln t/\sqrt{u}, \sqrt{u}) \to 0$ in the critical crossover limit.

Now, let us consider the two-point function. At one loop we have

$$\frac{t^2}{u}\chi_2 \approx \frac{t}{u} - \frac{r_c(u)}{u} - \frac{1}{2}\int_{\mathbf{p}} \left[\frac{V_4(\mathbf{p})}{K(\mathbf{p})+t} - \frac{V_3(\mathbf{p})^2}{(K(\mathbf{p})+t)^2}\right]. \tag{2.18}$$

The first one-loop term is the contribution of the tadpole that has to be considered in the pure φ^4 theory and which requires an appropriate subtraction to scale correctly, cf. eq. (2.7). The second one is due to the three-leg vertex and is finite for $t \to 0$. Therefore, if we define

$$r_c(u) = r_c^{\text{symm}}(u) + \frac{u}{2}\int_{\mathbf{p}} \frac{V_3(\mathbf{p})^2}{K(\mathbf{p})^2}, \tag{2.19}$$

where $r_c^{\text{symm}}(u)$ is given by eq. (2.7), we cancel all contributions of the φ^3 vertex.

Now, let us repeat the same discussion at two loops, in order to understand the general mechanism. There are four different topologies that must be considered, see Fig. 2.1.

Topology (a).

A contribution to χ_n is proportional to

$$\frac{u^{n/2+1}}{t^n}\int_{\mathbf{p}}\int_{\mathbf{q}} V^{(4)}(\mathbf{p},-\mathbf{p},\mathbf{q},-\mathbf{q}) \frac{V_4(\mathbf{p})^a V_4(\mathbf{q})^b V_3(\mathbf{p})^c V_3(\mathbf{q})^d}{(K(\mathbf{p})+t)^{a+c+1}(K(\mathbf{q})+t)^{b+d+1}}, \tag{2.20}$$

where $2a+2b+c+d=n$. The leading contribution for $t \to 0$ is obtained by setting $V^{(4)}(\mathbf{p},-\mathbf{p},\mathbf{q},-\mathbf{q}) \approx V^{(4)}(\mathbf{0},\mathbf{0},\mathbf{0},\mathbf{0}) = 1$. Then, the integral factorizes and we can use eq. (2.13). Ignoring logarithmic terms, we see that the corresponding contribution to $t^n\chi_n/u$ scales as

$$\left(\frac{u}{t}\right)^{n/2} t^{n/2-a-b} = \left(\frac{u}{t}\right)^{n/2} t^{(c+d)/2}. \tag{2.21}$$

Thus, a non-vanishing contribution is obtained only for $c+d=0$. Three-leg vertices can be neglected in the critical crossover limit.

Topology (b).

A contribution to χ_n has the form

$$\frac{u^{n/2+1}}{t^n}\int_{\mathbf{p}}\int_{\mathbf{q}} [V^{(4)}(\mathbf{0},\mathbf{p},\mathbf{q},-\mathbf{p}-\mathbf{q})]^2 \times \frac{V_4(\mathbf{p})^a V_4(\mathbf{q})^b V_4(\mathbf{p}+\mathbf{q})^c V_3(\mathbf{p})^d V_3(\mathbf{q})^e V_3(\mathbf{p}+\mathbf{q})^f}{(K(\mathbf{p})+t)^{a+d+1}(K(\mathbf{q})+t)^{b+e+1}(K(\mathbf{p}+\mathbf{q})+t)^{c+f+1}}, \tag{2.22}$$

where $2(a+b+c)+d+e+f=n-2$. The leading infrared contribution is obtained by approximating all expressions with their small-p behavior. Therefore, we can write for $t \to 0$

$$\frac{u^{n/2+1}}{t^n}\int_{\mathbf{p}}\int_{\mathbf{q}} \frac{(\hat{p}^2)^d(\hat{q}^2)^e(\widehat{p+q}^2)^f}{(\hat{p}^2+t)^{a+d+1}(\hat{q}^2+t)^{b+e+1}(\widehat{p+q}^2+t)^{c+f+1}}. \tag{2.23}$$

Integrals of this type can be easily evaluated. By writing $\hat{p}^2 = (\hat{p}^2 + t) - t$ in the numerator, we obtain integrals

$$I_{mnr} \equiv \int_{\mathbf{p}} \int_{\mathbf{q}} \frac{1}{(\hat{p}^2 + t)^m (\hat{q}^2 + t)^n (\widehat{p+q}^2 + t)^r}, \tag{2.24}$$

with $m > 0$, $n > 0$, $r > 0$. Then, we can rescale $\mathbf{p} \to t^{1/2}\mathbf{p}$, $\mathbf{q} \to t^{1/2}\mathbf{q}$ and extend the integration over all $\mathbb{R}^2$. This is possible since the corresponding continuum integral is finite. As a consequence the integral scales as $t^{2-m-n-r}$ and the corresponding contribution to $t^n \chi_n / u$ scales as

$$\left(\frac{u}{t}\right)^{n/2} t^{n/2-a-b-c-1} = \left(\frac{u}{t}\right)^{n/2} t^{(d+e+f)/2}. \tag{2.25}$$

Thus, a non vanishing contribution is obtained only for $d + e + f = 0$. Three-leg vertices can be neglected in the critical crossover limit.

Topology (c).

A contribution to χ_n has the form

$$\frac{u^{n/2+1}}{t^n} \int_{\mathbf{p}} \int_{\mathbf{q}} V^{(4)}(\mathbf{0}, \mathbf{p}, \mathbf{q}, -\mathbf{p} - \mathbf{q}) V^{(3)}(\mathbf{p}, \mathbf{q}, -\mathbf{p} - \mathbf{q}) \\ \times \frac{V_4(\mathbf{p})^a V_4(\mathbf{q})^b V_4(\mathbf{p} + \mathbf{q})^c V_3(\mathbf{p})^d V_3(\mathbf{q})^e V_3(\mathbf{p} + \mathbf{q})^f}{(K(\mathbf{p}) + t)^{a+d+1} (K(\mathbf{q}) + t)^{b+e+1} (K(\mathbf{p} + \mathbf{q}) + t)^{c+f+1}}, \tag{2.26}$$

where $2(a+b+c)+d+e+f = n-1$ and we assume without loss of generality $a \geq b \geq c$. We can now repeat the analysis performed for topology (b). We replace each quantity with its small-momentum behavior. In particular, we can replace $V^{(3)}(\mathbf{p}, \mathbf{q}, -\mathbf{p} - \mathbf{q})$ with $(\hat{p}^2 + \hat{q}^2 + \widehat{p+q}^2)$. Then, we rewrite each contribution in terms of the integrals I_{mnr}, cf. eq. (2.24). However, in this case it is possible that one (and only one) of the indices vanishes. If this the case, I_{mnr} factorizes and we can use the one-loop result (2.13). A careful analysis shows that in all cases the integral scales as t^{-a-b-c} for $t \to 0$ except when $b = c = 0$. In this case, if $a \neq 0$ the integral scales as $t^{-a} \ln t$, while for $a = 0$ it scales as $\log^2 t$. Thus, ignoring logarithms all integrals scale as t^{-a-b-c}. Therefore, the corresponding contribution to $t^n \chi_n / u$ scales as

$$\left(\frac{u}{t}\right)^{n/2} t^{n/2-a-b-c} = \left(\frac{u}{t}\right)^{n/2} t^{(d+e+f+1)/2}. \tag{2.27}$$

These contributions always vanish.

Topology (d).

A contribution to χ_n has the form

$$\frac{u^{n/2+1}}{t^n} \int_{\mathbf{p}} \int_{\mathbf{q}} [V^{(3)}(\mathbf{p}, \mathbf{q}, -\mathbf{p} - \mathbf{q})]^2 \frac{V_4(\mathbf{p})^a V_4(\mathbf{q})^b V_4(\mathbf{p} + \mathbf{q})^c V_3(\mathbf{p})^d V_3(\mathbf{q})^e V_3(\mathbf{p} + \mathbf{q})^f}{(K(\mathbf{p}) + t)^{a+d+1} (K(\mathbf{q}) + t)^{b+e+1} (K(\mathbf{p} + \mathbf{q}) + t)^{c+f+1}}, \tag{2.28}$$

where $2(a + b + c) + d + e + f = n$, $a \geq b \geq c$. We repeat the analysis done for topology (b) and (c). We find that the integral scales as

$$t^{-a-b-c+1} \begin{cases} \ln t / t & \text{for } a = b = c = 0; \\ 1/t & \text{for } b = c = 0,\ a \geq 1; \\ \ln t & \text{for } c = 0,\ b = 1,\ a \geq 1; \\ \text{constant} & \text{otherwise.} \end{cases} \tag{2.29}$$

Thus, if $b \neq 0$ and $c \neq 0$, ignoring logarithms, the contribution to $t^n \chi_n/u$ scales as

$$\left(\frac{u}{t}\right)^{n/2} t^{n/2-a-b-c+1} = \left(\frac{u}{t}\right)^{n/2} t^{(d+e+f)/2+1} \tag{2.30}$$

These contributions therefore always vanish in the critical crossover limit. If, however, $b = c = 0$, then

$$\left(\frac{u}{t}\right)^{n/2} t^{n/2-a-b-c} = \left(\frac{u}{t}\right)^{n/2} t^{(d+e+f)/2} \tag{2.31}$$

and thus one may have a finite (or a logarithmically divergent if $a = 0$) contribution for $d = e = f = 0$. Let us now focus on this last case in which $a = n/2 > 0$ with n even. Let us now show that these contributions are cancelled by the one-loop counterterm due to $r_c(u)$. Indeed, at two loops we obtain a contribution to χ_n of the form

$$r_c(u) \frac{u^{n/2}}{t^n} \int_{\mathbf{p}} \frac{V_3^b(\mathbf{p}) V_4^a(\mathbf{p})}{[K(\mathbf{p}) + t]^{a+b+1}} = r_c(u) \frac{u^{n/2}}{t^n} \begin{cases} \ln t & \text{for } b = 0 \\ t^{-a} & \text{for } b \geq 1 \end{cases} \tag{2.32}$$

where $2a + b = n$. Thus, contributions to $t^n \chi_n/u$ scale as $t^{n/2-a} = t^{b/2}$ and thus vanish unless $b = 0$. Thus, for each even n there are two contributions that should be considered: one with topology (d) and one associated with the counterterm $r_c(u)$. Taking properly into account the combinatorial factors, their sum is given by (of course, we only consider here the contribution to $r_c(u)$ due to the three-leg vertices)

$$\frac{u^{n/2+1}}{t^n} \int_{\mathbf{p}} \frac{1}{(K(\mathbf{p}) + t)^{a+1}} \int_{\mathbf{q}} \left[\frac{V^{(3)}(\mathbf{p}, \mathbf{q}, -\mathbf{p} - \mathbf{q})^2}{(K(\mathbf{q}) + t)(K(\mathbf{p} + \mathbf{q}) + t)} - \frac{V^{(3)}(0, \mathbf{q}, -\mathbf{q})^2}{(K(\mathbf{q}) + t)^2} \right] \tag{2.33}$$

For $a \geq 1$, the subtracted term improves the infrared behavior, and indeed the integral scales as $t^{-a+1} \ln t$ and is therefore irrelevant in the critical crossover limit.

2.1.2 Higher powers of the fields

It is interesting to consider also Hamiltonians with higher powers of the field φ. The standard scaling argument indicates that these additional terms are irrelevant for the critical behavior, but in principle they can contribute to the renormalization constants like h_c and r_c. For this purpose let us suppose that the Hamiltonian contains also terms of the form

$$\Delta \mathcal{H}_{\text{eff}} = \sum_{k>4} \frac{u^{(k-2)/2}}{k!} \int_{\mathbf{p}_1} \cdots \int_{\mathbf{p}_k} \delta(\mathbf{p}_1 + \cdots \mathbf{p}_k)\, V^{(k)}(\mathbf{p}_1, \cdots, \mathbf{p}_k) \varphi(\mathbf{p}_1) \cdots \varphi(\mathbf{p}_k). \tag{2.34}$$

Note the particular dependence on the coupling constant u, which is motivated by the large-N calculation and is crucial in the argument reported below.

Let us consider the contributions of these additional terms. At tree level we have an additional contribution to χ_n given by

$$\Delta \chi_n = \frac{u^{(n-2)/2}}{t^n} V^{(n)}(\mathbf{0}, \ldots, \mathbf{0}) \tag{2.35}$$

Thus, $t^n \Delta\chi_n/u \sim u^{(k-4)/2}$, that vanishes as $u \to 0$ for $k > 4$. At one-loop order there are additional contributions of the form

$$\frac{u^{n/2}}{t^n} \int_{\mathbf{p}} (K(\mathbf{p}) + t)^{-\sum a_i} V_3(\mathbf{p})^{a_3} \cdots V_{n+2}(\mathbf{p})^{a_{n+2}}, \tag{2.36}$$

where $V_k(\mathbf{p}) = V^{(k)}(-\mathbf{p}, \mathbf{p}, \mathbf{0}, \ldots, \mathbf{0})$ and $\sum_k (k-2)a_k = n$. Proceeding as in the previous section, using eq. (2.13), and noting that $\sum_{k>4} a_k > 0$ by hypothesis, we obtain

$$t^n \Delta\chi_n/u \sim u^{n/2-1} t^{1-\sum_{k>3} a_k} \sim u^{\frac{1}{2}a_3 + \frac{1}{2}\sum_{k\geq 5}(k-4)a_k}. \tag{2.37}$$

Here, possible logarithmic terms have been neglected. Then, since some a_k with $k \geq 5$ is non-vanishing by hypothesis, we find that this correction vanishes in the crossover limit. Therefore, no contribution survives at one loop. The same is expected at any perturbative order.

2.1.3 The general argument

The discussion reported above shows that at two loops one can define a critical crossover limit with crossover functions that are identical to those of the symmetric theory. This is expected to be a general result since formally the added interaction is irrelevant. This result can be understood diagrammatically.

Consider the continuum theory with Hamiltonian

$$\mathcal{H} = \int \mathrm{d}^2 x \, \frac{1}{2} \sum_\mu (\partial_\mu \phi(x))^2 + \frac{t}{2}\phi(x)^2 + \frac{\sqrt{u}}{3!}\phi(x)^2 \Box \phi(x) + \frac{u}{4!}\phi(x)^4. \tag{2.38}$$

Given an l-loop diagram contributing to the zero-momentum n-point irreducible correlation function, we can compute the superficial degree of divergence of Feynman integrals $D \sim \Lambda^\delta$ as

$$D \sim \Lambda^{d\ell + 2N_3 - 2N_i} \tag{2.39}$$

obtained rescaling each momenta with Λ. In (2.39) ℓ is the number of loop of the diagram, N_3 (N_4) is the number of the three (four) legs vertices and N_i is the number of the internal lines. Using the topological relations

$$\begin{aligned} n + 2N_i &= 3N_3 + 4N_4 \\ N_3 + 2N_4 &= n + 2\ell - 2 \end{aligned}$$

we obtain for $d = 2$

$$D \sim \Lambda^{2(1-N_4)} \tag{2.40}$$

Thus, there are primitively divergent diagrams for any n: those with $N_4 = 0$ (and correspondingly $N_3 = n + 2l - 2$) are quadratically divergent, while those with $N_4 = 1$ (and $N_3 = n + 2l - 4$) are logarithmically divergent. The previous considerations suggest that in the evaluation of the generic Feynman diagram with n external legs Λ^2 and $\log \Lambda^2$ divergences will be generated. To regularize the theory a counterterm $\delta_n \cdot \phi(\mathbf{p})^n$ is introduced.

However in principle this could not be sufficient. Indeed we observe that other divergences comes from second derivatives of the n-point irreducible correlation functions with respect to the external momenta $\phi(\mathbf{p})^{n-1}\Box_p\phi(\mathbf{p})$. Following the same step done before we find

$$\Box_p\langle\phi(\mathbf{p}=\mathbf{0})\phi(\mathbf{0})^{n-1}\rangle \sim \Lambda^{-2N_4} \tag{2.41}$$

which diverge logarithmically for every n when $N_4 = 0$, so that also these operators must be included in the renormalized Hamiltonian which will contain an infinite number of counterterms

$$\mathcal{H}^{\rm ren} = \mathcal{H} + \sum_n [Z_n(\Lambda)\phi^n + \zeta_n(\Lambda)\phi^{n-1}\Box\phi]. \tag{2.42}$$

Now, let us show that all counterterms except those computed in the previous section can be neglected in the critical crossover limit. Suppose that we wish to compute $Z_n(\Lambda)$ at l loops. Keeping into account that the divergence may be quadratic or logarithmic, we expect the l-loop divergent contribution to χ_n to be of the form

$$\frac{u^{n/2+l-1}}{t^n}(a_1\Lambda^2 + tP_1[\ln(\Lambda^2/t)] + P_2[\ln(\Lambda^2/t)]). \tag{2.43}$$

where $P_1(x)$ and $P_2(x)$ are polynomials and a_1 a constant. Therefore, the contribution to $t^n\chi_n/u$ vanishes unless $n/2 + l - 2 \leq 0$. The only two cases satisfying this condition (of course $n \geq 1$ and $l \geq 1$) are $l = n = 1$, $l = 1$ and $n = 2$, which are the cases considered before. Let us now consider the contributions to $\bar{\chi}_{n,i}$, which is the first derivative of the n-point connected correlation function with respect to the square of an external momentum $\mathbf{p}$ computed at zero momentum. Since momenta scale as $t^{1/2}$, in the critical crossover limit we should have $\bar{\chi}_{n,i} \approx ut^{-n-1}\bar{f}_n(t/u, H/u)$. The divergent contributions are logarithmic (diagrams with $N_4 = 0$) and therefore we expect an l-loop contribution of the form

$$\frac{u^{n/2+l-1}}{t^n}(P[\ln(\Lambda^2/t)] + \text{finite terms}). \tag{2.44}$$

Considering $t^{n+1}\bar{\chi}_{n,i}/u$, we see that this contribution always vanishes in the critical crossover limit. Therefore, the renormalization constants $\zeta_n(\Lambda)$ can be neglected. Thus, the only renormalizations needed are those that we have considered. Finally, let us show that correlation functions computed in the renormalized theory have the correct scaling behavior. Indeed, in the renormalized theory diagrams scale canonically with possible logarithmic corrections. Therefore, D introduced at the beginning of this section scales as $u^{N_4+N_3/2}t^{1-N_4}\times$logs, so that the contribution of D to $t^n\chi_n/u$ scales as

$$\frac{t^n}{u} \times \frac{1}{t^n} \times u^{N_4+N_3/2}t^{1-N_4} \sim u^{N_3/2}. \tag{2.45}$$

Therefore, the only non-vanishing diagrams have $N_3 = 0$, confirming the claim that three-leg vertices do not play any role.

2.1.4 A unique definition for the renormalization functions $h_c(u)$ and $r_c(u)$

In this section we wish to discuss again the definition of $r_c(u)$ and $h_c(u)$. It is obvious that these functions are not uniquely defined, since one can add a term proportional to u

without modifying the scaling behavior. We wish now to fix this ambiguity by requiring that $t = h = 0$ corresponds to the critical point.

It is easy to see that no modifications are needed for $h_c(u)$. Indeed, with the choice (2.17) one obtains the correlation functions of the symmetric theory and in this case the critical point is uniquely defined by $h = 0$ by symmetry. The proper definition of $r_c(u)$ requires more care, since we must perform a non-perturbative calculation in order to identify the critical point. For this purpose we will use the fact that in the critical crossover limit the perturbative expansion in powers of u is equivalent to the perturbative expansion in the continuum ϕ^4 theory once a proper mass renormalization is performed.

In the continuum theory, if $\tilde{t} \equiv t_{\rm cont}/u_{\rm cont}$ is the a-dimensional reduced temperature defined so that $\tilde{t} = 0$ corresponds to the critical point, we have at one loop, cf. eq. (2.10) of Ref. [32],

$$u_{\rm cont}\chi_{2,\rm cont} = \frac{1}{\tilde{t}} + \frac{1}{8\pi\tilde{t}^2}\left(\ln\frac{8\pi\tilde{t}}{3} + 3 + 8\pi D_2\right) + O(\tilde{t}^{-3}\ln\tilde{t}^2), \tag{2.46}$$

where D_2 is a non-perturbative constant that can be expressed in terms of renormalization-group functions, cf. eq. (2.11) of Ref. [32]. By using the four-loop perturbative results of Ref. [86], Ref. [32] obtained the estimate $D_2 = -0.0524(2)$. It is not clear whether the error can really be trusted, since in two dimensions the resummation of the perturbative expansion is not well behaved due to non-analyticities of the renormalization-group functions at the fixed point [87, 88]; still, the estimate should provide the correct order of magnitude.

The expansion (2.46) should be compared with the perturbative expansion of χ_2 in the lattice model. We write $r_c(u)$ as

$$\begin{aligned} r_c(u) &= \frac{u}{8\pi}\ln u + \frac{u}{2}\int_{\mathbf{p}}\frac{V_3(\mathbf{p})^2}{K(\mathbf{p})^2} + Au, \\ A &= -D_2 - \frac{1}{8\pi}\ln\frac{256\pi}{3} - \frac{3}{8\pi} - \frac{1}{2}\int_{\mathbf{p}}\left[\frac{V_4(\mathbf{p})}{K(\mathbf{p})} - \frac{1}{\hat{p}^2}\right]. \end{aligned} \tag{2.47}$$

where A has been determined comparing χ_2 with a lattice regularisation eq. (2.18)

$$u\chi_2 = \frac{u}{t} + \frac{u^2}{8\pi t^2}\left\{\log\frac{t}{32u} - 8\pi A - 4\pi\int_{\mathbf{p}}\left[\frac{V_4(\mathbf{p})}{K(\mathbf{p})} - \frac{1}{\hat{p}^2}\right]\right\} + O(u^3). \tag{2.48}$$

with χ_2 in the continuum limit given by eq. (2.46). If we use definition (2.47), the critical point corresponds to $\tilde{t} = 0$.

2.1.5 Higher than two dimension

In this section we want to generalize the previous results (obtained for $d = 2$) to higher dimension $2 \leq d < 4$, for which Ising criticality is still present. Cosidering the continuum action (2.49) one is able to predict the general scaling relations (2.52) and (2.53). On the other hand the critical parameters $h_c(u)$ and $r_c(u)$ will include more contributions with respect to the two dimensional case [56]. This is simple related to the fact that in three dimension for instance, the mass counterterm must be computed up to two loops. However in the case in which the theory is not symmetric, anomalous terms appear also for χ_3; these bad contributions cannot be deleted by using $h_c(u)$ or $r_c(u)$. In this section we show that the expected scaling relation (2.53) still survive if the critical field is translated by a constant factor[5] (i.e. $\varphi \to \varphi + u^{1/2}k_R$), so that the anomalous three legs diagrams can be deleted fixing k_R.

Let we start considering the continuum interaction in $d < 4$ dimension

$$\mathcal{S}_{\text{cont}}[\varphi] = \int d^d\mathbf{r} \left[H\varphi(\mathbf{r}) + \frac{1}{2}\Big(\partial\varphi(\mathbf{r})\Big)^2 + \frac{r}{2}\varphi(\mathbf{r})^2 + \frac{\sqrt{u}v_3}{3!}\varphi(\mathbf{r})^2\Box\varphi(\mathbf{r}) + \frac{u}{4!}\varphi(\mathbf{r})^4 \right], \quad (2.49)$$

generalizing the considerations done in (2.8), i.e. making a change of variable $\mathbf{r} = \mathbf{y}u^{-1/(4-d)}$ and defining a new bosonic field

$$\psi(\mathbf{x}) = u^{(d-2)/[2(d-4)]}\varphi(\mathbf{x}u^{-1/(4-d)}). \quad (2.50)$$

we can rewrite (2.49) as

$$\mathcal{S}_{\text{cont}}[\psi] = \int d^d\mathbf{s} \left[\tilde{H}\psi(\mathbf{s}) + \frac{1}{2}\Big(\partial\psi(\mathbf{s})\Big)^2 + \frac{\tilde{r}}{2}\psi(\mathbf{s})^2 + \frac{u^{\frac{d}{4-d}}v_3}{3!}\psi(\mathbf{s})^2\Box\psi(\mathbf{s}) + \frac{1}{4!}\psi(\mathbf{s})^4 \right], \quad (2.51)$$

where we have defined.

$$\tilde{H} \equiv Hu^{-(d+2)/[2(4-d)]}, \qquad \tilde{r} \equiv ru^{-2/(4-d)}. \quad (2.52)$$

Thus, formally, once the action is expressed in terms of ψ, the bare parameters appear only in the combinations $\tilde{H}$ and $\tilde{r}$ while the three fields coupling can be neglected. Then, consider the zero-momentum connected correlation function χ_n, neglecting the three-legs vertex, we have

$$\begin{aligned} \chi_n &\equiv \int d^d\mathbf{r}_2 \dots d^d\mathbf{r}_n \, \langle\varphi(\mathbf{0})\varphi(\mathbf{r}_2)\dots\varphi(\mathbf{r}_n)\rangle^{\text{conn}} \\ &= u^{[2d-n(2+d)]/[2(4-d)]} \int d^d\mathbf{s}_2 \dots d^d\mathbf{s}_n \, \langle\psi(\mathbf{0})\psi(\mathbf{s}_2)\dots\psi(\mathbf{s}_n)\rangle^{\text{conn}} \\ &= u^{[2d-n(2+d)]/[2(4-d)]} f_n(\tilde{H}, \tilde{r}), \end{aligned} \quad (2.53)$$

i.e. $u^{-[2d-n(2+d)]/[2(4-d)]}\chi_n$ is a scaling function that is universal given the normalization conditions for $\tilde{H}$ and $\tilde{r}$. The above-reported discussion is valid only at the formal level because we have not regularized the theory, or in other words a cut-off regularization breaks scale invariance.

Let us first discuss the symmetric case because it will be used in this work. In a similar way of what happens for $d = 2$, the previous relation (2.53) remains true if proper counterterms are included in the theory. For $d < 4$ we have to include only a mass counterterm $r_c(u)$ [$h_c(u) = 0$ due to the symmetry]. Having done this the correlation functions χ_n satisfy the scaling relations (2.53) with $\tilde{t} = tu^{-2/(4-d)}$, $t \equiv r - r_c(u)$ replacing $\tilde{r}$, and $\tilde{h} = hu^{-(d+2)/[2(4-d)]}$, $h \equiv H - h_c(u)$ replacing $\tilde{H}$

$$\chi_n = u^{[2d-n(2+d)]/[2(4-d)]} f_n(\tilde{h}, \tilde{t}) \quad (2.54)$$

---

[5] The normalization of k_R by using $u^{1/2}$, has been taken for convenience.

However in more than two dimensions more than one loop terms enter into the definition of $r_c(u)$ and $h_c(u)$. This is related to the fact that in the continuum theory, divergent diagrams are present beyond the one loop order. For instance in three dimension ($h_c(u) = 0$) we have[6]

$$r_c^{(\Lambda)}(u) = -\frac{\Lambda}{4\pi^2}u + \frac{u^2}{96\pi^2}\ln u + Ku^2 \tag{2.55}$$

where K is chosen so that $t = 0$ corresponds to the critical point (see sec. 2.1.4).

The non-symmetric case demands a more accurate analysis. Following the discussion of sec. 2.1.3 we have that a generic contribution to χ_n scales as[7] $\chi_n \sim G(\Lambda, t)t^{-n}u^{n/2+l-1}$. Using the scaling relation (2.54) $t \sim u^{2/(4-d)}$ we observe that

$$u^{\frac{n(2+d)-2d}{2(4-d)}}\chi_n \quad \sim \quad u^{\frac{n-4}{4-d}+\ell}G(\Lambda, u^2) \tag{2.56}$$

so that the anomalous diagram can be obtained by studying $\frac{n-4}{4-d} + \ell \leq 0$. If $d = 3$ there are the following dangerous contributions: a) $n = 1$, $\ell = 1, 2, 3$ (so that h_c can be obtained by a three loops computation), b) $n = 2$ $\ell = 1, 2$ [cancelled in the definition of $r_c(u)$], but also c) $n = 3$ $\ell = 1$ that in principle give us some problems. Now we show that the one loop $n = 3$ anomalous contributions can be deleted by introducing a new bosonic field $\phi(\mathbf{p})$[8]

$$\varphi(\mathbf{p}) \quad = \quad \phi(\mathbf{p}) - u^{1/2}k_R\delta(\mathbf{p}) \tag{2.57}$$

and taking k_R so that the effective three-legs vertex [computed up to $O(u)$ in $d = 3$] for the new bosonic fields is zero. Defining $\overline{V}^{(n)}(\mathbf{p}_1, \cdots \mathbf{p}_n)$ the $n-$legs vertex for the translated fields, we have

$$\overline{V}^{(3)}(\mathbf{p}_1, \mathbf{p}_2, \mathbf{p}_3) \quad = \quad V^{(3)}(\mathbf{p}_1, \mathbf{p}_2, \mathbf{p}_3) - uk_RV^{(4)}(\mathbf{p}_1, \mathbf{p}_2, \mathbf{p}_3, \mathbf{0}) \tag{2.58}$$

$$\begin{aligned}\overline{V}^{(2)}(\mathbf{p}_1, \mathbf{p}_2) \quad &= \quad V^{(2)}(\mathbf{p}_1, \mathbf{p}_2) - uk_RV^{(3)}(\mathbf{p}_1, \mathbf{p}_2, \mathbf{0}) \\ &\quad + \frac{u^2{k_R}^2}{2}V^{(4)}(\mathbf{p}_1, \mathbf{p}_2, \mathbf{0}, \mathbf{0})\end{aligned} \tag{2.59}$$

$$\begin{aligned}\overline{H} \quad &= \quad H - uk_RV^{(2)}(\mathbf{0}, \mathbf{0}) + \frac{u^2{k_R}^2}{2}V^{(3)}(\mathbf{0}, \mathbf{0}, \mathbf{0}) \\ &\quad - \frac{u^3{k_R}^3}{6}V^{(4)}(\mathbf{0}, \mathbf{0}, \mathbf{0}, \mathbf{0})\end{aligned} \tag{2.60}$$

Imposing that the first radiative correction for the three-legs vertex is null we get the result[9]

$$k_R \quad = \quad \frac{1}{V_4(\mathbf{0})}\left[\frac{1}{2}\int \mathrm{d}^3\mathbf{p}\frac{V_3(\mathbf{p})V_4(\mathbf{p})}{k(\mathbf{p})^2} - \frac{1}{6}\int \mathrm{d}^3\mathbf{p}\frac{V_3(\mathbf{p})^3}{k(\mathbf{p})^3}\right] \tag{2.61}$$

---

[6] The form of r_c and h_c depends on the explicit regularization used. Here we use a cut-off because it will be used for a fermionic model investigated in this work.

[7] $G_n(\Lambda)$ for $d = 3$ computed up to ℓ loops diverges as $\Lambda^{\ell+2}$. Indeed generalizing (2.40) we have that for a generic ℓ loops diagram $D \sim \Lambda^{\ell+2(1-N_4)} = \Lambda^{3-N_4+N_3/2-n/2}$

[8] This operation is exactly what we do when we obtain the effective action for the zero mode in the large N limit where in principle the condition $V^{(3)}(\mathbf{0}, \mathbf{0}, \mathbf{0}) = 0$ is not satisfied. For $d = 3$ one needs to take into account also radiative corrections.

[9] Notice that both the integrals are infra red finite in three dimensions.

that delete the the anomalous c) contributions. We have regularized the anomalous a) and b) contributions introducing respectively $h_c(u)$ and $r_c(u)$ similarly to what done for $d = 2$ (but with more diagram). But now new anomalous contributions appear due to the new terms (proportional to k_R) in (2.59) (2.60). It is straightforward to understand that this terms can be deleted recomputing $h_c(u)$ and $r_c(u)$ as a function of the new vertices $\overline{V}^{(n)}$. Indeed this is possible because the leading behavior of the vertices remain the same $\overline{V}_n(\mathbf{0}) \sim V_n(\mathbf{0})$.

2.2 Multicritical crossover limit

Now we want to generalize the previous considerations, considering more general interactions than (2.2). We want to take into account interactions in which we tune to zero at the same time all $V_j(\mathbf{0})$ for $j = 0, 1 \cdots \mathcal{N}+2$ (with $\mathcal{N}$ odd), while $V_{\mathcal{N}+3}(\mathbf{0})$ remain finite and positive.[10] In the continuum limit we want to study the following Hamiltonian

$$\mathcal{H} = H\chi + \frac{1}{2}\sum_{\mu}(\partial_\mu \chi)^2 + \sum_{n=2}^{\mathcal{N}+3} \frac{a_n}{n!}\frac{1}{N^{n/2-1}}\chi^n, \tag{2.62}$$

with $a_{\mathcal{N}+2} = 0$. Here we have disregarded the momentum dependence of the vertices—it is formally irrelevant in the continuum limit—and higher-order terms in the kinetic term. We are interested in the limit in which $a_i \to 0$ for $i = 2, \cdots \mathcal{N}+1$, so that the leading non-vanishing term is $a_{\mathcal{N}+3}\chi^{\mathcal{N}+3}$. In analogy to what have been done in the previous section 2.1 we wish now to compute the crossover from mean-field to multicritical behavior. The analysis is quite complex and thus we only consider explicitly the case $\mathcal{N} = 3$.

Using the lattice regularization we start from the following Hamiltonian

$$\begin{aligned} \mathcal{H} \;=\; & u_{01}\phi(\mathbf{0}) + \frac{1}{2}\int_{\mathbf{p}} (K(\mathbf{p}) + u_{02})\, \phi(\mathbf{p})\phi(-\mathbf{p}) \\ & + \frac{1}{3!}\left(\prod_{i=1}^{3}\int_{\mathbf{p}_i}\phi(\mathbf{p}_i)\right)\delta\left(\sum_{i=1}^{3}\mathbf{p}_i\right)\left[u_{03} + u_6^{1/4}V^{(3)}(\{\mathbf{p}_i\})\right] \\ & + \frac{1}{4!}\left(\prod_{i=1}^{4}\int_{\mathbf{p}_i}\phi(\mathbf{p}_i)\right)\delta\left(\sum_{i=1}^{4}\mathbf{p}_i\right)\left[u_{04} + u_6^{1/2}V^{(4)}(\{\mathbf{p_i}\})\right] \\ & + \frac{u_6^{3/4}}{5!}\left(\prod_{i=1}^{5}\int_{\mathbf{p}_i}\phi(\mathbf{p}_i)\right)\delta\left(\sum_{i=1}^{5}\mathbf{p}_i\right)V^{(5)}(\{\mathbf{p}_i\}) \\ & + \frac{u_6}{6!}\left(\prod_{i=1}^{6}\int_{\mathbf{p}_i}\phi(\mathbf{p}_i)\right)\delta\left(\sum_{i=1}^{6}\mathbf{p}_i\right)\left[1 + V^{(6)}(\{\mathbf{p}_i\})\right] \end{aligned} \tag{2.63}$$

where we have defined

$$V^{(i)}(\mathbf{0}, \ldots, \mathbf{0}) = 0 \tag{2.64}$$

for $i = 1, \cdots, 6$. We have written each vertex as a constant plus a function of the momenta multiplied by a power of u_6. This is indeed the expression that one would obtain from the effective Hamiltonian for the zero mode by setting $u_6 \sim 1/N^2$. Moreover, we have dropped the contributions of vertices with more than six fields. We will discuss them in sec. 2.2.4. The normalization of the field is fixed by requiring:

---

[10] The positive condition guarantees us that the stability of the theory.

$$K(\mathbf{p}) \approx \mathbf{p}^2 + O(\mathbf{p}^4), \tag{2.65}$$

while we introduce α_i to name the leading contribution in $\mathbf{p}$ for higher order than two vertices

$$V^{(i)}(\mathbf{p}, -\mathbf{p}, \mathbf{0}, \cdots \mathbf{0}) \approx \alpha_i \mathbf{p}^2 + O(\mathbf{p}^4). \tag{2.66}$$

We wish now to show that four critical parameters (u_{ci}, $i = 1, \ldots 4$) can be defined, such that for $u_i \equiv u_{0i} - u_{ci} \to 0$, ($i = 1, \ldots 4$), $u_6 \to 0$, the n-point susceptibility has the scaling form:

$$\chi_n = t^{1-n} f_n(x_1, x_3, x_4, x_6), \tag{2.67}$$

where we write for notational convenience $t \equiv u_2$ and we set $x_i \equiv u_i/t$. Moreover, we will show that the function f_n is independent of the vertices $V^{(i)}$ and it is thus a universal scaling function of the ϕ^6 theory. The non-universal features of the model appear only in the functions u_{ci}, which can be computed in perturbation theory up to an additive constant. In our case a two-loop calculation provides the full answer. Notice that, as pointed out in section 2.1 for the $\mathcal{N} = 1$ case, in order to prove eq. (2.67) it is enough to consider the case in which $u_1 = 0$. This is the case we shall consider below.

2.2.1 One-loop computation

We begin by considering a generic one-loop diagram with n_3 three-leg vertices and so on up to n_6 six-leg vertices contributing to χ_n. For $t \to 0$ its contribution is

$$\chi_n \sim t^{-n} \int_{\mathbf{p}} \frac{1}{[K(\mathbf{p}) + t]^{\sum n_i}} \prod_{i=3}^{6} [u_i + w_i V_i(\mathbf{p})]^{n_i} \tag{2.68}$$

where $V_i(\mathbf{p}) \equiv V^{(i)}(\mathbf{p}, -\mathbf{p}, \mathbf{0}, \ldots)$, $w_j = u_6^{(j-2)/4}$ ($j = 3, 4, 5, 6$), and $u_5 = 0$. Expanding we obtain contributions of the form

$$\chi_n \sim t^{-n} \prod_{i=3}^{6} u_i^{n_i - k_i} w_i^{k_i} \int_{\mathbf{p}} \frac{\prod_i [V_i(\mathbf{p})]^{k_i}}{[K(\mathbf{p}) + t]^{\sum n_i}}, \tag{2.69}$$

where $0 \leq k_i \leq n_i$ and $k_5 = n_5$. If $\sum (n_i - k_i) \geq 2$ the integral behaves as t^{-A} with $A = -1 + \sum (n_i - k_i)$, so that

$$t^{n-1} \chi_n \sim \prod_i x_i^{n_i - k_i} w_i^{k_i}. \tag{2.70}$$

Thus, in the scaling limit, the contributions of the formally-irrelevant vertices can be neglected and thus we can set $k_i = 0$. The remaining contributions (with $k_3 = k_4 = k_6 = n_5 = 0$) scale according to eq. (2.67). Note that in this case the integral can be computed in the continuum, by replacing $K(\mathbf{p})$ with p^2 and by integrating over the whole plane. Therefore, the result is independent of the explicit form of $K(\mathbf{p})$.

If $\sum(n_i - k_i) = 1$, we have similarly

$$t^{n-1}\chi_n \sim x_i^{n_i-k_i} w_i^{k_i} \log t. \tag{2.71}$$

The formally-irrelevant vertices can still be neglected. However, in this case there is an additional $\log t$ that breaks the scaling law for $k_i = 0$, i.e. for $n_3 + n_4 + n_6 = 1$. Anomalous contributions appear therefore in χ_1, χ_2, and χ_4.

Finally, if $\sum(n_i - k_i) = 0$ (this implies $n_3 = k_3$, $n_4 = k_4$, $n_6 = k_6$) the integral is constant as $t \to 0$. Therefore, we have

$$t^{n-1}\chi_n \sim \frac{1}{t}\prod_i w_i^{n_i} \sim \frac{u_6^{n/4}}{t}. \tag{2.72}$$

In the scaling limit this contribution is irrelevant except when $n \leq 4$.

In conclusion, at one loop, the only contributions that scale anomalously in χ_n are that whith $n \leq 4$. We shall now show that we can absorb these anomalous terms in the definition of the functions u_{ci} (in this section contributions to u_{ci} given by one-loop diagrams will be indicated as u_{ci}^{1l}).

Let us begin by considering the one-loop expression of χ_1:

$$\begin{aligned}
\chi_1^{1l} &= -\frac{u_{c1}^{1l}}{t} - \frac{1}{2t}\int_{\mathbf{p}} \frac{u_3 + u_6^{1/4} V_3(\mathbf{p})}{K(\mathbf{p}) + t} \\
&= -\frac{u_{c1}^{1l}}{t} - \frac{u_3}{2t}\left[-\frac{1}{4\pi}\log\frac{t}{32} + K_1\right] - \frac{u_6^{1/4}}{2t}\int_{\mathbf{p}} \frac{V_3(\mathbf{p})}{K(\mathbf{p})} + O(u_6^{1/4}\log t, u_3 \log t), \quad (2.73)
\end{aligned}$$

with

$$K_1 = \int_{\mathbf{p}} \left(\frac{1}{K(\mathbf{p})} - \frac{1}{\hat{p}^2}\right) \tag{2.74}$$

and $\hat{p}^2 = 4\sum_i \sin^2(p_i/2)$. Thus, if we define

$$\begin{aligned}
u_{c1}^{1l} &= \frac{u_3}{8\pi}(\log u_6 - 4\pi K_1) - \frac{u_6^{1/4}}{2}\int_{\mathbf{p}} \frac{V_3(\mathbf{p})}{K(\mathbf{p})}, \quad (2.75) \\
&\equiv U_1 + U_2
\end{aligned}$$

the anomalous contributions in χ_1 cancel out and the result is independent of $V^{(j)}$ and of $K(\mathbf{p})$

$$\chi_1^{1l} = -\frac{x_3}{8\pi}\log(32 x_6). \tag{2.76}$$

In order to render easier the analysis of the theory at two loop level, in (2.75) we have introduced U_1 and U_2, defined as

$$U_1 = \frac{u_3}{8\pi}(\log u_6 - 4\pi K_1) \tag{2.77}$$

$$U_2 = -\frac{u_6^{1/4}}{2}\int_{\mathbf{p}} \frac{V_3(\mathbf{p})}{K(\mathbf{p})}. \tag{2.78}$$

Let us now consider the susceptibility with $n = 2$. We have

$$\begin{aligned} t\chi_2^{1l} &= -\frac{u_{c2}^{1l}}{t} - \frac{1}{2t}\int_{\mathbf{p}} \frac{u_4 + w_4 V_4(\mathbf{p})}{K(\mathbf{p}) + t} + \frac{1}{2t}\int_{\mathbf{p}} \frac{[u_3 + w_3 V_3(\mathbf{p})]^2}{[K(\mathbf{p}) + t]^2} \\ &= -\frac{u_{c2}^{1l}}{t} - \frac{u_4}{2t}\left[-\frac{1}{4\pi}\log\frac{t}{32} + K_1\right] + \frac{u_3^2}{8\pi t^2} + \frac{u_6^{1/2}}{2t}\int_{\mathbf{p}}\left[\frac{V_3(\mathbf{p})^2}{K(\mathbf{p})^2} - \frac{V_4(\mathbf{p})}{K(\mathbf{p})}\right] + O(u_6^{1/4}\log t). \end{aligned} \tag{2.79}$$

Thus, if we define

$$\begin{aligned} u_{c2}^{1l} &\equiv D_1 + D_2 + D_3 \\ D_1 &= \frac{u_4}{8\pi}\left(\log u_6 - 4\pi K_1\right) \\ D_2 &= \frac{u_6^{1/2}}{2}\int_{\mathbf{p}} \frac{V_3(\mathbf{p})^2}{K(\mathbf{p})^2} \\ D_3 &= -\frac{u_6^{1/2}}{2}\int_{\mathbf{p}} \frac{V_4(\mathbf{p})}{K(\mathbf{p})} \end{aligned} \tag{2.80}$$

we obtain

$$t\chi_2^{1l} = \frac{x_3^2}{8\pi} - \frac{x_4}{8\pi}\log(32 x_6), \tag{2.81}$$

that is independent of the vertices and of $K(\mathbf{p})$.

Now let us consider χ_3. At one loop we have

$$\begin{aligned} t^2\chi_3^{1l} &= -\frac{u_{c3}^{1l}}{t} - \frac{1}{t}\int_{\mathbf{p}} \frac{[u_3 + w_3 V_3(\mathbf{p})]^3}{[K(\mathbf{p}) + t]^3} \\ &\quad + \frac{3}{2t}\int_{\mathbf{p}} \frac{[u_3 + w_3 V_3(\mathbf{p})][u_4 + w_4 V_4(\mathbf{p})]}{[K(\mathbf{p}) + t]^2} - \frac{1}{2t}\int_{\mathbf{p}} \frac{w_5 V_5(\mathbf{p})}{K(\mathbf{p}) + t} \\ &= -\frac{u_{c3}^{1l}}{t} - \frac{x_3^3 - 3x_3x_4}{8\pi} - \frac{u_6^{3/4}}{2t}\int_{\mathbf{p}}\left[\frac{2V_3(\mathbf{p})^3}{K(\mathbf{p})^3} - \frac{3V_3(\mathbf{p})V_4(\mathbf{p})}{K(\mathbf{p})^2} + \frac{V_5(\mathbf{p})}{K(\mathbf{p})}\right] + O(u_6^{3/4}\log t). \end{aligned} \tag{2.82}$$

Thus, the correct scaling is obtained by setting

$$\begin{aligned} u_{c3}^{1l} &\equiv T_1 + T_2 + T_3 \\ T_1 &= -{u_6}^{3/4}\int_{\mathbf{p}} \frac{2V_3(\mathbf{p})^3}{K(\mathbf{p})^3} \\ T_2 &= \frac{3{u_6}^{3/4}}{2}\int_{\mathbf{p}} \frac{V_3(\mathbf{p})V_4(\mathbf{p})}{K(\mathbf{p})^2} \\ T_3 &= -\frac{{u_6}^{3/4}}{2}\int_{\mathbf{p}} \frac{V_5(\mathbf{p})}{K(\mathbf{p})} \end{aligned} \tag{2.83}$$

Finally, let us consider the four-point function. There are five graphs contributing to it. It is easy to see that an anomalous contribution arises only from the insertion of the 6-leg vertex.

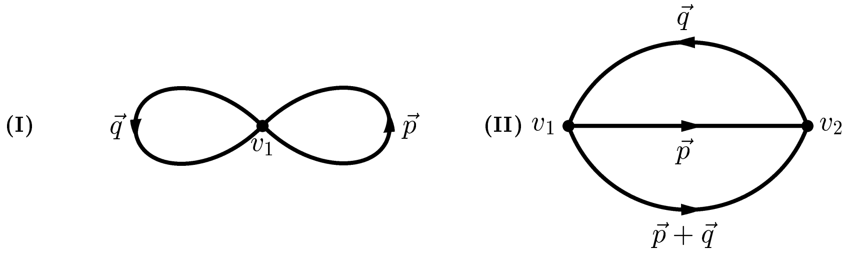

Figure 2.2: The general two loop topologies for χ_n. We report only the vertex (v_1 and v_2) for which more than two internal legs are contracted.

However, if we wish that χ_4 does not depend on any lattice detail we should also subtract other contributions that arise from the other graphs. We define therefore

$$\begin{aligned}
u_{c4}^{1l} &\equiv Q_1 + Q_2 + Q_3 + Q_4 + Q_5 + Q_6 \\
Q_1 &= \frac{u_6}{8\pi} \left(\log u_6 - 4\pi K_1\right) \\
Q_2 &= 3u_6 \int_{\mathbf{p}} \frac{V_3(\mathbf{p})^4}{K(\mathbf{p})^4} \\
Q_3 &= -6u_6 \int_{\mathbf{p}} \frac{V_4(\mathbf{p}) V_3(\mathbf{p})^2}{K(\mathbf{p})^3} \\
Q_4 &= \frac{3u_6}{2} \int_{\mathbf{p}} \frac{V_4(\mathbf{p})^2}{K(\mathbf{p})^2} \\
Q_5 &= 2u_6 \int_{\mathbf{p}} \frac{V_5(\mathbf{p}) V_3(\mathbf{p})}{K(\mathbf{p})^2} \\
Q_6 &= -\frac{u_6}{2} \int_{\mathbf{p}} \frac{V_6(\mathbf{p})}{K(\mathbf{p})}
\end{aligned} \tag{2.84}$$

2.2.2 Two loop computation

At two loops there many graphs contributing to χ_n. In general they can be grouped in two different topologies reported in Fig. 2.2. Graphs are obtained from these topologies by adding external legs to vertices v_1 and v_2 and to the internal lines. We will then distinguish the contributions in different classes, according to the nature of the vertex appearing in v_1 and v_2. We will thus consider contributions (IA) and (IB): in the first case we consider at the vertex v the zero-momentum part of the vertex, while in the opposite case we consider the remaining part. Analogously we distinguish contributions (IIA), (IIB), (IIC).

Case (IA)

In this case the contribution to χ_n can be written as

$$\begin{aligned} \chi_n \quad \sim \quad & u_j t^{-n} \int_{\mathbf{p}} [K(\mathbf{p}) + t]^{-\sum n_i - 1} \prod_i [u_i + w_i V_i(\mathbf{p})]^{n_i} \\ & \int_{\mathbf{q}} [K(\mathbf{q}) + t]^{-\sum m_i - 1} \prod_i [u_i + w_i V_i(\mathbf{q})]^{m_i} \end{aligned} \tag{2.85}$$

Expanding we obtain a sum of terms of the form

$$\begin{aligned} \chi_n \quad \sim \quad & u_j t^{-n} \prod_i u_i^{k_i + h_i} w_i^{n_i + m_i - k_i - h_i} \int_{\mathbf{p}} \int_{\mathbf{q}} [K(\mathbf{p}) + t]^{-\sum n_i - 1} \prod_i [V_i(\mathbf{p})]^{n_i - k_i} \\ & [K(\mathbf{q}) + t]^{-\sum m_i - 1} \prod_i [V_i(\mathbf{q})]^{m_i - h_i}. \end{aligned} \tag{2.86}$$

The integral scales as t^{-A} with $A = \sum_i (k_i + h_i)$ apart from logarithmic factors. Therefore,

$$t^{n-1} \chi_n \sim x_j \prod_i x_i^{k_i + h_i} w_i^{n_i + m_i - k_i - h_i}. \tag{2.87}$$

Thus, the contributions of the additional vertices can be neglected and we should only consider the case $n_i = k_i$, $m_i = h_i$. In this case, if there are no additional terms proportional to $\log t$, these contributions scale according to eq. (2.67). Logarithmic terms occur when $\sum n_i = 0$ or $\sum m_i = 0$, i.e. when there are tadpoles. Thus, an anomalous contribution occurs for the terms of the form

$$u_j t^{-n} \prod_i u_i^{m_i} \int_{\mathbf{p}} \frac{1}{K(\mathbf{p}) + t} \int_{\mathbf{q}} \frac{1}{[K(\mathbf{q}) + t]^{\sum m_i + 1}} \tag{2.88}$$

with $n = j + m_3 + 2m_4 + 4m_6 - 4$. However, at the same time we must consider the contributions of the one-loop counter-terms that give rise to terms of the form

$$\chi_n \sim u_{cj}^{1l} t^{-n} \int_{\mathbf{q}} [K(\mathbf{q}) + t]^{-\sum m_i - 1} \prod_i [u_i + w_i V_i(\mathbf{q})]^{m_i} \tag{2.89}$$

The analysis presented above can be repeated for these terms here, showing that one can neglect the contributions of the vertices V_i. Thus, we have a contribution

$$\chi_n \sim u_{cj}^{1l} t^{-n} \prod_i u_i \int_{\mathbf{q}} [K(\mathbf{q}) + t]^{-\sum m_i - 1} \tag{2.90}$$

Now, u_{cj}^{1l} is the sum of several contributions: we only consider here the logarithmic terms [U_1, D_1 and Q_1 in (2.75,2.80,2.84)]. The additional ones will be relevant for case (IIC) below. Taking into account the combinatorial factors we obtain

$$\chi_n \sim t^{-n} u_j \prod_i u_i \left[\int_{\mathbf{p}} \frac{1}{K(\mathbf{p}) + t} + \frac{1}{4\pi} \log u_6 - K_1 \right] \int_{\mathbf{q}} [K(\mathbf{q}) + t]^{-\sum m_i - 1} \tag{2.91}$$

The subtracted term replaces the $\log t$ term that arises from the integration over $\mathbf{p}$ with $\log(t/u_6)$. Thus, if no other logarithmic terms are generated by the integration over $\mathbf{q}$ this term scales correctly. However, when $m_i = 0$, another $\log t$ is generated. This occurs for $n = 2$ and $j = 6$. Thus taking into consideration this new anomalous contribution to χ_2 (and neglecting other contributions):

$$\begin{aligned} t{\chi_2}^{2\mathrm{l;IA}} &= -\frac{u_6}{4t}\Big[\int_{\mathbf{p}} \frac{1}{K(\mathbf{p})+t} + \frac{1}{4\pi}\log u_6 - K_1\Big] \int_{\mathbf{q}} [K(\mathbf{q})+t]^{-1} \\ &= -\frac{u_6}{4t}\left[\frac{1}{4\pi}\log 32x_6\right]\left[\frac{1}{4\pi}\log 32x_6 - \frac{1}{4\pi}\log u_6 + K_1\right] \end{aligned} \tag{2.92}$$

In order to cancel the previous anomalous contribution to χ_2, a correction to u_{c2} will be introduced in sec. 2.2.3.

(IB)

The general contribution scales according to

$$\begin{aligned} \chi_n \sim\ & w_j t^{-n} \prod_i u_i^{k_i+h_i} w_i^{n_i+m_i-k_i-h_i} \int_{\mathbf{p}}\int_{\mathbf{q}} V^{(j)}(\mathbf{p},-\mathbf{p},\mathbf{q},-\mathbf{q},\mathbf{0},\ldots) \\ & [K(\mathbf{p})+t]^{-\sum n_i - 1} \prod_i [V_i(\mathbf{p})]^{n_i-k_i} [K(\mathbf{q})+t]^{-\sum m_i - 1} \prod_i [V_i(\mathbf{q})]^{m_i-h_i}. \end{aligned} \tag{2.93}$$

Keeping into account the fact that $V^{(j)}(\mathbf{p},-\mathbf{p},\mathbf{q},-\mathbf{q},\mathbf{0},\ldots) \sim (p^2+q^2)$ for $p, q \to 0$, we find that, if $\sum_i k_i \neq 0$ and $\sum_i h_i \neq 0$, the integral scales as t^{-A} with $A = \sum_i (k_i + h_i) - 1$ apart from logarithmic factors. Thus

$$t^{n-1}\chi_n \sim w_j \prod_i x_i^{k_i+h_i} w_i^{n_i+m_i-k_i-h_i}; \tag{2.94}$$

such a term always vanishes in the critical crossover limit.

Let us now consider the case in which $\sum_i k_i = 0$ but $\sum_i h_i \neq 0$ There are several anomalous diagrams that come from this contributions. We are going to show now that all these non-scaling terms are eliminated by one loop diagrams with insertion of counter terms defined in the one loop computation. We define:

$$V^{(j)}(\mathbf{p},-\mathbf{p},\mathbf{q},-\mathbf{q},\mathbf{0},\cdots) \equiv V_j(\mathbf{p}) + V_j(\mathbf{q}) + \tilde{V}_j(\mathbf{p},\mathbf{q}) \tag{2.95}$$

then inserting (2.95) into (2.93) and following the discussion of the $\sum_i h_i \neq 0$ and $\sum_i k_i \neq 0$ case, we find that the anomalous terms only come from $V_j(\cdot)$ in (2.95), while $\tilde{V}_j$ terms are regular. At this point the integrals factorize and the discussion reduces to one loop computation of the previous section with the properly counter terms introduced. Explicitly we have

$$t^{n-1}\chi_n \sim \frac{w_j}{t} \prod_i {x_i}^{h_i} {w_i}^{n_i+m_i-h_i} \tag{2.96}$$

so that we have to take care all the diagram for which:

$$\sum_{i=3}^{6} \frac{(i-2)}{4}(n_i + d_i) + \frac{j-2}{4} \leq 1 \tag{2.97}$$

having defined $d_i = m_i - h_i$ and with $j = 4, 5, 6$.
If $j = 6$ we find a scaling diagram with $d_1 = 0$ and $n_i = 0$. This non-universal contribution is cancelled by Q_6 term of u_{c4}^{1l} (2.84), indeed for this terms (including combinatorial factors):

$$\begin{aligned} t^{n-1}\chi_n &\sim \frac{w_j}{t}\prod_i {x_i}^{h_i}{w_i}^{n_i+m_i-h_i}\int_{\mathbf{p}}\frac{V_6(\mathbf{p})}{K(\mathbf{p})+t}-\frac{V_6(\mathbf{p})}{K(\mathbf{p})} \\ &\sim w_j\prod_i {x_i}^{h_i}{w_i}^{n_i+m_i-h_i}\log t \end{aligned} \tag{2.98}$$

that can be neglected in the CCL limit. In a very similar manner using T_3 (2.83), we can delete the terms with $j = 5$, $d_i = 0$, $n_i = 0$ and $j = 5$, $n_i = 0$, $d_i = \delta_{i,3}$; while using D_3 (2.80) the diagrams with $j = 4$ and $n_i = 0$ are cancelled (anomalous one are $d_i = 0$, $d_i = \delta_{i,3}$, $d_i = 2\delta_{i,3}$ and $d_i = \delta_{i,4}$). The last diagrams with $j = 5$ we have to discuss is the $n_3 = 1$, $d_i = 0$. This diagrams are regularized by one loop-insertion of Q_5 (2.84). Indeed we have:

$$\begin{aligned} t^{n-1}\chi_n &\sim \frac{w_j}{t}w_3\prod_i {x_i}^{h_i}\int_{\mathbf{p}}\frac{V_3(\mathbf{p})V_5(\mathbf{p})}{(K(\mathbf{p})+t)^2}-\frac{V_3(\mathbf{p})V_5(\mathbf{p})}{K(\mathbf{p})^2} \\ &\sim w_j w_3\prod_i {x_i}^{h_i}\log t \end{aligned} \tag{2.99}$$

In a very similar way the remaining anomalous diagrams for $j = 4$ are regularized by T_2 ($n_3 = 1$ and $d_i = 0$, $n_3 = 1$ and $d_i = \delta_{i,3}$), Q_4 ($n_4 = 1$ and $d_i = 0$) and Q_3 ($n_3 = 2$ and $\delta_i = 0$). In the discussion above we do not have used Q_2, T_1 and D_2, we expect that these terms enter into topologies of type (II).

In the case in which $\sum_i k_i = \sum_i h_i = 0$ other counterterms must be included in order to regularize the theory. In this case (neglecting log):

$$t^{n-1}\chi_n \sim \frac{w_j}{t}\prod_i {w_i}^{n_i+m_i} = \frac{{u_6}^{\frac{n+2}{4}}}{t}, \tag{2.100}$$

so that we have to take care χ_1 and χ_2 in (IB). From now we take the following short-hand notation for the propagator

$$\Delta(\mathbf{p}) \equiv K(\mathbf{p}) + t, \tag{2.101}$$

then

$${\chi_1}^{2\text{l;IB}} = -\frac{u_6^{3/4}}{8t}\int_{\mathbf{p},\mathbf{q}}\frac{V_5(\mathbf{p},\mathbf{q})}{\Delta(\mathbf{p})\Delta(\mathbf{q})}+\frac{u_6^{3/4}}{4t}\int_{\mathbf{p},\mathbf{q}}\frac{V_3(\mathbf{p})V_4(\mathbf{p},\mathbf{q})}{\Delta(\mathbf{p})^2\Delta(\mathbf{q})} \tag{2.102}$$

Therefore in the CCL (i.e. for $t \to 0$):

$$\begin{aligned} {\chi_1}^{2\text{l;IB}} &= \frac{u_6^{3/4}}{t}\left(\mathcal{A}^{(1)}_{2\text{l;IB}}-\frac{\mathcal{B}^{(1)}_{2\text{l;IB}}}{4\pi}\log\frac{t}{32}\right) \\ \mathcal{A}^{(1)}_{2\text{l;IB}} &= -\frac{1}{8}\int_{\mathbf{p},\mathbf{q}}\frac{\tilde{V}_5(\mathbf{p},\mathbf{q})}{K(\mathbf{p})K(\mathbf{q})}+\frac{1}{4}\int_{\mathbf{p},\mathbf{q}}\frac{\tilde{V}_4(\mathbf{p},\mathbf{q})V_3(\mathbf{p})}{K(\mathbf{p})^2K(\mathbf{q})}-\frac{\alpha_3}{16\pi}\int_{\mathbf{q}}\frac{V_4(\mathbf{q})}{K(\mathbf{q})} \\ &\quad -\frac{1}{4}\int_{\mathbf{p},\mathbf{q}}\frac{V_5(\mathbf{p})}{K(\mathbf{p})}\left(\frac{1}{K(\mathbf{q})}-\frac{1}{\widehat{\mathbf{q}}^2}\right)+\frac{1}{4}\int_{\mathbf{p},\mathbf{q}}\frac{V_3(\mathbf{p})V_4(\mathbf{p})}{K(\mathbf{p})^2}\left(\frac{1}{K(\mathbf{q})}-\frac{1}{\widehat{\mathbf{q}}^2}\right) \end{aligned} \tag{2.103}$$

$$+\frac{1}{4}\int_{\mathbf{p},\mathbf{q}}\frac{V_4(\mathbf{p})}{K(\mathbf{p})}\left(\frac{V_3(\mathbf{q})}{K(\mathbf{q})}\frac{1}{K(\mathbf{q})}-\frac{\alpha_3}{\widehat{\mathbf{q}}^2}\right) \tag{2.104}$$

$$\mathcal{B}^{(1)}_{\mathrm{2l;IB}} = \frac{1}{4}\int_{\mathbf{p}}\frac{V_3(\mathbf{p})V_4(\mathbf{p})}{K(\mathbf{p})^2}-\frac{1}{4}\int_{\mathbf{p}}\frac{V_5(\mathbf{p})}{K(\mathbf{p})}+\frac{\alpha_3}{4}\int_{\mathbf{p}}\frac{V_4(\mathbf{p})}{K(\mathbf{p})} \tag{2.105}$$

where α_i was defined in (2.66). Now we compute the IB diagrams that enter into the computation of χ_2:

$$\begin{aligned} t{\chi_2}^{\mathrm{2l;IB}} &= -\frac{u_6}{8t}\int_{\mathbf{p},\mathbf{q}}\frac{V_6(\mathbf{p},\mathbf{q})}{\Delta(\mathbf{p})\Delta(\mathbf{q})}+\frac{u_6}{2t}\int_{\mathbf{p},\mathbf{q}}\frac{V_5(\mathbf{p},\mathbf{q})V_3(\mathbf{p})}{\Delta(\mathbf{p})^2\Delta(\mathbf{q})}-\frac{u_6}{2t}\int_{\mathbf{p},\mathbf{q}}\frac{V_4(\mathbf{p},\mathbf{q})V_3(\mathbf{p})^2}{\Delta(\mathbf{p})^3\Delta(\mathbf{q})} \\ &\quad -\frac{u_6}{4t}\int_{\mathbf{p},\mathbf{q}}\frac{V_3(\mathbf{p})V_3(\mathbf{q})V_4(\mathbf{p},\mathbf{q})}{\Delta(\mathbf{p})^2\Delta(\mathbf{q})^2}+\frac{u_6}{4t}\int_{\mathbf{p},\mathbf{q}}\frac{V_4(\mathbf{p})V_4(\mathbf{p},\mathbf{q})}{\Delta(\mathbf{p})^2\Delta(\mathbf{q})} \end{aligned} \tag{2.106}$$

Therefore in the CCL:

$$t{\chi_2}^{\mathrm{2l;IB}} = \frac{u_6}{t}\left(\mathcal{A}^{(2)}_{\mathrm{2l;IB}}-\frac{\mathcal{B}^{(2)}_{\mathrm{2l;IB}}}{4\pi}\log\frac{t}{32}\right) \tag{2.107}$$

$$\begin{aligned} \mathcal{A}^{(2)}_{\mathrm{2l;IB}} &= \int_{\mathbf{p},\mathbf{q}}\Big[-\frac{1}{8}\frac{\tilde{V}_6(\mathbf{p},\mathbf{q})}{K(\mathbf{p})K(\mathbf{q})}+\frac{1}{2}\frac{\tilde{V}_5(\mathbf{p},\mathbf{q})V_3(\mathbf{p})}{K(\mathbf{p})^2K(\mathbf{q})}-\frac{1}{2}\frac{V_3(\mathbf{p})^2\tilde{V}_4(\mathbf{p},\mathbf{q})}{K(\mathbf{p})^3K(\mathbf{q})}+\frac{1}{4}\frac{V_4(\mathbf{p})\tilde{V}_4(\mathbf{p},\mathbf{q})}{K(\mathbf{p})^2K(\mathbf{q})} \\ &\quad -\frac{1}{4}\frac{V_3(\mathbf{p})V_3(\mathbf{q})\tilde{V}_4(\mathbf{p},\mathbf{q})}{K(\mathbf{p})^2K(\mathbf{q})}\Big]-\frac{1}{4}\int_{\mathbf{p},\mathbf{q}}\frac{V_6(\mathbf{p})}{K(\mathbf{p})}\left(\frac{1}{K(\mathbf{q})}-\frac{1}{\widehat{\mathbf{q}}^2}\right)+\frac{1}{2}\int_{\mathbf{p},\mathbf{q}}\frac{V_5(\mathbf{p})}{K(\mathbf{p})} \\ &\quad \left(\frac{V_3(\mathbf{p})}{K(\mathbf{p})}\frac{1}{K(\mathbf{q})}+\frac{V_3(\mathbf{q})}{K(\mathbf{q})}\frac{1}{K(\mathbf{q})}-\frac{V_3(\mathbf{p})}{K(\mathbf{p})}\frac{1}{\widehat{\mathbf{q}}^2}-\alpha_3\frac{1}{\widehat{\mathbf{q}}^2}\right)-\frac{\alpha_3}{8\pi}\int_{\mathbf{q}}\frac{V_5(\mathbf{q})}{K(\mathbf{q})} \\ &\quad -\frac{1}{2}\int_{\mathbf{p},\mathbf{q}}\frac{V_4(\mathbf{p})}{K(\mathbf{p})}\left(\frac{V_3(\mathbf{p})^2}{K(\mathbf{p})^2}\Big(\frac{1}{K(\mathbf{q})}-\frac{1}{\widehat{\mathbf{q}}^2}\Big)+\frac{V_3(\mathbf{q})^2}{K(\mathbf{q})^2}\frac{1}{K(\mathbf{q})}-\frac{{\alpha_3}^2}{\widehat{\mathbf{q}}^2}\right)+\frac{3{\alpha_3}^2}{16\pi}\int_{\mathbf{q}}\frac{V_4(\mathbf{q})}{K(\mathbf{q})} \\ &\quad -\frac{1}{2}\int_{\mathbf{p},\mathbf{q}}\frac{V_3(\mathbf{p})V_4(\mathbf{p})}{K(\mathbf{p})^2}\left(\frac{V_3(\mathbf{q})}{K(\mathbf{q})}-\frac{\alpha_3}{\widehat{\mathbf{q}}^2}\right)+\frac{\alpha_3}{8\pi}\int_{\mathbf{q}}\frac{V_3(\mathbf{q})V_4(\mathbf{q})}{K(\mathbf{q})^2}-\frac{\alpha_4}{16\pi}\int_{\mathbf{q}}\frac{V_4(\mathbf{q})}{K(\mathbf{q})} \\ &\quad +\frac{1}{4}\int_{\mathbf{p},\mathbf{q}}\frac{V_4(\mathbf{p})^2}{K(\mathbf{p})^2}\left(\frac{1}{K(\mathbf{q})}-\frac{1}{\widehat{\mathbf{q}}^2}\right)+\frac{1}{4}\int_{\mathbf{p},\mathbf{q}}\frac{V_4(\mathbf{p})}{K(\mathbf{p})}\left(\frac{V_4(\mathbf{q})}{K(\mathbf{q})^2}-\frac{\alpha_4}{\widehat{\mathbf{q}}^2}\right) \end{aligned} \tag{2.108}$$

$$\begin{aligned} \mathcal{B}^{(2)}_{\mathrm{2l;IB}} &= -\frac{1}{4}\int_{\mathbf{p}}\frac{V_6(\mathbf{p})}{K(\mathbf{p})}+\frac{1}{2}\int_{\mathbf{p}}\frac{V_5(\mathbf{p})}{K(\mathbf{p})}\left(\alpha_3+\frac{V_3(\mathbf{p})}{K(\mathbf{p})}\right)-\frac{1}{2}\int_{\mathbf{p}}\frac{V_4(\mathbf{p})}{K(\mathbf{p})}\left({\alpha_3}^2+\frac{V_3(\mathbf{p})^2}{K(\mathbf{p})^2}\right) \\ &\quad -\frac{\alpha_3}{2}\int_{\mathbf{q}}\frac{V_3(\mathbf{q})V_4(\mathbf{q})}{K(\mathbf{q})^2}+\frac{1}{4}\int_{\mathbf{p}}\frac{V_4(\mathbf{p})}{K(\mathbf{p})}\left(\frac{V_4(\mathbf{p})}{K(\mathbf{p})}+\alpha_4\right) \end{aligned} \tag{2.109}$$

Case (IIA)

In this case the contributions of vertices v_1 and v_2 are simply $u_{j_1}u_{j_2}$. The contribution to χ_n has the general form

$$\begin{aligned} \chi_n &\sim t^{-n}u_{j_1}u_{j_2}\prod_i[u_i^{k_i+h_i+l_i}w_i^{n_i+m_i+p_i-k_i-h_i-l_i}] \\ &\quad \int_{\mathbf{p}}\int_{\mathbf{q}}(t+K(\mathbf{p}))^{-1-\sum n_i}(t+K(\mathbf{q}))^{-1-\sum m_i}(t+K(\mathbf{p}+\mathbf{q}))^{-1-\sum p_i} \\ &\quad\quad \prod_i[V_i(\mathbf{p})]^{n_i-k_i}[V_i(\mathbf{q})]^{m_i-h_i}[V_i(\mathbf{p}+\mathbf{q})]^{p_i-l_i}, \end{aligned} \tag{2.110}$$

with the topological relation $n = j_1 + j_2 - 6 + \sum_\ell (\ell - 2)(n_\ell + m_\ell + p_\ell)$. The analysis of this contribution is completely analogous to that presented in sec. 2.1.1 for the two-loop topology (b). The integral scales always as t^{-A} with $A = 1 + \sum_i (k_i + h_i + l_i)$ in the infrared limit. Thus, we have

$$t^{n-1}\chi_n \sim x_{j_1} x_{j_2} \prod_i [x_i^{k_i+h_i+l_i} w_i^{n_i+m_i+p_i-k_i-h_i-l_i}] \tag{2.111}$$

In the scaling limit, the only non-vanishing contributions are those with $n_i = k_i$, $m_i = h_i$, $p_i = l_i$: the formally irrelevant vertices can be disregarded. The remaining terms scale correctly.

Case (IIB)

In this case the vertex v_1 enters into the diagrams with the zero momentum part of a vertex u_{j_1}, while v_2 gives the contribution $V^{(j_2)}(\mathbf{p}, \mathbf{q}, -\mathbf{p} - \mathbf{q}, \mathbf{0}, \ldots)$. Then χ_n has the following form

$$\begin{aligned}\chi_n \sim\ & t^{-n} u_{j_1} w_{j_2} \prod_i [u_i^{k_i+h_i+l_i} w_i^{n_i+m_i+p_i-k_i-h_i-l_i}] \int_{\mathbf{p}} \int_{\mathbf{q}} V^{(j_2)}(\mathbf{p}, \mathbf{q}, -\mathbf{p} - \mathbf{q}, \mathbf{0}, \ldots) \\ & (t + K(\mathbf{p}))^{-1-\sum n_i} (t + K(\mathbf{q}))^{-1-\sum m_i} (t + K(\mathbf{p}+\mathbf{q}))^{-1-\sum p_i} \\ & \prod_i [V_i(\mathbf{p})]^{n_i-k_i} [V_i(\mathbf{q})]^{m_i-h_i} [V_i(\mathbf{p}+\mathbf{q})]^{p_i-l_i}.\end{aligned} \tag{2.112}$$

Here $n = j_1 + j_2 - 6 + \sum_\ell (\ell - 2)(n_\ell + m_\ell + p_\ell)$ as before. The analysis follows from the analogous one presented in sec. 2.1.1 for topology (c). Disregarding logarithmic factors the integral scales as t^{-A} with $A = \sum_i (k_i + h_i + l_i)$ in the infrared limit. Thus, we have

$$t^{n-1}\chi_n \sim x_{j_1} w_{j_2} \prod_i [x_i^{k_i+h_i+l_i} w_i^{n_i+m_i+p_i-k_i-h_i-l_i}], \tag{2.113}$$

which shows that these contributions can always be neglected.

Case (IIC)

Using a similar notation of case IIB, we have that χ_n has the following form

$$\begin{aligned}\chi_n \sim\ & t^{-n} w_{j_1} w_{j_2} \prod_i [u_i^{k_i+h_i+l_i} w_i^{n_i+m_i+p_i-k_i-h_i-l_i}] \\ & \int_{\mathbf{p}} \int_{\mathbf{q}} V^{(j_1)}(\mathbf{p}, \mathbf{q}, -\mathbf{p} - \mathbf{q}, \mathbf{0}, \ldots) V^{(j_2)}(\mathbf{p}, \mathbf{q}, -\mathbf{p} - \mathbf{q}, \mathbf{0}, \ldots) \\ & (t + K(\mathbf{p}))^{-1-\sum n_i} (t + K(\mathbf{q}))^{-1-\sum m_i} (t + K(\mathbf{p}+\mathbf{q}))^{-1-\sum p_i} \\ & \prod_i \left\{ [V_i(\mathbf{p})]^{n_i-k_i} [V_i(\mathbf{q})]^{m_i-h_i} [V_i(\mathbf{p}+\mathbf{q})]^{p_i-l_i} \right\}.\end{aligned} \tag{2.114}$$

Here $n = j_1 + j_2 - 6 + \sum_\ell (\ell - 2)(n_\ell + m_\ell + p_\ell)$ as before. The analysis follows from the analogous one presented in sec. 2.1.1 for topology (d). Assuming without loss of generality that $\sum k_i \le \sum h_i \le \sum l_i$, we should consider three cases: (a) $k_i = h_i = l_i = 0$; (b) $k_i = h_i = 0$, $\sum l_i > 0$; (c) $\sum h_i > 0$ and $\sum l_i > 0$.

In case (c) the integral behaves as t^{-A}, with with $A = \sum_i (k_i + h_i + l_i) - 1$ in the infrared limit. Thus,

$$t^{n-1}\chi_n \sim w_{j_1} w_{j_2} \prod_i [x_i^{k_i+h_i+l_i} w_i^{n_i+m_i+p_i-k_i-h_i-l_i}], \tag{2.115}$$

which can always be neglected. In case (a) the integral behaves as $\log t$, while in case (b) it behaves as $t^{-\sum l_i}$. Therefore,

$$t^{n-1}\chi_n \sim \frac{1}{t} w_{j_1} w_{j_2} \prod_i w_i^{n_i+m_i+p_i-l_i} x_i^{l_i} \sim \frac{u^{n/4+1/2}}{t} w^{-\sum l_i}, \tag{2.116}$$

so that we have to discuss some cases. First let us discuss the anomalous diagrams that can be cancelled by one-loop insertions. If $d_i = p_i - l_i$, they are the following (with $l_1 \geq 1$): (A) $d_i = \delta_{i,3}$, $n_i = m_i = 0$, $j_1 = j_2 = 3$ ($t^{n-1}\chi_n \sim {u_6}^{-1/4}$); (B) $d_i = 2\delta_{i,3}$, $n_i = m_i = 0$, $j_1 = j_2 = 3$ ($t^{n-1}\chi_n \sim {u_6}^0$); (C) $d_i = \delta_{i,4}$, $n_i = m_i = 0$, $j_1 = j_2 = 3$ ($t^{n-1}\chi_n \sim {u_6}^0$); (D) $d_i = \delta_{i,3}$, $n_i = m_i = 0$, $j_1 = 3$, $j_2 = 4$ ($t^{n-1}\chi_n \sim {u_6}^0$); (E) $d_i = \delta_{i,3}$, $n_i = \delta_{i,3}$, $m_i = 0$, $j_1 = 3$, $j_2 = 3$ ($t^{n-1}\chi_n \sim {u_6}^0$). Diagrams (A), (B) and (C) are regularized by insertion on respectively one-loop diagrams of D_2 counterterm of u_{c2} (2.80). Indeed, including combinatorial factors (let us consider A):

$$t^{n-1}\chi_n \quad \sim \quad \frac{{u_6}^{3/4}}{t} \prod_i {u_i}^{l_i} \int_{\mathbf{p},\mathbf{q}} \Big[\frac{V_3(\mathbf{p}) V^{(3)}(\mathbf{p},\mathbf{q},-\mathbf{p}-\mathbf{q})^2}{\Delta(\mathbf{p})^{\sum l_i+2} \Delta(\mathbf{p}+\mathbf{q}) \Delta(\mathbf{q})} - \frac{V_3(\mathbf{p}) V_3(\mathbf{q})^2}{\Delta(\mathbf{p})^{\sum l_i+2} K(\mathbf{q})^2}\Big]. \tag{2.117}$$

If we write $V^{(3)}(\mathbf{p},\mathbf{q},-\mathbf{p}-\mathbf{q}) =: V_3(\mathbf{p}) + V_3(\mathbf{q}) + \tilde{V}_3(\mathbf{p},\mathbf{q})$ in the first term in the r.h.s. of the previous expression (2.117), we find that only $V_3(\mathbf{q})$ terms are relevant [indeed for the other contributions the integral scale as t^{-A} with $A = \sum_i l_1 - 1$ as in the case (c)] but these are regularized by the second term on the r.h.s. of (2.117). The same happens for (B) and (C). Similar considerations follow for (D) and (E) using respectively T_2 and T_1 of u_{c3} (2.83).

Now we have to compute exactly the previous two loop contributions to χ_1 and χ_2. We define:

$$V^{(j)}(\mathbf{p},\mathbf{q},-\mathbf{p}-\mathbf{q},\mathbf{0},\cdots) = \frac{V_j(\mathbf{p}) + V_j(\mathbf{q}) + V_j(\mathbf{p}+\mathbf{q})}{2} + \overline{V}_j(\mathbf{p},\mathbf{q}). \tag{2.118}$$

We notice in particular that $\overline{V}_j = \mathbf{0}$ for $\mathbf{p} = \mathbf{0}$, $\mathbf{q} = \mathbf{0}$ or $\mathbf{p}+\mathbf{q} = \mathbf{0}$. One-point function is given by the following two diagrams:

$$\begin{aligned} \chi_1 \quad &= \quad -\frac{{u_6}^{3/4}}{4t} \int_{\mathbf{p},\mathbf{q}} \frac{V_3(\mathbf{p}) V^{(3)}(\mathbf{p},\mathbf{q},-\mathbf{p}-\mathbf{q})^2}{\Delta(\mathbf{p})^2 \Delta(\mathbf{q}) \Delta(\mathbf{p}+\mathbf{q})} \\ &\quad +\frac{{u_6}^{3/4}}{6t} \int_{\mathbf{p},\mathbf{q}} \frac{V^{(4)}(\mathbf{p},\mathbf{q},-\mathbf{p}-\mathbf{q},\mathbf{0}) V^{(3)}(\mathbf{p},\mathbf{q},-\mathbf{p}-\mathbf{q})}{\Delta(\mathbf{p}) \Delta(\mathbf{q}) \Delta(\mathbf{p}+\mathbf{q})} \end{aligned} \tag{2.119}$$

then in the CCL:

$${\chi_1}^{\text{2l;IIC}} \quad = \quad \frac{{u_6}^{3/4}}{t} \left(\mathcal{A}^{(1)}_{\text{2l;IIC}} - \frac{\mathcal{B}^{(1)}_{\text{2l;IIC}}}{4\pi} \log \frac{t}{32} \right) \tag{2.120}$$

$$\mathcal{B}^{(1)}_{\text{2l;IIC}} \quad = \quad -\frac{1}{4} \int_{\mathbf{p}} \left(2 \frac{V_3(\mathbf{p})^3}{K(\mathbf{p})^3} + \alpha_3 \frac{V_3(\mathbf{p})^2}{K(\mathbf{p})^2} \right) + \frac{1}{2} \int_{\mathbf{p}} \frac{V_4(\mathbf{p}) V_3(\mathbf{p})}{K(\mathbf{p})^2}. \tag{2.121}$$

The explicit expression for $\mathcal{A}^{(1)}_{2l;\mathrm{IIC}}$ is quite long and we not report here.

Two points function computation give us:

$$\begin{align} t\chi_2 &= \frac{u_6}{t}\int_{\mathbf{p},\mathbf{q}} V^{(3)}(\mathbf{p},\mathbf{q},-\mathbf{p}-\mathbf{q})^2\left[\frac{1}{2}\frac{V_3(\mathbf{p})V_3(\mathbf{q})}{\Delta(\mathbf{p})^2\Delta(\mathbf{q})^2\Delta(\mathbf{p}+\mathbf{q})}+\frac{1}{2}\frac{V_3(\mathbf{p})^2}{\Delta(\mathbf{p})^3\Delta(\mathbf{q})^2\Delta(\mathbf{p}+\mathbf{q})}\right. \nonumber\\ &\left.-\frac{1}{4}\frac{V_4(\mathbf{p})}{\Delta(\mathbf{p})^2\Delta(\mathbf{q})\Delta(\mathbf{p}+\mathbf{q})}\right]-\frac{V^{(3)}(\mathbf{p},\mathbf{q},-\mathbf{p}-\mathbf{q})V^{(4)}(\mathbf{p},\mathbf{q},-\mathbf{p}-\mathbf{q},\mathbf{0})V_3(\mathbf{p})}{\Delta(\mathbf{p})^2\Delta(\mathbf{q})\Delta(\mathbf{p}+\mathbf{q})} \nonumber\\ &+\frac{1}{6}\frac{V^{(4)}(\mathbf{p},\mathbf{q},-\mathbf{p}-\mathbf{q},\mathbf{0})^2}{\Delta(\mathbf{q})\Delta(\mathbf{p}+\mathbf{q})\Delta(\mathbf{p})}+\frac{1}{6}\frac{V^{(3)}(\mathbf{p},\mathbf{q},-\mathbf{p}-\mathbf{q})V^{(5)}(\mathbf{p},\mathbf{q},-\mathbf{p}-\mathbf{q},\mathbf{0},\mathbf{0})}{\Delta(\mathbf{p})\Delta(\mathbf{q})\Delta(\mathbf{p}+\mathbf{q})} \tag{2.122} \end{align}$$

and in the CCL:

$$\begin{align} t{\chi_2}^{2l;\mathrm{IIC}} &= \frac{u_6}{t}\left(\mathcal{A}^{(2)}_{2l;\mathrm{IIC}}-\frac{\mathcal{B}^{(2)}_{2l;\mathrm{IIC}}}{4\pi}\log\frac{t}{32}\right) \tag{2.123}\\ & \tag{2.124}\\ \mathcal{B}^{(2)}_{2l;\mathrm{IIC}} &= \frac{1}{2}\int_{\mathbf{p}}\frac{V_3(\mathbf{p})^2}{K(\mathbf{p})^2}\left({\alpha_3}^2+2\alpha_3\frac{V_3(\mathbf{p})}{K(\mathbf{p})}+3\frac{V_3(\mathbf{p})^2}{K(\mathbf{p})^2}\right)-\int_{\mathbf{p}}\frac{V_3(\mathbf{p})}{K(\mathbf{p})}\left(\frac{5}{2}\frac{V_4(\mathbf{p})V_3(\mathbf{p})}{K(\mathbf{p})^2}\right. \nonumber\\ &\left.+\alpha_3\frac{V_4(\mathbf{p})}{K(\mathbf{p})}+\frac{1}{4}\alpha_4\frac{V_3(\mathbf{p})}{K(\mathbf{p})}\right)+\frac{1}{2}\int_{\mathbf{p}}\frac{V_4(\mathbf{p})^2}{K(\mathbf{p})^2}+\frac{1}{2}\int_{\mathbf{p}}\frac{V_3(\mathbf{p})V_5(\mathbf{p})}{K(\mathbf{p})^2} \tag{2.125} \end{align}$$

also in this case we have reported explicitly only the *log* term of the previous expression.

2.2.3 Correction to u_{1c} and u_{2c} at two loop

In order to complete the two loop analysis we have to compute the contributions to χ_1 and to χ_2 of one loop diagrams with the insertion of counterterms u_{ci}. Then corrections to u_{c1} and u_{c2} are needed in order to delete non-scaling or non-universal terms. In the analysis of IA we have just used the logarithmic part of u_{ci} (U_1 and D_1) that will be neglected in this section. Using (2.75) (2.80) (2.83) (2.84) we have:

$$\chi_1^{1l;C} = -\frac{u_{3c}}{2t}\int_{\mathbf{p}}\frac{1}{K(\mathbf{p})+t}+{u_6}^{1/4}\frac{D_2+D_3}{2t}\int_{\mathbf{p}}\frac{V_3(\mathbf{p})}{\left(K(\mathbf{p})+t\right)^2} \tag{2.126}$$

and in the MCCL:

$$\begin{align} {\chi_1}^{1l;C} &= \frac{{u_6}^{3/4}}{t}\left(\mathcal{A}^{(1)}_{1l;C}-\frac{\mathcal{B}^{(1)}_{1l;C}}{4\pi}\log\frac{t}{32}\right) \tag{2.127}\\ \mathcal{A}^{(1)}_{1l;C} &= \frac{K_1}{4}\int_{\mathbf{p}}2\frac{V_3(\mathbf{p})^3}{K(\mathbf{p})^3}-3\frac{V_3(\mathbf{p})V_4(\mathbf{p})}{K(\mathbf{p})^2}+\frac{V_5(\mathbf{p})}{k(\mathbf{p})} \nonumber\\ &\qquad+\frac{\alpha_3}{4}\int_{\mathbf{p}}\left(\frac{V_3(\mathbf{p})^2}{K(\mathbf{p})^2}-\frac{V_4(\mathbf{p})}{K(\mathbf{p})}\right)\int_{\mathbf{q}}\left(\frac{V_3(\mathbf{q})}{K(\mathbf{q})^2}-\frac{\alpha_3}{\widehat{\mathbf{q}}^2}\right) \tag{2.128}\\ \mathcal{B}^{(1)}_{1l;C} &= \frac{1}{4}\int_{\mathbf{p}}2\frac{V_3(\mathbf{p})^3}{K(\mathbf{p})^3}-3\frac{V_3(\mathbf{p})V_4(\mathbf{p})}{K(\mathbf{p})^2}+\frac{V_5(\mathbf{p})}{k(\mathbf{p})}+\alpha_3\frac{V_3(\mathbf{p})^2}{K(\mathbf{p})^2}-\alpha_3\frac{V_4(\mathbf{p})}{K(\mathbf{p})} \tag{2.129} \end{align}$$

For χ_2 we have:

$$\begin{aligned}
{\chi_2}^{1l;C} &= -\frac{\sum_{i=2}^{6} Q_i}{2t^2}\int_{\mathbf{p}} \frac{1}{\Delta(\mathbf{p})} + \frac{u_{c3}u_6^{1/4}}{t^2}\int_{\mathbf{p}} \frac{V_3(\mathbf{p})}{\Delta(\mathbf{p})^2} - \frac{(D_2+D_3)u_6^{1/2}}{t^2}\int_{\mathbf{p}} \frac{V_3(\mathbf{p})^2}{\Delta(\mathbf{p})^3} \\
&\quad + \frac{(D_2+D_3)u_6^{1/2}}{t^2}\int_{\mathbf{p}} \frac{V_4(\mathbf{p})}{\Delta(\mathbf{p})^2} \qquad (2.130)
\end{aligned}$$

and in the MCCL limit:

$$\begin{aligned}
t{\chi_2}^{1l;C} &= \frac{u_6}{t}\left(\mathcal{A}^{(2)}_{1l;C} - \frac{\mathcal{B}^{(2)}_{1l;C}}{4\pi}\log\frac{t}{32}\right) \qquad (2.131) \\
\mathcal{A}^{(2)}_{1l;C} &= -\frac{\sum_{i=2}^{6} Q_i}{2u_6}K_1 + \frac{u_{c3}}{{u_6}^{3/4}}\int_{\mathbf{p}} \frac{V_3(\mathbf{p})}{K(\mathbf{p})^2} - \frac{\alpha_3}{\widehat{\mathbf{p}}^2} - \frac{\alpha_3 u_{c3}}{8\pi {u_6}^{3/4}} - \frac{D_2+D_3}{{u_6}^{1/2}}\int_{\mathbf{p}} \frac{V_3(\mathbf{p})^2}{K(\mathbf{p})^3} - \frac{{\alpha_3}^2}{\widehat{\mathbf{p}}^2} \\
&\quad + \frac{3}{8\pi}\frac{(D_2+D_3){\alpha_3}^2}{{u_6}^{1/2}} + \frac{D_2+D_3}{2{u_6}^{1/2}}\int_{\mathbf{p}} \frac{V_4(\mathbf{p})}{K(\mathbf{p})^2} - \frac{\alpha_4}{\widehat{\mathbf{p}}^2} - \frac{\alpha_4}{8\pi}\frac{D_2+D_3}{{u_6}^{1/2}} \qquad (2.132) \\
\mathcal{B}^{(2)}_{1l;C} &= -\frac{\sum_{i=2}^{6} Q_i}{2u_6} + \frac{u_{c3}\,\alpha_3}{{u_6}^{3/4}} - \frac{(D_2+D_3)\,{\alpha_3}^2}{{u_6}^{1/2}} + \frac{(D_2+D_3)\,\alpha_4}{2} \qquad (2.133)
\end{aligned}$$

where we have used (ref. to u_{ci}) At the end the only *log* correction comes from IA, while

$$\begin{aligned}
u_{c2}^{2l} &= -u_6\left(\mathcal{A}^{(2)}_{\mathrm{2l;IB}} + \mathcal{A}^{(2)}_{\mathrm{2l;IIC}} + \mathcal{A}^{(2)}_{\mathrm{1l;C}}\right) - \frac{u_6}{16\pi}\log 32x_6\left(K_1 - \frac{1}{4\pi}\log u_6\right) \qquad (2.134) \\
u_{c1}^{2l} &= -{u_6}^{3/4}\left(\mathcal{A}^{(1)}_{\mathrm{2l;IB}} + \mathcal{A}^{(1)}_{\mathrm{2l;IIC}} + \mathcal{A}^{(1)}_{\mathrm{1l;C}}\right) \qquad (2.135)
\end{aligned}$$

where we have used the fact that:

$$\begin{aligned}
0 &= \mathcal{B}^{(2)}_{\mathrm{2l;IB}} + \mathcal{B}^{(2)}_{\mathrm{2l;IIC}} + \mathcal{B}^{(2)}_{\mathrm{1l;C}} \qquad (2.136) \\
0 &= \mathcal{B}^{(1)}_{\mathrm{2l;IB}} + \mathcal{B}^{(1)}_{\mathrm{2l;IIC}} + \mathcal{B}^{(1)}_{\mathrm{1l;C}} \qquad (2.137)
\end{aligned}$$

The previous equalities are expected, indeed log terms come from the factorization of two loops integrals, so that the one-loop result is recovered.

2.2.4 Higher powers of the fields

We want to show that higher power of the fields in the starting interaction (2.63) does not affect the MCCL: indeed we want to give evidence of the fact that including higher power vertices the scaling equations (2.67) and the critical parameters u_{ci} do not change. In order to do that we have to show that every diagram, in which a more than six leg vertex appear, is suppressed in the MCCL. Let us consider an extra term in the Hamiltonian (2.63):

$$\Delta\mathcal{H} = \sum_{j>6} {u_6}^{(j-2)/4}\int\frac{d\mathbf{p}_1}{(2\pi)^2}\cdots\int\frac{d\mathbf{p}_j}{(2\pi)^2}\delta(\mathbf{p}_1+\cdots\mathbf{p}_j)[v_j + V^{(j)}(\mathbf{p}_1,\cdots\mathbf{p}_j)] \qquad (2.138)$$

At tree-level we have the following additional contributions $\Delta\chi_n$ to χ_n:

$$t^{n-1}\Delta\chi_n \sim \frac{{u_6}^{(j-2)/4}}{t} \sim {u_6}^{(j-6)/4} \qquad (2.139)$$

so that the contributions are null in the MCCL.

The generalization to one and two loops diagrams is direct. Suppose to have a diagram $\mathcal{G}_n$ with n-external legs and *at least* a vertex $V^{(j)}$ with $j > 6$. $\tilde{\mathcal{G}}^*_{n-j+6}$ is the diagram obtained replacing $V^{(j)}$ in $\mathcal{G}_n$ with $V^{(6)}$ in such a way that the topology remains unchanged.[11] In the previous section we have shown that the general behaviour for a diagram in which a six-legs vertex is present $\tilde{\mathcal{G}}^*_{n-j+6}$ is:

$$\tilde{\mathcal{G}}^*_{n-j+6} \sim t^{1-(n-j+6)}(\tilde{A} + \tilde{B} \log u_6) \tag{2.140}$$

where $\tilde{A}$ and $\tilde{B}$ are constants. Otherwise the loop-structure of $\mathcal{G}_n$ is exactly the same as the loop structure of $\tilde{\mathcal{G}}^*_{n-j+6}$; it follows that

$$t^{n-1}\mathcal{G}_n \sim {u_6}^{(j-6)/4}(A + B \log u_6) \tag{2.141}$$

that shows that graphs with higher order vertex are suppressed in the MCCL.

In this section we have obtained similar results of sec. 2.1 for Multicritical interactions eq. (2.63). In particular several critical parameters can be defined (sec. 2.2.3) so that taking the multicritical crossover limit (2.53) the connected n-point correlation functions χ_n behave in a universal way (2.52). The universality property is not affected by lattice details [$V^{(j)}(\mathbf{p}, \cdots)$ in eq. (2.63)] or by higher order vertex sec. 2.2.4, but can be defined using only $\phi^{\mathcal{N}+3}$ field theory.

---

[11] This can be done cutting $j-6$ external lines of $V^{(j)}$ in $\mathcal{G}$. We note that this operation is always possible up to two loops.

Chapter 3

Large-N expansion of $O(N)$ models: the critical zero mode

In sec. 1.5 we have shown as the standard $1/N$ expansion fails for certain $O(N)$ models at the finite temperature phase transition. Indeed in the $1/N$ expansion severe infra-red divergences appear that cannot be resummed including corrections to the leading ($N = \infty$) order. This means that one –in principle– needs to consider all the $1/N$ orders. However the failure of the expansion is suggested because, using a symmetry argument [82], one expects an Ising behaviour (if $\mathcal{N} = 1$) for every N finite. However, we have just pointed out, as in principle there is also the problem of the $1/N$ expansion: in [11] the study of $O(N)$ models in one dimension points out that the $N = \infty$ limit is affected by unphysical phase transitions that strictly disappear when N is taken finite.[1]

This chapter is organised in the following way. In sec. (3.1) we discuss the effective interaction of the models with a critical mode (i.e. $\mathcal{N} = 1$). We will find an interaction similar to what introduced in the past chapter 2, so that introducing proper scaling fields, we will be able to describe the crossover between the Ising criticality with the Mean Field one. More interesting, we will present also some numerical results (for the correction to the $N = \infty$ critical temperature) for a pair of model considered in literature [82] [81]. For the mixed O(N)-RP^{N-1} model [81], there are no numerical evidences of the existence of a phase transition for $N = 3$; however we predict the possibility that for $N < N_c$ ($N_c \approx 100$, see sec. 3.5), the critical point disappears. On the other hand, for the model simulated in [82], there are strong evidence that for $N = 3$ the system undergoes a phase transition. Our numerical prediction for the non universal critical constant p_c seems to have the same magnitude order of that measured in [82], however the accordance is not very good due to the big difference between $p_c(\infty)$ (≈ 5, see [55]) and $p_c(3)$ (≈ 20, see [82]). More stringent check will come from other $\mathcal{N} = 1$ models (see chapter 5), for which simulations with several N are available [50]. We stress that this could be an important test for the scheme presented in this work, and due to its universal setting, it could be applied to all the model with Mean Field crossover.

---

[1] A phase transition (i.e. a singularity in the partition function) can appear only if infinite degrees of freedom appear in the system (Yang-Lee Theorem [21] [22]). This can be realised both with a (physical) thermodynamic limit $V \to \infty$ or taking the (unphysical) $N \to \infty$ limit.

3.1 Effective Hamiltonian for the zero mode

We have discussed in the first Chapter that, for the class of phase transitions we are interested in, the propagator P has a zero mode at the critical point. In order to understand the role of $1/N$ fluctuations, a careful treatment of the zero mode is required. For this purpose, we are now going to integrate out the massive modes, obtaining an effective Hamiltonian for the critical field ϕ. More precisely, we define

$$e^{-\mathcal{H}_{\text{eff}}[\phi]} = \int \prod_{xa} d\varphi_{xa} e^{-\mathcal{H}[\Phi]}. \tag{3.1}$$

The effective Hamiltonian $\mathcal{H}_{\text{eff}}[\phi]$ has the following expansion

$$\begin{aligned}\mathcal{H}_{\text{eff}}[\phi] &= \frac{1}{\sqrt{N}}\tilde{H}\phi(\mathbf{0}) + \frac{1}{2}\int_{\mathbf{p}} \phi(-\mathbf{p})\tilde{P}^{-1}(\mathbf{p})\phi(\mathbf{p}) \\ &+ \sum_{n=3} \frac{1}{n!}\frac{1}{N^{n/2-1}} \int_{\mathbf{p}_1}\cdots\int_{\mathbf{p}_n} \delta(\sum_i \mathbf{p}_i)\ \tilde{V}^{(n)}(\mathbf{p}_1,\ldots,\mathbf{p}_n)\phi(\mathbf{p}_1)\cdots\phi(\mathbf{p}_n),\end{aligned} \tag{3.2}$$

where vertices and propagator also depend on N and have an expansion of the form

$$\begin{aligned}\tilde{H} &= \sum_{m=0} \frac{1}{N^m}\tilde{H}_m, \\ \tilde{P}^{-1}(\mathbf{p}) &= \sum_{m=0} \frac{1}{N^m}\tilde{P}^{-1}_m(\mathbf{p}), \\ \tilde{V}^{(n)}(\mathbf{p}_1,\ldots,\mathbf{p}_n) &= \sum_{m=0} \frac{1}{N^m}\tilde{V}^{(n)}_m(\mathbf{p}_1,\ldots,\mathbf{p}_n).\end{aligned} \tag{3.3}$$

We report here the explicit expressions that we shall need in the following:

$$\tilde{H}_0 = \frac{1}{2}\int_{\mathbf{p}}\sum_{ab} \hat{V}_{1ab}(\mathbf{0},\mathbf{p},-\mathbf{p})\hat{P}_{ab}(\mathbf{p}), \tag{3.4}$$

$$\tilde{P}^{-1}_0(\mathbf{p}) = \hat{P}^{-1}_{11}(\mathbf{p}), \tag{3.5}$$

$$\begin{aligned}\tilde{P}^{-1}_1(\mathbf{p}) = \frac{1}{2}\int_{\mathbf{q}} \Bigg[&\sum_{ab} \hat{V}^{(4)}_{11ab}(\mathbf{p},-\mathbf{p},\mathbf{q},-\mathbf{q})\hat{P}_{ab}(\mathbf{q}) - \\ &\sum_{abcd} \hat{V}^{(3)}_{11a}(\mathbf{p},-\mathbf{p},\mathbf{0})\hat{P}_{ab}(\mathbf{0})\hat{V}^{(3)}_{bcd}(\mathbf{0},\mathbf{q},-\mathbf{q})\ \hat{P}_{cd}(\mathbf{q}) - \\ &\sum_{abcd} \hat{V}^{(3)}_{1ab}(\mathbf{p},\mathbf{q},-\mathbf{p}-\mathbf{q})\hat{V}^{(3)}_{1cd}(\mathbf{p},\mathbf{q},-\mathbf{p}-\mathbf{q})\hat{P}_{ac}(\mathbf{q})\hat{P}_{bd}(\mathbf{p}+\mathbf{q})\Bigg],\end{aligned} \tag{3.6}$$

$$\tilde{V}^{(3)}_0(\mathbf{p},\mathbf{q},\mathbf{r}) = \hat{V}^{(3)}_{111}(\mathbf{p},\mathbf{q},\mathbf{r}), \tag{3.7}$$

$$\begin{aligned}\tilde{V}^{(4)}_0(\mathbf{p},\mathbf{q},\mathbf{r},\mathbf{s}) &= \hat{V}^{(4)}_{1111}(\mathbf{p},\mathbf{q},\mathbf{r},\mathbf{s}) - \\ &\sum_{ab} \hat{V}^{(3)}_{11a}(\mathbf{p},\mathbf{q},-\mathbf{p}-\mathbf{q})\hat{V}^{(3)}_{11b}(\mathbf{r},\mathbf{s},-\mathbf{r}-\mathbf{s})\hat{P}_{ab}(\mathbf{p}+\mathbf{q}) + \text{two permutations},\end{aligned} \tag{3.8}$$

$$\tilde{V}^{(5)}_0(\mathbf{p},\mathbf{q},\mathbf{r},\mathbf{s},\mathbf{t}) = \hat{V}^{(5)}_{1111}(\mathbf{p},\mathbf{q},\mathbf{r},\mathbf{s},\mathbf{t}) -$$

$$\left[\sum_{ab}\hat{V}^{(3)}_{11a}(\mathbf{p},\mathbf{q},-\mathbf{p}-\mathbf{q})\hat{V}^{(4)}_{111b}(\mathbf{r},\mathbf{s},\mathbf{t},-\mathbf{r}-\mathbf{s}-\mathbf{t})\hat{P}_{ab}(\mathbf{p}+\mathbf{q})+9\text{ permutations}\right]+$$
$$\left[\sum_{abcd}\hat{V}^{(3)}_{11a}(\mathbf{p},\mathbf{q},-\mathbf{p}-\mathbf{q})\hat{V}^{(3)}_{1bc}(\mathbf{r},\mathbf{p}+\mathbf{q},\mathbf{s}+\mathbf{t})\hat{V}^{(3)}_{11d}(\mathbf{s},\mathbf{t},-\mathbf{s}-\mathbf{t})\times\right.$$
$$\left.\times\hat{P}_{ab}(\mathbf{p}+\mathbf{q})\hat{P}_{cd}(\mathbf{s}+\mathbf{t})+14\text{ permutations}\right], \tag{3.9}$$

where a, b, c, d run from 1 to 4 over the massive modes.

The vertices introduced above are not independent, but near the critical point can be related to the scaling fields introduced to parametrize the gap equation eq. (1.10). The identities presented in sec. 3.1.1 allow us to derive several relations among the effective vertices at the critical point. We have for $p = p_c$ and $m_0^2 = m_{0c}^2$

$$\tilde{P}_0^{-1}(\mathbf{0}) = \frac{\partial \tilde{P}_0^{-1}(\mathbf{0})}{\partial m_0^2} = 0, \tag{3.10}$$

$$\tilde{V}_0^{(3)}(\mathbf{0},\mathbf{0},\mathbf{0}) = 0, \tag{3.11}$$

$$\left[\frac{\partial}{\partial m_0^2}\tilde{V}_0^{(3)}(\mathbf{0},\mathbf{0},\mathbf{0})\right]^2 = \frac{\partial^2 \tilde{P}_0^{-1}(\mathbf{0})}{\partial (m_0^2)^2}\tilde{V}_0^{(4)}(\mathbf{0},\mathbf{0},\mathbf{0},\mathbf{0}). \tag{3.12}$$

Relations (3.10), (3.11) and (3.12) are the first step to show the effective interaction for the zero mode is a weakly coupled interaction studied in the previous chapter. On the other hand (3.10) clearly confirm that the standard $1/N$ expansion fails close to the critical point. Indeed, outside the critical point, $\tilde{P}_0^{-1}(\mathbf{p})$ is nonsingular and for large N it is enough to expand the interaction Hamiltonian in powers of $1/N$. On the other hand, this not possible at the critical point. Since also the three-leg vertex vanishes at zero momentum in this case, cf. eq. (3.11), the zero-momentum leading term is the quartic one. Since the coupling constant is proportional to $1/N$, the model effectively corresponds to a weakly coupled ϕ^4 theory. In order to have a stable ϕ^4 theory, we must also have $\tilde{V}_0^{(4)}(\mathbf{0},\mathbf{0},\mathbf{0},\mathbf{0}) > 0$. For a generic solution of the gap equations satisfying eq. (1.14), this is not *a priori* guaranteed. Note, however, that if $\tilde{V}_0^{(4)}(\mathbf{0},\mathbf{0},\mathbf{0},\mathbf{0}) < 0$, then, for $p = p_c$, we have $\tilde{P}_0^{-1}(\mathbf{0}) \approx a(m_0^2 - m_{0c}^2)^2$, with $a < 0$, as a consequence of eq. (3.12): the propagator has a *negative* mass for $N = \infty$. We believe—but we have not been able to prove—that such a phenomenon signals the fact that the solution we are considering is not the relevant one. We expect the existence of another solution of the gap equation (1.10) with a lower free energy.

In the previous chapter we have seen that the weakly coupled ϕ^4 theory shows an interesting crossover limit. If one neglects fluctuations it corresponds to tune p and m_0^2 so that $\tilde{H}$ and $\tilde{P}^{-1}(\mathbf{0})$ go to zero as $N \to \infty$, in such a way that $\tilde{H}N$ and $\tilde{P}^{-1}(\mathbf{0})N$ remain constant. In this limit, Ising behavior is observed when the two scaling variables go to zero, while mean-field behavior is observed in the opposite case. Fluctuations change the simple scaling forms reported above and one must consider two additive renormalization constants ($h_c(u)$ and $r_c(u)$, in chap. 2).

However in order to strictly apply the results of the previous chapter (including also the computation of the renormalization constants with the lattice regularization) we need to impose the condition $V^{(3)}(\mathbf{0},\mathbf{0},\mathbf{0}) = 0$ for every values of the parameters, while in the case under investigation this happens only near the critical point (3.11).[2] In order to do that we change again the definition of the field so that the effective zero-momentum three-leg vertex vanishes for all p and m_0^2 in the limit $N \to \infty$. For this purpose we now define a new field

$$\alpha\chi(\mathbf{p}) = \phi(\mathbf{p}) + k\delta(\mathbf{p}), \tag{3.13}$$

where α and k are functions of p and m_0^2 to be fixed. The function k is fixed by requiring that the large-N zero-momentum three-leg vertex vanishes. Apparently, all $\tilde{V}^{(n)}$ contribute in this calculation. However, because of eq. (3.11), $\tilde{V}_0^{(3)}(\mathbf{0},\mathbf{0},\mathbf{0})$ vanishes at the critical point. As we already mentioned the interesting limit corresponds to considering $\Delta_m \equiv m_0^2 - m_{0c}^2 \to 0$ and $\Delta_p \equiv p - p_c \to 0$ together with $N \to \infty$. We will show in sec. 3.3 that this limit should be taken keeping fixed $\Delta_m N^{1/3}$ and $\Delta_p N$, so that $\tilde{V}_0^{(3)}(\mathbf{0},\mathbf{0},\mathbf{0})$ is effectively of order $N^{-1/3}$. Therefore, the equation defining k can be written in a compact form as

$$\frac{a_3}{N^{5/6}} + \sum_{n\geq 4} \frac{a_n k^{n-3}}{N^{n/2-1}} = 0, \tag{3.14}$$

where $a_n \approx a_{n0} + a_{n1}/N$ is the contribution of the n-point vertex at zero momentum. Eq. (3.14) can be rewritten as

$$\sum_{n=1}^{\infty} \frac{a_{n+3}}{N^{(n-1)/3}} \left(\frac{k}{N^{1/6}}\right)^n = -a_3 \tag{3.15}$$

which shows that k has an expansion of the form

$$k = k_0 N^{1/6}[1 + k_1 N^{-1/3} + O(N^{-2/3})]. \tag{3.16}$$

The leading constant k_0 depends only on the three- and four-leg vertex, the constant k_1 depends also on the five-leg vertex, and so on. The explicit calculation gives

$$\begin{aligned} k &= \sqrt{N}\frac{\tilde{V}_0^{(3)}(\mathbf{0},\mathbf{0},\mathbf{0})}{\tilde{V}_0^{(4)}(\mathbf{0},\mathbf{0},\mathbf{0},\mathbf{0})} + \\ &+ \frac{\sqrt{N}}{2}\frac{\tilde{V}_0^{(3)}(\mathbf{0},\mathbf{0},\mathbf{0})^2 \tilde{V}_0^{(5)}(\mathbf{0},\mathbf{0},\mathbf{0},\mathbf{0},\mathbf{0})}{[\tilde{V}_0^{(4)}(\mathbf{0},\mathbf{0},\mathbf{0},\mathbf{0})]^3} + O(N^{-1/2}). \end{aligned} \tag{3.17}$$

By performing this rescaling, the k-leg ϕ-vertex that scales with N as $N^{1-k/2}$ (except for $k \leq 3$) gives a contribution to the m-leg χ vertex (of course $m \leq k$) of order $N^{1-m/2+(m-k)/3}$, which is therefore always subleading. Taking this result into account we obtain

$$\begin{aligned} \mathcal{H}_{\rm eff} &= H\chi(\mathbf{0}) + \frac{1}{2}\int_{\mathbf{p}} \chi(\mathbf{p})\chi(-\mathbf{p})\bar{P}^{-1}(\mathbf{p}) + \\ &+ \frac{1}{3!\sqrt{N}}\int_{\mathbf{p},\mathbf{q}} \bar{V}^{(3)}(\mathbf{p},\mathbf{q},-\mathbf{p}-\mathbf{q})\chi(\mathbf{p})\chi(\mathbf{q})\chi(-\mathbf{p}-\mathbf{q}) \\ &+ \frac{1}{4!N}\int_{\mathbf{p},\mathbf{q},\mathbf{r}} \bar{V}^{(4)}(\mathbf{p},\mathbf{q},\mathbf{r},-\mathbf{p}-\mathbf{q}-\mathbf{r})\chi(\mathbf{p})\chi(\mathbf{q})\chi(\mathbf{r})\chi(-\mathbf{p}-\mathbf{q}-\mathbf{r}) + \ldots \end{aligned} \tag{3.18}$$

---

[2] However the fact that $V^{(3)}(\mathbf{0},\mathbf{0},\mathbf{0})$ goes to zero at the critical point is a fundamental topic in order to apply the following considerations. In particular this implies that k, defined in (3.13), can be computed perturbatively (3.17) near the critical point.

where

$$\begin{aligned}
H &= \frac{\alpha \tilde{H}_0}{\sqrt{N}} - \alpha k \left[\tilde{P}_0^{-1}(\mathbf{0}) + \frac{1}{N}\tilde{P}_1^{-1}(\mathbf{0})\right] + \frac{\alpha k^2}{2\sqrt{N}}\tilde{V}_0^{(3)}(\mathbf{0},\mathbf{0},\mathbf{0}) - \frac{\alpha k^3}{6N}\tilde{V}_0^{(4)}(\mathbf{0},\mathbf{0},\mathbf{0},\mathbf{0}) \\
&\qquad + \frac{\alpha k^4}{24N^{3/2}}\tilde{V}_0^{(5)}(\mathbf{0},\mathbf{0},\mathbf{0},\mathbf{0},\mathbf{0}) + O(N^{-7/6}), \\
\bar{P}^{-1}(\mathbf{p}) &= \alpha^2 \tilde{P}_0^{-1}(\mathbf{p}) + \frac{\alpha^2}{N}\tilde{P}_1^{-1}(\mathbf{p}) - \frac{\alpha^2 k}{\sqrt{N}}\tilde{V}_0^{(3)}(\mathbf{0},\mathbf{p},-\mathbf{p}) + \frac{\alpha^2 k^2}{2N}\tilde{V}_0^{(4)}(\mathbf{0},\mathbf{0},\mathbf{p},-\mathbf{p}) \\
&\qquad - \frac{\alpha^2 k^3}{6N^{3/2}}\tilde{V}_0^{(5)}(\mathbf{0},\mathbf{0},\mathbf{0},\mathbf{p},-\mathbf{p}) + O(N^{-4/3}), \\
\bar{V}^{(3)}(\mathbf{p},\mathbf{q},\mathbf{r}) &= \alpha^3 \tilde{V}_0^{(3)}(\mathbf{p},\mathbf{q},\mathbf{r}) - \frac{\alpha^3 k}{\sqrt{N}}\tilde{V}_0^{(4)}(\mathbf{0},\mathbf{p},\mathbf{q},\mathbf{r}) + O(N^{-2/3}), \\
\bar{V}^{(4)}(\mathbf{p},\mathbf{q},\mathbf{r},\mathbf{s}) &= \alpha^4 \tilde{V}_0^{(4)}(\mathbf{p},\mathbf{q},\mathbf{r},\mathbf{s}) + O(N^{-1/3}),
\end{aligned} \tag{3.19}$$

where $\alpha = \alpha_0 + \alpha_1 N^{-2/3} + O(N^{-4/3})$ is fixed by requiring that

$$\bar{P}^{-1}(\mathbf{p}) - \bar{P}^{-1}(\mathbf{0}) \equiv K(\mathbf{p}) \approx \mathbf{p}^2, \tag{3.20}$$

for $\mathbf{p} \to 0$.

3.1.1 Identities among effective vertices

In this section we wish to derive a general set of identities for the zero-momentum vertices in order to justify the relations introduced above (3.10,3.11,3.12). For this purpose we first rewrite the propagator and the vertices by considering the constants α, γ, and τ appearing in eq. (1.6) as independent variables *without* assuming the saddle-point relations. We define the integrals

$$\mathcal{A}_{ij,n}(\alpha,\gamma) = \int_{\mathbf{q}} \frac{\cos^i q_x \cos^j q_y}{(\gamma - \alpha \sum_\mu \cos q_\mu)^n}. \tag{3.21}$$

It is easy to verify that, if α and γ are replaced by their saddle-point values, $\alpha = 2W'(\bar{\tau})$ and $\gamma = (4 + m_0^2)W'(\bar{\tau})$, then

$$\mathcal{A}_{ij,n}(\alpha,\gamma) = \frac{1}{[W'(\bar{\tau})]^n} \int_{\mathbf{q}} \frac{\cos^i q_x \cos^j q_y}{(\hat{q}^2 + m_0^2)^n}. \tag{3.22}$$

In terms of α, γ, and τ the propagator is simply obtained by using eq. (1.57) and replacing $A_{i,j}(0,m_0^2)/[W'(\bar{\tau})]^2$ with $\mathcal{A}_{ij,2}(\alpha,\gamma)$. Let us now consider a generic n-leg vertex $V^{(n)}_{A_1,\ldots,A_n}$ at zero momentum. It is easy to verify that the only nonvanishing terms with $A_i = 4$ or $A_i = 5$ for some i are (in this section we do not explicitly write the momentum dependence since in all cases we are referring to zero-momentum quantities)

$$V^{(n)}_{4,\ldots 4} = V^{(n)}_{5,\ldots 5} = -\beta W^{(n)}(\tau)\ . \tag{3.23}$$

If all $A_i \le 3$, eq. (1.61) gives

$$V^{(n)}_{A_1,\ldots,A_n} = \frac{1}{2}(-1)^{i_2+i_3+n+1}(n-1)!\,\mathcal{A}_{i_2 i_3,n}(\alpha,\gamma), \tag{3.24}$$

where i_2 (resp. i_3) is the number of indices equal to 2 (resp. to 3). These expressions allow us to obtain simple recursion relations for the vertices.

$$\begin{aligned}
&V^{(n+1)}_{1,A_1,\dots,A_n} = \frac{\partial}{\partial\gamma} V^{(n)}_{A_1,\dots,A_n},\\
&V^{(n+1)}_{2,A_1,\dots,A_n} + V^{(n+1)}_{3,A_1,\dots,A_n} = \frac{\partial}{\partial\alpha} V^{(n)}_{A_1,\dots,A_n},\\
&V^{(n+1)}_{4,4,\dots,4} = \frac{\partial}{\partial\tau} V^{(n)}_{4,\dots,4},\\
&V^{(n+1)}_{5,5,\dots,5} = \frac{\partial}{\partial\tau} V^{(n)}_{5,\dots,5},
\end{aligned} \tag{3.25}$$

where α, γ, τ, and β are considered as independent variables. These relations also apply to the case $n = 2$, once we identify $V^{(2)}_{AB} = P^{-1}_{AB}$.

Let us consider the projector on the zero mode v_A, cf. eq. (1.70). Keeping into account that the symmetry of the matrix at zero momentum implies $v_2 = v_3$ and $v_4 = v_5$, we obtain

$$\sum_B v_B V^{(n+1)}_{B,A_1,\dots,A_n} = \left(v_1 \frac{\partial}{\partial\gamma} + v_2 \frac{\partial}{\partial\alpha} + v_4 \frac{\partial}{\partial\tau} \right) V^{(n)}_{A_1,\dots,A_n}. \tag{3.26}$$

Close to the critical point we can write, cf. eq. (1.66),

$$v_A = \hat{z}_A + O(s_1) \tag{3.27}$$

with

$$\hat{z}_A = K \left(2\frac{\mathcal{A}_{01,2}}{\mathcal{A}_{00,2}}, 1, 1, \frac{1}{2W''(\tau)}, \frac{1}{2W''(\tau)} \right), \tag{3.28}$$

where K is such to have $\sum_B \hat{z}_B^2 = 1$. Now, let us note that at the saddle point we have (we now think of α, τ, and γ as functions of m_0^2 and p)

$$\begin{aligned}
\frac{\partial\gamma}{\partial m_0^2} &= W'' \frac{\partial\tau}{\partial m_0^2} \left(4 + m_0^2 - \frac{B_1}{B_2} \right) + O(s_1) = \frac{2W''}{K} \frac{\partial\tau}{\partial m_0^2} \hat{z}_1 + O(s_1),\\
\frac{\partial\alpha}{\partial m_0^2} &= 2W'' \frac{\partial\tau}{\partial m_0^2} = \frac{2W''}{K} \frac{\partial\tau}{\partial m_0^2} \hat{z}_2 + O(s_1),
\end{aligned} \tag{3.29}$$

where we have used eqs. (1.65) and (1.59). Thus, if we define

$$C \equiv \left(\frac{2W''}{K} \frac{\partial\tau}{\partial m_0^2} \right)^{-1}, \tag{3.30}$$

we can rewrite

$$\begin{aligned}
\sum_B v_B V^{(n+1)}_{B,A_1,\dots,A_n} &= C \left(\frac{\partial\gamma}{\partial m_0^2} \frac{\partial}{\partial\gamma} + \frac{\partial\alpha}{\partial m_0^2} \frac{\partial}{\partial\alpha} + \frac{\partial\tau}{\partial m_0^2} \frac{\partial}{\partial\tau} \right) V^{(n)}_{A_1,\dots,A_n} + O(s_1)\\
&= C \frac{\partial}{\partial m_0^2} V^{(n)}_{A_1,\dots,A_n} + O(s_1),
\end{aligned} \tag{3.31}$$

where in the last term α, γ, τ, and β take their saddle-point values in terms of m_0^2 and p.

To go further we compute the derivative of $\hat{z}_A$ with respect to m_0^2. Since

$$\sum_B P^{-1}_{AB}\hat{z}_B = O(s_1), \tag{3.32}$$

we have

$$\sum_B P^{-1}_{AB}\frac{\partial \hat{z}_B}{\partial m_0^2} = -\sum_B \frac{\partial P^{-1}_{AB}}{\partial m_0^2}\hat{z}_B + O(s_2), \tag{3.33}$$

where $s_2 = \partial^2\beta/\partial(m_0^2)^2$ also vanishes at the critical point.

Since $\sum_A \hat{z}_A^2 = 1$, $\partial\hat{z}_B/\partial m_0^2$ belongs to the subspace orthogonal to $\hat{z}_A$. Thus, if $P^{\perp}_{AB}$ is the inverse of P^{-1} in the massive subspace, we obtain

$$\frac{\partial \hat{z}_A}{\partial m_0^2} = -\sum_{BC} P^{\perp}_{AB}\frac{\partial P^{-1}_{BC}}{\partial m_0^2}\hat{z}_C + O(s_2) = -\frac{1}{C}\sum_{BCD} P^{\perp}_{AB}V^{(3)}_{BCD}\hat{z}_C\hat{z}_D + O(s_2). \tag{3.34}$$

Finally, let us compute

$$\begin{aligned}
\hat{V}^{(n+1)}_{1,\dots 1} &= C\sum_{A_1,\dots,A_n} z_{A_1}\dots z_{A_n}\frac{\partial}{\partial m_0^2}V^{(n)}_{A_1,\dots,A_n} + O(s_1) \\
&= C\frac{\partial}{\partial m_0^2}\hat{V}^{(n)}_{1,\dots 1} - nC\sum_{A_1,\dots,A_n} z_{A_1}\dots z_{A_{n-1}}V^{(n)}_{A_1,\dots,A_n}\frac{\partial z_{A_n}}{\partial m_0^2} + O(s_1) \\
&= C\frac{\partial}{\partial m_0^2}\hat{V}^{(n)}_{1,\dots 1} + n\sum_{ab}\hat{V}^{(3)}_{11a}\hat{P}_{ab}\hat{V}^{(n)}_{b1\dots 1} + O(s_2),
\end{aligned} \tag{3.35}$$

where the indices a and b run from 1 to 4 over the massive subspace. Since s_2 is of order $p-p_c$ and $m_0^2 - m_{0c}^2$ this relation implies an identity only at the critical point. However, for $n = 2$ we can obtain another relation. Since $V^{(2)}_{AB} = P^{-1}_{AB}$ and $\sum_B P^{-1}_{AB}z_B = O(s_1)$ we do not need eq. (3.34) and obtain directly

$$\hat{V}_{111} = C\frac{\partial}{\partial m_0^2}P^{-1}_{11} + O(s_1). \tag{3.36}$$

The presence of corrections of order s_1 gives rise to two critical-point identities. Since $P^{-1}_{11} \sim s_1$ we obtain

$$\begin{aligned}
\hat{V}_{111} &= 0, \\
\frac{\partial}{\partial m_0^2}\hat{V}_{111} &= C\frac{\partial^2}{\partial(m_0^2)^2}P^{-1}_{11},
\end{aligned} \tag{3.37}$$

where all quantities are computed at the critical point.

3.2 Critical crossover limit in the large-N case

The main result of the previous section 3.1 is the identification of the zero mode Hamiltonian with the weakly coupled theory introduced in the previous chapter (2.2). One can work in order to apply the same results of chapter 2 by using the following identifications

$$\begin{aligned} &\text{chapter 2} && \text{chapter 3} \\ u &= && \frac{1}{N}\overline{V}^{(4)}(\mathbf{0},\mathbf{0},\mathbf{0},\mathbf{0}) && (3.38)\\ V^{(n)}(\mathbf{p}_1,\cdots\mathbf{p}_n) &= && \frac{\overline{V}^{(n)}(\mathbf{p}_1\cdots\mathbf{p}_n)}{\overline{V}^{(4)}(\mathbf{0},\mathbf{0},\mathbf{0},\mathbf{0})^{\frac{n-2}{2}}} && (3.39)\\ K(\mathbf{p}) &= && \overline{P}(\mathbf{p})-\overline{P}(\mathbf{0}) && (3.40)\\ r &= && \overline{P}(\mathbf{0}) && (3.41)\\ H &= && \overline{H} && (3.42) \end{aligned}$$

so that the normalization conditions assumed in sec. (2.1) are satisfied. In particular one can obtain the mass- and the magnetic-term regularisation (r_c and h_c) in the large N limit, using the function $h_c(u)$ and $r_c(u)$ obtained in the previous chapter[3] for the lattice regularisation using u defined in eq. (3.38).

However in our large-N case we have to take into the mind that the propagator and the vertices of the theory are function of $\Delta_m \equiv m_0^2 - m_{0c}^2$ and of $\Delta_p \equiv p - p_c$, and moreover all quantities, beside r and H, depend on these two variables. We have seen in the previous chapter that the Critical Crossover Limit (CCL) is defined having fixed two scaling variables x_t and x_h

$$x_t = N\frac{P(\mathbf{0})-r_c(u)}{\overline{V}^{(4)}(\mathbf{0},\mathbf{0},\mathbf{0},\mathbf{0})} \qquad (3.43)$$

$$x_h = N\frac{\overline{H}-h_c(u)}{\overline{V}^{(4)}(\mathbf{0},\mathbf{0},\mathbf{0},\mathbf{0})} \qquad (3.44)$$

Expanding the previous couple of equations (3.43,3.44) near the critical point one can obtain Δ_m and Δ_p as function of x_t x_h and N. As we will show in the next section Δ_m and Δ_p scale respectively as $1/N^{1/3}$ and $1/N$, so that we can assume an additional dependence on $u^{1/3}$ for the vertices, the propagator and the counterterms of the theory: i.e. we consider $K(\mathbf{p}; u^{1/3})$ and $V^{(k)}(\mathbf{p}_1,\ldots,\mathbf{p}_k; u^{1/3})$. Note that, by definition, $K(\mathbf{0}; u^{1/3}) = 0$ for all values of u. Moreover, we assume, as in the case of interest, that $V^{(3)}(\mathbf{0},\mathbf{0},\mathbf{0}; u^{1/3}) = 0$ for all values of u. Following the calculation presented in sec. 2.1.1, it is easy to realize that the dependence of the vertices on u is irrelevant except in $h_c(u)$. In this case, eq. (2.15) becomes

$$\frac{t}{u}\chi_1 = -\frac{h_c(u)}{u} - \frac{1}{2\sqrt{u}}\int_{\mathbf{p}} \frac{V_3(\mathbf{p}; u^{1/3})}{K(\mathbf{p}; u^{1/3})+t} + O(\sqrt{u}). \qquad (3.45)$$

Because of the prefactor $1/\sqrt{u}$ we must take here into account the first correction proportional to $u^{1/3}$. Thus, if $V_3(\mathbf{p}; u^{1/3}) \approx V_{3,0}(\mathbf{p}) + u^{1/3}V_{3,1}(\mathbf{p})$ and $K(\mathbf{p}; u^{1/3}) \approx K_0(\mathbf{p}) + u^{1/3}K_1(\mathbf{p})$, we obtain

$$\frac{t}{u}\chi_1 = -\frac{h_c(u)}{u} - \frac{1}{2\sqrt{u}}\int_{\mathbf{p}} \left[\frac{V_{3,0}(\mathbf{p}) + u^{1/3}V_{3,1}(\mathbf{p})}{K_0(\mathbf{p})+t} - \frac{u^{1/3}V_{3,0}(\mathbf{p})K_1(\mathbf{p})}{(K_0(\mathbf{p})+t)^2}\right] + O(u^{1/6}). \qquad (3.46)$$

---

[3] $r_c(u)$ and $h_c(u)$ are given by eq. (2.47) and by eq. (2.17).

Now, t can be set to zero without generating infrared divergences, neglecting corrections of order $u^{-1/2} t \ln t \sim u^{1/2} \ln u$. It follows

$$h_c(u) = -\frac{\sqrt{u}}{2} \int_{\mathbf{p}} \left[\frac{V_{3,0}(\mathbf{p})}{K_0(\mathbf{p})} + u^{1/3} \frac{V_{3,1}(\mathbf{p}) K_0(\mathbf{p}) - V_{3,0}(\mathbf{p}) K_1(\mathbf{p})}{K_0(\mathbf{p})^2} \right]. \tag{3.47}$$

Eq. (3.47) represents the only equation in which the explicit dependence of the vertices on Δ_m should be considered (Δ_p is proportional to u and thus it can always be set to zero). In all other cases, we can simply set $\Delta_m = \Delta_p = 0$.

3.3 Crossover between mean-field and Ising behavior

In this section we wish to apply the above-reported results for the critical crossover limit to the Hamiltonian (3.18) of the zero mode. With the identification (3.38-3.42) the effective Hamiltonian (3.2) corresponds to the Hamiltonian discussed in sec. 2.1.

We begin by reporting the additive renormalization constants. The mass renormalization constant is given by, cf. eqs. (2.47),

$$\begin{aligned} r_c(N) &= \frac{u}{8\pi} \ln\left(\frac{3u}{256\pi}\right) - \frac{u}{8\pi}(3 + 8\pi D_2) \\ &+ \frac{u}{2} \int_{\mathbf{p}} \left\{ \frac{[\bar{V}^{(3)}(\mathbf{0},\mathbf{p},-\mathbf{p})]^2}{\bar{V}^{(4)}(\mathbf{0},\mathbf{0},\mathbf{0},\mathbf{0}) K(\mathbf{p})^2} - \frac{\bar{V}^{(4)}(\mathbf{0},\mathbf{0},\mathbf{p},-\mathbf{p})}{\bar{V}^{(4)}(\mathbf{0},\mathbf{0},\mathbf{0},\mathbf{0}) K(\mathbf{p})} + \frac{1}{\hat{p}^2} \right\}, \end{aligned} \tag{3.48}$$

where D_2 is a nonperturbative constant defined in Ref. [32] (numerically $D_2 \approx -0.052$). As discussed in sec. 3.2, we can compute all quantities appearing in eq. (3.48) at the critical point and keep only the leading terms for $N \to \infty$. We thus obtain

$$\begin{aligned} r_c(N) &= \frac{u}{8\pi} \ln\left(\frac{3u}{256\pi}\right) - \frac{u}{8\pi}(3 + 8\pi D_2) \qquad (3.49) \\ &+ \frac{\alpha^2}{2N} \int_{\mathbf{p}} \left\{ [\tilde{V}_0^{(3)}(\mathbf{0},\mathbf{p},-\mathbf{p}) \tilde{P}_0(\mathbf{p})]^2 - \tilde{V}_0^{(4)}(\mathbf{0},\mathbf{0},\mathbf{p},-\mathbf{p}) \tilde{P}_0(\mathbf{p}) + \frac{\alpha^2}{\hat{p}^2} \tilde{V}_0^{(4)}(\mathbf{0},\mathbf{0},\mathbf{0},\mathbf{0}) \right\}, \end{aligned}$$

where all quantities are computed at the critical point.

Analogously, we should introduce a counterterm for the magnetic field:

$$h_c(N) = -\frac{1}{2}\sqrt{u} \int_{\mathbf{p}} \frac{\bar{V}^{(3)}(\mathbf{0},\mathbf{p},-\mathbf{p})}{[\bar{V}^{(4)}(\mathbf{0},\mathbf{0},\mathbf{0},\mathbf{0})]^{1/2} K(\mathbf{p})}. \tag{3.50}$$

As discussed in sec. 3.2, such a quantity should not be simply computed at the critical point, but one should also take into account the additional corrections of order $N^{-1/3}$. Since $k \sim O(N^{1/6})$ in the critical crossover limit, we have

$$\begin{aligned} h_c(N) &= -\frac{\alpha}{2\sqrt{N}} \int_{\mathbf{p}} \left[\tilde{V}_0^{(3)}(\mathbf{0},\mathbf{p},-\mathbf{p}) - \frac{\tilde{V}_0^{(3)}(\mathbf{0},\mathbf{0},\mathbf{0})}{\tilde{V}_0^{(4)}(\mathbf{0},\mathbf{0},\mathbf{0},\mathbf{0})} \tilde{V}_0^{(4)}(\mathbf{0},\mathbf{0},\mathbf{p},-\mathbf{p}) \right] \frac{1}{\tilde{P}_0^{-1}(\mathbf{p}) - \tilde{P}_0^{-1}(\mathbf{0})} \\ &- \frac{\alpha}{2\sqrt{N}} \frac{\tilde{V}_0^{(3)}(\mathbf{0},\mathbf{0},\mathbf{0})}{\tilde{V}_0^{(4)}(\mathbf{0},\mathbf{0},\mathbf{0},\mathbf{0})} \int_{\mathbf{p}} [\tilde{V}_0^{(3)}(\mathbf{0},\mathbf{p},-\mathbf{p}) \tilde{P}_0(\mathbf{p})]^2. \end{aligned} \tag{3.51}$$

The second integral should be computed at the critical point, while the first one and the prefactor of the second one should be expanded around the critical point. Since, as we shall show below, $\Delta_m \equiv m_0^2 - m_{0c}^2 \sim N^{-1/3}$ and $p - p_c \sim N^{-1}$, it is enough to compute the first correction in Δ_m. In practice, we find that the renormalization terms have the form

$$\begin{aligned} r_c(N) &= \frac{1}{N}(r_{c0}\ln N + r_{c1}), \\ h_c(N) &= \frac{1}{\sqrt{N}}(h_{c0} + \Delta_m h_{c1}). \end{aligned} \tag{3.52}$$

Once $r_c(N)$ and $h_c(N)$ are computed, we can define the scaling variables $x_t \sim t/u$ and $x_h \sim h/u$. Choosing the normalizations appropriately for later convenience, we define

$$\begin{aligned} x_t &\equiv \frac{N}{\alpha^2}[\bar{P}^{-1}(0) - r_c(N)], \\ x_h &\equiv \frac{N}{\alpha}[H - h_c(N)]. \end{aligned} \tag{3.53}$$

Now, the critical crossover limit is obtained by tuning p and m_0^2 around the critical point in such a way that x_t and x_h are kept constant, i.e. $p \to p_{\text{crit}}$, $m_0^2 \to m_{0,\text{crit}}^2$, $N \to \infty$ at fixed x_t and x_h. Note that here p_{crit} and $m_{0,\text{crit}}^2$ correspond to the position of the critical point as a function of N (thus $p_{\text{crit}} \to p_c$ and $m_{0,\text{crit}}^2 \to m_{0c}^2$ as $N \to \infty$) and are obtained by requiring $x_t = x_h = 0$ (cf. sec. 2.1.4).

In order to compute the relation between p, m_0^2 and x_t, x_h we set $\Delta_m \equiv m_0^2 - m_{0c}^2$ and $\Delta_p \equiv p - p_c$ and expand eq. (3.53) in powers of Δ_m and Δ_p. In the following we shall show that $\Delta_m \sim N^{-1/3}$ and $\Delta_p \sim N^{-1}$, so that the relevant terms are

$$x_t = N(b_{t0}\Delta_p + b_{t1}\Delta_p\Delta_m + b_{t2}\Delta_m^3) + d_1 \ln N + d_2 \tag{3.54}$$

$$\begin{aligned} x_h = {} & N^{3/2}(b_{h0}\Delta_p^2 + b_{h1}\Delta_p\Delta_m + b_{h2}\Delta_p\Delta_m^2 + b_{h3}\Delta_m^3 + b_{h4}\Delta_m^4) + \\ & + N^{1/2}(d_{30} + d_{31}\Delta_m). \end{aligned} \tag{3.55}$$

The constants are obtained by expanding $\bar{P}^{-1}(\mathbf{0})$ and H around the critical point and by using the expansions (3.52). All quantities are analytic in Δ_m and Δ_p and several terms are absent because of identities (3.10), (3.11), and (3.12). In particular, a term proportional to Δ_m^2 is absent in the equation for x_t. This is a consequence of eq. (3.12). Indeed, we have

$$\begin{aligned} \frac{1}{\alpha^2}\bar{P}^{-1}(\mathbf{0}) &= \tilde{P}_0^{-1}(\mathbf{0}) - \frac{[\tilde{V}_0^{(3)}(\mathbf{0},\mathbf{0},\mathbf{0})]^2}{2\tilde{V}_0^{(4)}(\mathbf{0},\mathbf{0},\mathbf{0},\mathbf{0})} + O(\Delta_m^3, N^{-1}) \\ &= \frac{1}{2}\left[\frac{\partial^2 \tilde{P}_0^{-1}(\mathbf{0})}{\partial(m_0^2)^2} - \frac{1}{\tilde{V}_0^{(4)}(\mathbf{0},\mathbf{0},\mathbf{0},\mathbf{0})}\left(\frac{\partial}{\partial m_0^2}\tilde{V}_0^{(3)}(\mathbf{0},\mathbf{0},\mathbf{0})\right)^2\right]\Delta_m^2 + O(\Delta_m^3, N^{-1}) \\ &= 0 + O(\Delta_m^3, N^{-1}), \end{aligned} \tag{3.56}$$

where in the last step we have used eq. (3.12).

We wish now to determine the behavior of Δ_m and Δ_p that is fixed by eqs. (3.54) and (3.55). We assume

$$\Delta_m = \frac{\delta_{m0}}{N^\alpha}, \qquad \Delta_p = \frac{\delta_{p0}}{N^\beta}, \tag{3.57}$$

where δ_{m0} and δ_{p0} are nonvanishing constants and α and β exponents to be determined. If $\beta < 1$, eq. (3.54) implies

$$b_{t0}\delta_{p0}N^{1-\beta} + b_{t2}\delta_{m0}N^{1-3\alpha} = o(N^{1-\beta}), \tag{3.58}$$

which requires $\beta = 3\alpha$. Now, consider eq. (3.55). The term $N^{3/2}\Delta_m^3$ is of order $N^{3/2-\alpha}$ and cannot be made to vanish. Therefore, we must have $\beta \geq 1$. Considering again eq. (3.55), it is easy to see that all terms containing Δ_p cannot increase as fast as $N^{1/2}$. Therefore, cancellation of the term $d_{30}N^{1/2}$ requires $\alpha = 1/3$. Consideration of eq. (3.54) implies finally $\beta = 1$. This analysis can be extended to the subleading corrections, obtaining an expansion of the form

$$\begin{aligned}
\Delta_m &= \frac{\delta_{m0}}{N^{1/3}} + \frac{\delta_{m1}}{N^{2/3}} + \frac{\delta_{m2}}{N^{5/6}}, + O(N^{-1}) \\
\Delta_p &= \frac{\delta_{p0}}{N} + \frac{\delta_{p1}}{N^{7/6}} + O(N^{-4/3}).
\end{aligned} \tag{3.59}$$

The coefficients are given by

$$\begin{aligned}
\delta_{m0} &= -\left(\frac{d_{30}}{b_{h3}}\right)^{1/3}, \\
\delta_{m1} &= \frac{\delta_{m0}^2}{3b_{t0}d_{30}}\left[b_{t0}d_{31} - b_{h1}(d_1 \ln N + d_2)\right] + \frac{b_{h1}\delta_{m0}^2}{3b_{t0}d_{30}}x_t + \\
&\quad + \frac{\delta_{m0}^5}{3b_{t0}d_{30}}(b_{h4}b_{t0} - b_{h1}b_{t2}), \\
\delta_{p0} &= -\frac{1}{b_{t0}}\left(\delta_{m0}^3 b_{t2} + d_1 \ln N + d_2 - x_t\right).
\end{aligned} \tag{3.60}$$

We are not able to compute δ_{m2} and δ_{p1} but we can however compute a relation between these two quantities. We obtain

$$\delta_{p1} = -\frac{3\delta_{m0}\delta_{m2}b_{h3}}{b_{h1}} + \frac{1}{b_{h1}\delta_{m0}}x_h. \tag{3.61}$$

Correspondingly, by using eq. (1.21), we can compute the expansion of u_h:

$$u_h = \frac{u_{h0}}{N} + \frac{u_{h1}}{N^{4/3}} + \frac{u_{h2}}{N^{3/2}}, \tag{3.62}$$

where u_{h1} depends on x_t and u_{h2} on x_h. We thus define a new scaling field by requiring that no term proportional to $x_tN^{-4/3}$ is present. For this purpose we set

$$\hat{u}_h = u_h + \frac{x_{\text{mix}}}{N^{1/3}}(p - p_c) \tag{3.63}$$

where the coefficient x_{mix} is given by

$$x_{\text{mix}} = \frac{(a_{03}b_{h1} - a_{11}b_{h3})\delta_{m0}}{b_{h3}}. \tag{3.64}$$

The new scaling field has an expansion of the form

$$\hat{u}_h = \frac{\hat{u}_{h0}}{N} + \frac{\hat{u}_{h1}}{N^{4/3}} + \frac{\hat{u}_{h2}}{N^{3/2}}, \tag{3.65}$$

where

$$\begin{aligned} \hat{u}_{h0} &= a_{03}\delta_{m0}^3, &(3.66)\\ \hat{u}_{h1} &= \frac{\delta_{m0}}{b_{h3}}[-a_{03}d_{31} + (a_{04}b_{h3} - a_{03}b_{h4})\delta_{m0}^3] &(3.67)\\ \hat{u}_{h2} &= \frac{a_{03}}{b_{h3}}x_h. &(3.68) \end{aligned}$$

Interestingly enough, in $\hat{u}_{h2}$ all terms proportional to the unknown quantity δ_{m2} cancel. At this point we can easily compute the $1/N$ expansion of the critical point p_{crit}, β_{crit}. It is enough to set $x_h = x_t = 0$ in the previous expansions, obtaining

$$\begin{aligned} p_{\text{crit}} &= p_c + \left.\frac{\delta_{p0}}{N}\right|_{x_t=0} + O(N^{-7/6}), &(3.69)\\ \beta_{\text{crit}} &= \beta_c + \frac{\hat{u}_{h0} + a_{10}\delta_{p0}|_{x_t=0}}{N} + O(N^{-7/6}). &(3.70) \end{aligned}$$

It follows that

$$\begin{aligned} p - p_{\text{crit}} &\approx \left(-\frac{2}{3}\frac{b_{t1}b_{h1}\delta_{m0}^2}{d_{30}} + 1\right)\frac{x_t}{b_{t0}N}, &(3.71)\\ \hat{u}_h - \hat{u}_{h,\text{crit}} &\approx \frac{3a_{03}b_{t0} - a_{11}b_{t1}}{3b_{h3}b_{t0} - b_{h1}b_{t1}}\frac{x_h}{N^{3/2}}, &(3.72) \end{aligned}$$

where $\hat{u}_{h,\text{crit}}$ is the value of $\hat{u}_h$ at the critical point. Therefore, the $1/N$ corrections modify the position of the critical point and change the magnetic scaling field which should now be identified with $\bar{u}_h = \hat{u}_h - \hat{u}_{h,\text{crit}}$ (as we already discussed the thermal magnetic field is not uniquely defined and we take again $p - p_{\text{crit}}$). Eqs. (3.71) and (3.72) also indicate which are the correct scaling variables. Ising behavior is observed only if $N(p - p_{\text{crit}})$ and $N^{3/2}(\hat{u}_h - \hat{u}_{h,\text{crit}})$ are both small; in the opposite case mean-field behavior is observed. Therefore, as N increases the width of the critical region decreases, and no Ising behavior is observed at $N = \infty$ exactly.

3.4 Critical behavior of $\langle \boldsymbol{\sigma}_x \cdot \boldsymbol{\sigma}_{x+\mu} \rangle$

In this section we wish to compute the large-N behavior of

$$\overline{E} = \langle \boldsymbol{\sigma}_x \cdot \boldsymbol{\sigma}_{x+\mu} \rangle. \tag{3.73}$$

Such a quantity does not coincide with the energy. However, as far as the critical behavior is concerned, there should not be any significant difference. In order to perform the computation, note that the equations of motion for the field $\lambda_{x\mu}$ give

$$\langle \rho_{x\mu} \rangle = 1 + \overline{E}. \tag{3.74}$$

Thus, we have

$$\overline{E} = \tau - 1 + \frac{1}{\sqrt{N}} \langle \hat{\rho}_{x\mu} \rangle = \tau - 1 + \frac{1}{\sqrt{N}} \sum_B U_{4B}(\mathbf{0}) \langle \Phi_{Bx} \rangle. \tag{3.75}$$

Therefore, we need to compute the correlations $\langle \phi \rangle$ and $\langle \varphi_a \rangle$. For the zero mode we have immediately

$$\langle \phi_x \rangle = \alpha \langle \chi_x \rangle - k = \frac{\alpha}{x_t} f_1^{\rm symm}(x_t, x_h) - k, \tag{3.76}$$

where $f_1^{\rm symm}(x_t, x_h)$ is the crossover function for the magnetization in the Ising model and the constant k diverges as $N^{1/6}$, modulo some obvious normalizations.

Let us now consider $\langle \varphi_a \rangle$ and show that such a correlation vanishes as $N \to \infty$ in the critical crossover limit. Indeed, we can write

$$\begin{aligned} \langle \varphi_a \rangle &= \frac{1}{\sqrt{N}} \hat{P}_{ab}(\mathbf{0}) \int_{\mathbf{p}} [\hat{V}_{bcd}(\mathbf{0}, \mathbf{p}, -\mathbf{p}) \hat{P}_{cd}(\mathbf{p}) + (\hat{V}_{b11}(\mathbf{0}, \mathbf{p}, -\mathbf{p}) - \hat{V}_{b11}(\mathbf{0}, \mathbf{0}, \mathbf{0})) \hat{P}_{11}(\mathbf{p})] \\ &\quad + \frac{1}{\sqrt{N}} \hat{P}_{ab}(\mathbf{0}) \hat{V}_{b11}(\mathbf{0}, \mathbf{0}, \mathbf{0}) \langle \phi_x^2 \rangle. \end{aligned} \tag{3.77}$$

Note that in the last term we have replaced

$$\int_{\mathbf{p}} \hat{P}_{11}(\mathbf{p}) = \langle \phi_x^2 \rangle, \tag{3.78}$$

a necessary step, since the integral diverges at the critical point and therefore should be computed in the effective theory for the zero mode. Now, we have

$$\langle \phi_x^2 \rangle = k^2 - 2\alpha k \langle \chi_x \rangle + \alpha^2 \langle \chi_x^2 \rangle. \tag{3.79}$$

In the critical crossover limit, the two expectation values are replaced by the crossover functions for the magnetization and the energy and by a regular term. Therefore, for $N \to \infty$, the leading behavior is $\langle \phi_x^2 \rangle = k^2 \sim N^{1/3}$. It follows that $\langle \varphi_a \rangle \sim N^{-1/6}$. In conclusion we can write

$$\begin{aligned} \overline{E} &= \tau - 1 + \frac{1}{\sqrt{N}} U_{41}(\mathbf{0}) \left[\frac{\alpha}{x_t} f_1^{\rm symm}(x_t, x_h) - k \right] \\ &= \overline{E}_{\rm reg} + \frac{1}{\sqrt{N}} U_{41}(\mathbf{0}) \frac{\alpha}{x_t} f_1^{\rm symm}(x_t, x_h) + O(N^{-2/3}), \end{aligned} \tag{3.80}$$

where $\overline{E}_{\rm reg}$ is the regular part of $\overline{E}$:

$$\begin{aligned} \overline{E}_{\rm reg} &= \tau - 1 - \frac{1}{\sqrt{N}} U_{41}(\mathbf{0}) k \\ &= \tau_0 - 1 + [\tau_1 - k_0 U_{41}(\mathbf{0})] \delta_{m0} N^{-1/3} + O(N^{-2/3}), \end{aligned} \tag{3.81}$$

where we have written $\tau \approx \tau_0 + \tau_1 \Delta_m$ and $k \approx k_0 \Delta_m \sqrt{N}$.

Equation (3.80) shows that the singular part of $\overline{E}$ behaves as the magnetization in the Ising model. For $x_t \ll 1$ and $x_h \ll 1$ one observes Ising behavior and thus

$$\begin{aligned} \overline{E} - \overline{E}_{\text{reg}} &\sim |x_t|^{\beta_I} && \text{for} \quad x_h = 0, \text{low } t \text{ phase} \\ \overline{E} - \overline{E}_{\text{reg}} &\sim |x_h|^{1/\delta_I} && \text{for} \quad x_h \neq 0, \end{aligned} \tag{3.82}$$

where $\beta_I = 1/8$ and $\delta_I = 15$. On the other hand, in the opposite limit we have

$$\begin{aligned} \overline{E} - \overline{E}_{\text{reg}} &\sim |x_t|^{\beta_{MF}} && \text{for} \quad x_h = 0, |x_t| \to \infty, \text{low } t \text{ phase} \\ \overline{E} - \overline{E}_{\text{reg}} &\sim |x_h|^{1/\delta_{MF}} && \text{for} \quad |x_h| \to \infty \end{aligned} \tag{3.83}$$

with $\beta_{MF} = 1/2$ and $\delta_{MF} = 3$. Note that the limit $|x_t| \to \infty$ and $|x_h| \to \infty$ should always be taken close to the critical limit. Therefore, $|x_h| \to \infty$ means that we should consider $N \to \infty$, $\hat{u}_h \to \hat{u}_{h,\text{crit}}$, $p \to p_{\text{crit}}$ in such a way that $N^{3/2}(\hat{u}_h - \hat{u}_{h,\text{crit}}) \to \infty$, i.e. N should increase much faster that the rate of approach to the critical point.

3.5 Numerical results for selected Hamiltonians

In this section we present some numerical results for some selected Hamiltonians. First, as in Ref. [82], we consider

$$W(x) = \frac{2}{p}\left(\frac{x}{2}\right)^p. \tag{3.84}$$

Second, we consider the mixed O(N)-RP^{N-1} model with Hamiltonian [81]

$$\mathcal{H} = -N\beta_V \sum_{x\mu} (\boldsymbol{\sigma}_x \cdot \boldsymbol{\sigma}_{x+\mu}) - \frac{N\beta_T}{2} \sum_{x\mu} (\boldsymbol{\sigma}_x \cdot \boldsymbol{\sigma}_{x+\mu})^2. \tag{3.85}$$

This Hamiltonian corresponds to the function

$$W(x) = px + \frac{1}{4}(1-p)x^2, \tag{3.86}$$

where we set $\beta_V = (1+p)\beta/2$ and $\beta_T = (1-p)\beta/2$. This Hamiltonian is ferromagnetic for $p > -1$. Note that for $p = -1$ we obtain the RP^{N-1} Hamiltonian [89], [81], [90], [91], [92], [93], [94], [84], [95], [85]

$$\mathcal{H} = -\frac{N\beta}{2} \sum_{x\mu} (\boldsymbol{\sigma}_x \cdot \boldsymbol{\sigma}_{x+\mu})^2, \tag{3.87}$$

that has the additional gauge invariance $\boldsymbol{\sigma}_x \to \epsilon_x \boldsymbol{\sigma}_x$, $\epsilon_x = \pm 1$. Under standard assumptions, the large-N analysis should apply also to this last model: the local gauge invariance should not play any role.[4]

---

[4] The irrelevance of the $\mathbb{Z}_2$ symmetry for the large-β behavior of RP^{N-1} models have been discussed in detail in Ref. [94, 95, 84]. Thus, in spite of the additional local invariance, RP^{N-1} models are expected to be asymptotically free and to be described by the perturbative renormalization group.

	W_1	W_2
β_c	1.334721915850	0.9181906464057
p_c	4.537856778637	-0.9707166650184
m_{0c}^2	0.1501849439193	0.8657494320430
a_{10}	0.4359516292302	-1.1359750388653
a_{11}	0.5042522341176	-0.6248171602172
a_{12}	-1.2793594495686	0.1122363376128
a_{03}	-1.3015714087645	-0.0061080440602
a_{04}	67.512019516378	0.2847340288532
b_{t0}	-0.04261881236908	0.21169346791995
b_{t1}	-0.0043954143923	0.05334711842197
b_{t2}	1.85335235385232	0.00015229016444
b_{h0}	-0.0077917231312	-0.664558775414698
b_{h1}	0.085888253027	-0.094120307536470
b_{h2}	-0.5785580673083	0.049596987743194
b_{h3}	-0.221693999401	-0.000920094744508
d_1	0.205	0.2678
d_2	0.614	-0.808514
d_{30}	0.374	1.1692
α^{-2}	0.0315969	0.00933367

Table 3.1: Numerical estimates for interaction (3.84) (W_1) and (3.86) (W_2).

In the large-N limit [55], the first Hamiltonian has a critical point at $\beta_c \approx 1.335$ and $p_c \approx 4.538$. By using the numerical results reported in Table 3.1 we can compute the first corrections to the critical parameters. We obtain

$$\beta_c \approx 1.335 + \frac{1}{N}(36.127 + 2.093 \ln N), \tag{3.88}$$

$$p_c \approx 4.538 + \frac{1}{N}(87.92 + 4.80 \ln N). \tag{3.89}$$

Note the presence of a $\ln N/N$ correction due to the nonanalytic nature of the renormalization counterterms. The correction terms are quite large, indicating that the large-N results are quantitatively predictive only for large values of N. This is not totally unexpected since [82] $p_c \approx 20$ for $N = 3$, that is quite far from the large-N estimate $p_c \approx 4.538$. If we substitute $N = 3$ in eq. (3.89), we obtain $p_c \approx 35$, which shows that the corrections have the correct sign and give at least the correct order of magnitude.

For $N = \infty$ the second Hamiltonian has a critical point at [81] $\beta_c \approx 0.918$ and $p_c \approx -0.971$. Including the first correction we obtain

$$\beta_c = 0.9182 - \frac{1}{N}(11.062 - 1.437 \ln N), \tag{3.90}$$

$$p_c = -0.9707 + \frac{1}{N}(2.905 - 1.265 \ln N). \tag{3.91}$$

In this case the corrections are smaller. However, for $N \leq 99.4$ they predict $p_c < -1$, although only slightly. This is of course not possible, since for $p < -1$ the system is no longer ferromagnetic. Thus, we expect the transition to disappear for some $N = N_c$, with $N_c \approx 100$ (this is of course a very rough estimate). Since $p_c \approx -1$, we also predict RP^{N-1} models to show a very weak first-order transition for large N.

3.6 Conclusions

In this chapter we have explicitly presented our technique to solve the problem of Infra Red Divergences in large N expansion, giving a detailed description of a class of one-parameter $O(N)$ models that present this kind of problem. This models show a line of first-order finite-β transitions. We focus on the endpoint of the first-order transition line where energy-energy correlations become critical, while the spin-spin correlation length remains finite, in agreement with Mermin-Wagner theorem [62]. In sec. 1.5 we showed that, at the critical point, the standard $1/N$ expansion breaks down, since the inverse propagator of the auxiliary fields has a zero eigenvalue. A careful treatment shows that the zero mode, i.e. the field associated with the vanishing eigenvalue, has an effective Hamiltonian that corresponds to a weakly coupled one-component ϕ^4 theory. Thus, the phase transition belongs to the Ising universality class for any N, in agreement with the argument of Ref. [82]. In Ref. [55] it was shown that for $N = \infty$ the transition has mean-field exponents. We reconcile here these two results. If u_t and u_h are the linear thermal and magnetic scaling fields, in the critical limit a generic long-distance quantity $\mathcal{O}$ has a behavior of the form

$$\langle \mathcal{O} \rangle_{\text{sing}} \approx u_t^{\sigma} f_{\mathcal{O}}(u_t N, u_h N^{3/2}), \tag{3.92}$$

where $f(x, y)$ is a crossover function. Only if $u_t N \ll 1$ and $u_h N^{3/2} \ll 1$ does one observe Ising behavior. In the opposite limit one observes mean-field criticality. Therefore, the width of the Ising critical region goes to zero as $N \to \infty$ and, even if the transition is an Ising one for any N, only mean-field behavior is observed for $N = \infty$. The behavior observed at the critical point for $N \to \infty$ resembles very closely what is observed in medium-range models [36], [37], [34], [35], with N playing the role of the interaction range. Our analysis fully confirms the conclusions of Ref. [82].

From a more quantitative point of view, we give explicit expressions for the critical values β_c and p_c and for the nonlinear scaling fields to order $1/N$. Numerical results are given for the Hamiltonian introduced in Ref. [82] and for mixed $O(N)$-RP^{N-1} models [81]. We plan to compute corrections to the critical parameters for other model for which more available data are present (for instance Yukawa models, chap. 5 and ref. [50]). This would provide a more evident check for the scheme proposed in this work.

The main result of this paper, i.e. the fact that the width of the Ising critical region goes to zero as $N \to \infty$, holds in any $d < 4$. However, in generic dimension d the natural scaling variables are $(p - p_{\text{crit}})N^{2/(4-d)}$ and $(\hat{u}_h - \hat{u}_{h,\text{crit}})N^{3/(4-d)}$,[5] while the scaling equation eq. (2.3) is now replaced by

$$\chi_n = u^{d/(4-d)} t^{-n(d+2)/4} f^{\text{symm}}_{d;n}(u t^{-(4-d)/2}, u h^{-2(4-d)/(2+d)}). \tag{3.93}$$

---

[5] Thus, for $d > 2$ the Ising critical region shrinks faster as N increases: in three dimensions as N^{-2} and N^{-3} in the thermal and magnetic directions respectively.

The claim simply follows from the fact that for any d the zero mode has a Hamiltonian that corresponds to a weakly coupled ϕ^4 theory. Thus, for $d < 4$, the phase transition is always Ising-like. One only needs to take into account the different definition of the scaling fields (3.93). Also the expressions for the renormalization constants r_c and h_c should be changed: for instance, in three dimensions we also expect contributions from two-loop graphs, as it happens in medium-range models [32]. More important, following the discussion of sec. (2.1.5) in order to get the previous scaling equation (3.93) one need to correct the definition of the zero mode (2.57) to impose that the three-leg vertex renormalized must be equal to zero unless contributions that are irrelevant in the Critical Crossover Limit.

Chapter 4

Large-N expansion of $O(N)$ models: the multicritical zero mode

In this chapter we want to generalize the considerations of the previous chapter to the case in which a multicritical zero mode appear $\mathcal{N} > 1$.[1] In this case the study of the effective interaction for the zero mode would require a more involved algebra which gives several non-trivial cancellations in the expansion of the scaling fields near the multicritical point. This cancellations generalize what found in chapter 3 [where for instance the Δ_m^2 term disappears in the expansion of x_t eq. (3.54)] and appear as soon as one consider the translated theory (3.13). The main effects of this cancellations will be the identification of the leading order of the effective vertices for the translated theory with the scaling fields for $N = \infty$ –i.e. without $1/N$ corrections– (1.48) introduced in order to parametrize the gap equation near the critical point (1.47).[2] Following the notations of the previous chapter, if we define $\tilde{V}^{(j)}(\mathbf{p}) \equiv \tilde{V}^{(j)}(\mathbf{0}, \cdots \mathbf{0}, \mathbf{p}, -\mathbf{p})$ the vertices of the zero mode, the first result will be to show that near the multicritical point

$$\begin{aligned} \tilde{V}^{(j)}(\mathbf{0}) &\sim {u_h}^{\frac{\mathcal{N}+2-j}{\mathcal{N}+2}} \\ &\sim u_{j-1},\, \Delta_m u_j,\, {\Delta_m}^2 u_{j+1} \cdots {\Delta_m}^{\mathcal{N}-j+3} \end{aligned} \tag{4.1}$$

for $j = 0, \cdots \mathcal{N}$. In the second line of (4.1) we have written all the contributions that scale in the same way in the $N = \infty$ critical limit defined by (1.48)

$$u_j \sim {u_h}^{\frac{\mathcal{N}+2-j}{\mathcal{N}+2}} \qquad\qquad \Delta_m \sim {u_h}^{\frac{1}{\mathcal{N}+2}}.$$

In the next section we will show that introducing a proper translation for the zero mode [similar to what introduced in (3.13)], one is able to cancel in eq. (4.1) all the contribution that factorize Δ_m so that $\overline{V}^{(j)}(\mathbf{0}) \sim u_{j-1}$.[3] This result is very important in order to include

---

[1] Referring to the notation introduced in the first chapter, we remember that only the $\mathcal{N}$ odd case is investigated, the other case being unstable for $N = \infty$.

[2] This identification will be exact apart some contribution that are irrelevant in the scaling limit taken in the past chapters (also called Critical Crossover Limit –CCL–).

[3] As in the previous chapter $\overline{V}^{(j)}$ refers to the vertices for the translated theory.

$1/N$ fluctuations to the $N=\infty$ theory of chapter 1. Indeed in chapter 2 we have obtained that the scaling fields describing the crossover to the multicritical point are given by

$$u_i(N) \equiv \overline{V}^{(i+1)}(\mathbf{0}) - u_{ci} \tag{4.2}$$

where u_{ci} regularise the theory and cancel the nonuniversal details. If the Δ_m contributions of the second line of eq. (4.1) do not cancel, inserting (4.1) in (4.2) one would obtain an expression similar to the following

$$u_i(N) \quad = \quad u_i(\infty) + \sum_{j=i+1}^{\mathcal{N}} c_j^{(i)} u_j(\infty) + O\Big(\frac{1}{N}\Big) \tag{4.3}$$

If $c_j^{(i)} \neq 0$ for *every* i and $j > i$, then the scaling fields would be discontinuous for $N=\infty$, so that our mechanism to explain crossover between the two different critical regime would fail. We remember that there is some freedom in the definition of the scaling fields u_i (1.48). Indeed also

$$u_i' = u_i + \sum_{j=0}^{i-1} a_j u_j \tag{4.4}$$

satisfy the scaling relations of the $N=\infty$ theory; however eq. (4.4) can never match with eq. (4.3). We stress how in principle the require to cancel $\mathcal{N}(\mathcal{N}-1)/2$ parameters [$c_i^{(j)}$ in eq. (4.3)] tuning a single parameter (the translation constant of the zero mode) looks an impossible work! The answer to this paradox relies on the fact that the vertices of the effective theory are not independent but are strictly related each other and at the end to the gap equation. In the first part of this chapter we want to elucidate this relations by using similar techniques of sec. 3.1.1, while in the last part of this chapter we will describe the crossover behaviour to mean field in a similar way of what done for the $\mathcal{N}=1$ case, chapter 2. In particular we will describe (in a general way), how to obtain the scaling field in the large N limit and how to include $1/N$ corrections to their $N=\infty$ definitions computing explicitly the $\mathcal{N}=3$ case.

4.1 Effective Hamiltonian for the zero mode

4.1.1 Basic definitions

As in the previous chapter the starting point is the definition of the effective interaction for the zero mode through the integration of the massive mode of the theory. However in this case, being interested in general relations, we need to take a more general point of view. If $v_A(\mathbf{p}; m_0^2, p_i)$ is the normalized eigenvector that corresponds to the zero eigenvalue for $\mathbf{p}=0$ at the MCP we have that we define the critical field (rescaled)

$$\varphi(\mathbf{p}) = \frac{1}{\sqrt{N}} \sum_A v_A(\mathbf{p}; m_0^2, p_i) \Psi_A, \tag{4.5}$$

while the effective Hamiltonian becomes

$$\mathcal{H}_{\rm eff}[\varphi] = -\frac{1}{N}\ln\frac{Z[\varphi]}{Z[0]}, \tag{4.6}$$

where

$$Z[\varphi] = \int \prod_{x,A} d\Psi_{xA}\,\delta(\Psi\cdot v - \varphi\sqrt{N})e^{-\mathcal{H}}, \tag{4.7}$$

where the functional δ function guarantees the identification (4.5) and $\Psi \cdot v = \sum_A \Psi_A v_A$. In this expression we assume that $v_A(\mathbf{p}; m_0^2, p_i)$ is normalized, i.e., $\sum_A v_A^2 = 1$. Note the additional factor $\sqrt{N}$ in the definition of φ. It guarantees that, in the large-N limit, the effective Hamiltonian becomes N independent.

The effective Hamiltonian can be expanded as before:

$$\begin{aligned}\mathcal{H}_{\rm eff}[\varphi] &= \tilde{H}\varphi + \frac{1}{2}\int_{\mathbf{p}} \tilde{P}^{-1}(\mathbf{p})\varphi(\mathbf{p})\varphi(-\mathbf{p}) \\ &\quad + \sum_{n=3}\frac{1}{n!}\int_{\mathbf{p}_1}\cdots\int_{\mathbf{p}_n}\delta\left(\sum_i \mathbf{p}_i\right)\tilde{V}^{(n)}(\mathbf{p}_1,\cdots,\mathbf{p}_n)\varphi(\mathbf{p}_1)\cdots\varphi(\mathbf{p}_n)\ .\end{aligned} \tag{4.8}$$

The magnetic field, the propagator, and the vertices acquire now an explicit N dependence and we can write

$$\tilde{H} = \sum_{n=1}\tilde{H}_n N^{-n}, \tag{4.9}$$

$$\tilde{P}^{-1}(\mathbf{p}) = \sum_{n=0}\tilde{P}_n^{-1}(\mathbf{p})N^{-n}, \tag{4.10}$$

$$\tilde{V}^{(j)}(\mathbf{p}_1,\ldots,\mathbf{p}_j) = \sum_{n=0}\tilde{V}_n^{(j)}(\mathbf{p}_1,\ldots,\mathbf{p}_j)N^{-n}. \tag{4.11}$$

4.1.2 Identities among the vertices of the effective Hamiltonian

Let us now derive some important relations concerning the zero-momentum vertices $\tilde{V}_0^{(j)}(\mathbf{0},\ldots,\mathbf{0})$ and propagator $\tilde{P}_0^{-1}(\mathbf{0})$ [that below will be denoted by $\tilde{V}_0^{(2)}(\mathbf{0})$]. Since we will discuss only zero-momentum quantities, in this section we will not write the explicit momentum dependence.

The leading behavior of $\mathcal{H}_{\rm eff}[\varphi]$ for $N \to \infty$ is obtained by considering the tree-level diagrams that arise from the perturbative expansion of (4.6) in powers of N. If we are only interested in zero-momentum correlations of the field φ at leading order in $1/N$ expansion[4], in $\mathcal{H}$ we can simply consider the zero-momentum vertices and in Z we need only to integrate over the five zero-momentum fields Ψ. In the following we take the point of view of sec. 3.1.1, in particular taking the short-hand notation

$$f_A \equiv (\gamma,\alpha,\alpha,\tau,\tau)$$

---

[4] In order to consider $1/N$ corrections to the vertices, one have to include radiative contributions in which vertices appear at every momenta.

we have that, using the gap-equations (1.7,1.8,1.9,1.10), the vertices of the theory that in principle depend on β and f_A are parametrized only by m_0^2. In particular we can write[5]

$$V^{(n)}_{A_1\cdots A_n} = V^{(n)}_{A_1\cdots A_n}(f_A(m_0^2), \beta(m_0^2)) \tag{4.12}$$

In (4.12) $f_A(m_0^2)$ and $\beta(m_0^2)$ are given in (1.7,1.8,1.9,1.10). We are not interested in the explicit form of $V^{(n)}_{A_i}$ that is given in [56], otherwise in the following we need only the following relations:

$$\begin{aligned} V^{(n+1)}_{A,A_1,\cdots A_n} &= \frac{\partial V^{(n)}_{A_1,\cdots A_n}}{\partial f_A} \\ \frac{\partial^2 V^{(n)}_{A_1,\cdots A_n}}{\partial \beta^2} &= 0 \end{aligned} \tag{4.13}$$

in particular the (4.13) easily follows from the fact that the action of the auxiliary fields is linear in β [55]. In section 3.1.1, it was shown that the derivative of f_A with respect to m_0^2 near the multicritical point is related to the zero mode v_A of the theory

$$\begin{aligned} \frac{\mathrm{d} f_A(m_0^2)}{\mathrm{d} m_0^2} &= \frac{1}{C(m_0^2, p_i)}\left(v_A(m_0^2, p_i) + \mathcal{O}(m_0^2, p_i)\xi_A(m_0^2, p_i)\right) \\ \mathcal{O}(m_0^2, p_i) &\sim \frac{\partial \beta(m_0^2, p_i)}{\partial m_0^2} \equiv s_1(m_0^2, p_i) \end{aligned} \tag{4.14}$$

ξ_A is a no-more specified vector while v_A is the zero mode at zero external momentum. $\mathcal{O}$ is a function of p_i and m_0^2 that goes to zero at the MCP (4.14). Since now we could neglect the explicit dependence on m_0^2 and p_i of $\mathcal{O}$, ξ_A, v_A and C. Using (4.14) and (4.13) we recover the following equality

$$\frac{\mathrm{d}}{\mathrm{d} m_0^2} V^{(n)}_{A_1,\ldots,A_n} = \frac{1}{C}\sum_B \Big(v_B + \mathcal{O}\xi_B\Big) V^{(n+1)}_{B,A_1,\ldots,A_n} + s_1 \frac{\partial}{\partial \beta} V^{(n)}_{A_1,\ldots,A_n}, \tag{4.15}$$

Identity (4.15) can also be written in the compact form

$$\frac{\mathrm{d}\mathcal{H}}{\mathrm{d} m_0^2} = \frac{\sqrt{N}}{C}\sum_B \Big(v_B + \mathcal{O}\xi_B\Big)\left[\frac{\partial \mathcal{H}}{\partial \Psi_B} - \sum_A V^{(2)}_{BA}\Psi_A\right] + s_1 \frac{\partial \mathcal{H}}{\partial \beta} \tag{4.16}$$

We begin by computing $d\mathcal{H}_{\text{eff}}/dm_0^2$. We have

$$\begin{aligned} \frac{d\mathcal{H}_{\text{eff}}}{dm_0^2} &= -\frac{1}{NZ[\varphi]}\left[\int \prod d\Psi\, \delta'(\Psi\cdot v - \varphi\sqrt{N})\Psi\cdot \frac{dv}{dm_0^2} e^{-\mathcal{H}} \right. \\ &\qquad \left. - \int \prod d\Psi\, \delta(\Psi\cdot v - \varphi\sqrt{N}) \frac{d\mathcal{H}}{dm_0^2} e^{-\mathcal{H}}\right] - (\varphi \to 0). \end{aligned} \tag{4.17}$$

The second term can be related to $d\mathcal{H}_{\text{eff}}/d\varphi$, by using identity (4.16). Indeed defining $\langle\cdot\rangle$ as

$$\langle \mathcal{F}[\Psi]\rangle \equiv \frac{1}{Z[\varphi]}\int d\Psi\, \delta(\Psi\cdot v - \varphi\sqrt{N})\mathcal{F}[\Psi] e^{-\mathcal{H}}. \tag{4.18}$$

---

[5] Here and in the following we are neglecting the dependence on W or p_i.

we find

$$\frac{d\mathcal{H}_{\rm eff}}{d\varphi} = \tilde{P}_0^{-1}\varphi + \frac{C}{N}\langle\frac{d\mathcal{H}}{dm_0^2}\rangle - \frac{Cs_1}{N}\langle\frac{\partial\mathcal{H}}{\partial\beta}\rangle + \frac{\mathcal{O}}{\sqrt{N}}\sum_B \xi_B\langle\sum_A V^{(2)}_{BA}\Psi_A - \frac{\partial\mathcal{H}}{\partial\Psi_B}\rangle \tag{4.19}$$

A simple calculation allows also to write

$$-\frac{1}{NZ[\varphi]}\int d\Psi\,\delta'(\Psi\cdot v - \varphi\sqrt{N})\Psi\cdot\frac{dv}{dm_0^2}e^{-\mathcal{H}} = \frac{1}{N^{3/2}}\frac{d}{d\varphi}\langle\Psi\cdot\frac{dv}{dm_0^2}\rangle - \frac{1}{N^{1/2}}\frac{d\mathcal{H}_{\rm eff}}{d\varphi}\langle\Psi\cdot\frac{dv}{dm_0^2}\rangle, \tag{4.20}$$

Thus, we obtain the following representation

$$\begin{aligned}\frac{d\mathcal{H}_{\rm eff}}{dm_0^2} &= \frac{1}{C}\frac{d\mathcal{H}_{\rm eff}}{d\varphi} + \frac{1}{N^{3/2}}\frac{d}{d\varphi}\langle\Psi\cdot\frac{dv}{dm_0^2}\rangle - \frac{1}{N^{1/2}}\frac{d\mathcal{H}_{\rm eff}}{d\varphi}\langle\Psi\cdot\frac{dv}{dm_0^2}\rangle \\ &\quad -\frac{\mathcal{O}}{C\sqrt{N}}\sum_B \xi_B\langle\sum_A V^{(2)}_{BA}\Psi_A - \frac{\partial\mathcal{H}}{\partial\Psi_B}\rangle - \frac{\tilde{P}_0\varphi}{C} + \frac{s_1}{N}\langle\frac{\partial\mathcal{H}}{\partial\beta}\rangle\end{aligned} \tag{4.21}$$

Now, let us show that the second term in the first line of (4.21) is of order $1/N$ and can therefore be dropped. Since $v\cdot dv/dm_0^2 = 0$, dv/dm_0^2 projects over the massive subspace, i.e. the field Ψ appearing in the mean value is a massive field. Thus, the leading contribution to the coefficient of φ^n is due to tree-level diagrams with n lines corresponding to the field φ and one line to the massive field $\Psi\cdot dv/dm_0^2$. The N-dependence of a tree-level graph contributing to the coefficient of φ^n is given by $N^{n/2-a}$ with

$$a = \frac{1}{2}\sum_{k=3}^{\infty}(k-2)n_k, \tag{4.22}$$

where n_k is the number of k-leg vertices appearing in the diagram. Now we use the fact that, for a tree-level diagram, $N_{\rm ext} = 2+\sum_{k=3}(k-2)n_k$, where $N_{\rm ext}$ is the number of external legs. Since $N_{\rm ext} = n+1$, we obtain $a = N_{\rm ext}/2 - 1 = (n-1)/2$, independently of the diagram. Thus,

$$\langle\Psi\cdot\frac{dv}{dm_0^2}\rangle \sim N^{1/2}, \tag{4.23}$$

independently of the number of φ legs. This proves that at leading order in $1/N$ the second term can be dropped, while the third one must be kept. Consider now the first term of the second line of (4.21):

$$\frac{\mathcal{O}}{C}\sum_{n\geq 2}\frac{1}{n!N^{n/2}}\langle\sum_{B\{A_i\}} V^{(n+1)}_{BA_1\cdots A_n}\xi_B\Psi_{A_1}\cdots\Psi_{A_n}\rangle \tag{4.24}$$

In (4.24) we decompose Ψ on the eigenvector of $\tilde{P}$ (one of which is the critical mode v_A, while the other four are massive modes $v^{(m)}$ with $m = 1, 2\cdots 4$)

$$\Psi_A = (v\cdot\Psi)v_A + \sum_{m=1}^{4}(v^{(m)}\cdot\Psi)v^{(m)}_A \tag{4.25}$$

Considering only mass-less component in (4.24) we find the following φ^n contribution:

$$\frac{\mathcal{O}}{C}\sum_{n\geq 2}\varphi^n\sum_{B\{A_i\}}V^{(n+1)}_{BA_1\cdots A_n}\xi_B v_{A_1}\cdots v_{A_n} \tag{4.26}$$

Otherwise inserting l $(1\leq l\leq n)$ massive vectors into (4.24) we have a contribution that looks like:

$$\frac{\mathcal{O}}{C}\sum_{n\geq 2}\frac{\varphi^{n-l}}{N^{l/2}}\sum_{B\{A_i\}}V^{(n+1)}_{BA_1\cdots A_n}\xi_B v_{A_1}\cdots v_{A_{n-l}}v^{(m_1)}_{A_{n-l+1}}\cdots v^{(m_l)}_{A_n}\langle(v^{(m_1)}\cdot\Psi)\cdots(v^{(m_l)}\cdot\Psi)\rangle \tag{4.27}$$

A leading order graph that enters into the evaluation of (4.27) is a tree graph with l external massive legs and an arbitrary number of massless one. It behaves independently of the massless legs like $N^{-l/2+1}$ so that we recover an $O(N^0)$ terms in (4.27) taking $l=1$. As a consequence of (4.26-4.27) (up to $1/N$) we have that the first term in the second line of (4.21) goes as φ^2 for $\varphi\to 0$. The same considerations follows for $\partial\mathcal{H}/N\partial\beta$ in (4.21), indeed following the same previous steps one can show that the leading order is $O(N^0)$ and that for $\varphi\to 0$ this behaves like φ^2. In the following we will write:

$$\sum_B\frac{\mathcal{O}\xi_B}{C\sqrt{N}}\langle\sum_A\frac{\partial\mathcal{H}}{\partial\Psi_B}-V^{(2)}_{BA}\Psi_A\rangle+\frac{s_1}{N}\langle\frac{\partial\mathcal{H}}{\partial\beta}\rangle \;=\; \sum_{k\geq 2}\frac{o_k}{k!}\varphi^k+O\left(\frac{1}{N}\right) \tag{4.28}$$

with $o_k\sim s_1$ near the MCP. Collecting all the previous results, at leading order in $1/N$ we have

$$\frac{d\mathcal{H}_{\rm eff}}{dm_0^2} \;=\; \frac{1}{C}\frac{d\mathcal{H}_{\rm eff}}{d\varphi}-\frac{1}{N^{1/2}}\frac{d\mathcal{H}_{\rm eff}}{d\varphi}\langle\Psi\cdot\frac{dv}{dm_0^2}\rangle+\sum_{n\geq 2}\frac{o_n}{n!}\varphi^n-\frac{\tilde{P}_0^{-1}\varphi}{C}+O\Big(\frac{1}{N}\Big) \tag{4.29}$$

Since $\langle\Psi\cdot dv/dm_0^2\rangle\sim\varphi^2$ for $\varphi\to 0$ we obtain a set of differential equation for the vertices

$$\frac{d\tilde{V}_0^{(n)}}{dm_0^2} \;=\; \frac{1-\delta_{n,1}}{C}\tilde{V}_0^{(n+1)}-n!\sum_{k=2}^{n-1}\frac{c^{(0)}_{n-1-k}}{(k-1)!}\tilde{V}_0^{(k)}+o_n \tag{4.30}$$

where coherently with (4.28) we have implicitly assumed $o_1=o_2=0$. In (4.30) we have defined

$$\frac{1}{\sqrt{N}}\langle\Psi\cdot\frac{dv}{dm_0^2}\rangle \;=\; \sum_{k\geq 0}c^{(0)}_k\varphi^{k+2}+O\Big(\frac{1}{N}\Big). \tag{4.31}$$

Eq. (4.30) allows us to compute the behavior close to the MCP of the zero-momentum vertices $\tilde{V}_0^{(k)}$ for $k\leq\mathcal{N}+3$. Using eq. (1.36) and the definition of the scaling fields (1.49) we have

$$\begin{aligned}\frac{d\beta}{dm_0^2} \;&=\; \sum_{k=1}^{\mathcal{N}}ku_k{\Delta_m}^{k-1}+a_{\mathbf{0}}^{(\mathcal{N}+2)}(\mathcal{N}+2){\Delta_m}^{\mathcal{N}+1}\\ &\quad +O\Big[{\Delta_m}^{\mathcal{N}+2},\Big\{{\Delta_m}^{i-1}\prod_{l=1}^{m_i+1}u_{k_l}\Big\}_{i=1,2\cdots\mathcal{N}},\{{\Delta_m}^{\mathcal{N}}u_k\}_{k=1,\cdots\mathcal{N}}\Big],\end{aligned} \tag{4.32}$$

where $\Delta_m \equiv m_0^2 - m_{0c}^2$. All the terms in the first line of (4.32) go as u_h near the MCP; the next to leading contribution ($\sim {u_h}^{\frac{\mathcal{N}+3}{\mathcal{N}+2}}$) is obtained considering the three terms of the second line of (4.32) with i even and $u_{k_l} = u_{\mathcal{N}}$ concerning the second term, and with $u_k = u_{\mathcal{N}}$ in the third term. We will now show that for $2 \leq k \leq \mathcal{N}+3$ zero-momentum vertices can be expanded close to the MCP as

$$\tilde{V}_0^{(k)} = a_k {\Delta_m}^{\mathcal{N}+3-k} + \sum_{j=1}^{k-2} b_j^{(k)} u_j + \sum_{j=k-1}^{\mathcal{N}} b_j^{(k)} u_j {\Delta_m}^{j-k+1} + \ldots \tag{4.33}$$

For $k = 2$ the second term is absent.

The (4.33) can be obtained starting from the following equality

$$\tilde{V}_0^{(2)} = \tilde{P}_0^{-1} = f(m_0^2, p_i)\frac{d\beta}{dm_0^2} \tag{4.34}$$

(that was demonstrated in [56] and recovered in chapter 1) and using recursively (4.30). We notice that for $k = 1$ the r.h.s. of (4.30) cancels in agreement with the condition $\tilde{V}_0^{(1)} = 0$ given by the gap equation. For $k = 2$ expansion (4.33) follows from eq. (4.32) and it is enough to identify $a_2 = f(0,0)a_{000}^{(\mathcal{N}+2)}(\mathcal{N}+2)$, $b_j^{(2)} = jf(0,0)$. For $k = 3$ the expansion follows from eq. (4.30) and indeed all coefficients can be related with those appearing in the expansion of $\tilde{V}_0^{(2)}$ and $\mathcal{O}$. We will need the explicit expression for a_k and $b_j^{(k)}$ for $j \geq k-1$. Applying eq. (4.30) recursively we obtain

$$a_k = \frac{(\mathcal{N}+1)!}{(\mathcal{N}-k+3)!}\mathcal{C}^{k-2}a_2 \tag{4.35}$$

$$b_j^{(k)} = \frac{(j-1)!}{(j-k+1)!}\mathcal{C}^{k-2}b_j^{(2)}, \tag{4.36}$$

where the second relation applies only for $j \geq k-1$. For $j < k-1$ the expression for $b_j^{(k)}$ is not so simple, indeed it will appear also contributions coming from $\mathcal{O}$ and higher derivative of f. However we are not interested in the explicit expression of $b_j^{(k)}$ for $j \geq k-1$ because this coefficients are not involved in the cancellations of the translated theory. This will be clarified in the next section 4.1.3.

4.1.3 Translated zero-mode Hamiltonian

In the previous section we have shown that all zero-momentum vertices with $k < \mathcal{N}+3$ vanish at the MCP. We shall now perform a field redefinition in order to have $V^{(\mathcal{N}+2)}(\mathbf{0},\ldots,\mathbf{0}) = 0$ for all values of the parameters. Proceeding in a similar way of what done in chapter 3 eq. (3.13) we write

$$\varphi(\mathbf{p}) = \alpha\chi(\mathbf{p}) + k\delta(\mathbf{p}). \tag{4.37}$$

In terms of χ, the effective Hamiltonian has the expansion

$$\begin{aligned}\mathcal{H}_{\text{eff}}[\chi] &= \overline{H}\chi + \frac{1}{2}\int_{\mathbf{p}} \overline{P}^{-1}(\mathbf{p})\chi(\mathbf{p})\chi(-\mathbf{p}) \\ &+\sum_{n=3}\frac{1}{n!}\int_{\mathbf{p}_1}\cdots\int_{\mathbf{p}_n}\delta\left(\sum_i \mathbf{p}_i\right)\overline{V}^{(n)}(\mathbf{p}_1,\cdots,\mathbf{p}_n)\chi(\mathbf{p}_1)\cdots\chi(\mathbf{p}_n).\end{aligned} \tag{4.38}$$

The parameters α and k are determined by requiring that

$$\overline{V}^{(\mathcal{N}+2)}(\mathbf{0},\ldots,\mathbf{0}) = 0, \tag{4.39}$$

$$\overline{P}^{-1}(\mathbf{p}) - \overline{P}^{-1}(\mathbf{0}) = \mathbf{p}^2 + O(\mathbf{p}^4) \tag{4.40}$$

for all values of the parameters. Condition (4.39) is satisfied if

$$\sum_{j=0}^{\infty} \frac{k^j}{j!} \tilde{V}^{(\mathcal{N}+2+j)}(\mathbf{0},\ldots,\mathbf{0}) = 0. \tag{4.41}$$

Since $\tilde{V}^{(\mathcal{N}+2)}(\mathbf{0},\ldots,\mathbf{0})$ vanishes at the MCP for $N \to \infty$, close to the MCP we can expand k as

$$k = \sum_{n=1}^{\infty} k_n \left[\tilde{V}^{(\mathcal{N}+2)}(\mathbf{0},\ldots,\mathbf{0})\right]^n. \tag{4.42}$$

The first term is easily computed:

$$k_1 = -\frac{1}{\tilde{V}_0^{(\mathcal{N}+3)}(\mathbf{0},\ldots,\mathbf{0})} + O(1/N). \tag{4.43}$$

by using eq. (4.30) and eq. (4.33) it is easy to see that

$$k = -\frac{1}{C}\Delta_m + O[{\Delta_m}^2, u_i, N^{-1}]. \tag{4.44}$$

Since k vanishes at the MCP for $N \to \infty$, we have at the MCP

$$\overline{V}^{(j)}(\mathbf{0},\ldots,\mathbf{0}) = \tilde{V}^{(j)}(\mathbf{0},\ldots,\mathbf{0}) + O(1/N), \tag{4.45}$$

for any $j \geq \mathcal{N}+3$. In principle one can observe that due to the leading behaviour of k (4.44) $\overline{V}^{(j)}$ will have the same general expansion of $\tilde{V}^{(j)}$ (4.33), for $j \leq \mathcal{N}+2$:

$$\overline{V}^{(j)} \;=\; \sum_{i=1}^{j-2} \overline{b}_i^{(j)} u_i + \sum_{i=j-1}^{\mathcal{N}} \overline{b}_i^{(j)} u_i {\Delta_m}^{i-j+1} + \overline{a}_j {\Delta_m}^{\mathcal{N}-j+3} + \cdots \tag{4.46}$$

On the other hand in this case an important cancellation occurs (for $j \leq \mathcal{N}+2$). Indeed one can show that $\overline{b}_i^{(j)} = 0$ for $i \geq j$ and that $\overline{a}_j = 0$ so that at leading order in u_h one has $\overline{V}^{(j)} \sim u_{j-1}$. This implies that the translated vertices vanishes faster as $\Delta_m \to 0$.

We start from

$$\overline{V}^{(j)} = \alpha^j \sum_{n=0}^{\mathcal{N}+3-j} \frac{k^n}{n!} \tilde{V}_0^{(n+j)} + O(k^{\mathcal{N}+4-j}, N^{-1}). \tag{4.47}$$

The leading contribution independent of the scaling fields is given by [using the notations given in (4.33)]

$$\begin{aligned}
&\alpha^j \sum_{n=0}^{\mathcal{N}+3-j} \frac{k^n a_{n+j}}{n!} (\Delta_m)^{\mathcal{N}+3-j-n} + O[(\Delta_m)^{\mathcal{N}+4-j}, N^{-1}] = \\
&\alpha^j \frac{a_2(\mathcal{N}+1)!C^{j-2}}{(\mathcal{N}+3-j)!} (Ck+\Delta_m)^{\mathcal{N}+3-j} + O[(\Delta_m)^{\mathcal{N}+4-j}, N^{-1}] = O[(\Delta_m)^{\mathcal{N}+4-j}, N^{-1}],
\end{aligned} \tag{4.48}$$

where we have used eqs. (4.36) and (4.44). As for the contributions proportional to the scaling fields u_i, no cancellation occurs for $i \leq j-2$. If $i \geq j-1$ the coefficient of u_i is given by

$$\begin{aligned}
&\alpha^j \sum_{n=0}^{i-j+1} \frac{k^n b_i^{(n+j)}}{n!}(\Delta_m)^{i-j-n+1} + O[(\Delta_m)^{i-j+2}, N^{-1}] = \\
&\alpha^j \frac{b_i^{(j)}(i-1)!C^{j-2}}{(i-j+1)!}(Ck+\Delta_m)^{i-j+1} + O[(\Delta_m)^{i-j+2}, N^{-1}] = O[(\Delta_m)^{i-j+2}, N^{-1}]
\end{aligned} \tag{4.49}$$

The previous equations (4.48-4.49) show that $\overline{a}_j = 0$ and $\overline{b}_i^{(j)} = 0$ if $i \geq j$ in (4.46) confirming the starting claim. Otherwise other cancellations appear at next to leading order, so that the general structure of the translated vertices is not given by the corrections of (4.46). This is investigated in the next sub-section 4.1.4 and in 4.1.5 where the structure of k is investigated in detail, in particular it is shown that the ${\Delta_m}^2$ correction of k in (4.44) is due only to contribution coming from C. The strategy of the next sub-section 4.1.4 is to generalize the set of differential equations for $\tilde{V}^{(j)}$ (4.30) to to the translated one $\overline{V}^{(j)}$. Near the MCP this set of differential equations decouple so that we can easily recover the cancellations discovered in this section. Otherwise using the new set of equations one is able to discover other cancellations. One can think to have in mind the final results for the translated vertices (4.63,4.72, 4.73) and in particular the translated vertices for the $\mathcal{N} = 3$ case (4.74,4.75,4.76) that will be used in the final section of this chapter 4.2, where $1/N$ corrections for the scaling fields and the scaling variables will be explicitly built for the $\mathcal{N} = 3$ case.

4.1.4 Structure of the translated vertices: another derivation

For convenience in this section we will take $\alpha = 1$ in eq. (4.37) (at the end $\overline{V}^{(j)}$ must be rescaled by α^j). One can try to solve in a more direct way the structure of the translated vertices $\overline{V}^{(j)}$. In a similar way of what done in previous sections we define

$$Z[\chi] = \int \mathrm{d}\Psi \delta(\psi \cdot v - \sqrt{N}\chi - \sqrt{N}k) e^{-\mathcal{H}} \tag{4.50}$$

$$\mathcal{H}_{\text{eff}} = -\frac{1}{N} \log \frac{Z[\chi]}{Z[0]} \tag{4.51}$$

and we follow the same steps of sec 4.1.2. The first change is in equation (4.17). Using an obvious definition for $\langle\cdot\rangle$ and (4.20) we have:

$$\begin{aligned}
\frac{\mathrm{d}\mathcal{H}_{\text{eff}}}{\mathrm{d}m_0^2} = & \frac{1}{N}\langle\frac{\mathrm{d}\mathcal{H}}{\mathrm{d}m_0^2}\rangle - \frac{1}{\sqrt{N}}\frac{\mathrm{d}\mathcal{H}_{\text{eff}}}{\mathrm{d}\chi}\langle\Psi \cdot \frac{\mathrm{d}v}{\mathrm{d}m_0^2}\rangle + \frac{\mathrm{d}\mathcal{H}_{\text{eff}}}{\mathrm{d}\chi}\frac{\mathrm{d}k}{\mathrm{d}m_0^2} + O\left(\frac{1}{N}\right) \\
& -\Big[\chi \to 0\Big]
\end{aligned} \tag{4.52}$$

On the other hand (4.19) does not change apart the substitution $\varphi \to \chi + k$ (notice however that the explicit k dependence disappear in (4.52) because the subtraction in the second line). So we generalize (4.29) in:

$$\begin{aligned}\frac{\mathrm{d}\mathcal{H}_{\text{eff}}}{\mathrm{d}m_0^2} &= \left(\frac{1}{C}+\frac{\mathrm{d}k}{\mathrm{d}m_0^2}\right)\frac{\mathrm{d}\mathcal{H}_{\text{eff}}}{\mathrm{d}\chi}-\frac{\tilde{V}_0^{(2)}}{C}\chi+\sum_n\frac{o_n}{n!}(\chi+k)^n-\frac{1}{\sqrt{N}}\frac{\mathrm{d}\mathcal{H}_{\text{eff}}}{\mathrm{d}\chi}\langle\Psi\cdot\frac{\mathrm{d}v}{\mathrm{d}m_0^2}\rangle\\ &\quad +O\left(\frac{1}{N}\right)-\Big[\chi\to 0\Big] \qquad (4.53)\end{aligned}$$

Using (4.31) we are now able to generalize (4.30) for the translated vertices:

$$\begin{aligned}k_s(m_0^2)\overline{V}^{(n+1)} &= \frac{\mathrm{d}\overline{V}^{(n)}}{\mathrm{d}m_0^2}+n!\Bigg[\frac{c_0^{(0)}\overline{V}^{(n-1)}}{(n-2)!}+\frac{c_1^{(0)}\overline{V}^{(n-2)}}{(n-3)!}+\cdots+c_{n-2}^{(0)}\overline{V}^{(1)}\\ &\qquad +k\left(2\frac{c_0^{(0)}\overline{V}^{(n)}}{(n-1)!}+3\frac{c_1^{(0)}\overline{V}^{(n-1)}}{(n-2)!}+\cdots+(n+1)c_{n-1}^{(0)}\overline{V}^{(1)}\right)\\ &\qquad +\frac{k^2}{2}\left(2\frac{c_0^{(0)}\overline{V}^{(n+1)}}{n!}+6\frac{c_1^{(0)}\overline{V}^{(n)}}{(n-1)!}+\cdots+(n+1)nc_{n-1}^{(0)}\overline{V}^{(1)}\right)\\ &\qquad +O(k^3)\Bigg]\\ o_j\,\text{with}\,j\geq 2 \qquad &+\Big[o_n+(n+1)o_{n+1}k+(n+2)(n+1)o_{n+2}\frac{k^2}{2}+O(k^3)\Big]\\ &+\frac{\tilde{V}_0^{(2)}}{C}\delta_{n,1} \qquad (4.54)\end{aligned}$$

In (4.54) we have defined

$$k_s(m_0^2) = \frac{1}{C}+\frac{\mathrm{d}k}{\mathrm{d}m_0^2}. \qquad (4.55)$$

k_s is studied in detail in sec. 4.1.5. There we have shown that

$$\begin{aligned}k_s(m_0^2) &= \frac{\alpha c_0^{(0)}(\mathcal{N}+2)}{A_0C}u_{\mathcal{N}}+\frac{c_0^{(0)}{\Delta_m}^2}{C^2}+O\left({\Delta_m}^3,{u_h}^{\frac{3}{\mathcal{N}+2}}\right) \qquad (4.56)\\ k_s(m_0^2)-c_0^{(0)}k^2 &= \frac{\alpha c_0^{(0)}(\mathcal{N}+2)}{A_0C}u_{\mathcal{N}}+O\left({\Delta_m}^3,{u_h}^{\frac{3}{\mathcal{N}+2}}\right) \qquad (4.57)\end{aligned}$$

in (4.56) the Δ_m term cancels in a non trivial way, while in (4.57) also the ${\Delta_m}^2$ term disappears.

We have just noticed that $\overline{V}^{(j)}$ in principle has the same structure of $\tilde{V}^{(j)}$ (4.46) near the MCP. Otherwise we notice that at leading order in u_h due to the relations (4.56) and (4.57), eq. (4.54) becomes

$$\frac{\mathrm{d}\overline{V}^{(j)}}{\mathrm{d}m_0^2}=0 \implies \overline{V}^{(j)}\sim u_{j-1} \qquad (4.58)$$

so that we recover the cancellations discovered in the previous section 4.1.3:

$$\begin{aligned}\overline{b}_i^{(j)} &= 0 \qquad\qquad i=j,j+1,\cdots\mathcal{N} \qquad (4.59)\\ \overline{a}_j &= 0. \qquad (4.60)\end{aligned}$$

We can complete (4.59) with

$$\overline{b}_i^{(j)} = b_i^{(j)} \qquad\qquad i = 1, \cdots j-1 \tag{4.61}$$

that follows from the fact that k goes to zero at the MCP. If $n = 1$ (4.54) becomes:

$$\frac{\mathrm{d}\overline{V}^{(1)}}{\mathrm{d}m_0^2} = -\frac{1}{C}\tilde{V}_0^{(2)} - 2o_2 k \approx -\frac{1}{C}\tilde{V}_0^{(2)} \qquad\qquad \overline{V}^{(1)} = b_0^{(1)} u_h \tag{4.62}$$

where we have used the gap equation (in the following $u_0 \equiv u_h$). Eq. (4.62) is expected if compared with similar results for higher order vertices eq. (4.58).

Now we consider corrections to (4.58). In particular we have to compute at what order (in Δ_m) u_j enters into $\overline{V}^{(k)}$ for $j > k-1$, i.e. we want to compute $\chi^{(j)}$ and $\chi_i^{(j)}$ $(j \le i \le \mathcal{N})$ in the following expression

$$\overline{V}^{(j)} = \sum_{i=1}^{j-1} b_i^{(j)} u_i + \mathcal{V}_0^{(j)} \Delta_m{}^{\chi^{(j)}} + \sum_{i=j}^{\mathcal{N}} \mathcal{V}_i^{(j)} u_i \Delta_m{}^{\chi_i^{(j)}}. \tag{4.63}$$

Writing (4.54) for $n = \mathcal{N} + 2$ (taking into account the constraint $\overline{V}^{(\mathcal{N}+2)} = 0$) we have:

$$\begin{aligned}(k_s(m_0^2) - k^2)\overline{V}^{(\mathcal{N}+3)} \quad &= \quad c_0^{(0)}(\mathcal{N}+2)(\mathcal{N}+1)(1+O(k))\overline{V}^{(\mathcal{N}+1)} \\ &\quad + c_1^{(0)}(\mathcal{N}+2)(\mathcal{N}+1)\mathcal{N}(1+O(k))\overline{V}^{(\mathcal{N})} + \cdots \end{aligned}\tag{4.64}$$

this show the importance of cancellations that happen in (4.56) and (4.57), indeed the previous equations tell us that the $\Delta_m{}^2$ term in $\overline{V}^{(\mathcal{N}+1)}$ disappears according with (4.60). However in principle solving (4.64) one is able to compute the following expression

$$k_s(m_0^2) - c_0^{(0)} k^2 = \sum_{i=1}^{\mathcal{N}} \mathcal{K}_i u_i + \mathcal{K}_0 \Delta_m{}^3 \tag{4.65}$$

that can be recovered simply using the leading behaviour of the translated field. Then one can try to find $\chi_i^{(j)}$. If we consider $n = 1$ case of (4.54) [defining $\eta(m_0^2) \equiv k_s(m_0^2) - c_0^{(0)} k(m_0^2)^2$]

$$\eta\overline{V}^{(2)} = \frac{\mathrm{d}\overline{V}^{(1)}}{\mathrm{d}m_0^2} + \alpha\tilde{V}^{(2)} \tag{4.66}$$

where α is an appropriate constant that can be obtained including all the proper terms in (4.54). Remembering that $\tilde{V}^{(2)} = f(m_0^2)s_1$, we easily obtain that the correction to the leading behavior $\overline{V}^{(1)} \sim u_h$ is of order Δ_m and comes from $f(m_0^2)$ so that

$$\chi_i^{(1)} = i + 1 \qquad\qquad \chi^{(1)} = \mathcal{N} + 3. \tag{4.67}$$

Considering the $n = 2$ case of (4.54):

$$\eta\overline{V}^{(3)} = \frac{\mathrm{d}\overline{V}^{(2)}}{\mathrm{d}m_0^2} + o_2\Big[1 + O(k)\Big] + 2c_0^{(0)}\overline{V}^{(1)} + 2kc_0^{(0)}\overline{V}^{(2)}. \tag{4.68}$$

The leading corrections comes from o_2 terms so we find

$$\chi_i^{(2)} = i \qquad\qquad \chi^{(2)} = \mathcal{N} + 2. \tag{4.69}$$

Using (4.54) is then quite easy to compute the terms that appear in the expansion (4.63). Indeed we can rewrite the differential equation (4.54) including only the terms we are interested in as

$$\frac{\mathrm{d}\overline{V}_0^{(n)}}{\mathrm{d}m_0^2} = o_n + t_n {\Delta_m}^3 \overline{V}_0^{(n+1)} + \sum_{j=n+2}^{\mathcal{N}+3} t_{j,n} {\Delta_m}^{j+1-n} \overline{V}_0^{(j)}. \tag{4.70}$$

Integrating the previous equation, using $\overline{V}_0^{(j)} \sim u_{j-1}$, we get

$$\begin{aligned} \overline{V}_0^{(n)}(\Delta_m) - \overline{V}_0^{(n)}(0) &= \left[\int_0^{\Delta_m} o_n\right] + \frac{t_n}{4} {\Delta_m}^4 u_n + \sum_{j=n+1}^{\mathcal{N}} \frac{t_{j+1,n}}{j+3-n} {\Delta_m}^{j+3-n} u_j \\ &\quad + \frac{t_{\mathcal{N}+3}}{\mathcal{N}+5-n} \overline{V}_0^{(\mathcal{N}+3)} {\Delta_m}^{\mathcal{N}+5-n}. \end{aligned} \tag{4.71}$$

Using the previous equation (4.71) we are able to give our final result (for $j > 2$)

$$\begin{aligned} \chi_j^{(j)} &= \mathrm{Min}[j, 4] \\ \chi_i^{(j)} &= \mathrm{Min}[i, i+3-j] \qquad j \neq i & (4.72) \\ \chi^{(j)} &= \mathrm{Min}[\mathcal{N}+2, \mathcal{N}+5-j]. & (4.73) \end{aligned}$$

To finish this section we give an explicit expression of the translated vertices for the $\mathcal{N} = 3$ case that will be studied in detail in the rest of this chapter:

$$\begin{aligned} \overline{V}^{(1)} &= b_0^{(1)} u_h + \mathcal{V}_1^{(1)} {\Delta_m}^2 u_1 + \mathcal{V}_2^{(1)} {\Delta_m}^3 u_2 + \mathcal{V}_3^{(1)} {\Delta_m}^4 u_3 + \mathcal{V}^{(1)} {\Delta_m}^6 & (4.74) \\ \overline{V}^{(2)} &= b_1^{(2)} u_1 + \mathcal{V}_2^{(2)} u_2 {\Delta_m}^2 + \mathcal{V}_3^{(2)} u_3 {\Delta_m}^3 + \mathcal{V}^{(2)} {\Delta_m}^5 & (4.75) \\ \overline{V}^{(3)} &= b_1^{(3)} u_1 + b_2^{(3)} u_2 + \mathcal{V}_3^{(3)} u_3 {\Delta_m}^3 + \mathcal{V}^{(3)} {\Delta_m}^5 & (4.76) \\ \overline{V}^{(4)} &= b_1^{(4)} u_1 + b_2^{(4)} u_2 + b_2^{(4)} u_3 + \mathcal{V}^{(4)} {\Delta_m}^4. & (4.77) \end{aligned}$$

4.1.5 $k(m_0^2)$ near the MCP

In this section we want to investigate the structure of $k(m_0^2)$ (4.37) as a power of Δ_m in order to recover the claims of the previous section [see eqs. (4.56) and (4.57)]. This is the fundamental issue in order to investigate the algebraic structure of the translated vertices $\overline{V}^{(j)}$. In particular we want to show that the Δ_m and ${\Delta_m}^2$ terms that enter into the expression of $k_s(m_0^2)$ near the MCP are due only to the $C(m_0^2)$ expansion near the MCP. We want to investigate only the structure in Δ_m [notice that the scaling fields u_i trivially appear linearly in $k(m_0^2)$] so in the following we can think to put $u_i = 0$. This allows us to think to the expansion (4.78) as an expansion in Δ_m. Otherwise the considerations are general in the MCCL, the expression (4.78) being an expansion in u_h.

An easy computation gives us:

$$\begin{aligned} k(m_0^2) \;&=\; -\frac{\tilde{V}^{(\mathcal{N}+2)}}{\tilde{V}^{(\mathcal{N}+3)}} - \frac{1}{2}\frac{\tilde{V}^{(\mathcal{N}+4)}}{\tilde{V}^{(\mathcal{N}+3)}}\left(\frac{\tilde{V}^{(\mathcal{N}+2)}}{\tilde{V}^{(\mathcal{N}+3)}}\right)^2 + \left(\frac{1}{6}\frac{\tilde{V}^{(\mathcal{N}+5)}}{\tilde{V}^{(\mathcal{N}+3)}} - \frac{1}{2}\left[\frac{\tilde{V}^{(\mathcal{N}+4)}}{\tilde{V}^{(\mathcal{N}+3)}}\right]^2\right)\left(\frac{\tilde{V}^{(\mathcal{N}+2)}}{\tilde{V}^{(\mathcal{N}+3)}}\right)^3 \\ &\quad + O\left({\Delta_m}^4\right) \end{aligned} \tag{4.78}$$

In this subsection we limit ourself to $\mathcal{N} > 1$. In this case we have that $\mathrm{d}\beta/\mathrm{d}{m_0}^2$ is taken into account in the ${\Delta_m}^4$ term in (4.78). This allows us to neglect in (4.30) the terms that are order s_1 near the MCP

$$\frac{\mathrm{d}\tilde{V}_0^{(n)}}{\mathrm{d}{m_0}^2} = \frac{1}{C(m_0^2)}\tilde{V}_0^{(n+1)} - n(n-1)c_0^{(0)}\tilde{V}_0^{(n-1)} + \cdots \tag{4.79}$$

where the dots mean that in the following the corrections can be neglected. Using (4.79) and (4.78) we get a very easy expression

$$\begin{aligned} \frac{\mathrm{d}k(m_0^2)}{\mathrm{d}m_0^2} \;&=\; -\frac{1}{C(m_0^2)} + c_0^{(0)}(\mathcal{N}^2 + 3\mathcal{N} + 2)\frac{\tilde{V}_0^{(\mathcal{N}+1)}}{\tilde{V}_0^{(\mathcal{N}+3)}} - c_0^{(0)}\frac{\mathcal{N}^2 + 3\mathcal{N}}{2}\left[\frac{\tilde{V}_0^{(\mathcal{N}+2)}}{\tilde{V}_0^{(\mathcal{N}+3)}}\right]^2 \\ &\quad + O\left({\Delta_m}^3, \frac{1}{N}\right) \end{aligned} \tag{4.80}$$

In the previous expression we have taken the convention used in this work

$$\tilde{V}^{(n)} \;=\; \tilde{V}_0^{(n)} + O\left(\frac{1}{N}\right)$$

As a straightforward consequence of (4.79), we have that

$$\frac{\tilde{V}_0^{(\mathcal{N}+1)}}{\tilde{V}_0^{(\mathcal{N}+3)}} \;=\; \frac{1}{2C(m_0^2)^2}{\Delta_m}^2 + O({\Delta_m}^3) \tag{4.81}$$

$$\left[\frac{\tilde{V}_0^{(\mathcal{N}+2)}}{\tilde{V}_0^{(\mathcal{N}+3)}}\right]^2 \;=\; \frac{1}{C(m_0^2)^2}{\Delta_m}^2 + O({\Delta_m}^3), \tag{4.82}$$

so that we recover the wanted result

$$\frac{\mathrm{d}k(m_0^2)}{\mathrm{d}m_0^2} \;=\; -\frac{1}{C(m_0^2)} + \frac{c_0^{(0)}}{C(m_0^2)^2}{\Delta_m}^2 + O({\Delta_m}^3) \tag{4.83}$$

$$\begin{aligned} k_s(m_0^2) \;&\equiv\; \frac{1}{C(m_0^2)} + \frac{\mathrm{d}k(m_0^2)}{\mathrm{d}m_0^2} \\ &=\; \frac{c_0^{(0)}{\Delta_m}^2}{C(m_0^2)^2} + O({\Delta_m}^3), \end{aligned} \tag{4.84}$$

and finally

$$k_s(m_0^2) - k(m_0^2)^2 \;=\; O({\Delta_m}^3). \tag{4.85}$$

In (4.83) the Δ_m is due only to $C(m_0^2)$, this disappears with the ${\Delta_m}^2$ term in the (4.85).

4.2 Scaling Fields and the large N limit

In the previous section we have obtained a detailed description of the zero mode Hamiltonian near the MCP. We are now in a position to apply the results of chapter 2 concerning the multicritical points. In particular we have verified that at the $\mathcal{N}$-th order multicritical point all the vertices $\tilde{V}_0^{(j)}(\mathbf{0})$ (with $j = 1, \cdots \mathcal{N}+2$) go to zero in a proper way that has been careful characterized above.[6] This is a necessary condition in order to apply the results of chapter 2 concerning the crossover to multicritical points.

Taking a pedagogical point of view we will give a detail description of the $\mathcal{N}=3$ case for which one can apply the results of sec. 2.2. Following the same step of sec. 3.2, we want to investigate *i*) the scaling variables that describe the crossover between classical behavior to Mean Field behavior eq. (2.67), *ii*) the correction to the critical point $p_i = p_{ic}$ and $\beta = \beta_c$ given by (1.15) and *iii*) the $1/N$ corrections to the classical scaling fields defined in (1.48) and to the classical scaling relations (1.49). We have just pointed out at the beginning of this chapter that the cancellations we have found in the previous sections are very important to solve the point *iii*).

4.2.1 $\mathcal{N}=3$ case in two dimension

For the $\mathcal{N}=3$ the translated vertices near the MCP has been explicitly given in eqs. (4.74), (4.75) and (4.76). Using them we are now in a position to apply the result of sec. 2.2, in particular the results for the Hamiltonian (2.63) can be used with the following identification (for $i = 1, 2, 3, 4$)

$$u_{0i} = \overline{V}^{(i)}(\mathbf{0}) \qquad\qquad u_6 = \frac{\overline{V}^{(6)}(\mathbf{0})}{N^2}. \tag{4.86}$$

Notice in particular that the normalization conditions assumed in eq. (2.63) are satisfied due to the definition of u_6 (4.86) and to eq. (4.37) that ensures $\overline{V}^{(5)}(\mathbf{0}) = 0$ and $K(\mathbf{p}) \approx \mathbf{p}^2$. We will consider only the two dimensions. Otherwise, as pointed out for $\mathcal{N}=1$, for $d>2$ one has to translate the theory to impose that the renormalized five legs vertex is zero. The scaling variable are then simply given by

$$\begin{aligned}
x_h &= -\frac{N^2}{\alpha}(\overline{H} - h_c) &(4.87)\\
x_1 &= \frac{N^2}{\alpha^2}(\overline{V}^{(2)}(\mathbf{0}) - u_{c1}) &(4.88)\\
x_2 &= \frac{N^2}{\alpha^3}(\overline{V}^{(3)}(\mathbf{0}) - u_{c2}) &(4.89)\\
x_3 &= \frac{N^2}{\alpha^4}(\overline{V}^{(4)}(\mathbf{0}) - u_{c3}) &(4.90)
\end{aligned}$$

where u_{ci} have been computed using a lattice regularization in chapter 4. We are not interested in the exact form of this variable but we will develop them in the most general way around the MCP. Notice that in the computation of u_{c1} and u_{c3} we are not able to give $1/N^2$ terms: indeed it would require an hard fine tuning not available until now. On the other hand h_c and u_{c1} can be obtained imposing $\mathbb{Z}_2$ symmetry at the transition.

---

[6] We are neglecting $1/N$ corrections and the counterterms that one needs to include in the effective action in order to regularize the theory. This contributions will be deleted including corrections to the $N=\infty$ multicritical point.

Scaling fields equations. Using the results of the tree-level translated theory we have:

$$\begin{aligned} x_h &= N^{5/2}\Big(b_0^{(1)}u_h + \mathcal{V}_1^{(1)}{\Delta_m}^2 u_1 + \mathcal{V}_2^{(1)}{\Delta_m}^3 u_2 + \mathcal{V}_3^{(1)}{\Delta_m}^4 u_3 + \mathcal{V}^{(1)}{\Delta_m}^6 + \cdots\Big) \\ &\quad + N^{3/2}(H_0 + H_1\Delta_m + \cdots) + N^{1/2}\cdots \qquad (4.91) \\ x_1 &= N^2\Big(b_1^{(2)}u_1 + \mathcal{V}_2^{(2)}u_2{\Delta_m}^2 + \mathcal{V}_3^{(2)}u_3{\Delta_m}^3 + \mathcal{V}^{(2)}{\Delta_m}^5 + \cdots\Big) \\ &\quad + N(U_0 + U_1\Delta_m + \cdots) \qquad (4.92) \\ x_2 &= N^{3/2}\Big(b_1^{(3)}u_1 + b_2^{(3)}u_2 + \mathcal{V}_3^{(3)}u_3{\Delta_m}^3 + \mathcal{V}^{(3)}{\Delta_m}^5 + \cdots\Big) \\ &\quad + N^{1/2}(D_0 + D_1\Delta_m + \cdots) \qquad (4.93) \\ x_3 &= N\Big(b_1^{(4)}u_1 + b_2^{(4)}u_2 + b_3^{(4)}u_3 + \mathcal{V}^{(4)}{\Delta_m}^4 + \cdots\Big) \\ &\quad + (T_0 + T_1\Delta_m) \qquad (4.94) \end{aligned}$$

In the previous expression we do not have considered the possibility of cancellations at one loop order, this is not necessary for the considerations we are going to do. Otherwise if one is searching for particular symmetries some cancellation could be model dependent.[7]

We notice that at the classical level, the scaling fields u_i are not defined in a unique way. Indeed we are able to re-define:

$$u_i' = k_i u_i + \sum_{j=0}^{i-1} f_j u_j \qquad (4.95)$$

so that we can eventually resum *at classical level* the $b_j^{(i)}$ contribution in (4.91-4.94). On the other hand in order to cancel the $\mathcal{V}_l^{(i)}$ terms in (4.91-4.94) we have to include $1/N$ correction in the definition of the scaling fields.

Correction to the critical point. Solving (4.92-4.94) in u_i and putting the result into (4.91) we argue that $\Delta_m \sim m_0/N^{1/5}$ in the MCCL. Using then (4.92,4.93,4.94) we find:

$$u_i \sim \frac{u_i^{(0)}}{N} + O\left(\frac{1}{N^{6/5}}\right) \qquad i = 1, 2 \qquad (4.96)$$

$$u_3 \sim \frac{u_3^{(0)}}{N^{4/5}} + O\left(\frac{1}{N}\right) \qquad (4.97)$$

with:

$${m_0}^5 = -\frac{H_0}{b_0^{(1)} a_{000}^{(5)}} \qquad (4.98)$$

---

[7] For instance if $\mathcal{N} = 1$ and the action is $\mathbb{Z}_2$ symmetric, then in chapter 5 we will show that some cancellations are present also at one loop order. These cancellations give the obvious result $h_c = 0$ (i.e. explicit symmetry is not broken).

$$u_1^{(0)} = -\frac{\mathcal{V}^{(2)} {m_0}^5 + U_0}{b_1^{(2)}} \tag{4.99}$$

$$u_2^{(0)} = \frac{(\mathcal{V}^{(2)} - \mathcal{V}^{(3)}) {m_0}^5 + U_0 - D_0}{b_2^{(3)}} \tag{4.100}$$

$$u_3^{(0)} = -\frac{\mathcal{V}^{(4)} {m_0}^4}{b_3^{(4)}} \tag{4.101}$$

The previous equations (4.96-4.101) are the leading correction to the position of the critical point (notice they are independent of x_i). Otherwise the position of the critical point (u_{ci}) can be obtained studying (4.91-4.94) with $x_i = 0$. It is not hard to see that for u_{ci} we have the following developments in powers of $N^{-1/5}$:

$$\Delta_{mc} = \frac{m_{0c}}{N^{1/5}} + \frac{m_{1c}}{N^{2/5}} + \frac{m_{3c}}{N^{3/5}} + \cdots \tag{4.102}$$

$$u_{1c} = \frac{u_{1c}^{(0)}}{N} + \frac{u_{1c}^{(1)}}{N^{6/5}} + \frac{u_{1c}^{(2)}}{N^{7/5}} + \cdots \tag{4.103}$$

$$u_{2c} = \frac{u_{2c}^{(0)}}{N} + \frac{u_{2c}^{(1)}}{N^{6/5}} + \frac{u_{2c}^{(2)}}{N^{7/5}} + \cdots \tag{4.104}$$

$$u_{3c} = \frac{u_{3c}^{(0)}}{N^{4/5}} + \frac{u_{3c}^{(1)}}{N} + \frac{u_{3c}^{(2)}}{N^{6/5}} + \cdots \tag{4.105}$$

in particular $m_{0c} = m_0$ and $u_{ic}^{(0)} = u_i^{(0)}$ (4.98-4.101).

Redefinitions of the scaling fields. Now we take $x_i \neq 0$ in (4.91-4.94). Defining $\tilde{m} \equiv \Delta_m - \Delta_{mc}$ $\tilde{u}_i \equiv u_i - u_{ic}$, taking into account (4.102-4.105) the (4.91-4.94) now become:

$$\frac{x_h}{b_0^{(1)} N^{5/2}} = \frac{m_{0c}}{N^{1/5}} \tilde{u}_1 + \frac{{m_{0c}}^2}{N^{2/5}} \tilde{u}_2 + \frac{{m_{0c}}^3}{N^{3/5}} \tilde{u}_3 + 5 a_{000}^{(5)} \frac{{m_{0c}}^4}{N^{4/5}} \tilde{m} + \cdots \tag{4.106}$$

$$\frac{x_1}{N^2} = b_1^{(2)} \tilde{u}_1 + \frac{\mathcal{V}_2^{(2)} {m_{0c}}^2}{N^{2/5}} \tilde{u}_2 + \frac{\mathcal{V}_3^{(2)} {m_{0c}}^3}{N^{3/5}} \tilde{u}_3 + 5 \frac{\mathcal{V}^{(2)} {m_{0c}}^4}{N^{4/5}} \tilde{m} + \cdots \tag{4.107}$$

$$\frac{x_2}{N^{3/2}} = b_1^{(3)} \tilde{u}_1 + b_2^{(3)} \tilde{u}_2 + \frac{\mathcal{V}_3^{(3)} {m_{0c}}^3}{N^{3/5}} \tilde{u}_3 + 5 \frac{\mathcal{V}^{(3)} {m_{0c}}^4}{N^{4/5}} \tilde{m} + \cdots \tag{4.108}$$

$$\frac{x_3}{N} = b_1^{(4)} \tilde{u}_1 + b_2^{(4)} \tilde{u}_2 + b_3^{(4)} \tilde{u}_3 + \frac{4 \mathcal{V}^{(4)} {m_{0c}}^3}{N^{3/5}} \tilde{m} + \cdots \tag{4.109}$$

where dots indicate sub-leading contributions. In principle one can solve the previous equations (4.106-4.109) obtaining the following expansion:

$$\tilde{m} = \sum_{i,j,k,l} \mathcal{M}_{ijkl} {x_3}^i {x_2}^j {x_1}^k {x_h}^l \tag{4.110}$$

$$\tilde{u}_p = \sum_{i,j,k,l} \mathcal{U}_{ijkl}^{(p)} {x_3}^i {x_2}^j {x_1}^k {x_h}^l \tag{4.111}$$

with $\mathcal{M}$,$\mathcal{U} \to 0$ when $N \to \infty$. Following chapter 3 and [56], then one tries to solve the previous mixing defining new scaling fields that have to take into account $1/N$ corrections respect the mean-field definition. As a first step we compute (at leading order) the linear terms (in which only one x_i appears) in (4.110-4.111). We easily obtain the following expressions:

$$\begin{aligned}
\tilde{u}_1 &= \mathcal{U}^{(1)}_{x_1}\frac{x_1}{N^2}+\mathcal{U}^{(1)}_{x_2}\frac{x_2}{N^{19/10}}+\mathcal{U}^{(1)}_{x_3}\frac{x_3}{N^{8/5}}+\mathcal{U}^{(1)}_{x_h}\frac{x_h}{N^{5/2}}+\cdots\\
\mathcal{U}^{(1)}_{x_1} &\equiv N^2\mathcal{U}^{(1)}_{0010}=\frac{1}{b^{(2)}_1}+O\left(\frac{1}{N^{1/10}}\right)\\
\mathcal{U}^{(1)}_{x_2} &\equiv N^{19/10}\mathcal{U}^{(1)}_{0100}=\frac{{m_{0c}}^2\mathcal{V}^{(2)}}{a^{(5)}_{000}b^{(3)}_2b^{(2)}_1}-\frac{{m_{0c}}^2\mathcal{V}^{(2)}_2}{b^{(3)}_2b^{(2)}_1}+O\left(\frac{1}{N^{1/10}}\right)\\
\mathcal{U}^{(1)}_{x_3} &\equiv N^{8/5}\mathcal{U}^{(1)}_{1000}=\frac{{m_{0c}}^3\mathcal{V}^{(2)}}{a^{(5)}_{000}b^{(4)}_3b^{(2)}_1}-\frac{{m_{0c}}^3\mathcal{V}^{(2)}_3}{b^{(4)}_3b^{(2)}_1}+O\left(\frac{1}{N^{1/10}}\right)\\
\mathcal{U}^{(1)}_{x_h} &\equiv N^{5/2}\mathcal{U}^{(1)}_{0001}=-\frac{\mathcal{V}^{(2)}}{a^{(5)}_{000}b^{(2)}_1b^{(1)}_0}+O\left(\frac{1}{N^{1/10}}\right)
\end{aligned}\tag{4.112}$$

$$\begin{aligned}
\tilde{u}_2 &= \mathcal{U}^{(2)}_{x_1}\frac{x_1}{N^2}+\mathcal{U}^{(2)}_{x_2}\frac{x_2}{N^{3/2}}+\mathcal{U}^{(2)}_{x_3}\frac{x_3}{N^{8/5}}+\mathcal{U}^{(2)}_{x_h}\frac{x_h}{N^{5/2}}+\cdots\\
\mathcal{U}^{(2)}_{x_1} &\equiv N^2\mathcal{U}^{(2)}_{0010}=-\frac{b^{(3)}_1}{b^{(2)}_1b^{(3)}_2}+O\left(\frac{1}{N^{1/10}}\right)\\
\mathcal{U}^{(2)}_{x_2} &\equiv N^{3/2}\mathcal{U}^{(2)}_{0100}=\frac{1}{b^{(3)}_2}+O\left(\frac{1}{N^{1/10}}\right)\\
\mathcal{U}^{(2)}_{x_3} &\equiv N^{8/5}\mathcal{U}^{(2)}_{1000}=\frac{b^{(3)}_1{m_{0c}}^3\mathcal{V}^{(2)}_3-b^{(2)}_1\mathcal{V}^{(3)}_3{m_{0c}}^3}{b^{(2)}_1b^{(3)}_2b^{(4)}_3}-\frac{{m_{0c}}^3}{a^{(5)}_{000}b^{(2)}_1b^{(3)}_2b^{(4)}_3}(b^{(3)}_1\mathcal{V}^{(2)}-b^{(2)}_1\mathcal{V}^{(3)})\\
&\quad +O\left(\frac{1}{N^{1/10}}\right)\\
\mathcal{U}^{(2)}_{x_h} &\equiv N^{5/2}\mathcal{U}^{(2)}_{0001}=\frac{b^{(3)}_1\mathcal{V}^{(2)}}{a^{(5)}_{000}b^{(1)}_0b^{(2)}_1b^{(3)}_2}-\frac{\mathcal{V}^{(3)}}{a^{(5)}_{000}b^{(1)}_0b^{(3)}_2}+O\left(\frac{1}{N^{1/10}}\right)
\end{aligned}\tag{4.113}$$

$$\begin{aligned}
\tilde{u}_3 &= \mathcal{U}^{(3)}_{x_1}\frac{x_1}{N^2}+\mathcal{U}^{(3)}_{x_2}\frac{x_2}{N^{3/2}}+\mathcal{U}^{(3)}_{x_3}\frac{x_3}{N}+\mathcal{U}^{(3)}_{x_h}\frac{x_h}{N^{23/10}}+\cdots\\
\mathcal{U}^{(3)}_{x_1} &\equiv N^2\mathcal{U}^{(3)}_{0010}=\frac{4\mathcal{V}^{(4)}}{5a^{(5)}_{000}b^{(2)}_1b^{(4)}_3}+\frac{b^{(3)}_1b^{(4)}_2}{b^{(2)}_1b^{(3)}_2b^{(4)}_3}-\frac{b^{(4)}_1}{b^{(2)}_1b^{(4)}_3}+O\left(\frac{1}{N^{1/10}}\right)\\
\mathcal{U}^{(3)}_{x_2} &\equiv N^{3/2}\mathcal{U}^{(3)}_{0100}=-\frac{b^{(4)}_2}{b^{(3)}_2b^{(4)}_3}+O\left(\frac{1}{N^{1/10}}\right)\\
\mathcal{U}^{(3)}_{x_3} &\equiv N\mathcal{U}^{(2)}_{1000}=\frac{1}{b^{(4)}_3}+O\left(\frac{1}{N^{1/10}}\right)\\
\mathcal{U}^{(3)}_{x_h} &\equiv N^{23/10}\mathcal{U}^{(3)}_{0001}=-\frac{4\mathcal{V}^{(4)}}{5a^{(5)}_{000}b^{(1)}_0m_{0c}b^{(4)}_3}+O\left(\frac{1}{N^{1/10}}\right)
\end{aligned}\tag{4.114}$$

$$\tilde{m} = \mathcal{U}^{(m)}_{x_1}\frac{x_1}{N^{14/10}}+\mathcal{U}^{(m)}_{x_2}\frac{x_2}{N^{11/10}}+\mathcal{U}^{(m)}_{x_3}\frac{x_3}{N^{4/5}}+\mathcal{U}^{(m)}_{x_h}\frac{x_h}{N^{17/10}}+\cdots\tag{4.115}$$

$$
\begin{aligned}
\mathcal{U}^{(m)}_{x_1} &\equiv N^{14/10}\mathcal{M}_{0010} = -\frac{1}{5a^{(5)}_{000}{m_{0c}}^3 b^{(2)}_1} + O\left(\frac{1}{N^{1/10}}\right) \\
\mathcal{U}^{(m)}_{x_2} &\equiv N^{11/10}\mathcal{M}_{0100} = -\frac{1}{5b^{(3)}_2 {m_{0c}}^2 a^{(5)}_{000}} + O\left(\frac{1}{N^{1/10}}\right) \\
\mathcal{U}^{(m)}_{x_3} &\equiv N^{4/5}\mathcal{M}_{1000} = -\frac{1}{5a^{(5)}_{000} m_{0c} b^{(4)}_3} + O\left(\frac{1}{N^{1/10}}\right) \\
\mathcal{U}^{(m)}_{x_h} &\equiv N^{17/10}\mathcal{M}_{0001} = \frac{1}{5a^{(5)}_{000}{m_0}^4 b^{(1)}_0} + O\left(\frac{1}{N^{1/10}}\right) \qquad (4.116)
\end{aligned}
$$

We see that at leading order in $1/N$ (4.114) becomes:

$$\overline{u}_3 \equiv \tilde{u}_3 \sim \mathcal{U}^{(3)}_{x_3}\frac{x_3}{N} \qquad (4.117)$$

so that the new scaling field ($\overline{u}_3$) does not need any corrections with respect the older one ($\tilde{u}_3$). The same happen for $\overline{u}_2$:

$$\overline{u}_2 \equiv \tilde{u}_2 \sim \mathcal{U}^{(2)}_{x_2}\frac{x_2}{N^{3/2}} \qquad (4.118)$$

In the expression for $\tilde{u}_1$ (4.112) we see that the terms in x_2 and x_3 are sub-leading with respect to x_1. So one has to include correction to this scaling fields in the following way [using (4.117) and (4.118)]:

$$\overline{u}_1 \equiv \tilde{u}_1 - \frac{1}{N^{2/5}}\frac{\mathcal{U}^{(1)}_{x_2}}{\mathcal{U}^{(2)}_{x_2}}\tilde{u}_2 - \frac{1}{N^{3/5}}\frac{\mathcal{U}^{(1)}_{x_3}}{\mathcal{U}^{(3)}_{x_3}}\tilde{u}_3 \sim \mathcal{U}^{(2)}_{x_1}\frac{x_1}{N^2} \qquad (4.119)$$

Notice that in the previous expression $\mathcal{U}^{(1)}_{x_2}/\mathcal{U}^{(2)}_{x_2}$ and $\mathcal{U}^{(1)}_{x_3}/\mathcal{U}^{(3)}_{x_3}$ need to be computed up to corrections of order $N^{-3/5}$ and $N^{-2/5}$ with respect the value reported in (4.112,4.113,4.114). This implies that if one wants to compute exactly the mixing coefficients in (4.119) one needs to include in (4.106-4.109) almost $N^{-3/5}$ corrections to the leading behaviour, in particular also radiative corrections will enter in the effective computation. Now we have to discuss the effect of having discarded the non-linear terms in (4.110) and (4.111). But it is easy to see that [including contributions that correct (4.107)] for instance the ${x_3}^2$ contribution scales as $1/N^{22/10}$. This shows that this contributions can be neglected.

Now we pass to discuss the $\tilde{u}_h$ field. Using the gap-equation and (4.91) we include corrections to (4.106) in the following way

$$\frac{x_h}{b^{(1)}_0 N^{5/2}} = \tilde{u}_h + \frac{\mathcal{H}_1}{N^{2/5}}\tilde{u}_1 + \frac{\mathcal{H}_2}{N^{3/5}}\tilde{u}_2 + \frac{\mathcal{H}_3}{N^{4/5}}\tilde{u}_3 + \frac{\mathcal{H}^{(1)}_m}{N}\tilde{m} + \frac{\mathcal{H}^{(2)}_m}{N^{4/5}}\tilde{m}\tilde{m} \qquad (4.120)$$

Notice that in the previous expansion (4.120), the $\tilde{u}_3\tilde{u}_3$ term ($\sim {x_3}^2 N^{-2}$) is not present; indeed it has been adsorbed in the definition of u_h. At leading order in N we have (4.91-4.94)

$$
\begin{aligned}
\mathcal{H}_1, \mathcal{H}_2, \mathcal{H}_3 &= \mathcal{V}^{(1)}_1 {m_{0c}}^2, \mathcal{V}^{(1)}_2 {m_{0c}}^3, \mathcal{V}^{(1)}_3 {m_{0c}}^3 \qquad (4.121) \\
\mathcal{H}^{(1)}_m &= 6m^5_{0c}\mathcal{V}^{(1)} + H_1 \qquad (4.122) \\
\mathcal{H}^{(2)}_m &= 15m^4_{0c}\mathcal{V}^{(1)} \qquad (4.123)
\end{aligned}
$$

while in order to compute completely the mixing-coefficients many other contributions (in $1/N^{10}$) are needed. Using then (4.120) and (4.116) we can define the new scaling field $\overline{u}_h$

$$\begin{aligned}\overline{u}_h &= \tilde{u}_h - \frac{1}{\mathcal{U}^{(1)}_{x_1}}\left(\frac{\mathcal{H}_1\mathcal{U}^{(1)}_{x_1}}{N^{2/5}} + \frac{\mathcal{H}^{(1)}_m\mathcal{U}^{(m)}_{x_1}}{N^{2/5}}\right)\overline{u}_1 - \frac{1}{\mathcal{U}^{(2)}_{x_2}}\left(\frac{\mathcal{H}_1\mathcal{U}^{(1)}_{x_2}}{N^{4/5}} + \frac{\mathcal{H}_2\mathcal{U}^{(2)}_{x_2}}{N^{3/5}} + \frac{\mathcal{H}_3\mathcal{U}^{(3)}_{x_2}}{N^{4/5}}\right.\\ &\quad \left.+\frac{\mathcal{H}^{(1)}_m\mathcal{U}^{(m)}_{x_2}}{N^{3/5}}\right)\overline{u}_2 - \frac{1}{\mathcal{U}^{(3)}_{x_3}}\left(\frac{\mathcal{H}_1\mathcal{U}^{(1)}_{x_3}}{N} + \frac{\mathcal{H}_2\mathcal{U}^{(2)}_{x_3}}{N^{6/5}} + \frac{\mathcal{H}_3\mathcal{U}^{(3)}_{x_3}}{N^{4/5}} + \frac{\mathcal{H}^{(1)}_m\mathcal{U}^{(m)}_{x_3}}{N^{4/5}}\right)\overline{u}_3\\ &\quad -\frac{\mathcal{H}^{(2)}_m}{(\mathcal{U}^{(3)}_{x_3})^2}\frac{1}{N^{2/5}}\overline{u}_3^2 \end{aligned} \tag{4.124}$$

so that we can write:

$$\overline{u}_h \sim \frac{x_h}{N^{5/2}} \tag{4.125}$$

4.3 Conclusions

In this chapter we have investigate the critical behavior of $O(N)$ models with a generalized ferromagnetic nearest neighbour interaction depending on $\mathcal{N}$ tunable parameters that undergo a phase transition at finite temperature (see chapter 1). In sec. 4.1 we have studied in detail the algebraic structure of the zero Mode Hamiltonian near the critical point, parametrizing the vertices using the scaling fields of the $N = \infty$ theory (chapter 1). Using the results of chapter 2 in two dimension, in sec. 4.2 we have applied the theory of Multicritical Crossover Limit to the specific case $\mathcal{N} = 3$. The approach we have given is only algebraic (for instance we do not have taken care of the explicit form of u_{ci}[8] but we have taken the most general behavior near the MCP) but shows the steps that one need to follow in order to study the critical limit when $N \to \infty$. In particular it shows the definition of the scaling fields and corrections to the critical point that in principle could be compared with available numerical results (in a similar way of what reported in sec. 3.5). Using the scheme presented in this chapter we believe several physical system could be investigate. For instance finite temperature Yukawa model with N_f fermions (for $N_f \to \infty$) has been investigate in chapter 5. There we have shown as the system, for every N_f finite, undergoes an Ising phase transition that crosses on a Mean Field phase transition for $N_f = \infty$ in the same way of the $\mathcal{N} = 1$ models introduced in chapter 1 and studied in chapter 3. It is usually claimed that if one tune also a chemical potential the phase diagram exhibit also a tricritical point. We plan to apply the method developed in this chapter for the investigation of this multicritical point.

---

[8] The explicit form of u_{ic} has been computed in chapter 2

Chapter 5

Fermionic Models with chiral symmetry

In the previous chapters we have investigated several problems related to the $1/N$ expansion in models with global symmetry. In order to investigate such kinds of problems we have used generalized Heisenberg models. However we believe that the presentation given is general because in the effective action for the zero mode (translated or not) noone symmetries was assumed, but the most general expansions was taken.[1] For this reason we have tried to investigate the large N limit of other Infra Red divergent models [49]. In this chapter we present our analysis of fermionic models with global symmetry at finite temperature. This kind of studies could be significant in order to investigate the nature of the QCD phase diagram. The finite-temperature transition in QCD has been extensively studied in the last twenty years and is becoming increasingly important because of the recent experimental progress in the physics of ultrarelativistic heavy-ion collisions. Some general features of the transition, which is associated with the restoration of chiral symmetry, can be studied in dimensionally-reduced three-dimensional models [44, 45]. However, a detailed understanding requires a direct analysis in QCD. Being the phenomenon intrinsically nonperturbative, our present knowledge comes mainly from numerical simulations [46, 47]. Due to the many technical difficulties—finite-size effects, proper inclusion of fermions, etc. —results are not yet conclusive and thus it is worthwhile to study simplified models that show the same basic features but are significantly simpler.

---

[1] This is not completely correct. We have seen that in $O(N)$ models the sign of the effective four leg vertex at the Critical Point has the same sign of the mass term of the zero mode near the CP [the claim follows from eq. (3.12)]. In principle this fact could not necessary holds for other models which share with Heisenberg models the existence of a zero mode.

5.1 The model

In this chapter we shall consider a Yukawa model in which N_f fermions are coupled with a scalar field through a Yukawa interaction.

$$\mathcal{S} \;=\; DN_f \int \mathrm{d}^{d+1}\mathbf{x} \left(\frac{1}{2}(\partial\phi)^2 + \frac{\mu}{2}\phi^2 + \frac{\lambda}{4!}\phi^4\right) + \sum_{f=1}^{N_f} \int \mathrm{d}^{d+1}\mathbf{x}\, \overline{\psi}_f \Big(\partial\!\!\!/ + g\phi + M\Big)\psi_f \tag{5.1}$$

where $\partial\!\!\!/ \equiv \sum_{\mu=1}^{d+1} \gamma_\mu \partial_\mu$ and γ_μ, $\mu = 1, \cdots, d+1$ are the generator of a Clifford Algebra satisfying the anti-commutation relations $\{\gamma_\mu, \gamma_\nu\} = 2\delta_{\mu,\nu}\mathbf{1}$ where $\mathrm{tr}\,\gamma_\mu^2 = D$,[2] and $\mathbf{1}$ is the identity $D \times D$ matrix. The integration is over $\mathbb{R}^d \times [0, T^{-1}]$, and $\lambda \geq 0$ to ensure the stability of the quartic potential. Along the *thermal* direction we take periodic boundary conditions for the bosonic field ϕ and antiperiodic ones for the fermionic fields ψ_f

$$\phi(\mathbf{x}, 0) = \phi(\mathbf{x}, T^{-1}) \qquad \psi(\mathbf{x}, 0) = -\psi(\mathbf{x}, T^{-1}) \qquad \overline{\psi}(\mathbf{x}, 0) = -\overline{\psi}(\mathbf{x}, T^{-1}). \tag{5.2}$$

The theory must be properly regularized. We shall consider a sharp-cutoff regularization, restricting the momentum integrations in the *spatial* directions to $p < \Lambda$. However, the discussion presented here can be extended without difficulty to any other regularization that maintains at least a remnant of chiral symmetry. For instance an explicit lattice calculation involving staggered fermions has been considered. However all the computations strictly follow the presentation of this chapter without any new consideration;[3] in particular the relations that protect the symmetry of the theory are satisfied also for chiral fermions on the lattice (in the following this fact will guarantee that $M_c = 0$ for every N_f).

Given a representation of the Clifford Algebra in even dimension (see e.g. [24]), $\gamma_{\mathcal{C}}$ is introduced

$$\gamma_{\mathcal{C}} := \gamma_1 \gamma_2 \cdots \gamma_d, \tag{5.3}$$

so that it anti-commutes with all the generators of the algebra $\{\gamma_{\mathcal{C}}\,, \gamma_\mu\} = 0$, $\mu = 1, 2 \cdots d$. On the other hand an odd dimensional representation can be built by using the standard $d-1$-dimensional representation, plus $\gamma_{\mathcal{C}}$ (5.3) multiplied by a proper $\mathbb{C}$ number

$$\gamma_\mu(2d+1) = \begin{cases} \gamma_u(2d) & \text{if } \mu < 2d+1 \\ \sqrt{(-1)^k}\,\gamma_{\mathcal{C}}(2d) & \text{if } \mu = 2d+1. \end{cases}$$

The interaction (5.1) has a discrete symmetry for $M = 0$. If d is even this can be realized by the following transformations

$$\psi \to \gamma_{\mathcal{C}}\,\psi \qquad \overline{\psi} \to -\overline{\psi}\,\gamma_{\mathcal{C}} \qquad \phi \to -\phi \tag{5.4}$$

---

[2] One can chooses a representation so that $D = 2^{d/2}$ if d is even, $D = 2^{(d+1)/2}$ if d is odd

[3] The only significant differences are related to the doubling problem (partially solved by staggered fermions) that gives additional degrees of freedom.

In odd dimension $\gamma_{\mathcal{C}}$ is trivial $\gamma_{\mathcal{C}} = (-1)^k \mathbf{1}$. Actually the previous symmetry (5.4) can be realized using a γ_i coupled with a reflection in the Euclidean space along the i-th direction [24]:

$$\begin{gathered}\psi \to \gamma_i \psi \qquad \overline{\psi} \to -\overline{\psi}\gamma_i \qquad \phi \to -\phi \\ \{x_1, \cdots x_i, \cdots x_{d+1}\} \to \{x_1, \cdots - x_i, \cdots x_{d+1}\}\end{gathered} \tag{5.5}$$

We present an unified picture using (5.5) with $i = d+1$. We are interested to study the reduced-dimensional action which is obtained integrating out the *thermal* component so that the minus sign appearing in (5.5) can be neglected. The previous symmetries (5.4-5.5) protect by fermions mass generation and can be investigate studying the expectation value of the bosonic field $< \phi >$ that will be used as an order parameter to investigate the phase diagram of the model (5.1).

In the limit $N_f \to \infty$ this model can be solved analytically and one finds that there is a range of parameters in which it shows a transition analogous to that observed in QCD [48, 49]. It separates a low-temperature phase in which chiral symmetry is broken from a high-temperature phase in which chiral symmetry is restored. For $N_f = \infty$ this transition shows mean-field behavior, in contrast with general arguments that predict the transition to belong to the Ising universality class. This apparent contradiction was explained in Ref. [50] where, by means of scaling arguments, it was shown that the width of the Ising critical region scales as a power of $1/N_f$, so that only mean-field behavior can be observed in the limit $N_f = \infty$.

This picture is strictly like what we have observed in a generalized $O(N)$ σ model in the first part of this work: for finite values of N the transition was expected to be in the Ising universality class, while the $N = \infty$ solution predicted mean-field behavior. In chap. 3 we performed a detailed calculation of the $1/N$ corrections, explaining the observed behavior in terms of a critical-region suppression. The analytic technique presented in this work can be applied to model (5.1). It allows us to obtain an analytic description of the crossover from mean-field to Ising behavior that occurs when N_f is large and to extend the discussion of Ref. [50] to the case $M \neq 0$. More importantly, we are able to show that the phenomenon is universal. In field-theoretical terms, it can be characterized as a crossover between two fixed points: the Gaussian fixed point and the Ising fixed point. This implies that quantitative predictions for model (5.1) can be obtained in completely different settings. One can use field theory and compute the crossover functions by resumming the perturbative series [29, 30, 31, 32]. Alternatively, one can use the fact that the field-theoretical crossover is equivalent to the critical crossover that occurs in models with medium-range interactions [33, 34, 32, 35, 26]. This allows one to use the wealth of results available for these spin systems [33, 36, 37, 34, 32, 26]. Finally, we should note that the phenomenon is quite general and occurs in any situation in which there is a crossover from the Gaussian fixed point to a nonclassical stable fixed point. For instance, similar considerations have been recently presented for finite-temperature QCD in some very specific limit [58], while for other models the scenario presented above is questionable [43].

In sec. 5.2 we review the behavior in the limit $N_f = \infty$. In sec. 5.3 we consider the $1/N_f$ fluctuations and determine the effective theory of the excitations that are responsible for the Ising behavior at the critical point. These modes are described by an effective weakly-coupled ϕ^4 Hamiltonian. These considerations are applied to the Yukawa model in sec. 5.5.2

and in sec. 5.5.3. We determine the relevant scaling variables and show how to compute the crossover behavior of the correlation functions. In the appendix B we carefully discuss the relations among medium-ranged spin models, field theory, and the Yukawa model. The presentation given strictly follows Ref. [59] and Ref. [60].

5.2 Behavior for $N_f = \infty$

The solution of the model for $N_f = \infty$ is quite standard. We briefly summarize here the main steps, following the presentation of Ref. [49]. As a first step we integrate the fermionic fields obtaining an effective action $\mathcal{S}_{\rm eff}[\phi]$ given by

$$e^{-DN_f \mathcal{S}_{\rm eff}[\phi]} \;=\; \int \prod_{f=1}^{N_f} \mathrm{d}\overline{\psi}_f \mathrm{d}\psi_f \, e^{-\mathcal{S}[\phi,\overline{\psi},\psi]}, \tag{5.6}$$

where

$$\mathcal{S}_{\rm eff}[\phi] \;=\; \int \mathrm{d}^{d+1}\mathbf{x} \Big(\frac{1}{2}(\partial\phi)^2 + \frac{\mu}{2}\phi^2 + \frac{\lambda}{4!}\phi^4\Big) - \frac{1}{D}\int \mathrm{d}^{d+1}\mathbf{x}\; \mathrm{tr}\log\Big(\not\partial + g\phi + M\Big). \tag{5.7}$$

For $N_f \to \infty$ one can expand around the saddle point $\phi = \overline{\phi}$, that is determined by the gap equation $\delta\mathcal{S}_{\rm eff}[\overline{\phi}]/\delta\phi = 0$

$$\overline{\mu} m + \frac{\overline{\lambda}}{6} m^3 = (m+M)T \sum_{n\in\mathbb{Z}} \int_{p<\Lambda} \frac{\mathrm{d}^d\mathbf{p}}{(2\pi)^d} \frac{1}{p^2 + \omega_n^2 + (m+M)^2}, \tag{5.8}$$

where we define the *frequencies* $\omega_n \equiv (2n+1)\pi T$, and

$$m \equiv g\,\overline{\phi} \qquad \overline{\mu} \equiv \mu\, g^{-2} \qquad \overline{\lambda} \equiv \lambda\, g^{-4}\;.$$

The action corresponding to a saddle-point solution m is:

$$\overline{\mathcal{S}}_{\rm eff}(m, M, T) \;=\; \frac{\overline{\mu}}{2} m^2 + \frac{\overline{\lambda}}{4!} m^4 - \frac{T}{2}\sum_{n\in\mathbb{Z}} \int_{p<\Lambda} \frac{\mathrm{d}^d\mathbf{p}}{(2\pi)^d} \log\left[\frac{p^2 + \omega_n^2 + (m+M)^2}{p^2 + \omega_n^2}\right], \tag{5.9}$$

where we have added a mass-independent counterterm to regularize the sum [49]. Such a quantity has been chosen so that the action for $M = m = 0$ vanishes. Summations can be done analytically using the identity[4]

$$\sum_n \frac{x}{(n+1/2)^2 + x^2} = \pi\tanh(\pi x) = \pi\Big(1 - \frac{2}{e^{2\pi x} + 1}\Big). \tag{5.10}$$

---

[4] The (5.10) can be proved considering the identity $0 = \pi \int_{\mathcal{C}} \mathrm{d}z \frac{\mathrm{ctg}(\pi z)}{(z+1/2)^2 + x^2}$, that holds considering for instance $\mathcal{C}$ a rectangular in the complex plain with the vertex on semi-integer number [i.e. $v_i = (m_i + 1/2, in_i + 1/2)$, $m_i, n_i \in \mathbb{Z}$ and $i = 1, 2\cdots 4$], and taking the limit $m_i, n_i \to \pm\infty$, with the proper sign so that $\mathcal{C}$ encloses all the plane. Using Cauchy theorem one can evaluate the series (5.10) computing the residues of the previous integrand at $z = -1/2 \pm ix$.

The gap equation can then be written as

$$p(m) \;=\; (m+M)\,\mathcal{G}(m+M,T), \tag{5.11}$$

where the functions $p(m)$ and $\mathcal{G}(x,T)$ are defined by

$$p(m) \;\equiv\; \overline{\mu}\,m + \frac{\overline{\lambda}}{6}m^3, \tag{5.12}$$

$$\mathcal{G}(x,T) \;\equiv\; \int_{p<\Lambda} \frac{\mathrm{d}^d\mathbf{p}}{(2\pi)^d}\,\frac{1}{\sqrt{p^2+x^2}}\left(\frac{1}{2} - \frac{1}{e^{\sqrt{p^2+x^2}/T}+1}\right). \tag{5.13}$$

Analogously we can rewrite eq. (5.9) as

$$\begin{aligned}\overline{\mathcal{S}}_{\text{eff}}(m,M,T) \;=\;& \frac{\overline{\mu}}{2}m^2 + \frac{\overline{\lambda}}{4!}m^4 \\ &-T\int_{p<\Lambda}\frac{\mathrm{d}^d\mathbf{p}}{(2\pi)^d}\left[\log\left(\cosh\frac{\sqrt{p^2+(m+M)^2}}{2T}\right) - \log\cosh\frac{p}{2T}\right]\end{aligned} \tag{5.14}$$

Using eqs. (5.11) and (5.14) we can determine the phase diagram of the model. Given $\overline{\mu}$ and $\overline{\lambda}$, for each value of T and M we determine the solutions m of the gap equations. When the solutions are more than one, the physical one is that with the lowest action $\overline{\mathcal{S}}_{\text{eff}}(m,M,T)$. Note that eqs. (5.11) and (5.14) are invariant under the transformations $m \to -m$ and $M \to -M$. Thus, we can limit our study to the case $M \geq 0$. In general, we can find either one solution or three different solutions m_0, m_+, and m_- with $m_- \leq m_0 \leq m_+$ (for some specific values of the parameters two of them may coincide). The previous claim can be proved using the following identities (see app. A)

$$\frac{\mathrm{d}}{\mathrm{d}x}x\,\mathcal{G}(x,T) \geq 0 \qquad\qquad \frac{\mathrm{d}^2}{\mathrm{d}x^2}x\,\mathcal{G}(x,T)\theta(x) \leq 0\,, \tag{5.15}$$

[$\theta(x)$ is the step function] and straightforward consideration on the gap equation (5.11). There are four different possibilities:

(a) If $\overline{\mu} \geq \mathcal{G}(0,0) = C_0\Lambda^{d-1}$ with

$$C_0 \;\equiv\; \left[2^d\pi^{d/2}(d-1)\Gamma\!\left(\frac{d}{2}\right)\right]^{-1}, \tag{5.16}$$

then, for every $M \geq 0$, there is only one solution $m_+ \geq 0$; for $M = 0$ we have $m_+ = 0$.

(b) If $0 < \overline{\mu} < C_0\Lambda^{d-1}$, there exists a critical temperature $T_c(\overline{\mu})$ (see fig. 5.1). For $T > T_c(\overline{\mu})$ and any M there is only one solution $m_+ \geq 0$ (for $M = 0$ we have $m_+ = 0$). For $T < T_c(\overline{\mu})$ and $M < \tilde{M}$ there are three solutions m_0, m_+, and m_- with $m_- \leq m_0 \leq m_+$ and $m_+ \geq 0$ and $m_- \leq 0$. For $T < T_c(\overline{\mu})$ and $M > \tilde{M}$ there is only one solution corresponding to m_+. The physical solution is always m_+ so that $\tilde{M}$ has no physical

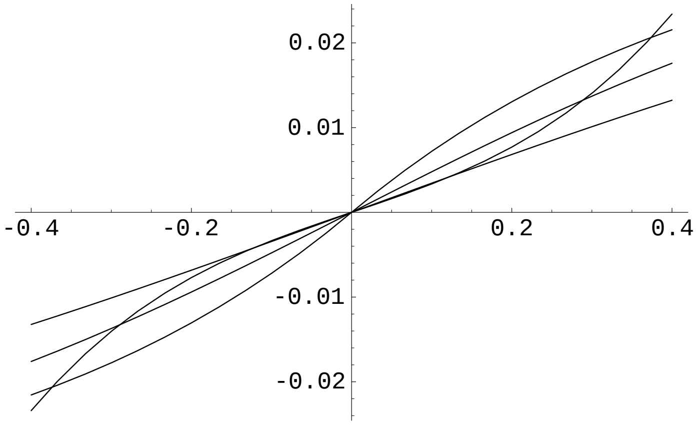

Figure 5.1: Plot of $p(m)$ and $m\mathcal{G}(m)$ for $C_0\Lambda^{d-1} > \overline{\mu} > 0$ taking different temperature. The symmetry is broken at low temperature ($m_+ \neq 0$)

meaning. Moreover, for $T < T_c(\overline{\mu})$ and $M = 0$, $m_+ > 0$. The critical temperature can be computed from the following relation:

$$\begin{aligned} \overline{\mu} = \mathcal{G}(0, T_c) &= T_c \sum_{n \in \mathbb{Z}} \int_{p<\Lambda} \frac{\mathrm{d}^d\mathbf{p}}{(2\pi)^d} \frac{1}{p^2 + \omega_{c,n}^2} \\ &= \Lambda^{d-1} C_0 - \Lambda^{d-1} \int_{p<1} \frac{\mathrm{d}^d\mathbf{p}}{(2\pi)^d} \frac{1}{p[e^{p/t_c} + 1]}, \end{aligned} \tag{5.17}$$

where $\omega_{c,n} \equiv (2n+1)\pi T_c$ and $T_c(\overline{\mu}) = t_c(\overline{\mu})\Lambda$. For $\overline{\mu} \to 0$, we have $T_c(\overline{\mu}) \to \infty$.

(c) If $-C_1 < \overline{\mu} \leq 0$ (see fig. 5.2 left), with[5]

$$C_1^{3/2} \equiv \lambda^{1/2} \frac{3\Lambda^d}{2^{d+2}\pi^{d/2}\sqrt{2}} \Gamma\Big(\frac{d+2}{2}\Big)^{-1}, \tag{5.18}$$

there is a critical mass $\tilde{M}$ such that there are three solutions for $M < \tilde{M}$, two of them coincide for $M = \tilde{M}$, while for $M > \tilde{M}$ the only solution is m_+. The physical solution—the one with the lowest action—is always m_+ so that $\tilde{M}$ has no physical meaning. Note that $m_+ > 0$ for $M = 0$.

(d) For $\overline{\mu} \leq -C_1$ (see fig. 5.1 right) there are three solutions for all values of T and M. The relevant solution is always $m_+ > 0$.

In order to compute the more stable solutions (if more than one are present) one can use the previous consideration, the figs. 5.2 5.1 and[6]

$$S_{\text{eff}}(m) = c(M,T) + \int_0^m \mathrm{d}x\, p(x) - (x+M)\mathcal{G}(x+M,T) \tag{5.19}$$

---

[5] C_1 is the solution of the equation $p(-x) = \lim_{M\to\infty} M\mathcal{G}(M,0)$ with $x = (2C_1/\overline{\lambda})^{1/2}$. The value x corresponds to the position of a maximum of $p(m)$ for $\overline{\mu} = -C_1$.

[6] $c(M,T)$ can easily be computed using eq. (5.9), in particular $c(0,T) = 0$.

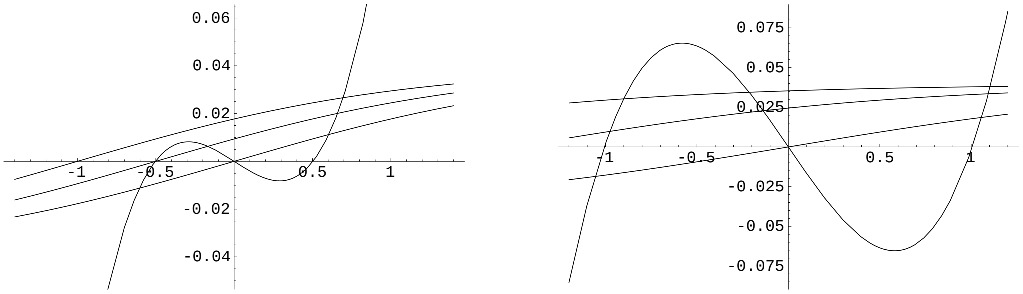

Figure 5.2: Plot of $p(m)$ and $(m{+}M)\mathcal{G}(m{+}M)$ for several M and with $\overline{\mu} < 0$ (the intersection points are the solutions of the gap equation 5.11). (Left) Case (c): there could be one or three solution, however $m_+ > 0$ is always present and is always the more stable. (Right) Case (d): there are always three solutions.

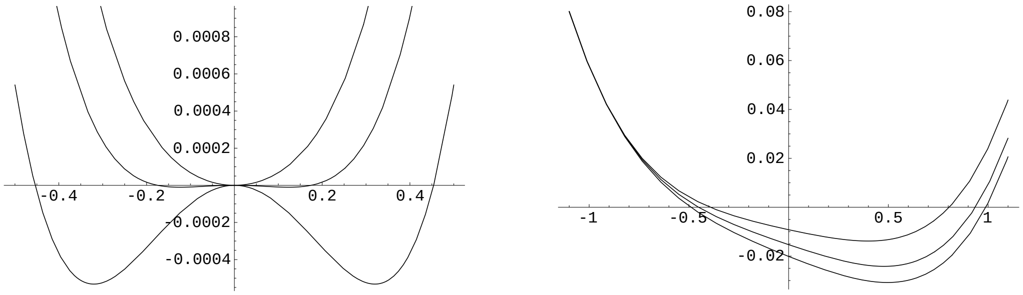

Figure 5.3: S_{eff} for $M = 0$ and $M > 0$

to evaluate the more stable solution. Using the symmetry of $p(x)$ and $x\mathcal{G}(x)$ we get that in case (a) chiral symmetry is never broken, while in cases (c) and (d) chiral symmetry is never restored. Thus, the only case of interest—and the only one we shall consider in the following—is case (b), in which there is a chirally-symmetric high-temperature phase and a low-temperature phase in which chiral symmetry is broken (see fig. 5.3).

The nature of the transition is easily determined. We expand

$$\mathcal{G}(x,T) \;=\; \sum_{m,n} g_{mn}\, x^{2m}(T-T_c)^n, \tag{5.20}$$

where

$$\begin{aligned}
g_{00} &= T_c \sum_{n\in\mathbb{Z}} \int_{p<\Lambda} \frac{\mathrm{d}^d\mathbf{p}}{(2\pi)^d}\,\frac{1}{p^2+\omega_{c,n}^2},\\
g_{01} &= \sum_{n\in\mathbb{Z}} \int_{p<\Lambda} \frac{\mathrm{d}^d\mathbf{p}}{(2\pi)^d}\,\frac{p^2-\omega_{c,n}^2}{(p^2+\omega_{c,n}^2)^2}\\
&= -\frac{1}{T_c^2}\int_{p<\Lambda} \frac{\mathrm{d}^d\mathbf{p}}{(2\pi)^d}\frac{e^{p/T_c}}{(e^{p/T_c}+1)^2},\\
g_{10} &= -T_c \sum_{n\in\mathbb{Z}} \int_{p<\Lambda} \frac{\mathrm{d}^d\mathbf{p}}{(2\pi)^d}\,\frac{1}{(p^2+\omega_{c,n}^2)^2},
\end{aligned} \tag{5.21}$$

and $\omega_{c,n} \equiv (2n+1)\pi T_c$. Since $g_{00} = \mathcal{G}(0,T_c) = \overline{\mu}$ [eq. (5.17)], the gap equation (5.11) becomes:

$$\frac{\overline{\lambda}}{6}m^3 \;=\; \overline{\mu}M + g_{01}(T-T_c)(m+M) + g_{10}(m+M)^3 + \cdots \tag{5.22}$$

where we have neglected subleading terms in $m+M$ and $T-T_c$. Defining

$$u_h \equiv \frac{6\overline{\mu}}{6g_{10}-\overline{\lambda}}\,M \qquad\qquad u_t \equiv \frac{6g_{01}}{6g_{10}-\overline{\lambda}}\,(T-T_c), \tag{5.23}$$

and taking the limit $u_h, u_t \to 0$ at fixed $x \equiv u_t/u_h^{2/3}$ we obtain the equation of state

$$m \;=\; {u_h}^{1/3} f(x) \tag{5.24}$$

$$0 \;=\; f(x)^3 + x f(x) + 1. \tag{5.25}$$

Note that the prefactor of $T-T_c$ in u_t is always positive to ensure the existence of only one solution for $T > T_c$. Such an equation is exactly the mean-field equation of state that relates magnetization φ, magnetic field h, and reduced temperature t. Indeed, if we consider the mean-field Hamiltonian

$$\mathcal{H} = h\varphi + \frac{t}{2}\varphi^2 + \frac{u}{24}\varphi^4, \tag{5.26}$$

the stationarity condition gives

$$h + t\varphi + \frac{u}{6}\varphi^3 = 0, \tag{5.27}$$

which is solved by $\varphi = A h^{1/3} f(Bt|h|^{-2/3})$, where $f(x)$ satisfies eq. (5.25), and A and B are constants depending on u. This identification also shows that M plays the role of an external field, while $m \sim \overline{\phi}$ is the magnetization.

5.3 Vertex, Propagator and the failure of $1/N$ expansion

In order to perform the $1/N_f$ calculation, we expand the field ϕ around the saddle-point solution,

$$\phi(\mathbf{x}) = \overline{\phi} + \frac{1}{g\sqrt{N}}\hat{\phi}(\mathbf{x}), \tag{5.28}$$

where $N \equiv DN_f$, and $\hat{\phi}(\mathbf{x})$ in Fourier modes:

$$\hat{\phi}(\mathbf{x}_d, x_{d+1}) = T\sum_{n\in\mathbb{Z}} e^{2i\pi nTx_{d+1}} \int \frac{\mathrm{d}^d\mathbf{p}}{(2\pi)^d}\,\hat{\phi}_n(\mathbf{p})e^{i\mathbf{p}\cdot\mathbf{x}_d}\;. \tag{5.29}$$

In the following we will refer to the integers n—or more precisely to $2\pi nT$—as frequencies. In this way we obtain the following expansion for the effective action:

$$\hat{\mathcal{S}}_{\text{eff}}[\hat{\phi}_n] \;=\; N\{\mathcal{S}_{\text{eff}}[\phi] - \mathcal{S}_{\text{eff}}[\overline{\phi}]\}$$

$$
\begin{aligned}
= \ & \frac{T}{2}\sum_n \int_{p<\Lambda} \frac{\mathrm{d}^d\mathbf{p}}{(2\pi)^d}\, P(\mathbf{p},n)\hat{\phi}_n(\mathbf{p})\hat{\phi}_{-n}(-\mathbf{p}) \\
& + \sum_{l\geq 3} \frac{T^{l-1}}{l!N^{l/2-1}} \sum_{\{n_i\}} \int_{p_i<\Lambda} \frac{\mathrm{d}^d\mathbf{p}_1}{(2\pi)^d} \cdots \frac{\mathrm{d}^d\mathbf{p}_l}{(2\pi)^d} (2\pi)^d \delta\Big(\sum_{j=1}^l \mathbf{p}_j\Big) \delta_{\sum_i n_i, 0} \\
& \qquad \hat{\phi}_{n_1}(\mathbf{p}_1)\cdots\hat{\phi}_{n_l}(\mathbf{p}_l) V^{(l)}(\mathbf{p}_1, n_1; \cdots; \mathbf{p}_l, n_l).
\end{aligned} \tag{5.30}
$$

Note the Kronecker δ on the frequencies that ensures that vertices are nonvanishing only for $\sum_i^l n_i = 0$. In particular—this property will be important in order to obtain the effective action for the zero mode—if only one frequency is nonvanishing $V^{(l)}(\mathbf{p}_1, n; \mathbf{p}_2, 0; \cdots; \mathbf{p}_l, 0) = 0$.

The vertices appearing in expansion (5.30) are easily computed. The fermion contribution is obtained by considering the one-loop fermionic graphs in theory (5.1). If we define the free fermion propagator

$$
\Delta_F(\mathbf{p}, n; m) \equiv \frac{-i\sum_{j=1}^d \gamma_j p_j - i\gamma_{d+1}\omega_n + m}{p^2 + \omega_n^2 + m^2} \tag{5.31}
$$

with $\omega_n \equiv (2n+1)\pi T$, the fermion contribution is

$$
\begin{aligned}
& V_f^{(l)}(\mathbf{p}_1, n_1; \cdots; \mathbf{p}_l, n_l) = \\
& \qquad (-1)^l \frac{T}{D} \sum_{a\in\mathbb{Z}} \int_{q<\Lambda} \frac{\mathrm{d}^d\mathbf{q}}{(2\pi)^d} \operatorname{tr}\left[\prod_{i=1}^l \Delta_F\Big(\mathbf{q} + \sum_{j=1}^i \mathbf{p}_j; a + \sum_{j=1}^i n_j; m+M\Big)\right] \\
& \qquad + \text{permutations},
\end{aligned} \tag{5.32}
$$

where the permutations make the vertex completely symmetric [there are $(l-1)!$ terms]. Note that the frequencies ω_n never vanish and thus the vertices have a regular expansion in powers of $m+M$. Vertices $V_f^{(l)}$ satisfy an important symmetry relation. First, note that

$$
\gamma_{d+1}\Delta_F(\mathbf{p}, n; m)\gamma_{d+1} = -\Delta_F(\mathbf{p}, -n-1; -m). \tag{5.33}
$$

It follows

$$
\begin{aligned}
& \sum_{a\in\mathbb{Z}} \operatorname{tr}\left[\prod_{i=1}^l \Delta_F(\mathbf{q}_i; a+b_i; m)\right] = \sum_{a\in\mathbb{Z}} \operatorname{tr}\left[\prod_{i=1}^l \gamma_{d+1}\Delta_F(\mathbf{q}_i; a+b_i; m)\gamma_{d+1}\right] = \\
& (-1)^l \sum_{a\in\mathbb{Z}} \operatorname{tr}\left[\prod_{i=1}^l \Delta_F(\mathbf{q}_i; -a-b_i-1; -m)\right] = (-1)^l \sum_{a\in\mathbb{Z}} \operatorname{tr}\left[\prod_{i=1}^l \Delta_F(\mathbf{q}_i; a-b_i; -m)\right].
\end{aligned} \tag{5.34}
$$

In the second step we used $\gamma_{d+1}^2 = 1$, while in the last one we redefined $a \to -a+1$. This relation implies (we write here explicitly the dependence of the vertices on m and M)[7]

$$
V_f^{(l)}(\mathbf{p}_1, n_1; \ldots; \mathbf{p}_l, n_l; m+M) = (-1)^l V_f^{(l)}(\mathbf{p}_1, -n_1; \ldots; \mathbf{p}_l, -n_l; -m-M). \tag{5.35}
$$

---

[7] If d is odd, one can repeat the same argument using $\gamma_{\mathcal{C}}$ defined in (5.3). It shows that vertices with l legs are multiplied by $(-1)^l$ if one changes the sign of $m+M$ at fixed momenta and *frequencies*.

For every $l > 4$, the vertex is due only to the fermion loops, so that $V^{(l)} = V_f^{(l)}$. For $l \leq 4$ we must also take into account the contribution of the bosonic part of the action, so that

$$\begin{aligned} V^{(3)}(\mathbf{p}, n_1; \mathbf{q}, n_2; \mathbf{r}, n_3) &= \overline{\lambda} m + V_f^{(3)}(\mathbf{p}, n_1; \mathbf{q}, n_2; \mathbf{r}, n_3), \\ V^{(4)}(\mathbf{p}, n_1; \mathbf{q}, n_2; \mathbf{r}, n_3; \mathbf{s}, n_4) &= \overline{\lambda} + V_f^{(4)}(\mathbf{p}, n_1; \mathbf{q}, n_2; \mathbf{r}, n_3; \mathbf{s}, n_4). \end{aligned} \tag{5.36}$$

Finally, for the inverse propagator we have

$$P(\mathbf{p}, n) = \frac{\mathbf{p}^2}{g^2} + \frac{(2\pi T n)^2}{g^2} + \overline{\mu} + \frac{\overline{\lambda}}{2} m^2 + V_f^{(2)}(-\mathbf{p}, -n; \mathbf{p}, n). \tag{5.37}$$

Vertices $V^{(l)}$ also satisfy the symmetry relation (5.35), while the inverse propagator $P(\mathbf{p}, n)$ satisfies $P(\mathbf{p}, n; m, M) = P(\mathbf{p}, -n; -m, -M)$. In order to clarify the equation of the critical crossover limit we need to explicitly compute $P(\mathbf{p}, n)$, $V_3(\mathbf{p}, n) \equiv V^{(3)}(\mathbf{p}, n; -\mathbf{p}, -n; \mathbf{0}, 0)$ and $V_3(\mathbf{p}, n) \equiv V^{(4)}(\mathbf{p}, n; -\mathbf{p}, -n; \mathbf{0}, 0; \mathbf{0}, 0)$ for $M, m \to 0$. Using standard formula $\mathrm{Tr}\, \gamma_\mu \gamma_\nu = D\, \delta_{\mu,\nu}$, $\mathrm{Tr}\, \gamma_\mu \gamma_\nu \gamma_\delta = 0$ and $\mathrm{Tr}\, \gamma_\alpha \gamma_\beta \gamma_\gamma \gamma_\delta = D\, (\delta_{\alpha,\beta}\delta_{\gamma,\delta} - \delta_{\alpha,\gamma}\delta_{\beta,\delta} + \delta_{\alpha,\delta}\delta_{\beta,\gamma})$ and defining

$$\begin{aligned} \tau_h(\mathbf{p}, n) &= 2 v_h(\mathbf{p}, n) + v_h(\mathbf{0}, 0) \\ &\quad - T\Big(\mathbf{p}^2 + (2\pi T n)^2\Big) \sum_{a \in \mathbb{Z}} \int_{q < \Lambda} \eta_h(\mathbf{q}, a)^2 \eta_h(\mathbf{q} + \mathbf{p}, a + n) \\ v_h(\mathbf{p}, n) &= T \sum_{a \in \mathbb{Z}} \int_{q < \Lambda} \eta_h(\mathbf{q}, a) \eta_h(\mathbf{q} + \mathbf{p}, a + n) \end{aligned} \tag{5.38}$$

with $\eta_h(\mathbf{p}, n) := \Big(\mathbf{p}^2 + \pi^2 T^2 (2n+1)^2 + h^2\Big)^{-1}$, we get the final result

$$\begin{aligned} P(\mathbf{p}, n) &= \frac{\mathbf{p}^2}{g^2} + \frac{(2\pi T n)^2}{g^2} + \overline{\mu} + \frac{\overline{\lambda}}{2} m^2 - T \sum_a \int^{\Lambda} \mathrm{d}^d \mathbf{q}\, \eta_h(\mathbf{q}, a) \\ &\quad + \Big(\frac{\mathbf{p}^2}{2} + \frac{(2\pi n)^2}{2}\Big) v_h(\mathbf{p}, n) + 2h^2 v_h(\mathbf{0}, 0) && (5.39) \\ V_3(\mathbf{p}, n) &= \overline{\lambda} m + 2(m + M)\tau_{m+M}(\mathbf{p}, n) && (5.40) \\ &\quad - 8(m+M)^3 T \sum_{a \in \mathbb{Z}} \int_{q < \Lambda} \eta_{m+M}(\mathbf{q}, a)^2 \eta_{m+M}(\mathbf{q} + \mathbf{p}, a + n) && (5.41) \\ V_4(\mathbf{p}, n) &= \overline{\lambda} + 2\tau_{m+M}(\mathbf{p}, n) + O(m+M)^2 && (5.42) \end{aligned}$$

The similarity of (5.41) with (5.42) simplifies the equations of the critical crossover limit with respect to the general case. This is due to the symmetry of the model (5.35) that is not present in other models investigated in this work. Indeed in the general case one has to tune the model at the critical point recovering the symmetry which is than dynamically broken. However in this case the critical point remain fixed at $M = 0$ without $1/N_f$ fluctuations, technically this follows from (5.41) and (5.42).

Finally, note that $V^{(4)}(\mathbf{0}, 0; \mathbf{0}, 0; \mathbf{0}, 0; \mathbf{0}, 0)$ is positive at the transition. Indeed, one obtains explicitly (note that $\lambda \geq 0$ to ensure the stability of the quartic potential)

$$V^{(4)}(\mathbf{0}, 0; \mathbf{0}, 0; \mathbf{0}, 0; \mathbf{0}, 0) = \overline{\lambda} + 6 T_c \sum_a \int_{q < \Lambda} \frac{\mathrm{d}^d \mathbf{q}}{(2\pi)^d} \frac{1}{(q^2 + \omega_{c,n}^2)^2} > 0. \tag{5.43}$$

It is easy to verify that $P(\mathbf{0},0)$ vanishes at the transition. Indeed, for $m=M=0$ we have

$$\begin{aligned} P(\mathbf{0},0) &= \overline{\mu} - T\sum_{n\in\mathbb{Z}}\int_{q<\Lambda}\frac{\mathrm{d}^d\mathbf{q}}{(2\pi)^d}\frac{1}{q^2+\omega_n^2} \\ &= -g_{01}(T-T_c)+O(T-T_c)^2, \end{aligned} \tag{5.44}$$

where we used eqs. (5.20) and (5.17). Thus, the mode with $n=0$ is singular at the critical point. It is exactly this singularity that forbids a standard $1/N_f$ expansion at $T=T_c$ and gives rise to the Ising behavior. This type of singular behavior is the main topic of this work and has been described in the first chapter of this works in a general way using generalized Heisenberg Models. The strategy proposed there consists in integrating all the nonsingular modes $\hat{\phi}_n$, $n\neq 0$, and study the effective theory for the zero mode $\hat{\phi}_0$ and is the same we are going to apply for the model under investigation.

5.4 The effective theory of the zero mode

Following the conclusion of the previous section and the standard protocol developed in the first chapter, we compute now the effective action for the zero mode integrating the non critical degrees of freedom. Integrating all fields $\hat{\phi}_n$ with $n\neq 0$ we obtain the effective action

$$e^{-\tilde{\mathcal{S}}_{\text{eff}}[\hat{\phi}_0]} = \int\prod_{n\neq 0}\mathrm{d}\hat{\phi}_n\, e^{-\hat{\mathcal{S}}_{\text{eff}}[\hat{\phi}_n]}, \tag{5.45}$$

with

$$\begin{aligned} \tilde{\mathcal{S}}_{\text{eff}} &= \sqrt{N}\tilde{H}\hat{\phi}_0(\mathbf{0}) + \frac{T}{2}\int_{q<\Lambda}\frac{\mathrm{d}^d\mathbf{p}}{(2\pi)^d}\,\hat{\phi}_0(\mathbf{p})\,\tilde{P}(\mathbf{p})\,\hat{\phi}_0(-\mathbf{p}) \\ &\quad +\sum_{l\geq 3}\frac{T^{l-1}}{l!N^{l/2-1}}\int_{p_i<\Lambda}\frac{\mathrm{d}^d\mathbf{p}_1}{(2\pi)^d}\cdots\frac{\mathrm{d}^d\mathbf{p}_l}{(2\pi)^d}\,(2\pi)^d\delta\Big(\sum_{i=1}^{l}\mathbf{p}_i\Big) \\ &\quad \times\tilde{V}^{(l)}(\mathbf{p}_1,\dots\mathbf{p}_l)\hat{\phi}_0(\mathbf{p}_1)\cdots\hat{\phi}_0(\mathbf{p}_l) \end{aligned} \tag{5.46}$$

where H, $\tilde{P}$, and $\tilde{V}^{(l)}$ have an expansion in powers of $1/N$. The computation of these quantities is quite simple. The contribution of order $1/N^k$ to $\tilde{V}^{(l)}$ is obtained by considering all k-loop diagrams contributing to the l-point connected correlation function of $\hat{\phi}_0$ and considering only the nonsingular fields (i.e. propagators with $n\neq 0$) on the internal lines. Frequency conservation $V^{(n)}(\mathbf{p},n;\mathbf{0},0;\cdots\mathbf{0},0)\sim\delta_{n,0}$ implies that all tree-level diagrams with more than one vertex vanish.[8] Therefore, $\tilde{H}=O(N^{-1})$, $\tilde{P}(\mathbf{p})=P(\mathbf{p},0)+O(N^{-1})$, and $\tilde{V}^{(l)}=V^{(l)}_{n_i=0}+O(N^{-1})$ ($V^{(l)}_{n_i=0}$ is the vertex $V^{(l)}$ with all frequencies set to zero). For the inverse propagator $\tilde{P}$ and for the magnetic field $\tilde{H}$ we shall also need the $1/N$ corrections. We obtain

---

[8] For a tree-level graph, the usual topological arguments give the relation $\sum_n(n-2)N_n=-2$, where N_n is the number of vertices belonging to the graph such that n legs belong to internal lines. Since $n\geq 1$ if there is more than one vertex, the previous equality requires $N_1\geq 2$. But frequency conservation implies that V_l vanishes if all frequencies but one vanish. Therefore, each nontrivial tree-level diagram vanishes.

$$\tilde{H} = \frac{H_1}{N} + O(N^{-2}) \tag{5.47}$$

$$\tilde{P}(\mathbf{p}) = P(\mathbf{p},0) + \frac{P^{(1)}(\mathbf{p})}{N} + O(N^{-2}), \tag{5.48}$$

with

$$H_1 = \frac{T}{2}\sum_{n\neq 0}\int_{p<\Lambda}\frac{\mathrm{d}^d\mathbf{p}}{(2\pi)^d}\, V_3(\mathbf{p},n)P(\mathbf{p},n)^{-1} \tag{5.49}$$

$$P^{(1)}(\mathbf{0}) = \frac{T}{2}\sum_{n\neq 0}\int_{p<\Lambda}\frac{\mathrm{d}^d\mathbf{p}}{(2\pi)^d}\,\Big[V_4(\mathbf{p},n)P(\mathbf{p},n)^{-1} - V_3(\mathbf{p},n)^2P(\mathbf{p},n)^{-2}\Big], \tag{5.50}$$

where $V_l(\mathbf{p},n) \equiv V^{(l)}(\mathbf{p},n;-\mathbf{p},-n;\mathbf{0},0;\ldots)$. Note that relation (5.35) implies an analogous symmetry relation for $\tilde{V}^{(l)}$[9]:

$$\tilde{V}^{(l)}(\mathbf{p}_1,\ldots,\mathbf{p}_l;m,M) = (-1)^l\tilde{V}^{(l)}(\mathbf{p}_1,\ldots,\mathbf{p}_l;-m,-M), \tag{5.51}$$

where we have written explicitly the dependence on m and M. Analogously $\tilde{P}(\mathbf{p})$ and $\tilde{H}$ are respectively symmetric and antisymmetric under $m,M \to -m,-M$.

In order to obtain the final effective theory we introduce a new field $\chi(\mathbf{p})$ such that the corresponding zero-momentum three-leg vertex vanishes for any value of the parameters. For this purpose we write

$$\alpha\chi(\mathbf{p}) = T\hat{\phi}_0(\mathbf{p}) + \sqrt{N}k\delta(\mathbf{p}), \tag{5.52}$$

where α and k are functions to be determined. If we write $a_l \equiv \tilde{V}^{(l)}(\mathbf{0},0;\ldots;\mathbf{0},0)$, k is determined by the equation

$$\sum_{l=0}\frac{(-1)^l k(m,M)^l}{l!}a_{l+3}(m,M) = 0, \tag{5.53}$$

where we have written explicitly the dependence on m and M. Now, symmetry (5.51) implies also

$$\sum_{l=0}\frac{(-1)^l[-k(-m,-M)]^l}{l!}a_{l+3}(m,M) = 0, \tag{5.54}$$

so that $k(m,M) = -k(-m,-M)$. Therefore, k has an expansion of the form

$$k = \sum_{ab,a+b\,\mathrm{odd}} k_{ab}m^aM^b, \tag{5.55}$$

where the coefficients k_{ab} have a regular expansion in powers of $1/N$. The leading behavior close to the transition is easily computed:

$$k = \frac{a_3}{a_4} + O(m^aM^b, a+b=3). \tag{5.56}$$

---

[9] For a diagram $D(m,M)$, with n_j $j-$legs vertices, entering in the computation of $V^{(l)}$ we have $D(m,M) = (-1)^{\sum_j n_j j}D(-m,-M) = (-1)^l D(-m,-M)$. We have used the relation $\sum_j n_j j = l + 2n_I$, n_I being the internal line

In terms of χ the effective action can be written as

$$\begin{aligned}\tilde{\mathcal{S}}_{\text{eff}} &= N^{1/2}\overline{H}\chi(\mathbf{0}) + \frac{1}{2}\int_{q<\Lambda}\frac{\mathrm{d}^d\mathbf{p}}{(2\pi)^d}\,\chi(\mathbf{p})\,\overline{P}(\mathbf{p})\,\chi(-\mathbf{p}) \qquad (5.57)\\ &\quad+\sum_{l\geq 3}\frac{1}{l!N^{l/2-1}}\int_{p_i<\Lambda}\frac{\mathrm{d}^d\mathbf{p}_1}{(2\pi)^d}\cdots\frac{\mathrm{d}^d\mathbf{p}_l}{(2\pi)^d}\,(2\pi)^d\delta\Big(\sum_{i=1}^{l}\mathbf{p}_i\Big)\,\overline{V}^{(l)}(\mathbf{p}_1,\ldots\mathbf{p}_l)\chi(\mathbf{p}_1)\cdots\chi(\mathbf{p}_l).\end{aligned}$$

The quantities $\overline{H}$, $\overline{P}$, and $\overline{V}^{(l)}$ have an expansion in terms of m, M, and $1/N$. Explicitly we have:

$$\overline{H} = \alpha T^{-1}[\tilde{H} - k\tilde{P}(\mathbf{0}) + \frac{k^2}{2}\tilde{V}_3(\mathbf{0}) - \frac{k^3}{6}\tilde{V}_4(\mathbf{0}) + O(m^aM^b, a+b=5)], \qquad (5.58)$$

$$\overline{P}(\mathbf{p}) = \alpha^2T^{-1}[\tilde{P}(\mathbf{p}) - k\tilde{V}_3(\mathbf{p}) + \frac{k^2}{2}\tilde{V}_4(\mathbf{p}) + O(m^aM^b, a+b=4)], \qquad (5.59)$$

$$\begin{aligned}\overline{V}^{(2l+1)}(\mathbf{p}_1,\ldots,\mathbf{p}_{2l+1}) &= \alpha^{2l+1}T^{-1}[\tilde{V}^{(2l+1)}(\mathbf{p}_1,\ldots,\mathbf{p}_{2l+1}) - k\tilde{V}^{(2l+2)}(\mathbf{p}_1,\ldots,\mathbf{p}_{2l+1},\mathbf{0})\\ &\quad+O(m^aM^b, a+b=3)], \qquad (5.60)\end{aligned}$$

$$\overline{V}^{(2l)}(\mathbf{p}_1,\ldots,\mathbf{p}_{2l}) = \alpha^{2l}T^{-1}\tilde{V}^{(2l)}(\mathbf{p}_1,\ldots,\mathbf{p}_{2l}) + O(m^aM^b, a+b=2). \qquad (5.61)$$

Up to now we have not defined the parameter α. We will fix it by requiring

$$\left.\frac{d\overline{P}(\mathbf{p})}{dp^2}\right|_{p=0} = 1, \qquad (5.62)$$

for all values of the parameters. The parameter α is a function of m, M, and $1/N$. The symmetry properties of k and of the vertices imply that α is invariant under $m, M \to -m, -M$. As a consequence, under $m, M \to -m, -M$, the quantities $\overline{H}$, $\overline{P}$, and $\overline{V}^{(l)}$ have the same symmetry properties as $\tilde{H}$, $\tilde{P}$, and $\tilde{V}^{(l)}$.

In the following we shall need the expansions of $\overline{H}$, $\overline{P}(\mathbf{0})$, and $\overline{V}^{(3)}(\mathbf{p},-\mathbf{p},\mathbf{0})$ close to the critical point. Using (5.39), (5.41) and (5.42) we get

$$\begin{aligned}P(\mathbf{0},0) &\approx \frac{\overline{\lambda}}{2}m^2 - (T-T_c)g_{01} - 3(M+m)^2g_{10},\\ V_3(\mathbf{0},0) &\approx \overline{\lambda}m - 6(M+m)g_{10},\\ V_4(\mathbf{0},0) &\approx \overline{\lambda} - 6g_{10}, \qquad (5.63)\end{aligned}$$

Notice the relation

$$V_f^{(3)}(\mathbf{p},n;-\mathbf{p},-n;\mathbf{0},0;m) = mV_f^{(4)}(\mathbf{p},n;-\mathbf{p},-n;\mathbf{0},0;\mathbf{0},0;m) + O(m^3), \qquad (5.64)$$

(we have explicitly written the mass dependence of the vertices) that we have just commented in the previous section. In the relations (5.63) we have used $g_{10} = -v_0(\mathbf{0},0)$ that can easily obtained using the development of the gap equation near the critical point. We expand $\overline{H}$ and $\overline{P}(\mathbf{0})$ is powers of $1/N$ as

$$\frac{T\overline{H}}{\alpha} = h_0 + \frac{h_1}{N} + O(N^{-2}), \qquad (5.65)$$

$$\frac{T\overline{P}(\mathbf{0})}{\alpha^2} = p_0 + \frac{p_1}{N} + O(N^{-2}). \qquad (5.66)$$

By using expansions (5.63) we obtain

$$\begin{aligned}
h_0 &\approx -\frac{V_3(\mathbf{0},0)}{V_4(\mathbf{0},0)}P(\mathbf{0},0)+\frac{1}{3}\frac{V_3(\mathbf{0},0)^3}{V_4(\mathbf{0},0)^2}\\
&\approx -\overline{\mu}M+\frac{g_{01}\overline{\lambda}}{6g_{10}-\overline{\lambda}}M(T-T_c)-\frac{g_{10}\overline{\lambda}(6g_{10}+\overline{\lambda})}{(6g_{10}-\overline{\lambda})^2}M^3+O(m^aM^b,a+b=5),\\
h_1 &\approx H_1-\frac{V_3(\mathbf{0},0)}{V_4(\mathbf{0},0)}P^{(1)}(\mathbf{0})\\
&\approx -\frac{\overline{\lambda}MT}{2(6g_{10}-\overline{\lambda})}\sum_{n\neq 0}\int_{p<\Lambda}\frac{\mathrm{d}^d\mathbf{p}}{(2\pi)^d}[6g_{10}+V_f^{(4)}(\mathbf{p},n;-\mathbf{p},-n;\mathbf{0},0;\mathbf{0},0)]P(\mathbf{p},n)^{-1}\\
&\quad +O(m^aM^b,a+b=3),\\
p_0 &\approx P(\mathbf{0},0)-\frac{V_3(\mathbf{0},0)^2}{2V_4(\mathbf{0},0)}\\
&\approx -g_{01}(T-T_c)+\frac{3g_{10}\overline{\lambda}}{6g_{10}-\overline{\lambda}}M^2+O(m^aM^b,a+b=4),\\
p_1 &\approx P^{(1)}(\mathbf{0},0)\approx e+O(m^aM^b,a+b=2),
\end{aligned}\tag{5.67}$$

where e is the value of $P^{(1)}(\mathbf{0},0)$ for $M=m=0$. Note that several terms that are allowed by the symmetry $m,M\to -m,-M$ are missing in these expansions. In the case of h_0 we used the gap equation to eliminate the term proportional to m^3. This substitution is responsible for the appearance of the term linear in M and cancels the terms proportional to $m(T-T_c)$, m^2M, and mM^2. In the case of h_1 and p_0 note that the terms proportional to m, and m^2, mM cancel out. Finally, we compute the three-leg vertex. At leading order in $1/N$ we obtain

$$\begin{aligned}
\frac{T}{\alpha^3}\overline{V}^{(3)}(\mathbf{p},-\mathbf{p},\mathbf{0}) &= V_3(\mathbf{p},0)-\frac{V_3(\mathbf{0},0)}{V_4(\mathbf{0},0)}V_4(\mathbf{p},0)\\
&\approx \frac{-\overline{\lambda}M}{6g_{10}-\overline{\lambda}}[6g_{10}+V_f^{(4)}(\mathbf{p},0;-\mathbf{p},0;\mathbf{0},0;\mathbf{0},0)]+O(m^aM^b,a+b=3).
\end{aligned}\tag{5.68}$$

Note that the term proportional to m is missing as a consequence of relation (5.64).

Having computed the expansion of translated vertices of the theory with one incoming momenta (5.67,5.68) and at zero external momenta (5.63) we are now in a position to define the critical crossover limit for the model under investigation.

5.5 The critical crossover limit

The manipulations presented in the previous section allowed us to compute the effective action for the zero mode $\chi(\mathbf{p})$. Far from the critical point $\overline{P}(\mathbf{p})\neq 0$ for all momenta and thus one can perform a standard $1/N_f$ expansion. At the critical point instead this expansion fails because $\overline{P}(\mathbf{0})=0$. At the critical point, for $N\to\infty$ the long-distance behavior is controlled by the action

$$\tilde{S}_{\text{eff}}\approx\int \mathrm{d}^d\mathbf{x}\left[\frac{1}{2}(\partial\chi)^2+\frac{u}{4!}\chi^4\right]+O(N^{-2}),\tag{5.69}$$

where

$$u = \frac{1}{N}\overline{V}^{(4)}(\mathbf{0},\mathbf{0},\mathbf{0},\mathbf{0}). \tag{5.70}$$

Here we have used the fact that vertices with an odd number of fields vanish at the critical point and the normalisation condition (5.62). Moreover, since the critical mode corresponds to $\mathbf{p} = \mathbf{0}$, we have performed an expansion in powers of the momenta, keeping only the leading term. Since for $N \to \infty$, $\overline{V}^{(4)}(\mathbf{0},\mathbf{0},\mathbf{0},\mathbf{0}) = \alpha^4 T^{-1} V^{(4)}(\mathbf{0},\mathbf{0},\mathbf{0},\mathbf{0})$, inequality (5.43) implies $u > 0$ at the critical point. eq. (5.69) is the action of the critical ϕ^4 theory which should be studied in the weak-coupling limit $u \to 0$. In this regime the model shows an interesting scaling behavior—we named it *critical crossover*—that describes the crossover between Mean-Field and Ising behavior and has been studied in detail in the chapter 2 and applied for a specific model in chapter 3. In this chapter we want to recover the results obtained for Heisenberg models in chapter 3 for Yukawa model (5.1) using the general $\mathcal{N} = 1$ theory presented in chapter 2.

5.5.1 The general theory

Following Ref. [56] in chapter 2 and 3 we extended these considerations to the general two-dimensional Hamiltonian

$$\begin{aligned}\mathcal{S}_{\text{eff}}[\varphi] &= H\varphi(\mathbf{0}) + \frac{1}{2}\int \frac{d^2\mathbf{p}}{(2\pi)^2}[K(\mathbf{p}) + r]\varphi(\mathbf{p})\varphi(-\mathbf{p}) \\ &\quad + \sum_{l\geq 3}\frac{u^{l/2-1}}{l!}\int \frac{d^2\mathbf{p}_1}{(2\pi)^2}\dots\frac{d^2\mathbf{p}_l}{(2\pi)^2}(2\pi)^d\delta\left(\sum_i \mathbf{p}_i\right)\mathcal{V}^{(l)}(\mathbf{p}_1,\dots,\mathbf{p}_l)\varphi(\mathbf{p}_1)\dots\varphi(\mathbf{p}_l),\end{aligned} \tag{5.71}$$

where $K(\mathbf{p}) = p^2 + O(p^4)$, $\mathcal{V}^{(3)}(\mathbf{0},\mathbf{0},\mathbf{0}) = 0$, and $\mathcal{V}^{(4)}(\mathbf{0},\mathbf{0},\mathbf{0},\mathbf{0}) = 1$. The presence of vertices with an odd number of legs requires an additional counterterm for the magnetic field. Indeed, we showed that it was possible to find functions $r_c(u)$ and $H_c(u)$ such that for $t \equiv r - r_c(u)$ (infrared limit), $h \equiv H - H_c(u)$, $u \to 0$ (weak-coupling limit), at fixed t/u, h/u one has

$$\chi_n = u^{1-n} f_n(\tilde{h},\tilde{t}), \tag{5.72}$$

where the scaling function $f_n(x,y)$ is the same as that computed in the continuum theory. In particular, $\chi_n u^{n-1}$ vanishes in the crossover limit if n is odd. The counterterms are regularization-dependent. In the continuum theory with a cutoff we have

$$h_c = -\frac{\sqrt{u}}{2}\int_{p<\Lambda}\frac{d^2\mathbf{p}}{(2\pi)^2}\frac{\mathcal{V}_3(\mathbf{p})}{K(\mathbf{p})}, \tag{5.73}$$

$$r_c = \frac{u}{8\pi}\ln\frac{u}{\Lambda^2} + \frac{u}{2}\int_{p<\Lambda}\frac{d^2\mathbf{p}}{(2\pi)^2}\frac{\mathcal{V}_3(\mathbf{p})^2}{K(\mathbf{p})^2} + A_0 u, \tag{5.74}$$

with $\mathcal{V}_3(\mathbf{p}) \equiv \mathcal{V}^{(3)}(\mathbf{p},-\mathbf{p},\mathbf{0})$ and

$$A_0 = -D_2 - \frac{3}{8\pi} + \frac{1}{8\pi}\log\frac{3}{8\pi} - \frac{1}{2}\int_{p<\Lambda}\frac{d^2\mathbf{p}}{(2\pi)^2}\left[\frac{\mathcal{V}^{(4)}(\mathbf{p},-\mathbf{p},\mathbf{0},\mathbf{0})}{K(\mathbf{p})} - \frac{1}{p^2}\right]. \tag{5.75}$$

The nonperturbative constant D_2 was estimated in Ref. [32]: $D_2 = -0.0524(2)$. The relations (5.73) and (5.74) generalize the lattice expressions found in chapter 2 [see eqs. (2.47) (2.75)] to a sharp cut off regularisation. However as will be clear later in this case (in which chiral symmetry is not broken in the starting action) h_c is irrelevant in the scaling limit.

5.5.2 Scaling behavior

In this section we wish to use the previous results to compute the crossover behavior of model (5.1) in 2+1 dimensions. Since $u \sim 1/N$ the relevant scaling variables are

$$\begin{aligned} x_h &= \frac{NT_c}{\alpha}(N^{1/2}\overline{H} - H_c) \\ x_t &= \frac{NT_c}{\alpha^2}(\overline{P}(\mathbf{0}) - r_c), \end{aligned} \tag{5.76}$$

where the factors α/T_c and α^2/T_c are introduced for convenience. The critical crossover limit is obtained by tuning T, M, and N close to the critical point so that x_h and x_t are kept constant. The expansions of $\overline{H}$ and $\overline{P}(\mathbf{0})$ are reported in eq. (5.67). The expansions of H_c and r_c are easily derived. For H_c we have

$$H_c = -\frac{1}{2\sqrt{N}} \int_{p<\Lambda} \frac{\mathrm{d}^2\mathbf{p}}{(2\pi)^2} \frac{\overline{V}^{(3)}(\mathbf{p}, -\mathbf{p}, \mathbf{0})}{\overline{P}(\mathbf{p})}, \tag{5.77}$$

where all quantities are computed for $M = m = 0$. Using eq. (5.68) we have

$$H_c = \frac{\alpha h_{c0} M}{T_c\sqrt{N}} + O(m^a M^b, a+b=3), \tag{5.78}$$

where h_{c0} is a constant. Using eq. (5.74) we obtain for r_c the expansion

$$r_c = \frac{\alpha^2}{T_c N}(r_0 \ln N + r_1) + O(m^a M^b, a+b=2), \tag{5.79}$$

where

$$r_0 = -\frac{\alpha^2 V_4(\mathbf{0},0)}{8\pi}, \tag{5.80}$$

$$\begin{aligned} r_1 &= \alpha^2 V_4(\mathbf{0},0)\left[\frac{1}{8\pi}\ln\frac{3\alpha^4 V_4(\mathbf{0},0)}{8\pi T_c \Lambda^2} - D_2 - \frac{3}{8\pi}\right] \\ &\quad -\frac{1}{2}\int_{p<\Lambda}\frac{\mathrm{d}^2\mathbf{p}}{(2\pi)^2}\left[\frac{T_c V_4(\mathbf{p},0)}{P(\mathbf{p},0)} - \frac{\alpha^2 V_4(\mathbf{0},0)}{p^2}\right]. \end{aligned} \tag{5.81}$$

Note that the three-leg vertex that appears in eq. (5.74) does not contribute to this order, since it vanishes for $m = M = 0$. Thus, eqs. (5.76) can be written as

$$x_h \approx N^{3/2}\left[-\overline{\mu}M + a_0 M(T - T_c) + a_1 M^3 + \frac{a_2 M}{N} + \cdots\right] - h_{c0} M\sqrt{N}, \tag{5.82}$$

$$x_t \approx N\left[-g_{01}(T - T_c) + a_3 M^2 + \frac{e}{N} + \cdots\right] - r_0 \ln N - r_1, \tag{5.83}$$

where a_0, a_1, a_2, a_3, and e are coefficients that can be read from eq. (5.67). These expansions show that

$$\overline{\mu} M = -x_h N^{-3/2}, \tag{5.84}$$

$$T - T_c = \frac{e - r_0 \ln N - r_1 - x_t}{N g_{01}}. \tag{5.85}$$

The critical point is specified by the condition $x_t = x_h = 0$. The symmetry under $m, M \to -m, -M$ guarantees that the critical point corresponds to $M = 0$. On the other hand, $1/N$ fluctuations give rise to a shift of the critical temperature. If $T_c(N)$ is the finite-N critical temperature, we obtain

$$T_c(N) \approx T_c + \frac{1}{N} \frac{e - r_0 \ln N - r_1}{g_{01}}. \tag{5.86}$$

Note that, beside the expected $1/N$ correction there is also a $\ln N/N$ term that is related to the nontrivial renormalization. It follows

$$T - T_c(N) = -\frac{x_t}{N g_{01}}. \tag{5.87}$$

Note that g_{01} is negative [see eq. (5.21)] and thus we have $x_t > 0$ for $T > T_c(N)$, as expected. Using the gap equation we can also derive the behavior of m in the critical crossover limit. We obtain

$$m \equiv \frac{m_0}{N^{1/2}}, \tag{5.88}$$

where m_0 is a function of $\ln N$ that satisfies the equation

$$\frac{1}{6}(\overline{\lambda} - 6 g_{10}) m_0^3 + (r_0 \ln N + r_1 - e + x_t) m_0 + x_h = 0. \tag{5.89}$$

For $N \to \infty$, m_0 has an expansion in inverse powers of $\ln N$, the leading term being

$$m_0 \approx -\frac{x_h}{r_0} \frac{1}{\ln N} + O(\ln^{-2} N). \tag{5.90}$$

Note that $m_0 \to 0$ as $x_h \to 0$.

These results confirm the scaling predictions of Ref. [50]. For the massless theory with $M = 0$, there are two regimes: for $N(T - T_c(N)) \ll 1$ one observes Ising behavior, while for $N(T - T_c(N)) \gg 1$ mean-field behavior occurs. If $M \neq 0$ the same considerations apply, the relevant variable being $MN^{3/2}$. It is important to note the role played in the derivation by the symmetry $m, M \to -m, -M$, that is present because the regularization preserves chiral invariance. Even though vertices with an odd number of legs are present, the symmetry makes them irrelevant in the crossover limit. Thus, the additional renormalizations computed in Ref. [56] do not play any role here.

The results reported above can be extended to d dimensions for $d < 4$, the relevant scaling variables being eqs. (2.52)

$$x_h \sim M N^{(d+2)/[2(4-d)]}, \qquad x_t \sim [T - T_c(N)] N^{2/(4-d)}. \tag{5.91}$$

In $d = 3$, on the basis of eq. (2.55), we also predict for $T_c(N)$ an expansion of the form

$$T_c(N) \approx T_c + \frac{a}{N} + \frac{b \ln N + c}{N^2}, \tag{5.92}$$

where a, b, and c are constants that can be computed as in the two-dimensional case. However notice that, as pointed out in sec. 2.1.5, in three dimension (and in general for $d > 2$) one have to translate the critical field by a constant k_R (2.57) that have to be taken into account in order to cancel some diagram for χ_3 that do not go to zero in the Critical Crossover Limit eq. (2.61). However in the symmetric case this is not necessary because the explicit $\mathbb{Z}_2$ symmetry of the action is protected in the scaling limit. Indeed the two one loop anomalous contributions ($\equiv D_1^{(3)}, D_2^{(3)}$) for χ_3 [see point c) in 2.1.5] are[10]

$$D_1^{(3)} = \frac{1}{t^3 N^{3/2}} \int \mathrm{d}^3\mathbf{p} \frac{\overline{V}^{(3)}(\mathbf{p})^3}{K(\mathbf{p})^3} \sim \frac{M^3}{t^3 N^{3/2}} \tag{5.93}$$

$$D_2^{(3)} = \frac{1}{t^3 N^{3/2}} \int \mathrm{d}^3\mathbf{p} \frac{\overline{V}^{(3)}(\mathbf{p})^2 \overline{V}^{(4)}(\mathbf{p})}{K(\mathbf{p})^2} \sim \frac{M}{t^3 N^{3/2}}. \tag{5.94}$$

In the critical crossover limit in $d = 3$ from eq. (2.54) follows that $\chi_3 \sim N^{9/2}$ and that $t \sim N^{-2}$ so that

$$N^{-9/2} D_1^{(3)} \sim M^3 \qquad\qquad N^{-9/2} D_2^{(3)} \sim M \tag{5.95}$$

that are obviously irrelevant in the CCL. We stress that the reason $D_1^{(3)}$ and $D_2^{(3)}$ are negligible is the equation (5.64) that holds for all models which are chiral symmetric. In general the effect of k_R must be taken into account for all Hamiltonian which broke chiral symmetry as for instance in the case of Wilson fermions. This system is currently under investigation.

5.5.3 Correlation functions

The results reported in sec. 5.5.2 allow us to compute the scaling behavior of the correlation functions. For instance, we have

$$\langle \phi(\mathbf{x}_d, x_{d+1}) \rangle = \overline{\phi} - \frac{k}{g} + \frac{\alpha}{g\sqrt{N}} \langle \chi(\mathbf{x}_d) \rangle \tag{5.96}$$

Using eq. (2.54) with $n = 1$ and $d = 2$, we have $\langle \chi(\mathbf{x}_d) \rangle = f_1(x_h, x_t)$ in the critical crossover limit. The background term can be neglected in the crossover limit since

$$\overline{\phi} - \frac{k}{g} \approx \frac{1}{g} \left[m - \frac{V_3(\mathbf{0}, 0)}{V_4(\mathbf{0}, 0)} \right] \approx \frac{M}{g} \frac{6 g_{10}}{\overline{\lambda} - 6 g_{10}} \sim N^{-3/2}. \tag{5.97}$$

Thus, we obtain

$$\langle \phi(\mathbf{x}_d, x_{d+1}) \rangle \approx \frac{\alpha}{g\sqrt{N}} f_1(x_h, x_t) \tag{5.98}$$

---

[10] In three dimension the integrals are both Infra Red finite.

The factor $1/\sqrt{N}$ is related to the particular normalization of ϕ used in (5.1) and disappears if we redefine $\varphi = \sqrt{N}\phi$ in order to have a canonical kinetic term for φ. The function $f_1(x_h, x_t)$ is the scaling function for the magnetization in the Ising model. For instance, for $x_h = 0$ and $x_t < 0$ (low-temperature phase), we have $f_1(0, x_t) \sim (-x_t)^{\beta_I}$ and $f_1(0, x_t) \sim (-x_t)^{\beta_{MF}}$ respectively for $|x_t| \ll 1$ and $|x_t| \gg 1$, where $\beta_I = 1/8$ and $\beta_{MF} = 1/2$ are the magnetization exponents in the Ising and in the Gaussian model. The universality of the crossover allows us to compute the scaling functions in any other model in which there exists a crossover between the Gaussian and the Ising fixed point. In particular, we can use the results for systems with medium-range interactions [33, 36] (see also the appendix B). In Ref. [36] (LBB) the authors report $\langle |m|R\rangle$ versus tR^2 (see their Fig. 9), where m is the magnetization, t the reduced temperature, and R the effective interaction range. These results give us $\langle \phi(\mathbf{x}_d, x_{d+1})\rangle$ for $x_h = 0$. One only needs to take into account the different normalizations of the fields, of the coupling constant, and of the scaling variable. In the crossover limit $N \to \infty$, $T \to T_c(N)$ at fixed $N(T - T_c(N))$ we have

$$g\sqrt{N}\langle \phi(\mathbf{x}_d, x_{d+1})\rangle = K_{1,\mathrm{LBB}}\langle |m|R\rangle_{\mathrm{LBB}} \tag{5.99}$$

$$(tR^2)_{\mathrm{LBB}} = K_{\mathrm{LBB}} N[T - T_c(N)]. \tag{5.100}$$

The nonuniversal constants K_{LBB} and $K_{1,\mathrm{LBB}}$ are computed in the app. B.

It is customary to define an effective exponent $\beta_{\mathrm{eff}}(T)$ as

$$\beta_{\mathrm{eff}}(T) = [T - T_c(N)]\frac{d}{dT}\ln\langle \phi(\mathbf{x}_d, x_{d+1})\rangle, \tag{5.101}$$

for $M = 0$ and $T < T_c(N)$. In the crossover limit $T \to T_c(N)$, $N \to \infty$ at fixed $N[T - T_c(N)]$, the exponent $\beta_{\mathrm{eff}}(T)$ interpolates between the Ising value $\beta_I = 1/8$ and the mean-field $\beta_{MF} = 1/2$. Again, this effective exponent can be derived from the results of Ref. [36]. The curve reported in Fig. 15 of Ref. [36] gives β_{eff} in the Yukawa model once tR^2 is replaced by $K_{\mathrm{LBB}}[T - T_c(N)]N$.

The same considerations apply to the connected zero-momentum n-point function χ_n:

$$\begin{aligned}
\chi_n &= \int \mathrm{d}^{d+1}\mathbf{x}_2 \ldots \mathrm{d}^{d+1}\mathbf{x}_n \,\langle \phi(\mathbf{0})\phi(\mathbf{x}_2)\ldots\phi(\mathbf{x}_n)\rangle^{\mathrm{conn}} \\
&= \frac{\alpha^n}{T^{n-1}g^n N^{n/2}} \int \mathrm{d}^{d}\mathbf{x}_2 \ldots \mathrm{d}^{d}\mathbf{x}_n \,\langle \chi(\mathbf{0})\chi(\mathbf{x}_2)\ldots\chi(\mathbf{x}_n)\rangle^{\mathrm{conn}} \\
&= \frac{\alpha^{4-3n}V_4(\mathbf{0},0)^{1-n}}{g^n} N^{n/2-1} f_n(x_h, x_t),
\end{aligned} \tag{5.102}$$

For $n = 2$ the crossover function for $x_h = 0$ can be obtained from the results of Ref. [36], since $g^2\chi_2 = K_{2,\mathrm{LBB}}(\tilde{\chi}R^2)_{\mathrm{LBB}}$. The constant $K_{2,\mathrm{LBB}}$ is given in the Appendix.

One can also use field theory to compute the crossover curves and thus use the results of Ref. [32]. For instance, in the high-temperature phase, for $M = 0$ we have in the crossover limit

$$g^2\chi_2 = K_{2,\mathrm{FT}}F_\chi(\tilde{t}), \qquad \tilde{t} = K_{\mathrm{FT}} N[T - T_c(N)], \tag{5.103}$$

where $F_\chi(\tilde{t})$ is reported in Ref. [32] and K_{FT}, $K_{2,\mathrm{FT}}$ are nonuniversal constants computed in the appendix B.

In the discussion presented above we have focused on the case $d = 2$, but it is immediate to generalize all these considerations to the three-dimensional case. For $d = 3$ the universal crossover curves have been computed in Refs. [29, 30, 32, 31] (field theory) and in Ref. [37] (medium-range models). These results apply directly to the Yukawa model.

5.6 Conclusions

In this chapter we have considered the Yukawa model in the limit $N_f \to \infty$, focusing on the crossover between mean-field and Ising behavior. For this purpose we have determined the action of the mode that becomes critical at the transition. In the long-distance limit, it becomes equivalent to that of a weakly coupled ϕ^4 theory. This identification allows us to use the results available for this model summarized in chapter 2 ([29] [56]). In particular, we have identified a universal critical crossover occurring for $N_f \to \infty$, $M \to 0$, and $T - T_c(N) \to 0$ at fixed x_t and x_h, see eqs. (5.84), (5.87), (5.91). In field-theoretical terms, this behavior represents the crossover induced by the flow from the unstable Gaussian fixed point to the stable Ising fixed point. Quantitative results for the Yukawa model can be obtained by using the field-theoretical results of Refs. [29], [32], [31], or the Monte Carlo results available for medium-range models [36, 37]. The necessary nonuniversal renormalization constants can be computed in perturbation theory. Results for $d = 2$ are reported in the appendix.

We should stress that our results are not specific of the chosen regularization, but can be extended to other regularization as well. In particular, the extension to Kogut-Susskind fermions [61], the model considered in Ref. [50], is essentially straightforward and have not been presented here. The Wilson case is more involved. Indeed, the absence of chiral symmetry implies that the symmetry relations satisfied here by the effective vertices [see eq. (5.35)] are no longer valid. In turn, this may imply additional mixing as it happens in the generalized Heisenberg model [56]. Also the higher than two dimension is more complicate for Wilson fermions, due to the necessity of introducing and tune another parameter k_R.

Let us note that all calculations presented here refer to the model in infinite spatial volume. However, the crossover behavior can also be observed in the finite-size scaling limit. The discussion in sec. 5.5.1 can be easily extended to this case too. It is trivial to verify that the correct scaling variable is $\tilde{L} = L u^{1/(4-d)}$, i.e. $\tilde{L} = L N^{-1/(4-d)}$ in the Yukawa model. Again, one can use universality and obtain predictions for the Yukawa model from the results obtained in other contexts. In particular, one can use the finite-size scaling results of Refs. [33, 36, 37] that refer to medium-range models at the critical point.

Finally, we should mention that one could also generalize the model and consider fermion fields $\psi_{\alpha f}$ transforming according to a representation of a group G and a coupling of the form $\overline{\psi}_f T^a \phi^a \psi_f$, where T^a are the generators of the algebra of G. The discussion is essentially unchanged, though in this case one would obtain the vector ϕ^4 theory; several models have been just studied pointing out the reduction of the critical zone [51] [52] [53]. Field-theory results relevant for this case are given in Refs. [29], [32], [31]. More in general we believe that the considerations and the results obtained in this chapter are not peculiar of fermion models but could be recovered for instance also for vectorial models at finite temperature.[11] This is not an unexpected result in the light of chapter 6 where the large N scheme studied in this work is applied to a vectorial ϕ^6 interaction. Indeed using standard arguments one can see as the introduction of a cut off (the temperature in the ϕ^4 interaction) can be resummed in higher order vertices.

---

[11] See for instance [54].

We have just stressed that a careful numerical investigation of fermionic models (of the type presented in this chapter) could be a very precise test of the idea presented in this work, due to the fact that a lot of available simulations (also for several N_f) are present [50] [51] [52] [53]. The goals of such a studies would be the determination of the $1/N$ correction to the critical parameter $T_c(N)$ [and $M_c(N)$ in the case of Wilson fermions] to compare with the simulation data for several N. This step could be require few time and is actually under study. On the other hand is not clear to us if the data available in literature could confirm the claim that all the crossover considered in this work are universal, i.e. if for instance medium range models can be compared with Yukawa models. It is our opinion that such a question merit further investigations.

Chapter 6

Crossover in tricritical models

In this chapter we want to give another example in which our technique can be used to elucidate some aspects of a tricritical phase diagram in the large N limit. The Hamiltonian (6.1) is usually used in order to investigate systems that exhibit a tricritical phase transition like for instance metamagnet [97] or fluid ^{3}He-^{4}He mixtures. The large N limit has been investigated long time ago [96]. The standard scenario predicts (for $H \neq 0$) two lines of continuous phase transitions (that usually are called wing lines) that end joining together in a tricritical point. However some questions remain open. Indeed the ref. [96] shows that the continuous transitions observed along the wing lines are Mean Field like while because of symmetry argumentation, the authors expect a Ising behavior for every N. In this chapter we want to show as the two different critical behavior can be reconciled defining the Critical Crossover Limit for Hamiltonian (6.1). The presentation strictly follows chapter 1 and 3 and some steps are missed. In particular we take care to define (sec. 6.2) the $N = \infty$ scaling fields of the theory (with which using results of sec. 1.3 one can recover the $N = \infty$ phase diagram) and to study the stability of the weakly coupled theory (sec. 6.4) that is the basic point in order to define the Critical Crossover Limit which implementation for interaction (6.1) is identical to what done in chapter 3 for $\mathcal{N} = 1$ Heisenberg models.

6.1 The model

In this chapter we will consider a vectorial model with a ϕ^6 interaction. Let us discuss the following lattice regularization

$$\mathcal{H}[\phi] \;=\; -\frac{1}{2}\sum_{x,\mu}\vec{\phi}_x\vec{\phi}_{x+\mu} - \sum_x\Big(\vec{H}\vec{\phi}_x + (\vec{H}_3\vec{\phi}_x)\frac{|\vec{\phi}_x|^2}{N} - \frac{r}{2}|\vec{\phi}_x|^2 - \frac{u}{4!}\frac{|\vec{\phi}_x|^4}{N} - \frac{v}{6!}\frac{|\vec{\phi}_x|^6}{N^2}\Big) \tag{6.1}$$

where $\vec{H}$ and $\vec{H}_3$ are two vectors with N components equal respectively to H and H_3. Hamiltonian (6.1) has been used to investigate tricritical point. In particular the common accepted phase diagram exhibits two lines of continuous phase transition (that are usually called wing lines) that end in a tricritical point. Detecting the tricritical point in general is not an easy work and it requires an accurate fine tuning of r, u and v (while for symmetric reasons at the tricritical point one has $H = H_3 = 0)^1$ (for more details we refer to [98]).

The large N limit can be studied introducing auxiliary fields as done in chapter 1. In this case we need only two auxiliary fields (λ, μ), because we relax the unit spin constraint in order to follow $[96]^2$. Thus we can write

$$\begin{aligned}
\mathcal{Z} &= \int \prod_x \mathrm{d}\vec{\phi}_x \, e^{-\mathcal{H}[\phi]} \\
&\sim \int \prod_x \mathrm{d}\vec{\phi}_x \mathrm{d}\mu_x \mathrm{d}\lambda_x \, \exp\Bigg[\frac{1}{2}\sum_{x,\mu} \vec{\phi}_x \vec{\phi}_{x+\mu} + \sum_x \left(\frac{N}{2}\lambda_x\Big(\mu_x - \frac{|\vec{\phi}_x|^2}{N}\Big) + \vec{H}\vec{\phi}_x + (\vec{H}_3\vec{\phi}_x)\mu_x \right. \\
&\quad \left. -\frac{Nr}{2}\mu_x - \frac{Nu}{4!}{\mu_x}^2 - \frac{Nv}{6!}{\mu_x}^3\right)\Bigg] \qquad (6.2)
\end{aligned}$$

Integrating the ϕ field in the previous expression we obtain the effective action A for the auxiliary fields that is the starting point for every $1/N$ investigation:

$$\begin{aligned}
\mathcal{Z} &\sim \int \prod_x \mathrm{d}\mu_x \mathrm{d}\lambda_x \, \exp\Bigg[-\frac{N}{2}\operatorname{tr}\log \mathcal{O}[\lambda] + \frac{N}{2}(H + H_3\mu, \mathcal{O}^{-1}[\lambda], H + H_3\mu) \\
&\quad + \sum_x \left(\frac{N}{2}\lambda_x\mu_x - \frac{Nr}{2}\mu_x - \frac{Nu}{4!}{\mu_x}^2 - \frac{Nv}{6!}{\mu_x}^3\right)\Bigg] \\
&\equiv \int \prod_x \mathrm{d}\mu_x \mathrm{d}\lambda_x \, e^{-NA[\mu,\lambda]} \qquad (6.3)
\end{aligned}$$

where we have introduced the operator $\mathcal{O}$ that acts on scalar fields in the following manner:

$$(\varphi, \mathcal{O}[\lambda], \varphi) = -\sum_{x,\mu} \varphi_x \varphi_{x+\mu} + \sum_x \lambda_x {\varphi_x}^2 \qquad (6.4)$$

For constant value of $\lambda_x = \lambda$, $\mathcal{O}$ can be diagonalized in momenta space so that

$$\mathcal{O}[\overline{\lambda}](\mathbf{p}) = \frac{1}{2}(\widehat{\mathbf{p}}^2 + 2\lambda - 2d). \qquad (6.5)$$

6.2 Gap-Equation. The $H_3 = 0$ case

We are interested to understand the crossover from Mean Field criticality to Ising criticality on the wing lines of the tricritical phase diagram. In order to do that it it is expected [96] we can put $H_3 = 0$ without destroy the qualitative picture. Indeed imposing the stationarity of the effective action (6.3) we obtain two equations for the fields at the stationary point $\overline{\mu}$ and $\overline{\lambda}$

$$\begin{aligned}
\overline{\mu} &= 2B_1(m_0^2) + 4H^2 B_2(m_0^2) \\
\overline{\lambda} &= r + \frac{u}{3!}\overline{\mu} + \frac{v}{5!}\overline{\mu}^2 \qquad (6.6)
\end{aligned}$$

---

[1] However the study of interaction (6.1) in the weak coupling limit (chap. 2 for $\mathcal{N} = 3$), could give the leading term of the expansion of $r_c(v)$ and $u_c(v)$ apart a $\sim v$-factor similar to A defined in sec. 2.1.4.

[2] However as we have just noticed during this work, in the large N limit unit spin constraint is usually irrelevant [24] [49].

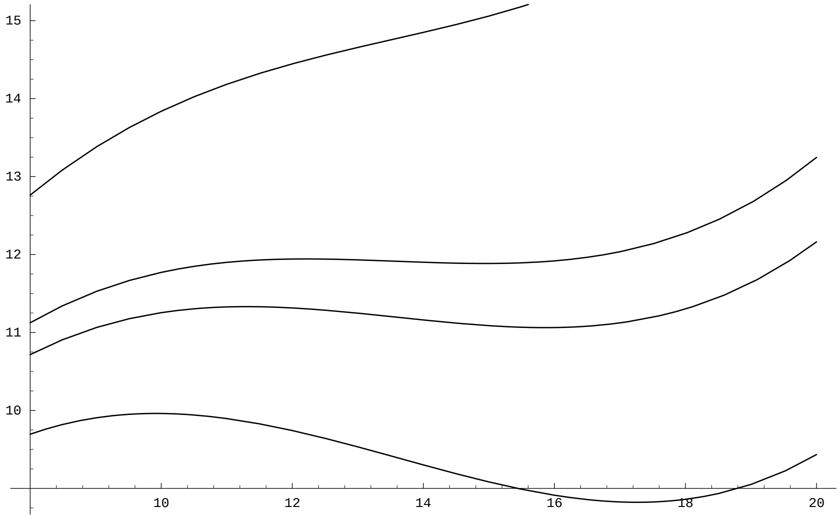

Figure 6.1: H^2 versus $\overline{\mu}$ with $v = 1/4$, $u = -1/2$ and (from below) $r = 5$, 5.05, 5.07 and 5.15

where we have defined

$$m_0^2 \equiv 2\overline{\lambda} - 2d. \tag{6.7}$$

In eq. (6.6) we have taken the notation of the previous chapters defining

$$B_n(m_0^2) = \int_{\mathbf{p}} \frac{1}{(\widehat{p}^2 + m_0^2)^n} \tag{6.8}$$

From the previous equation (6.6) we can obtain H (and of course $\overline{\lambda}$) as a function of the $O(N)$ symmetric observable $\overline{\mu}$:[3]

$$H^2 = \frac{\overline{\mu} - 2B_1(m_0^2)}{4B_2(m_0^2)} \tag{6.9}$$

where m_0^2 as a function of $\overline{\mu}$ is obtained using eq. (6.7) and the second of eqs. (6.6). Interesting enough is the fact that H^2 as a function of $\overline{\mu}$ in general cannot be inverted as depicted in fig. 6.1. This is the sign of the appearance of a phase transition, the mechanism being the same of what presented in chapter 1 or ref. [55] for Heisenberg models. In this case the magnetic field H plays the role of the temperature (or spin-spin correlation length) in Heisenberg models. The key point is that in both model phase transitions happen at finite temperature ($\beta < \infty$ for the Heisenberg models) and at finite Magnetic Field ($H \neq 0$ for the model studied in this chapter). This fact is the reason for which infrared divergences appear and the standard expansion fails, so that the crossover mechanism is observed instead of a one parameter (N) family of critical points.

Figure 6.1 gives evidence of the existence of a line of critical point (wing line) near which we have (in the following we reduce to the $H > 0$ case):

$$H - H_c \sim (\overline{\mu} - \overline{\mu}_c)^3 \tag{6.10}$$

---

[3] Indeed using the equations of motions we get $\overline{\mu} = < |\vec{\phi}_x|^2/N >$

At this point the Mean Field considerations of the chapter 1 and of reference [55] can easily be applied with analogous results. In order to elucidate this claim, if we take as tunable parameters of our theory r and H (u and v remaining fixed for instance at the value reported in fig. 6.1) and expanding the gap-equation near the critical point $H_c \approx 23$, $r_c \approx 5.07$ and $\overline{\mu}_c \approx 14$ (see fig. 6.1) we get the following expansion

$$\begin{aligned} H^2 - H_c^2 &= \sum_{n,m} a_{nm}(r-r_c)^n(\overline{\mu}-\overline{\mu}_c)^m \\ a_{0i} &= 0 \qquad \text{for } i = 0,1,2. \end{aligned} \tag{6.11}$$

Equation (6.11) and the gap equation for $\mathcal{N} = 1$ Heisenberg models (1.21) are identical apart replacing r with p and $\overline{\mu}$ with m_0^2. In particular proceeding in such a way the $N = \infty$ scaling fields can be obtained using eq. (1.24) and eq. (1.28). Then following the considerations of chapter 3 we expect to extend the $N = \infty$ analysis including also $1/N$ fluctuations. In particular this allows us to explain the crossover between Mean-Field to Ising behavior using universal crossover functions that have been investigated in chapter 2 and have been used in all the rest of this work.

In the next section 6.3 we will obtain the Propagator and the vertices of the auxiliary fields μ, λ, in particular we want to show the presence of the zero mode of the theory. Having done this it will be clear that the $1/N$ results obtained for the Heisenberg models (chap. 3) or for the Yukawa model (chap. 5) strictly apply also for Hamiltonian (6.1), confirming the claim that for every N finite on the wing lines one observes Ising phase transitions that cross –in a universal way– on Mean field phase transitions for $N = \infty$.

6.3 $1/N$ Expansion and Crossover to Ising Behavior

Now we are going to show that eq. (6.10) implies the existence of a zero mode, so that the picture developed in chapter 3 can be applied also in this case. Introducing fluctuations for the auxiliary fields to the saddle point solutions (6.6)

$$\begin{aligned} \mu_x &= \overline{\mu} + \frac{\widehat{\mu}_x}{\sqrt{N}} \\ \lambda_x &= \overline{\lambda} + \frac{\widehat{\lambda}_x}{\sqrt{N}} \end{aligned} \tag{6.12}$$

the standard $1/N$ expansion [characterized by the inverse of the propagator $P^{-1}_{AB;\overline{\mu}}(\mathbf{p})$ and by the effective vertices $V^{(j)}_{A_1\cdots A_j;\overline{\mu}}(\mathbf{p_1}, \cdots \mathbf{p_j})$] is easily obtained. In order to give an outlook on how a zero mode appears near a gap equation that exhibits criticality like that presented in fig. 6.1 we try to differentiate the gap-equation (6.3) (rewritten below)

$$\frac{\delta}{\delta\Psi_A(\mathbf{0})} A[\overline{\Psi}(\overline{\mu}), H(\overline{\mu})] = 0 \tag{6.13}$$

[$\Psi_1(\mathbf{p}) \equiv \widehat{\mu}(\mathbf{p})$ and $\Psi_2(\mathbf{p}) \equiv \widehat{\lambda}(\mathbf{p})$] with respect to $\overline{\mu}$ obtaining

$$\sum_B \frac{\delta^2 S[\overline{\Psi}(\overline{\mu}), H(\overline{\mu})]}{\delta\Psi_A(\mathbf{0})\delta\Psi_B(\mathbf{0})} \frac{\mathrm{d}\overline{\Psi}_B}{\mathrm{d}\overline{\mu}} + \frac{\delta^2 S[\overline{\Psi}(\overline{\mu}), H(\overline{\mu})]}{\delta\Psi_A(\mathbf{0})\delta H} \frac{\mathrm{d}H}{\mathrm{d}\overline{\mu}} = 0. \tag{6.14}$$

In the previous equation (6.14) at the critical point the second term cancels [like $(\overline{\mu}-\overline{\mu}_c)^2$] pointing out that P^{-1} is singular at the critical point confirming the starting claim. In particular (denoting with $z_A(\mathbf{p})$ the zero mode of the theory), neglecting a normalization factor, from eq. (6.14) easily follows

$$\begin{aligned}\sum_B P^{-1}_{AB}(\mathbf{0})z_B(\mathbf{0}) &\sim (\overline{\mu}-\overline{\mu}_c)^2 z_A(\mathbf{0})\\ z_B(\mathbf{0}) &= \frac{\mathrm{d}\overline{\Psi}_B}{\mathrm{d}\overline{\mu}}+O(\overline{\mu}-\overline{\mu}_c)^2. \end{aligned}\tag{6.15}$$

The previous equation is similar to relation (3.29) found for Heisenberg models.[4]

To explicitly verify the previous consideration we compute $\det P^{-1}$. It is easy to obtain the following formula

$$\begin{aligned}P^{-1}_{11}(\mathbf{0}) &= \frac{2u}{4!}+\frac{v\overline{\mu}}{5!}=\frac{1}{4}\frac{\mathrm{d}m_0^2}{\mathrm{d}\overline{\mu}}\\ P^{-1}_{12}(\mathbf{0}) &= -\frac{1}{2}\\ P^{-1}_{22}(\mathbf{0}) &= -8H^2B_3(m_0^2)-2B_2(m_0^2)=\left(\frac{\mathrm{d}m_0^2}{\mathrm{d}\overline{\mu}}\right)^{-1}\left(1-B_2(m_0^2)\frac{\mathrm{d}H^2}{\mathrm{d}\overline{\mu}}\right)\end{aligned}\tag{6.16}$$

Using (6.9) we obtain

$$\det P^{-1}(\mathbf{0})=-B_2(m_0^2)\frac{\mathrm{d}H^2}{\mathrm{d}\overline{\mu}}\tag{6.17}$$

confirming the presence of the zero mode at the critical point (fig. 6.1). Notice that the sign of $\mathrm{d}H^2/\mathrm{d}\overline{\mu}$ is positive near the critical point [i.e. $a_{03}>0$ in eq. (6.11)], this will be relevant to discuss the stability of the theory.

6.4 On the stability of the Weakly-Coupled theory

In this chapter we want to do some considerations on the stability of the weakly coupled theory describing the crossover between Ising to Mean Field behavior. This is in principle the unique think that could destroy the picture we have presented in the previous sections. We have just noticed in sec. 3.1 how the positivity[5] of the zero mode four legs vertex is related to the positivity of the zero mode mass near the critical point (see eq. 3.12).

Using equations (6.16) it is easy to compute the critical eigenvalue λ_0 of P^{-1}. If we define

$$m' \equiv \frac{\mathrm{d}m_0^2}{\mathrm{d}\overline{\mu}}\tag{6.18}$$

---

[4] In this case the auxiliary fields are two instead of five. However relation (6.15) is general once A is taken to run on the number of auxiliary fields present in the theory

[5] This is related to the stability of the weakly ϕ^4 theory in the sense that if the positivity condition fails than one needs to consider also higher than four legs vertex that have been discarded in chapter 2 simply using scaling arguments.

we find

$$\lambda_0 \ = \ -\frac{B_2(m_0^2)}{4}\left(\frac{m'}{4}+\frac{1}{m'}\right)^{-1}\frac{\mathrm{d}H^2}{\mathrm{d}\overline{\mu}}+O\left(\frac{\mathrm{d}H^2}{\mathrm{d}\overline{\mu}}\right)^2 \qquad (6.19)$$

so that our stability condition becomes $m' < 0$ (we have just noticed that $a_{03} > 0$), and using eq. (6.7) we get the following condition

$$v\overline{\mu}_c < -10u \qquad (6.20)$$

Figure 6.1 gives numerical evidence that the critical point we have considered satisfies previous relation (6.20). However we expect that the same result holds on all the wing lines.

Appendix A

Properties of $x\mathcal{G}$ eq. (5.11)

We want to proof relations (5.15). Due to the symmetry $\mathcal{G}(-x,T) = \mathcal{G}(x,T)$ we will consider here only $x > 0$. Notice that

$$\begin{aligned} x\mathcal{G}(x) &:= \frac{1}{2}\int^{\Lambda} \mathrm{d}\mathbf{p}\, f_T(x,\mathbf{p}) \\ f_T(x,\mathbf{p}) &= \frac{\mathrm{d}w_x(\mathbf{p})}{\mathrm{d}x}\tanh\frac{w_x(\mathbf{p})}{2T} \end{aligned} \tag{A.1}$$

where we have defined:

$$w_x(\mathbf{p}) = \sqrt{\mathbf{p}^2 + x^2} \tag{A.2}$$

Then using the previous we have:

$$\frac{\mathrm{d}w_x(\mathbf{p})}{\mathrm{d}x} = \frac{x}{w_x(\mathbf{p})} \tag{A.3}$$

$$\frac{\mathrm{d}^2w_x(\mathbf{p})}{\mathrm{d}x^2} = \frac{1}{w_x(\mathbf{p})}\Big(1 - \Big(\frac{\mathrm{d}w_x(\mathbf{p})}{\mathrm{d}x}\Big)^2\Big) \tag{A.4}$$

$$\begin{aligned} \frac{\mathrm{d}^3w_x(\mathbf{p})}{\mathrm{d}x^3} &= -\frac{3}{w_x(\mathbf{p})^2}\frac{\mathrm{d}w_x(\mathbf{p})}{\mathrm{d}x}\Big(1 - \Big(\frac{\mathrm{d}w_x(\mathbf{p})}{\mathrm{d}x}\Big)^2\Big) \\ &= -\frac{3}{w_x(\mathbf{p})}\frac{\mathrm{d}w_x(\mathbf{p})}{\mathrm{d}x}\frac{\mathrm{d}^2w_x(\mathbf{p})}{\mathrm{d}x^2} \end{aligned} \tag{A.5}$$

We have $x \le w_x(\mathbf{p})$ (A.2), so that both the first and second derivative or w are positive while the third derivative is always negative. Then we have:

$$\frac{\mathrm{d}f_T(x,\mathbf{p})}{\mathrm{d}x} = \frac{\mathrm{d}^2w_x(\mathbf{p})}{\mathrm{d}x^2}\tanh\frac{w_x(\mathbf{p})}{2T} + \frac{1}{2T}\Big(\frac{\mathrm{d}w_x(\mathbf{p})}{\mathrm{d}x}\Big)^2\cosh^{-2}\frac{w_x(\mathbf{p})}{2T} \tag{A.6}$$

which is always positive for the previous considerations. For the second derivative we find:

$$\begin{aligned} \frac{\mathrm{d}^2f_T(x,\mathbf{p})}{\mathrm{d}x^2} = {} & \frac{\mathrm{d}^3w_x(\mathbf{p})}{\mathrm{d}x^3}\tanh\frac{w_x(\mathbf{p})}{2T} + \frac{3}{2T}\frac{\mathrm{d}w_x(\mathbf{p})}{\mathrm{d}x}\frac{\mathrm{d}^2w_x(\mathbf{p})}{\mathrm{d}x^2}\cosh^{-2}\frac{w_x(\mathbf{p})}{2T} \\ & -\frac{1}{2T^2}\Big(\frac{\mathrm{d}w_x(\mathbf{p})}{\mathrm{d}x}\Big)^3\sinh\frac{w_x(\mathbf{p})}{2T}\cosh^{-3}\frac{w_x(\mathbf{p})}{2T} \end{aligned}$$

$$\begin{aligned}
&= -\frac{3}{w_x(\mathbf{p})}\frac{\mathrm{d}w_x(\mathbf{p})}{\mathrm{d}x}\frac{\mathrm{d}^2w_x(\mathbf{p})}{\mathrm{d}x^2}\Big(\tanh\frac{w_x(\mathbf{p})}{2T}-\frac{w_x(\mathbf{p})}{2T}\cosh^{-2}\frac{w_x(\mathbf{p})}{2T}\Big)\\
&\quad -\frac{1}{2T^2}\Big(\frac{\mathrm{d}w_x(\mathbf{p})}{\mathrm{d}x}\Big)^3\sinh\frac{w_x(\mathbf{p})}{2T}\cosh^{-3}\frac{w_x(\mathbf{p})}{2T}\\
&\leq 0 \qquad \text{(A.7)}
\end{aligned}$$

having used the fact that:

$$\tanh x = \frac{1}{2}\frac{\sinh 2x}{\cosh^2 x} \geq \frac{x}{\cosh^2 x} \qquad \text{(A.8)}$$

Immediately (A.6) and (A.7) give us the relations (5.15). Otherwise similar results show that $\mathcal{G}(x,T)$

$$\mathcal{G}(x,T) = \frac{1}{2}\int^{\Lambda}\mathrm{d}\mathbf{p}\frac{1}{w_x(\mathbf{p})}\tanh\frac{w_x(\mathbf{p})}{2T} \qquad \text{(A.9)}$$

is a decreasing function of x. Indeed we find

$$\frac{\mathrm{d}\mathcal{G}(x,T)}{\mathrm{d}x} = -\frac{1}{2}\int^{\Lambda}\mathrm{d}\mathbf{p}\frac{1}{w_x(\mathbf{p})^2}\frac{\mathrm{d}w_x(\mathbf{p})}{\mathrm{d}x}\Big(\tanh\frac{w_x(\mathbf{p})}{2T}-\frac{w_x(\mathbf{p})}{2T}\cosh^{-2}\frac{w_x(\mathbf{p})}{2T}\Big) \qquad \text{(A.10)}$$

and the claim follows using the (A.8).

Appendix B

Relations among the Yukawa model, medium-range models, and field theory

In this appendix we want to relate the weakly coupled φ^4 theory, medium-range models, and the Yukawa model for $d = 2$. This models have been considered in this work as prototype for large-$\mathcal{N}$ phase transition with infrared singularities. More interesting the solution proposed (i.e. to resum the divergences introducing N-dependent scaling variables with scaling relations given by a weakly coupled φ^4 theory) has given us the possibility to identify the crossover between Ising behavior to Mean Field behavior in all such models. In this appendix we want to elucidate how one can use numerical available data on medium range model to obtain numerical informations on Yukawa models (or vice-versa).

For simplicity, we only consider the case $H = 0$, corresponding to $M = 0$ in the Yukawa model. The field-theory model has been discussed in sec. 2.1, where it was shown that the n-point zero momentum connected correlation function $\chi_{\mathrm{FT},n}$ shows a scaling behavior of the form

$$u^{n-1}\chi_{\mathrm{FT},n} = f_{\mathrm{FT},n}(\tilde{t}_{\mathrm{FT}}) \qquad \tilde{t}_{\mathrm{FT}} \equiv [r - r_c(u)]/u. \tag{B.1}$$

Next, we consider systems with medium-range interactions. Consider a square lattice, Ising spins σ_x at the sites of the lattice, and the Hamiltonian

$$\mathcal{H} = -\frac{1}{2}\sum_{\mathbf{xy}} J(\mathbf{x}-\mathbf{y})\sigma_{\mathbf{x}}\sigma_{\mathbf{y}}. \tag{B.2}$$

We assume[1] that $J(\mathbf{x}) = 1$ for $|x| \leq R_m$, $J(\mathbf{x}) = 0$ for $|x| > R_m$. The behavior of these models is very similar to that observed in the Yukawa model, R_m playing the role of N. For any finite R_m, the system belongs to the Ising universality class, while for $R_m = \infty$ all spins are coupled together and one obtains mean-field behavior. In Ref. [33] it was shown that this model shows a crossover that interpolates between mean-field and Ising behavior. If one defines an effective interaction range R by

$$R^2 = \frac{\sum_{\mathbf{x},\mathbf{y}}(\mathbf{x}-\mathbf{y})^2 J(\mathbf{x}-\mathbf{y})}{\sum_{\mathbf{x},\mathbf{y}} J(\mathbf{x}-\mathbf{y})}, \tag{B.3}$$

---

[1] One can also consider a much more general class of medium-ranged models, see Ref. [32].

then for $R, R_m \to \infty$, $t \equiv (T - T_c(R))/T_c(R) \to 0$ at fixed $\tilde{t}_{\rm MR} \equiv tR^2$ one has

$$R^{4-3n} \chi_{{\rm MR},n} = f_{{\rm MR},n}(\tilde{t}_{\rm MR}), \tag{B.4}$$

where $\chi_{{\rm MR},n}$ is the connected zero-momentum n-points correlation function of the fields σ. In Ref. [32] it was shown that $f_{{\rm MR},n}(x)$ and $f_{{\rm FT},n}(x)$ are closely related. Indeed, we have

$$f_{{\rm MR},n}(x) = \mu_{1,{\rm MR}} \mu^n_{2,{\rm MR}} f_{{\rm FT},n}(\lambda_{\rm MR} x), \tag{B.5}$$

where $\mu_{i,{\rm MR}}$ and $\lambda_{\rm MR}$ are model-dependent constants that reflect the arbitrariness in the definitions of the fields, of the range R, and of the scaling variable $\tilde{t}$. The constants can be computed using the results of Ref. [32], sec. 4.2.[2] Explicitly, we have for the two-point and four-point zero-momentum connected correlation functions:

$$\begin{aligned}
\chi_{{\rm MR},2} R^{-2} &= \frac{1}{\tilde{t}_{\rm MR}} + \frac{1}{4\pi \tilde{t}^2_{\rm MR}} \left[\ln \left(\frac{4\pi \tilde{t}_{\rm MR}}{3} \right) + 8\pi D_2 + 3 \right] + O(\tilde{t}^{-3}_{\rm MR}), \\
\chi_{{\rm MR},4} R^{-8} &= -\frac{2}{\tilde{t}^4_{\rm MR}} + O(\tilde{t}^{-5}_{\rm MR}).
\end{aligned} \tag{B.6}$$

In the field-theory model we have instead

$$u\chi_2 = \frac{1}{\tilde{t}} + \frac{1}{8\pi \tilde{t}^2} \left[\ln \frac{8\pi \tilde{t}}{3} + 8\pi D_2 + 3 \right] + O(\tilde{t}^{-3}). \tag{B.7}$$

$$u^2 \chi_4 = -\frac{1}{\tilde{t}^4} + O(\tilde{t}^{-5}). \tag{B.8}$$

Comparing we obtain

$$\mu_{1,{\rm MR}} = 2, \qquad \mu_{\rm MR} = \lambda_{\rm MR} = \frac{1}{2}. \tag{B.9}$$

In sec. 5.5 we have shown a similar relation for the Yukawa model. If $x_t \equiv -g_{01} N[T - T_c(N)]$, we find for the zero-momentum correlation functions of the field ϕ

$$\tilde{\chi}_n \equiv g^n \chi_n = N^{n/2-1} f_{Y,n}(x_t), \tag{B.10}$$

and

$$f_{Y,n}(x) = \mu_{1,Y} \mu^n_{2,Y} f_{{\rm FT},n}(\lambda_Y x). \tag{B.11}$$

In order to compute these constants we compare the one-loop expansions of the two-point function in field theory and in the Yukawa model. In the Yukawa model we find

$$\begin{aligned}
\int {\rm d}^d\mathbf{x} \langle \chi(\mathbf{0}) \chi(\mathbf{x}) \rangle &= \frac{NT}{\alpha^2 x_t} - \left(\frac{NT}{\alpha^2 x_t} \right)^2 r_c \\
&\quad - \frac{1}{2N} \left(\frac{NT}{\alpha^2 x_t} \right)^2 \int_{p<\Lambda} \frac{{\rm d}^2\mathbf{p}}{(2\pi)^2} \frac{\overline{V}^{(4)}(\mathbf{p}, -\mathbf{p}, \mathbf{0}, \mathbf{0})}{\overline{P}(\mathbf{p})} + O(x_t^{-3}).
\end{aligned} \tag{B.12}$$

---

[2] Note that the function $f_\chi(\hat{t})$ defined in Ref. [32] refers to correlations of the fields ϕ and not of the original fields φ. However, relation (4.12) of Ref. [32] shows that in the critical crossover limit $\sum_x \langle \varphi_0 \varphi_x \rangle \approx \sum_x \langle \phi_0 \phi_x \rangle$. The same holds for χ_4. The expression reported here are obtained from those reported in Ref. [32] by setting $\overline{a}_2 = 1$, $\overline{a}_4 = -2$, $N = 1$, $c_0 = \hat{c}_0 = \tau$, and $\tilde{t}_{\rm MR} = \hat{t} + \hat{c}_0$.

Using the explicit expression for r_c we obtain

$$\tilde{\chi}_2 = \frac{1}{x_t} + \frac{\alpha^2 V_4(\mathbf{0},0)}{8\pi x_t^2}\left[\ln\frac{8\pi x_t}{3\alpha^2 V_4(\mathbf{0},0)} + 8\pi D_2 + 3\right] + O(x_t^{-3}). \tag{B.13}$$

For the four-point function we have instead

$$\tilde{\chi}_4 N^{-1} = -\frac{V_4(\mathbf{0},0)}{x_t^4} + O(x_t^{-5}). \tag{B.14}$$

Comparing we obtain

$$\mu_{1,Y} = \alpha^4 V_4(\mathbf{0},0), \qquad \mu_{2,Y} = \frac{1}{\alpha^3 V_4(\mathbf{0},0)}, \qquad \lambda_Y = \frac{1}{\alpha^2 V_4(\mathbf{0},0)}. \tag{B.15}$$

The constants reported in sec. 5.5.3 are easily derived:

$$K_{\rm FT} = -\lambda_Y g_{01}, \qquad K_{2,\rm FT} = \mu_{1,Y}\mu_{2,Y}^2, \tag{B.16}$$

$$K_{\rm LBB} = -\frac{\lambda_Y g_{01}}{\lambda_{\rm MR}}, \qquad K_{n,\rm LBB} = \frac{\mu_{1,Y}\mu_{2,Y}^n}{\mu_{1,\rm MR}\mu_{2,\rm MR}^n}, \tag{B.17}$$

where $n = 1, 2$. Note that g_{01} is negative, so that $K_{\rm FT}$ and $K_{\rm LBB}$ are positive as expected.

The generalization to $\mathcal{N} = 1$ Heisenberg models is straightforward and can be obtained repeating the previous considerations of the Yukawa model with which shares the same large N expansion.

Bibliography

[1] A. D. Sokal "Monte Carlo Methods in Statistical Mechanics: Foundation and New Algorithms", lecture given at the Lausanne summer school 1989.
A. Pelissetto "Introduction to the Monte Carlo Method, " lecture given at the 2^{nd} National Seminar of Theoretical Physics, Parma 1992.

[2] C. Schmidt "Lattice QCD at finite density," to appear on proceeding of LATTICE 2006, Tucson.

[3] E. Marinari and G. Parisi "Trattatello di Probabilità e statistica. "

[4] S. R. Coleman "Aspects of Symmetry, " Cambridge University Press, (1985).

[5] W. A. Bardeen and M. Moshe, Phys. Rev. D **28** (1983) 1372.

[6] T. H. Berlin and M. Kac, Phys. Rev. **86** (1952) 821.

[7] H. E. Stanley, Phys. Rev. **176** (1968) 718.

[8] H. K. Janssen, B. Schaub and B. Schmittmann, Z. Phys. B **73** (1989).

[9] K. G. Wilson, Phys. Rev. D **7** (1973) 2911.

[10] D. J. Gross and A. Neveu, Phys. Rev. D **10** (1974) 3235.

[11] A. D. Sokal and A. O. Starinets, Nucl. Phys. B **601** (2001) 425 [arXiv:hep-lat/0011043].

[12] J. P. Blaizot, R. Mendez-Galain and N. Wschebor, Annals Phys. **307** (2003) 209 [arXiv:hep-ph/0212084].

[13] S. Hands, A. Kocic and J. B. Kogut, Annals Phys. **224** (1993) 29 [arXiv:hep-lat/9208022].

[14] H. Yamada, Int. J. Mod. Phys. A **13** (1998) 4133 [arXiv:hep-th/9704001].

[15] J. I. Kapusta, "Finite Temperature Field Theory," Cambridge University Press, (2006).

[16] D. O'Connor C. R. Stephens, Phys. Rep. **363** (2002) 425-545.

[17] R. Abe, Prog. Theor. Phys. **48** (1972) 1414.

[18] S. K. Ma, Phys. Rev. Lett. **29** (1972) 1311.

[19] E. Brezin and D. J. Wallace, Phys. Rev. B **7** (1973) 1967.

[20] S. K. Ma, Phys. Rev. A **10** (1974) 1818.

[21] C. N. Yang and T. D. Lie, Phys. Rev. **87** (1952) 404.

[22] T. D. Lie and C. N. Yang, Phys. Rev. **87** (1952) 410.

[23] "Phase Transitions and Critical Phenomena", edited by C. Domb and M. S. Green (Academic, New York, 1976), Vol. VI.

[24] J. Zinn-Justin, "Quantum field theory and critical phenomena," Fourth Edition Clarendon Press Oxford (2002).

[25] C. Itzykson and J. M. Drouffe, "Statistical Field Theory," Cambridge University Press, Cambridge, (1989).

[26] A. Pelissetto and E. Vicari, Phys. Rep. 368 (2002) 549 [cond-mat/0012164].

[27] C. Bagnuls and C. Berviller, J. Phys. Lett. 45 (1984) L95.

[28] C. Bagnuls, C. Berviller and Y. Garrabos, J. Phys. Lett. 45 (1984) L127.

[29] C. Bagnuls and C. Berviller, Phys. Rev. B 32 (1985) 7209.

[30] C. Bagnuls, C. Bervillier, D.I. Meiron, and B.G. Nickel, Phys. Rev. B 35 (1987) 3585; (Erratum) B 65 (2002) 149901 [hep-th/0006187];

[31] C. Bagnuls and C. Bervillier, Phys. Rev. E 65 (2002) 066132 [hep-th/011220].

[32] A. Pelissetto, P. Rossi, and E. Vicari, Nucl. Phys. B 554 (1999) 552 [cond-mat/9903410].

[33] E. Luijten, H.W.J. Blöte, and K. Binder, Phys. Rev. E 54 (1996) 4626 [cond-mat/9607019].

[34] A. Pelissetto, P. Rossi, and E. Vicari, Phys. Rev. E 58 (1998) 7146 [cond-mat/9804264].

[35] S. Caracciolo, M.S. Causo, A. Pelissetto, P. Rossi, and E. Vicari, Phys. Rev. E 64 (2001) 046130 [cond-mat/0105160].

[36] E. Luijten, H.W.J. Blöte, and K. Binder, Phys. Rev. E 56 (1997) 6540 [cond-mat/9706257]

[37] E. Luijten and K. Binder, Phys. Rev. E 58 (1998) 4060(R) [cond-mat/9807415]; 59 (1999) 7254.

[38] M. Corti and V. Degiorgio, Phys. Rev. Lett. 55 (1985) 2005.

[39] G. Dietler and D. S. Cannel, Phys. Rev. Lett. 60 (1988) 1852.

[40] M. A. Anisimov, A. A. Povodyrev, V. D. Kulikov and J. V. Sengers, Phys. Rev. Lett. 75 (1995) 3146.

[41] C. Bagnuls, C. Bervillier, Phys. Rev. Lett. 76 (1996) 4094.

[42] M. A. Anisimov, A. A. Povodyrev, V. D. Kulikov and J. V. Sengers, Phys. Rev. Lett. 76 (1996) 4095.

[43] S. Chandrasekharan and F. J. Jiang, Phys. Rev. D **74** (2006) 014506 [arXiv:hep-lat/0602031].

[44] R.D. Pisarski and F. Wilczek, Phys. Rev. D 29 (1984) 338.

[45] A. Butti, A. Pelissetto, and E. Vicari, J. High Energy Phys. 08 (2003) 029 [hep-ph/0307036]; F. Basile, A. Pelissetto, and E. Vicari, Proceedings of the XXIII International Symposium on Lattice Field Theory, Dublin, July 2005, Proc. of Science (LAT2005) 199 [hep-lat/0509018]; F. Basile, A. Pelissetto and E. Vicari, JHEP **0502** (2005) 044 [arXiv:hep-th/0412026].

[46] F. Karsch, *Lectures on Quark Matter*, Proceedings of the 40 Internationale Universitätswochen für Kern und Teilchenphysik, Lecture Notes in Physics 583, edited by W. Plessas and L. Mathelisch (Springer, Berlin, 2002) [hep-lat/0106019].

[47] F. Karsch and E. Laermann, *Thermodynamics and in-medium hadron properties from lattice QCD*, in Quark-Gluon Plasma 3, edited by R.C. Hwa (World Scientific, Singapore, 2003) [hep-lat/0305025].

[48] B. Rosenstein, A.D. Speliotopoulos and H.L. Yu, Phys. Rev. D 49 (1994) 6822.

[49] M. Moshe and J. Zinn-Justin, Phys. Rept. 385 (2003) 69 [hep-th/0306133].

[50] J.B. Kogut, M.A. Stephanov, and C.G. Strouthos, Phys. Rev. D 58 (1998) 096001 [hep-lat/9805023]

[51] C. Strouthos and S. Christofi, JHEP **0501** (2005) 057 [arXiv:hep-lat/0501001].

[52] C. G. Strouthos, Nucl. Phys. A **749** (2005) 182 [arXiv:hep-lat/0410003].

[53] C. G. Strouthos, arXiv:hep-ph/0301085.

[54] C. G. Strouthos and I. N. Tziligakis, JHEP **0302** (2003) 034 [arXiv:hep-lat/0212040].

[55] S. Caracciolo and A. Pelissetto, Phys. Rev. E 66 (2002) 016120 [cond-mat/0202506].

[56] S. Caracciolo, B.M. Mognetti, and A. Pelissetto, Nucl. Phys. B 707 (2005) 458 [cond-mat/0409536].

[57] S. Caracciolo, B.M. Mognetti, and A. Pelissetto, “Two-Dimensional Heisenberg Model with Nonlinear Interactions: Multicritical Points,” in preparation.

[58] B. Bringoltz, Phys. Rev. D **73** (2006) 076002 [arXiv:hep-lat/0511058].

[59] S. Caracciolo, B.M. Mognetti, and A. Pelissetto, Proceedings of the XXIII International Symposium on Lattice Field Theory, Dublin, July 2005, Proc. of Science (LAT2005) 187 [hep-lat/0509063].

[60] S. Caracciolo, B. M. Mognetti and A. Pelissetto, Nucl. Phys. B **741** (2006) 421 [arXiv:hep-lat/0601018].

[61] J. B. Kogut and L. Susskind, "Hamiltonian Formulation Of Wilson's Lattice Gauge Theories," Phys. Rev. D **11** (1975) 395.

[62] N.D. Mermin and H. Wagner, Phys. Rev. Lett. **17** (1966) 1133.

[63] A.M. Polyakov, Phys. Lett. B **59** (1975) 79.

[64] E. Brézin and J. Zinn-Justin, Phys. Rev. B **14** (1976) 3110.

[65] W.A. Bardeen, B.W. Lee, and R.E. Shrock, Phys. Rev. D **14** (1976) 985.

[66] U. Wolff, Phys. Rev. Lett. **62** (1989) 361; Nucl. Phys. B **334** (1990) 581; Phys. Lett. B **248** (1990) 335.

[67] R.G. Edwards, S.J. Ferreira, J. Goodman, and A.D. Sokal, Nucl. Phys. B **380** (1992) 621.

[68] J.-K. Kim, Phys. Rev. Lett. **70** (1993) 1735; Phys. Rev. D **50** (1994) 4663.

[69] S. Caracciolo, R.G. Edwards, A. Pelissetto, and A.D. Sokal, Phys. Rev. Lett. **75** (1995) 1891 [hep-lat/9411009]; Nucl. Phys. B (Proc. Suppl.) **42** (1995) 752 [hep-lat/9411064].

[70] S. Caracciolo, R.G. Edwards, T. Mendes, A. Pelissetto, and A.D. Sokal, Nucl. Phys. B (Proc. Suppl.) **47** (1996) 763 [hep-lat/9509033].

[71] T. Mendes, A. Pelissetto, and A.D. Sokal, Nucl. Phys. B **477** (1996) 203 [hep-lat/9604015].

[72] M. Falcioni and A. Treves, Nucl. Phys. B **265** (1986) 671.

[73] S. Caracciolo and A. Pelissetto, Nucl. Phys. B **420** (1994) 141 [hep-lat/9401015].

[74] S. Caracciolo and A. Pelissetto, Nucl. Phys. B **455** (1995) 619) [hep-lat/9510015]; B. Allés, S. Caracciolo, A. Pelissetto, and M. Pepe, Nucl. Phys. B **562**, 581 (1999) [hep-lat/9906014].

[75] B. Allés, A. Buonanno, and G. Cella, Nucl. Phys. B **500** (1997) 513 [hep-lat/9701001]; Nucl. Phys. B (Proc. Suppl.) **53** (1997) 677 [hep-lat/9608002].

[76] P. Hasenfratz, M. Maggiore, and F. Niedermayer, Phys. Lett. B **245** (1990) 522.

[77] P. Hasenfratz and F. Niedermayer, Phys. Lett. B **245** (1990) 529.

[78] M. Campostrini, A. Pelissetto, P. Rossi, and E. Vicari, Phys. Lett. B **402** (1997) 141 [hep-lat/9702010].

[79] A.C.D. van Enter and S.B. Shlosman, Phys. Rev. Lett. **89** (2002) 285702 [cond-mat/0205455].

[80] A.C.D. van Enter and S.B. Shlosman, *Provable first-order transitions for liquid crystal and lattice gauge models with continuous symmetries*, cond-mat/0306362.

[81] N. Magnoli and F. Ravanini, Z. Phys. C **34** (1987) 43.

[82] H.W.J. Blöte, W. Guo, and H.J. Hilhorst, Phys. Rev. Lett. **88** (2002) 047203 [cond-mat/0201174].

[83] A. Pal and S.K. Roy, Phys. Rev. E **67** (2003) 011705.

[84] F. Niedermayer, P. Weisz, and D.-S. Shin, Phys. Rev. D **53** (1996) 5918 [hep-lat/9507005].

[85] A.D. Sokal and A.O. Starinets, Nucl. Phys. B **601** (2001) 425 [hep-lat/0011043].

[86] G.A. Baker, Jr., B.G. Nickel, M.S. Green, and D.I. Meiron, Phys. Rev. Lett. **36** (1977) 1351; G.A. Baker, Jr., B.G. Nickel, and D.I. Meiron, Phys. Rev. B **17** (1978) 1365.

[87] P. Calabrese, M. Caselle, A. Celi, A. Pelissetto, and E. Vicari, J. Phys. A **33** (2000) 8155 [hep-th/0005254].

[88] M. Caselle, A. Pelissetto, and E. Vicari, in *Fluctuating Paths and Fields*, W. Janke, A. Pelster, H.-J. Schmidt, and M. Bachmann eds., (World Scientific, Singapore, 2001) [hep-th/0010228].

[89] S. Hikami and T. Maskawa, Prog. Theor. Phys. **67** (1982) 1038.

[90] K. Ohno, H.-O. Carmesin, H. Kawamura, and Y. Okabe, Phys. Rev. B **42** (1990) 10360.

[91] H. Kunz and G. Zumbach, J. Phys. A **22** (1989) L1043; Phys. Lett. B **257** (1991) 299; Phys. Rev. B **46** (1992) 662; J. Phys. A **25** (1992) 6155.

[92] P. Butera and M. Comi, Phys. Rev. B **46** (1992) 11141 [hep-lat/9205027].

[93] S. Caracciolo, R.G. Edwards, A. Pelissetto, and A.D. Sokal, Nucl. Phys. B (Proc. Suppl.) **26** (1992) 595 [hep-lat/9201003]; Nucl. Phys. B (Proc. Suppl.) **30** (1993) 815 [hep-lat/9212012]; Phys. Rev. Lett. **71** (1993) 3906 [hep-lat/9307022].

[94] M. Hasenbusch, Phys. Rev. D **53** (1996) 3445 [hep-lat/9507008].

[95] S. M. Catterall, M. Hasenbusch, R. R. Horgan and R. Renken, Phys. Rev. D **58** (1998) 074510 [hep-lat/9801032].

[96] S. Sarbach and M. Fisher, Phys. Rev. B **18** (1978) 2350

[97] M. E. Fisher, AIP Conf. Proc. **24**, 273 (1975)

[98] "Phase Transitions and Critical Phenomena", edited by C. Domb and M. S. Green (Academic, New York, 1976), Vol. IX.